

Investigating the Role of Glutathione Transferases in the Phytodetoxification of Explosives

Kyriakos Tzafestas
PhD

University of York
Biology

February 2016

Abstract

The explosive 2,4,6-trinitrotoluene (TNT) is a major worldwide environmental pollutant. Highly persistent to degradation the presence of this toxic pollutant presents various health and environmental concerns. In the present study the role of two glutathione transferases (GSTs), in the detoxification of TNT is investigated. The Tau class GSTs from *Arabidopsis thaliana* (*Arabidopsis*), GST-U24 and GST-U25, were strongly upregulated in response to TNT. Following affinity chromatography purification and characterisation of recombinant forms of both enzymes, three distinct TNT-glutathionyl products were identified. GSTU-25 was able to convert TNT to 2-glutathionyl-4,6-dinitrotoluene, with the concurrent release of nitrite. This conjugate could be chemically weaker than TNT and as a result, potentially more susceptible to biodegradation. To further investigate the detoxification abilities of GST-U24 and GST-U25 *in planta* 35S-GST-U24 and GST-U25 *Arabidopsis* lines were generated. These GST overexpressing lines exhibited significantly increased ability to withstand and detoxify TNT with a corresponding reduction in glutathione levels, and displayed higher shoot and root biomass than untransformed plants when grown in the presence of TNT.

A *Drosophila melanogaster* Epsilon class GST (*DmGSTE6*) was subsequently assessed for its potential for phytoremediation. *DmGSTE6* exhibited higher activity than GST-U24 and GST-U25 towards TNT *in vitro* and produced almost exclusively 2-glutathionyl-4,6-dinitrotoluene. Expressing *DmGSTE6* in *Arabidopsis* resulted in enhanced biomass, when grown on TNT-containing media, when compared to the GST-U24/U25 overexpressing lines, but a similar TNT uptake rate.

Finally, to identify key amino residues involved in the catalytic activity of GSTs towards TNT, a site-directed mutagenesis approach was employed. The results highlighted Tyr107 as important to catalytic activity with additional aromatic residues contributing to the stabilisation of aromatic substrates such as TNT. Ultimately the GST-mediated detoxification pathway demonstrated here can be exploited in robust plant species for the phytoremediation of TNT.

List of contents

Abstract	<i>iii</i>
List of contents	<i>iv</i>
List of Figures	<i>ix</i>
List of Tables	<i>xiii</i>
Acknowledgments	<i>xv</i>
Author's declaration	<i>xvi</i>
Chapter 1: Introduction	1
1.1 Explosives.....	1
1.2 TNT.....	2
1.2.1 TNT pollution.....	3
1.2.2 TNT toxicity.....	4
1.2.2.1 TNT toxicity in plants.....	4
1.2.2.2 TNT toxicity in mammals and bacteria.....	5
1.3 TNT detoxification by microbes.....	6
1.4 Xenobiotic detoxification in plants.....	9
1.4.1 Uptake and metabolism of TNT in plants.....	11
1.4.1.1 Uptake.....	11
1.4.1.2 Transformation.....	12
1.4.1.3 Conjugation.....	12
1.5 Glutathione transferases.....	14
1.5.1 GST activities.....	14
1.5.2 Classification.....	15
1.5.3 Evolution of GSTs.....	16
1.5.4 Gene organisation.....	17
1.5.5 Structural features.....	18
1.5.6 GST functions.....	21
1.5.6.1 Zeta.....	21
1.5.6.2 DHAR.....	21
1.5.6.3 Lamda.....	22

1.5.6.4 Theta.....	22
1.5.6.5 Phi.....	23
1.5.6.6 Tau.....	23
1.5.6.7 TCHQD.....	24
1.5.6.8 MAPEG.....	24
1.6 Glutathione.....	24
1.7 Catabolism of glutathione conjugates.....	27
1.8 Current remediation strategies.....	29
1.8.1 Incineration.....	29
1.8.2 Composting.....	30
1.8.3 Bioslurry.....	30
1.8.4 Phytoremediation.....	31
1.9 Phytoremediation of TNT.....	35
1.10 Aims of the current study.....	36
Chapter 2: General Materials and Methods.....	37
2.1 Consumables and reagents.....	37
2.2 Plasmids, bacteria and growth conditions.....	37
2.2.1 Plasmids.....	37
2.2.2 Bacterial strains.....	38
2.2.3 Preparation of high competency Escherichia coli cells.....	38
2.2.4 Transformation of chemically competent Escherichia coli.....	40
2.2.5 Transformation of electro-competent Agrobacterium tumefaciens.....	40
2.2.6 Bacterial growth conditions.....	41
2.2.6.1 Growth conditions for liquid media.....	41
2.2.6.2 Growth conditions for solid media.....	41
2.3 Molecular biology techniques.....	41
2.3.1 Agarose gel electrophoresis.....	41
2.3.2 Plasmid preparation.....	42
2.3.3 DNA fragment purification.....	42
2.3.4 Nucleotide sequencing and analysis.....	42
2.3.5 Polymerase chain reaction (PCR).....	43
2.3.6 Restriction endonuclease digestion of DNA.....	43
2.3.7 Dephosphorylation of a linearised vector.....	43
2.3.8 DNA ligation.....	44
2.3.9 Blue/white colony screening.....	44
2.4 Protein expression and purification.....	44

2.4.1 Protein expression	44
2.4.2 Cell lysis by sonication	46
2.4.3 Protein purification	46
2.4.4 Protein visualisation	46
2.4.5 Protein quantification	47
2.5 Plant methods	47
2.5.1 Seed sterilisation	47
2.5.2 Stratification	48
2.5.3 Growth conditions	48
2.5.3.1 Growth conditions for soil	48
2.5.3.2 Growth conditions for solid media	48
2.5.4 Genomic DNA isolation from plants	48
2.6 Statistical analysis	49

Chapter 3: AtGSTU24 and AtGSTU25 over-expressing Arabidopsis

lines	50
3.1 Introduction	50
3.2 Methods	55
3.2.1 Protein extraction from plant tissue	55
3.2.2 CDNB activity assay on plant protein extract	55
3.2.3 TNT-containing soil reparation	56
3.2.4 Soil studies	56
3.2.5 Extraction of TNT and derivatives from soil	57
3.2.6 LC/MS analysis of soil extraction products	57
3.2.7 Glutathione measurements	58
3.2.8 GPOX assay	59
3.3 Results	61
3.3.1 CDNB Activity of plant protein extracts	61
3.3.2 Biomass of GST-U24 and U25 OE Arabidopsis lines	62
3.3.3 TNT uptake from soil	66
3.3.4 Glutathione abundance	70
3.3.5 GPOX activity	73
3.4 Discussion	75

Chapter 4: Biochemical characterisation of a TNT detoxifying

Drosophila GST and recombinant expression in Arabidopsis	80
4.1 Introduction	80

4.2 Methods.....	82
4.2.1 Cloning of <i>DmGSTE6</i> in pET-YSBLIC3C.....	82
4.2.2 Expression and purification of <i>DmGSTE6</i>	83
4.2.3 Kinetic assay with CDNB.....	83
4.2.4 TNT activity assay.....	84
4.2.5 Kinetic assay with TNT.....	85
4.2.6 LC-MS analysis of conjugation products.....	86
4.2.7 HADNTs and ADNTs activity assay.....	86
4.2.8 GPOX activity.....	86
4.2.9 Expression of <i>DmGSTE6</i> in Arabidopsis.....	87
4.2.10 Protein extraction from plant tissue.....	87
4.2.11 CDNB activity assay on plant protein extract.....	88
4.2.12 Griess assay.....	88
4.2.13 RT-PCR.....	90
4.2.14 Root length studies and analysis.....	91
4.2.15 TNT-containing soil preparation.....	91
4.2.16 Soil studies.....	91
4.2.17 Extraction of TNT and derivatives in soil.....	92
4.2.18 Hydroponic culture setup.....	92
4.2.19 Liquid culture setup.....	92
4.2.20 Chlorophyll measurement.....	93
4.2.21 Glutathione measurements.....	94
4.2.22 Glutathione depletion studies.....	94
4.2.23 ggt3/1 knockout lines grown on TNT-containing media.....	94
4.3 Results.....	95
4.3.1 Cloning, expression and purification of <i>DmGSTE6</i>	95
4.3.2 Kinetic analysis of <i>DmGSTE6</i> with CDNB.....	95
4.3.3 Effect of pH on GST activity.....	97
4.3.4 Effect of temperature on GST activity.....	100
4.3.5 Kinetic analysis with TNT.....	103
4.3.6 Griess assay.....	104
4.3.7 Activity towards ADNTs and HADNTs.....	105
4.3.8 GPOX activity.....	106
4.3.9 Recombinant expression of <i>DmGSTE6</i> in Arabidopsis.....	107
4.3.10 Preliminary screening of the <i>DmGSTE6</i> transgenic Arabidopsis lines.....	109

4.3.10.1 Preliminary screening of <i>DmGSTE6</i> expressing Arabidopsis	109
4.3.10.2 CDNB activity of plant protein extracts	111
4.3.10.3 RT-PCR on <i>DmGSTE6</i> expressing Arabidopsis lines	112
4.3.10.4 Griess assay on plant protein extracts	113
4.3.11 Root length studies	114
4.3.12 Biomass of transgenic lines grown on TNT-containing soil	121
4.3.13 TNT uptake by the transgenic lines from soil	124
4.3.14 Hydroponic cultures	125
4.3.15 Liquid cultures supplemented with TNT and GSH	132
4.3.15.1 Effect of exogenous GSH on intervals levels of GSH	137
4.3.16 Glutathione depletion studies	139
4.3.17 GGT1 and GGT3 involvement in the catabolism of TNT-GSH conjugates	141
4.4 Discussion	143
Chapter 5: Site-directed-mutagenesis on AtGSTU24 and U25	149
5.1 Introduction	149
5.2 Methods	153
5.2.1 Generation, expression and purification of mutants	153
5.2.2 Homology modelling	155
5.2.3 Activity assays towards TNT	155
5.2.4 Activity assays towards CDNB	156
5.2.5 ANS binding assays	156
5.3 Results	157
5.3.1 Selection and production of GST-U24 and GST-U25 mutants	157
5.3.2 Activity of GST-U24 and GST-U25 mutants towards TNT	159
5.3.3 Activity of GST-U24 and GST-U25 mutants towards CDNB	161
5.3.4 Probing the GST-U24 and GST-U25 mutants for conformational changes	163
5.4 Discussion	165
5.4.1 Residues important to the activity towards TNT	165
5.4.2 Leu211 involved in the production of conjugate 3	166
5.4.3 Engineering the GST-U25 conjugate profile into GST-U24	167
Chapter 6: Final discussion	168
Abbreviations	178
References	181

List of figures

Figure 1.1: Chemical structures of the main secondary explosives.....	2
Figure 1.2: Chemical structure of TNT.....	4
Figure 1.3: TNT toxicity in plants.....	5
Figure 1.4: Structure of TNT and its primary reduced derivatives.....	6
Figure 1.5: Hydride addition to the aromatic ring of TNT, catalysed by microbial enzymes.....	8
Figure 1.6: Plant xenobiotic metabolism.....	9
Figure 1.7: Autoradiography of [U-14C]-TNT in poplar and switchgrass.....	11
Figure 1.8: The proposed metabolic pathway for TNT in plants.....	13
Figure 1.9: Phylogenetic tree of Arabidopsis GSTs.....	17
Figure 1.10: Distribution of GST genes in the Arabidopsis genome.....	18
Figure 1.11: Overview of the GST structure.....	20
Figure 1.12: Known GSH functions in plants.....	26
Figure 1.13: Schematic representation of the most likely catabolic pathway for GSH-conjugates.....	29
Figure 1.14: Main types of phytoremediation.....	32
Figure 3.1: Upregulation of Arabidopsis GSTs in response to TNT.....	51
Figure 3.2: Glutathionylation of TNT.....	53
Figure 3.3: Appearance of GST OE and WT plants treated with TNT.....	54
Figure 3.4: GST catalysed conjugation of CDNB with GSH.....	55
Figure 3.5: Overview of the process used to determine GSH abundance.....	59
Figure 3.6: Overview of the process used to measure GPOX activity.....	59
Figure 3.7: Appearance and conjugation activities of roots of GST OE and WT plants.....	61
Figure 3.8: Appearance of GST OE and WT plants grown on TNT-containing soil.....	63

Figure 3.9: Biomass of GST OE and WT plants grown on TNT-containing soil.....	65
Figure 3.10: HPLC analysis of samples extracted from soil.....	67
Figure 3.11: Mass spectrometry of samples extracted from soil.....	68
Figure 3.12: TNT uptake from soil by GST OE and WT plants.....	69
Figure 3.13: GSH abundance in the leaves and roots of GST OE and WT plants.....	70
Figure 3.14: GSH and GSSG levels in the leaves and roots of GST OE and WT plants.....	72
Figure 3.15: SDS-PAGE analysis of GST-U24/U25 expression and purification..	73
Figure 3.16: Enzyme kinetics and Lineweaver-Burk double reciprocal plots for the GPOX activity of GST-U24 and GST-U25.....	74
Figure 4.1: Vector map of the pET-YSBLIC3C plasmid.....	82
Figure 4.2: The chemical reactions of Griess assay.....	88
Figure 4.3: Standard curve of nitrite concentrations versus absorbance.....	89
Figure 4.4: SDS-PAGE gel showing the expression and purification of <i>DmGSTE6</i>	95
Figure 4.5: Michaelis-Menten plot of <i>DmGSTE6</i> with CDNB.....	96
Figure 4.6: Effect of pH on the conjugation activity of <i>DmGSTE6</i>	98
Figure 4.7: Conjugate production profile of <i>DmGSTE6</i> across different pH values.....	99
Figure 4.8: Effect of temperature on the conjugation activity of <i>DmGSTE6</i>	101
Figure 4.9: Conjugate production profile of <i>DmGSTE6</i> across different temperatures.....	102
Figure 4.10: Michaelis-Menten plot of <i>DmGSTE6</i> with TNT.....	103
Figure 4.11: Griess assay with purified GST-U24, GST-U25 and <i>DmGSTE6</i>	105
Figure 4.12: Activity of <i>DmGSTE6</i> towards HADNTs and ADNTs.....	106
Figure 4.13: GPOX activity of <i>DmGSTE6</i>	107

Figure 4.14: Diagnostic digestions of pART7 and pART27 carrying the <i>DmGSTE6</i> gene.....	108
Figure 4.15: Diagnostic PCR to confirm successful insertion of the <i>DmGSTE6</i> in the <i>Arabidopsis</i> genome.....	108
Figure 4.16: Preliminary screening of the <i>DmGSTE6</i> expressing lines detoxification abilities.....	110
Figure 4.17: Activity of plant protein extracts with CDNB.....	112
Figure 4.18: RT-PCR on <i>DmGSTE6</i> expressing <i>Arabidopsis</i>	113
Figure 4.19: Griess assay with plant protein extracts.....	114
Figure 4.20: Effect of TNT on root growth of <i>Arabidopsis</i> seedlings.....	119
Figure 4.21: Root length of <i>Arabidopsis</i> seedlings grown on TNT-containing media.....	120
Figure 4.22: Appearance of <i>Arabidopsis</i> seedlings grown in soil containing TNT.....	122
Figure 4.23: Biomass of <i>Arabidopsis</i> seedlings grown in soil containing TNT.....	123
Figure 4.24: Levels of nitrotoluenes recovered from TNT-containing soil where <i>Arabidopsis</i> seedlings were grown.....	125
Figure 4.25: Hydroponic culture assembly of <i>Arabidopsis</i> seedlings.....	126
Figure 4.26: TNT uptake from hydroponic cultures by <i>Arabidopsis</i> seedlings.....	127
Figure 4.27: Coloration and HPLC analysis of TNT-containing media where <i>Arabidopsis</i> seedlings were grown.....	128
Figure 4.28: LC/MS analysis of unidentified peaks from TNT-containing media where <i>Arabidopsis</i> seedlings were grown.....	130
Figure 4.29: TNT uptake by plants grown in TNT-containing liquid media supplemented with GSH.....	134
Figure 4.30: Appearance of plants grown in TNT-containing liquid media supplemented with GSH.....	135
Figure 4.31: Chlorophyll content of plants grown in TNT-containing liquid media supplemented with GSH.....	136
Figure 4.32: Levels of GSH in liquid cultures containing both TNT and GSH.....	136

Figure 4.33: Levels of GSSG in liquid cultures containing both TNT and GSH...	137
Figure 4.34: Internal GSH levels of plants grown on TNT-containing liquid media supplemented with GSH.....	138
Figure 4.35: Root length and appearance of plants grown on media containing BSO.....	140
Figure 4.36: Root length and surface area of <i>ggt</i> KO lines grown on TNT-containing media.....	142
Figure 5.1: Degradation of 2,4-dinitrotoluene (2,4-DNT) by <i>Burkholderia</i> sp. DNT.....	149
Figure 5.2: Chemical structures of naturally occurring nitro-substituted compounds.....	150
Figure 5.3: Protein sequence alignment of GST-U24, GST-U25 and <i>DmGSTE6</i>	152
Figure 5.4: Protein sequence alignment of GST-U24 and GST-U25 with <i>TaGSTU4-4</i> and <i>GmGSTU4-4</i>	157
Figure 5.5: Models of monomeric forms of GST-U24 and GST-U25 based on homology modelling.....	158
Figure 5.6: Activity towards TNT and conjugate production profile of GST-U24 and its respective mutants.....	160
Figure 5.7: Activity towards TNT and conjugate production profile of GST-U25 and its respective mutants.....	161
Figure 5.8: Activity of GST-U24, GST-U25 and their respective mutants towards CDNB.....	162
Figure 5.9: Fluorescence emission spectra of ANS binding to the active site of GST-U24, GST-U25 and their respective mutants.....	164
Figure 6.1: The proposed pathway for the detoxification of TNT in the roots of <i>Arabidopsis</i>	169

List of tables

Table 2.1: Plasmids used for gene cloning and enzyme expression	38
Table 2.2: Bacterial strains used for gene cloning and enzyme expression	38
Table 2.3: The components of SOB medium	39
Table 2.4: The components of TfbI solution	39
Table 2.5: The components of TfbII solution	39
Table 2.6: Sequencing primers	43
Table 2.7: The components of AI medium	45
Table 2.8: Composition of stock solutions for AI medium	45
Table 2.9: The components of PBS	46
Table 2.10: The composition of 4x sample loading buffer	47
Table 2.11: The composition of 2x CTAB buffer	49
Table 3.1: Kinetic data of GST-U24 and GST-U25 GPOX activity	74
Table 4.1: Primers for cloning <i>DmGSTE6</i> in pET-YSB LIC3C	83
Table 4.2: HPLC conditions for the separation of the TNT-GSH conjugates	85
Table 4.3: Primers used for RT-PCR	90
Table 4.4: HPLC conditions for the detection of both TNT and GSH	93
Table 4.5: Kinetic analysis of CDNB-conjugating activity by <i>DmGSTE6</i> , GST-U24 and GST-U25	96
Table 4.6: Activity of <i>DmGSTE6</i> across the range of pH values tested	99
Table 4.7: Activity of <i>DmGSTE6</i> across the range of temperatures tested	102
Table 4.8: Kinetic analysis of TNT-conjugating activity by <i>DmGSTE6</i> , GST-U24 and GST-U25	103
Table 4.9: Root length of 10-day-old plants grown on TNT-containing media	116
Table 4.10: Root surface area of 20-day-old plants grown on TNT- containing media	116
Table 4.11: Possible TNT photo-degradation products	131

Table 5.1: Primers used for the site-directed-mutagenesis of GST-U24 and GST-U25	154
Table 5.2: HPLC conditions for the separation of the TNT-GSH conjugates	155
Table 5.3: The GST-U24 and GST-U25 mutants	159

Acknowledgements

Many thanks go to a great deal of people who have helped me along the way to my PhD and have made the past three years an enjoyable and memorable experience, however, above everyone else I would like to thank Mr. Ashley Burgess for supporting me and funding this project. Without him none of this would have been possible. He has been very kind and generous to me.

Special thanks to Professor Neil C. Bruce for trusting me with this project, as well as for his continuous support, guidance and encouragement. I have very much enjoyed working in his lab and will always be grateful for this opportunity.

To Dr. Elizabeth L. Rylott for her supervision and regular advice regarding the project. Her door was always open and I probably cannot thank her enough for the endless meetings we had, the energy, the enthusiasm and the thought she put in the project.

Thanks to Professor Simon McQueen Mason and Dr. Frans Maathuis for their participation and valuable input in the thesis advisory panel.

I would also like to thank all the members of the Bruce and McQueen-Mason group. I will not name them individually in the fear of forgetting someone. They have all been excellent and helpful colleagues but above everything else they have been great friends. Big thanks go to Louise and Dave for their excellent work in the lab and always offering their help when needed.

I would also like to thank Professors B. Mannervik and N. Ohkama-Otsu who very kindly provided the Epsilon class GST from *D. melanogaster* and the γ -glutamyl transpeptidase knockout plant lines respectively.

At last I would like to thank my family for their continuous motivational support and encouragement, and Maria M. Razalan, my partner in both lab and life, who has been extremely supportive in and out of the lab and has helped me achieve so much.

Author's Declaration

I declare that I am the sole author of this work and that it is original except where indicated by reference in the text. No part of this work has been submitted for any other degree to any other institution.

Publications arising from this work:

- Gunning, V., et al., Arabidopsis Glutathione Transferases U24 and U25 Exhibit a Range of Detoxification Activities with the Environmental Pollutant and Explosive, 2,4,6-Trinitrotoluene. *Plant Physiol*, 2014. 165(2): p. 854-865.
- Rylott, E.L., et al., Phytodetoxification of the environmental pollutant and explosive 2,4,6-trinitrotoluene. *Plant Signal Behav*, 2015. 10(1): p. e977714.

Chapter 1: Introduction

1.1 Explosives

An explosive is a reactive material that can generate high volume of rapidly expanding gas that exerts pressure on its surroundings. The first explosive compound originated in China, a mixture of saltpetre (potassium nitrate), sulphur and charcoal, known as gunpowder [1]. However, the explosive power of gunpowder could not be enhanced and it was particularly sensitive. Since 1840, chemists around the world were able to synthesise a number of new compounds by nitration. In the years to follow the explosive properties of these compounds were realised and applications for military and industrial purposes soon followed.

Explosives can be separated into primary and secondary or high explosives. Primary explosives include compounds such as nitroglycerin, which are highly unstable and were soon replaced by secondary explosives that offered distinct advantages over their predecessors. In 1771 British chemist Peter Woulfe discovered picric acid and by 1863, when 2,4,6-trinitrotoluene (TNT) was discovered by Joseph Wilbrand, the age of secondary explosives was at full swing. These new explosives came with inherent stability until detonation and could resist friction, heat and mechanical shock [2]. The invention of efficient detonators, along with refinement in production processes and sufficient scale up, allowed the incorporation of TNT into ordnance [3]. By World War I TNT was the most widely used military explosive due to its stability and relatively easy manufacture. The demands of World War II, along with an increase in petroleum production which resulted in an increased abundance of toluene, rocketed TNT manufacture. By 1945 global TNT production reached 150,000 tonnes per month [4]. During World War II organic explosives with more nitrated groups on them were invented. To date secondary explosives can be split into three major categories according to their chemical structure; the nitrate esters, nitramines and nitroaromatics (Figure 1.1). Nitroaromatics form

an important group of compounds recalcitrant to degradation. Chemically stable, they are composed of an aromatic ring with one or more nitro groups. The most commonly used explosives by military are 2,4,6-trinitrotoluene (TNT), hexahydro-1,3,5-trinitro-1,3,5-triazine (RDX) and octahydro-1,3,5,7-tetranitro-1,3,5,7-tetrazocine (HMX).

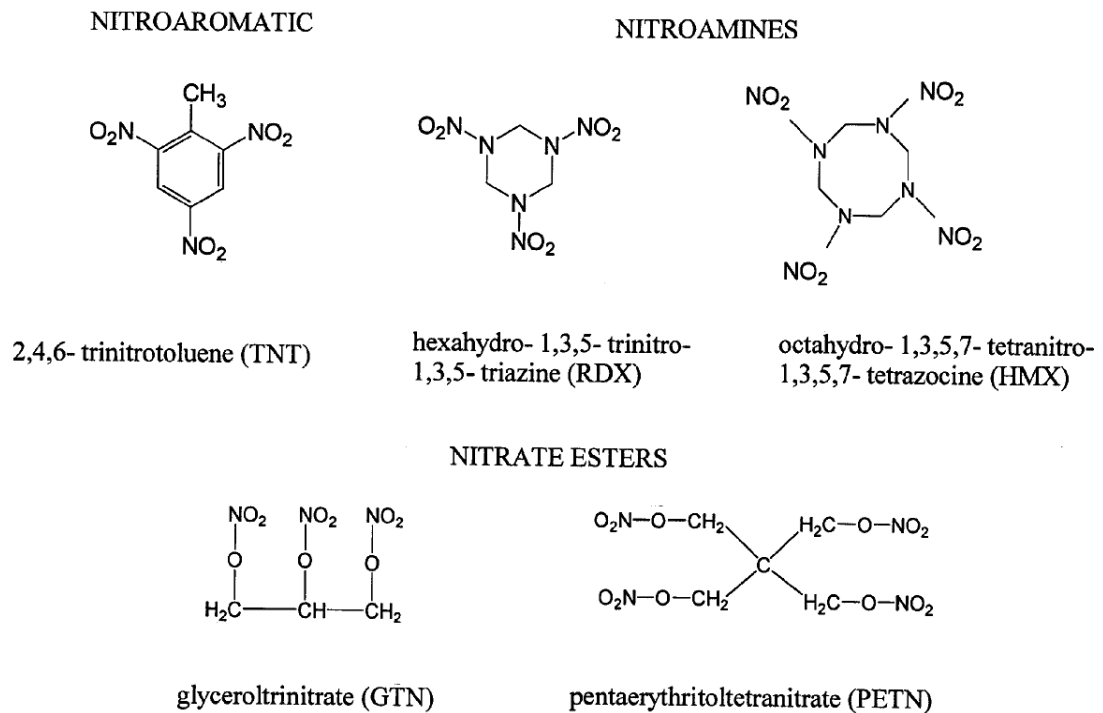


Figure 1.1: Chemical structures of the most representative members of the three classes of secondary explosives. Figure taken from Rosser et al [5].

1.2 TNT

The explosive TNT is perhaps the best-known nitroaromatic compound. It is a toxic odourless yellow compound, and a xenobiotic; a manmade compound that does not occur naturally in the environment. TNT is produced by sequential nitration of toluene [2]. During manufacture the by-products 2,4-dinitrotoluene (2,4-DNT) and 2,6-dinitrotoluene (2,6-DNT) are produced.

1.2.1 TNT pollution

The continual use of explosives, along with production and decommissioning is progressively contaminating millions of hectares of military land [6]. The most widely used explosive, TNT is associated with extensive soil and water contamination [2]. High explosive compound contamination has been reported for many military training ranges worldwide [7, 8], with the contamination being heterogeneous. Contaminated training ranges have hotspots of TNT that can reach concentrations of up to 87000 mg kg⁻¹ soil [9]. However, the average contamination is in the range of 100 to 1000 mg kg⁻¹, or lower for surface soils in artillery training ranges and 1 to 36 mg kg⁻¹ for hand grenade ranges [10, 11]. The United States Department of Defense has identified more than 1000 sites heavily contaminated with explosives, of which more than 95 % contained TNT [12]. The total area of operational ranges in the United States contaminated with munitions constituents, is estimated to be more than 10 million hectares [13]. Besides the United States, such sites have also been identified in Germany and other European countries [14]. Besides the training ranges contamination derives also from discarded and unexploded ordnance, as well as former manufacturing and WWII sites. It is important to control such extensive pollution and remediate those sites and in accordance with this the United States Environmental Protection Agency (USEPA) has established a remediation goal of 17.2 mg kg⁻¹ for TNT in soils [15].

The structure of TNT makes bioremediation particularly challenging. Both nitrogen and oxygen are highly electro-negative elements, with oxygen possessing the highest electro-negativity. The electron-withdrawing properties of the nitro groups delocalize the π electrons of the aromatic ring, turning the ring from electron-rich to electron-deficient (Figure 1.2) and thus particularly resistant to oxidative attack and subsequent ring cleavage by microbial oxygenases [16-18].

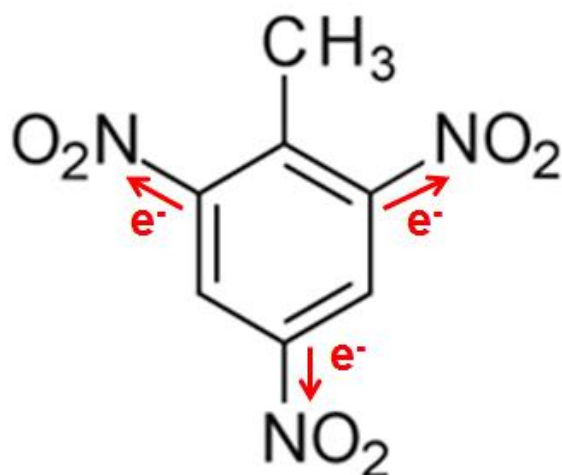


Figure 1.2: Chemical structure of TNT. The electron-withdrawing properties of the nitro groups delocalise the electrons of the aromatic ring to such an extent that they are no longer available for oxidative attack by microbial oxygenases.

1.2.2 TNT toxicity

Classified by the US Environmental Protection Agency (EPA) as a Class C (possible human) carcinogen, TNT has been shown to be toxic to all organisms tested.

1.2.2.1 TNT toxicity in plants

TNT has been found to exhibit phytotoxic effects to all plants tested. The toxicity of TNT to plants is species dependent with most species able to tolerate TNT levels of 50 to 100 mg kg⁻¹ soil [19]. Plants grown in the presence of toxic levels of TNT exhibit symptoms of chlorosis, stunting of the roots and inhibition of lateral growth [20-22]. Plants have also been reported to suffer growth suppression, with TNT reducing seedling biomass and seed germination [23-25]. As a consequence, root length and/or biomass of plants grown on media containing TNT serves as a good indicator of the plant's tolerance towards TNT [23, 26, 27]. The mechanism underlying TNT toxicity to plants has recently been revealed.

Arabidopsis monodehydroascorbate reductase 6 (MDHAR6), an FAD-dependent oxidoreductase that recycles ascorbate by reducing monodehydroascorbate (MDA), the primary oxidation product of ascorbate,

was found to have activity towards TNT [28]. MDHAR6 which is targeted to the plastids and mitochondria reduces TNT by a single electron to form a TNT nitro-radical that is subsequently auto-oxidised back to TNT with the concurrent generation of superoxide. This futile cycle depletes NADPH and causes oxidative damage within mitochondria and plastids, where important biochemical pathways are located (Figure 1.3). This study confirms that the main reason of TNT toxicity derives from the generation of ROS.

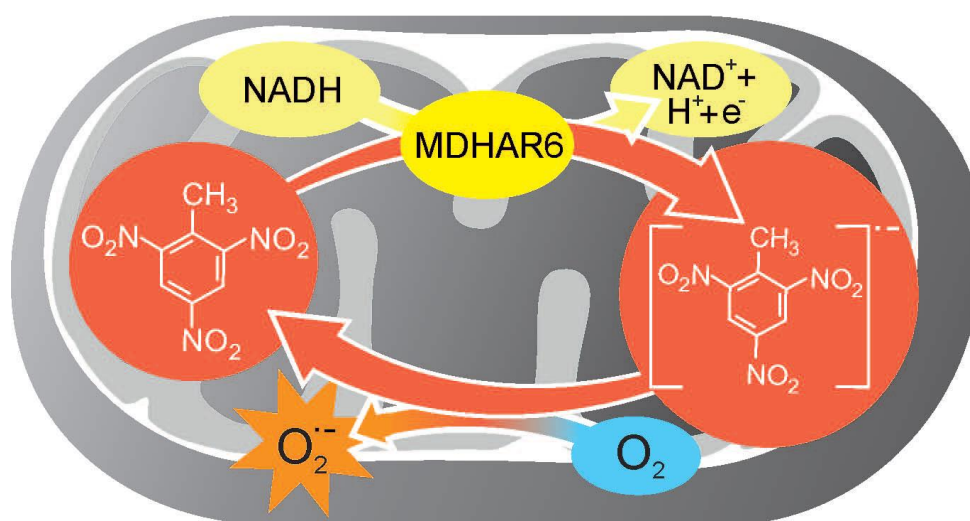


Figure 1.3: A schematic representation of the catalytic activity of mitochondrial MDHAR6 towards TNT. Figure taken from Johnston et al [28].

1.2.2.2 TNT toxicity in mammals and bacteria

Protein sequence alignments suggest that MDHAR6 is unique to plants and algae. In bacteria and mammals, TNT causes strong cytotoxic and genotoxic effects *in vitro* [29-32]. In humans TNT can be readily absorbed through the skin, respiratory and gastrointestinal tract [33]. Exposure to TNT can result in aplastic anemia, hepatitis, rashes and skin hemorrhages [34]. Further symptoms of TNT toxicity include dermatitis, gastritis, cyanosis, nausea, dizziness and reduced sperm count [35]. Nitroreductases present in the human liver can reduce TNT to hydroxylamino-dinitrotoluene (HADNTs) and amino-dinitrotoluene derivatives (ADNTs) which react with biological molecules and can lead to carcinogenic and mutagenic effects [33]. The primary reduced metabolites of TNT (HADNTs and ADNTs) (Figure 1.4) have

been proven to be equally or slightly less toxic than their parent compound, depending on the cell type, and to possess mutagenic potential [29-32]. Their cytotoxicity seems to be inversely related to their state of reduction, confirming that one of the main reasons for the toxicity of TNT is the presence of the nitro groups [29, 31]. In soil, TNT has a significant impact on the microbial population, selecting a narrow range of Gram-negative bacterial species that belong mainly to the *Pseudomonadaceae* and *Xanthomonadaceae* families [36].

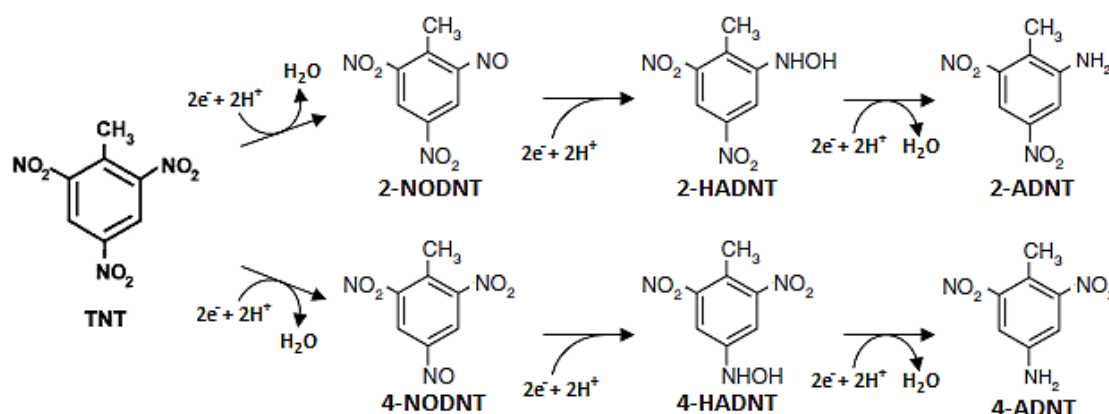


Figure 1.4: Structure of TNT and its primary reduced derivatives.

1.3 TNT detoxification by microbes

Bioremediation uses the metabolic processes of microorganisms, to transform or degrade environmental pollutants such as TNT. Research on the bioremediation of TNT has revealed several bacteria that are able to metabolise this toxic compound. Although some studies refer to microbial transformation of TNT as degradation, a ring-cleavage or mineralisation pathway has yet to be identified in bacteria. Because TNT is a highly oxidised molecule most of the microorganisms metabolise it by reducing its nitro groups, a well characterised process [4, 37].

Under aerobic conditions bacterial nitroreductases are able to reduce TNT to HADNT, ADNTs and diaminonitrotoluenes (DANTs). Characteristic examples are enteric bacteria and the *nfsI* nitroreductase from *Enterobacter cloacae* [38,

39]. Besides their activity as nitroreductases, some members of the old yellow enzyme (OYE) family of flavoproteins are able to transform TNT by addition of a hydride to the aromatic ring, resulting in the formation of monohydride- or dihydride-Meisenheimer complexes that can condense with HADNT to form diarylamines and release nitrogen in the form of nitrite (Figure 1.5) [40-42]. Characteristic examples of such enzymes are the pentaerythritol tetranitrate reductase (PETNr) from *E. cloacae* PB2 [43] and the xenobiotic reductase XenB from *Pseudomonas fluorescens* I-C [44]. Hydride addition to TNT has also been observed for other bacteria, without however identifying the enzymes involved [40, 45]. Directed evolution, in the form of genome shuffling has been used to enhance the TNT transformation rate of *Stenotrophomonas maltophilia* OK-5 [46]; however, the mechanism still follows the reductive pathway.

Aerobic bacteria are able to reduce two of the three nitro groups. For the third nitro group, anaerobic conditions are required, and this is considered as a more efficient process than aerobic transformation due to the low redox potential that allows for rapid reduction of substrates [47]. Anaerobic bacteria that have such ability include mainly *Clostridia* and *Desulfovibrio* sp. [37, 48, 49]. Anaerobic TNT transformation results in accumulation of triaminotoluene (TAT) in the environment.

Although bacteria isolated from contaminated soil can rapidly detoxify explosives in laboratory conditions, the explosives persist in the environment suggesting that bacteria do not have enough biomass or metabolic activity to decontaminate these areas *in situ*. In addition, there have been several cases where it has been reported that partially reduced forms of TNT can react with each other, yielding azoxytetranitrotoluene [50], a compound more mutagenic than TNT itself [51].

Fungi have also been reported to transform TNT and in certain cases completely mineralise it [52, 53]. The most well characterised among fungi is the white rot fungus *Phanerochaete chrysosporium* [52]. The efficient mineralization of TNT requires lignolytic conditions and it is hypothesized to proceed through the sequential reduction of TNT to HADNT and ADNT during

the initial steps of the pathway. The complete process and enzymes involved are not fully understood but the mineralization of TNT is believed to result from the activity of multiple enzymes, including lignin and manganese peroxidases [54]. Nevertheless, the practical application of fungi for the remediation of contaminated sites is limited by their low tolerance towards TNT toxicity [55].

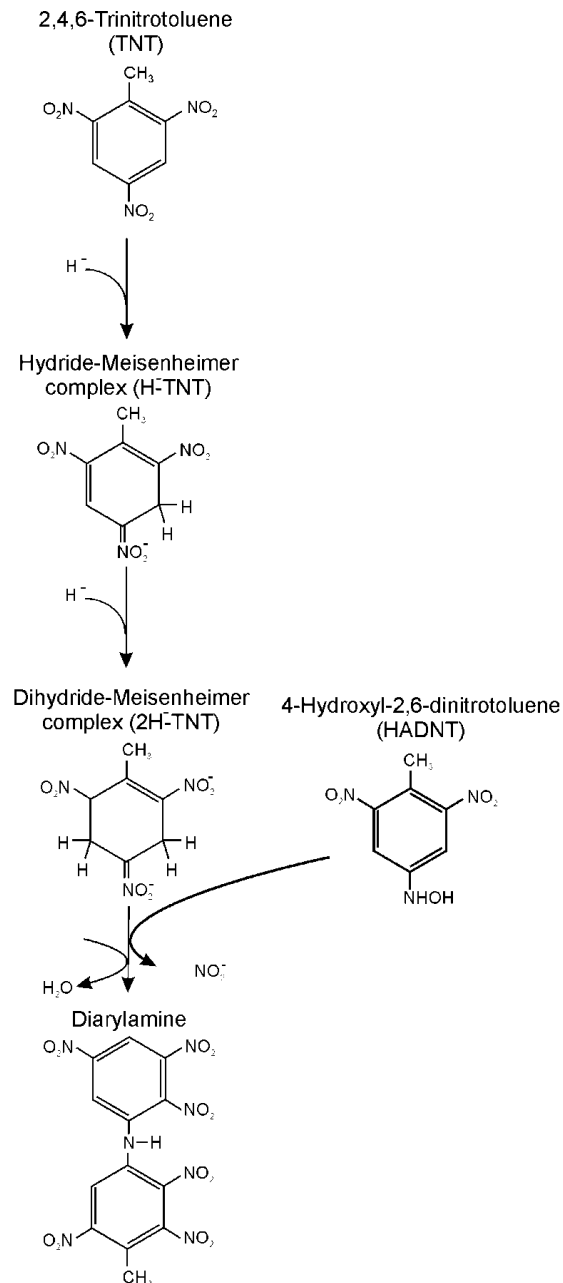


Figure 1.5: Hydride addition to the aromatic ring of TNT catalysed by microbial enzymes. Sequential addition of hydride leads to monohydride and dihydride-Meisenheimer complexes that can condensate with HADNT to form diarylamines with concurrent nitrite release. Figure adapted from Rylott et al. [56].

1.4 Xenobiotic detoxification in plants

Following uptake by the plant, metabolism of xenobiotics can be separated into three distinct phases: activation, conjugation and compartmentation (Figure 1.6) [19, 57, 58].

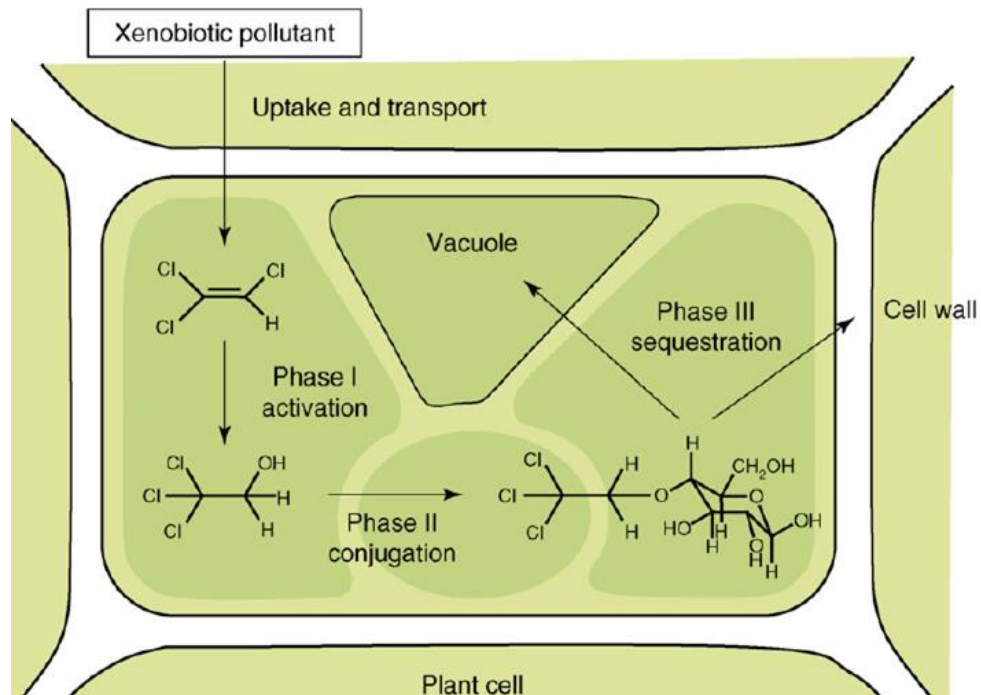


Figure 1.6: Summary of plant xenobiotic metabolism. The process can be separated into three phases. Phase I introduces or exposes functional groups to the xenobiotic through reactions such as, oxidation, reduction and hydrolysis. Phase II deactivates the compound from phase I by covalent linkage to an endogenous hydrophilic molecule such as glucose, malonate and glutathione. Phase III exports the conjugates from the cytosol and sequesters them in the vacuole or apoplast. Figure taken from Van Aken [59].

- Phase I – Activation:** During this phase the compound undergoes reactions such as oxidation, reduction and hydrolysis, resulting in the addition or exposure of a functional group [19, 58]. Enzymes including P450s, other monooxygenases, esterases and reductases, introduce functional groups such as hydroxyl (-OH), amino (-NH₂) and sulphhydryl (-SH) to the substrate. The products of phase I are often more hydrophilic than the parent compound, decreasing the ability of the compound to partition into the biological membranes and thus restricting its distribution

within cells and tissues [19]. In some cases, the functional groups can result in increased toxicity [19]. The newly introduced reactive sites allow phase II reactions to occur [57, 60]. If the xenobiotic already has a suitable functional group, the compound can proceed straight to phase II reactions [58].

- **Phase II – Conjugation:** Reactive sites present on the xenobiotic from phase I are used as sites for covalent conjugation to endogenous hydrophilic molecules such as glucose, malonate and glutathione forming a water soluble conjugate. In contrast to phase I products, products of phase II are either non-toxic, or less toxic than the parent compound [19, 57]. Phase II enzymes include a variety of transferases such as malonyl-transferases, glucosyl-transferases, and glutathione-transferases. Malonate can be conjugated to hydroxyl and amino groups, while glucose can be conjugated to hydroxyl, sulphhydryl, amino and carboxyl groups of activated xenobiotics. Glutathione can mainly conjugate electrophilic sites of the xenobiotic, often with a concurrent release of a nitro or halogen group [19]. The conjugation that occurs during the phase II reactions 'labels' the compounds for immediate sequestration.
- **Phase III – Compartmentation:** The inactive, water-soluble xenobiotic conjugates of Phase II are exported from the cytosol by membrane-located transport proteins. Conjugates remaining in the cytosol could potentially inhibit the phase II reactions or loose conjugation, thus restoring toxicity [57]. The xenobiotic conjugates can be sequestered in the apoplast or vacuole. Conjugates have been found to be associated with the pectin, lignin and hemicellulose fraction of the cell wall [57, 60]. ATP-binding cassette (ABC) transporters mediate the transportation of the conjugates [61]. In the case of the vacuole, further metabolism of the conjugate may take place, however the steps and enzymes involved remain vague [62] (see section 1.7).

1.4.1 Uptake and metabolism of TNT in plants

1.4.1.1 Uptake

The efficient uptake and translocation of a compound is dependent upon a number of factors, including plant species, soil and environmental conditions and bioavailability of the compound [63]. The bioavailability of a compound relies mainly on its chemical properties and especially its hydrophobicity. Hydrophobicity is usually expressed as the octanol:water partition co-efficient ($\text{Log } K_{\text{OW}}$). Compounds with a high $\text{Log } K_{\text{OW}}$ (> 3) are particularly hydrophobic and bind strongly to the soil organic matter, making them less soluble and hence less bioavailable [63]. Compounds with a lower $\text{Log } K_{\text{OW}}$ (< 3) have higher water solubility and are able to migrate in the soil pore water, allowing for efficient take up by the plants. Therefore TNT with a $\text{Log } K_{\text{OW}}$ of 1.6 can be efficiently taken up by plants and is suitable for phytoremediation. After uptake, in all species tested so far (tobacco, poplar, switchgrass, orchardgrass, perennial ryegrass, tall fescue, bean and wheat), with the exception of some conifer trees [64], TNT is predominantly localized in the roots ($>95\%$) (Figure 1.7) [65-70].

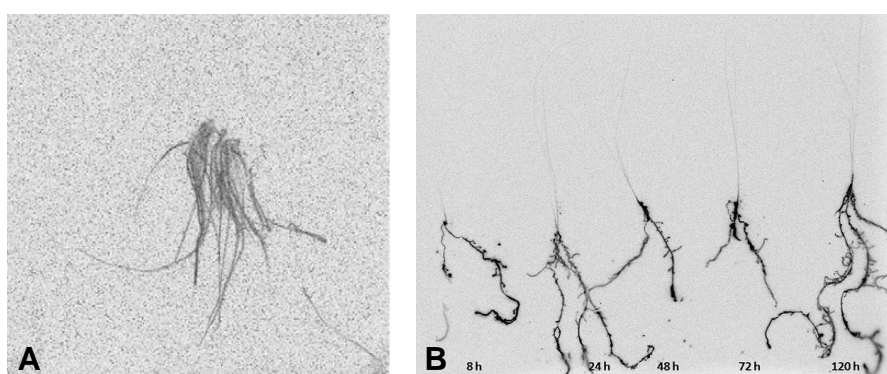


Figure 1.7: Phosphor imager autoradiograph of (A) four week-old poplar plantlets, spiked with $[\text{U-}^{14}\text{C}]\text{-TNT}$ for 48 h before leaf and root sections were excised from the woody cutting, and (B) four week-old switchgrass plants spiked with $[\text{U-}^{14}\text{C}]\text{-TNT}$, harvested (as whole plants) after 8, 24, 48, 72, and 120 h. In both species TNT remains predominantly ($>95\%$) in the roots throughout the time course. Figure from Brentner et al. [68].

1.4.1.2 Transformation

The metabolism of TNT *in planta* has been extensively reviewed [6, 56, 71]. During phase I, TNT follows the reductive pathway that is usually observed with microbial metabolism. The TNT molecule is reduced by nitroreductases to HADNT via a nitroso intermediate and subsequently to ADNT [56]. It is not clear whether HADNT or ADNT is predominantly produced, as HADNT is unstable [72, 73]. In *Arabidopsis* it has been reported that reductive transformations are catalysed by oxophytodione reductases (OPRs) without excluding the possibility of other contributing nitroreductases. OPRs are OYE homologues that are upregulated in response to TNT treatment [25] and are able to produce both HADNTs and ADNTs [27]. Over-expression of OPR1, OPR2 and OPR3 (all exhibit activity towards TNT) results in faster TNT uptake and increased production of ADNTs compared to untransformed plants [27]. Evidence suggests that oxidative transformation of TNT is also occurring. In the aquatic plant *Myriophyllum aquaticum* TNT metabolites including those arising from oxidative transformation of the methyl group and/or aromatic hydroxylation have been identified [74]. Cytochromes P450 are likely candidates for these reactions, and several are upregulated in response to TNT [75], although no enzymes catalysing oxidative transformations of TNT have yet been identified.

1.4.1.3 Conjugation

Subsequent conjugation of HADNTs and ADNTs to glucose has been well characterised and is catalysed by UDP-glucosyl transferases (UGTs), creating conjugation products that are likely to be subsequently incorporated into the plant biomass (Figure 1.8) [26]. The *Arabidopsis* UGTs are able to conjugate both HADNTs and ADNTs as part of the phase II reactions to form O- and C-glucosidic bonds. Over-expression of some of these UGTs results in increased conjugate production and enhanced resistance towards TNT as displayed by higher root growth compared to untransformed plants [26]. Conjugation to other molecules and organic acids (e.g. malonate and glutathione) may also occur. Glutathione transferases (GSTs) are also upregulated in response to TNT treatment in *Arabidopsis* and poplar [75, 76]

while commercially available equine liver GST is able to conjugate TNT producing 2-S-glutathionyl-4,6-dinitrotoluene [76].

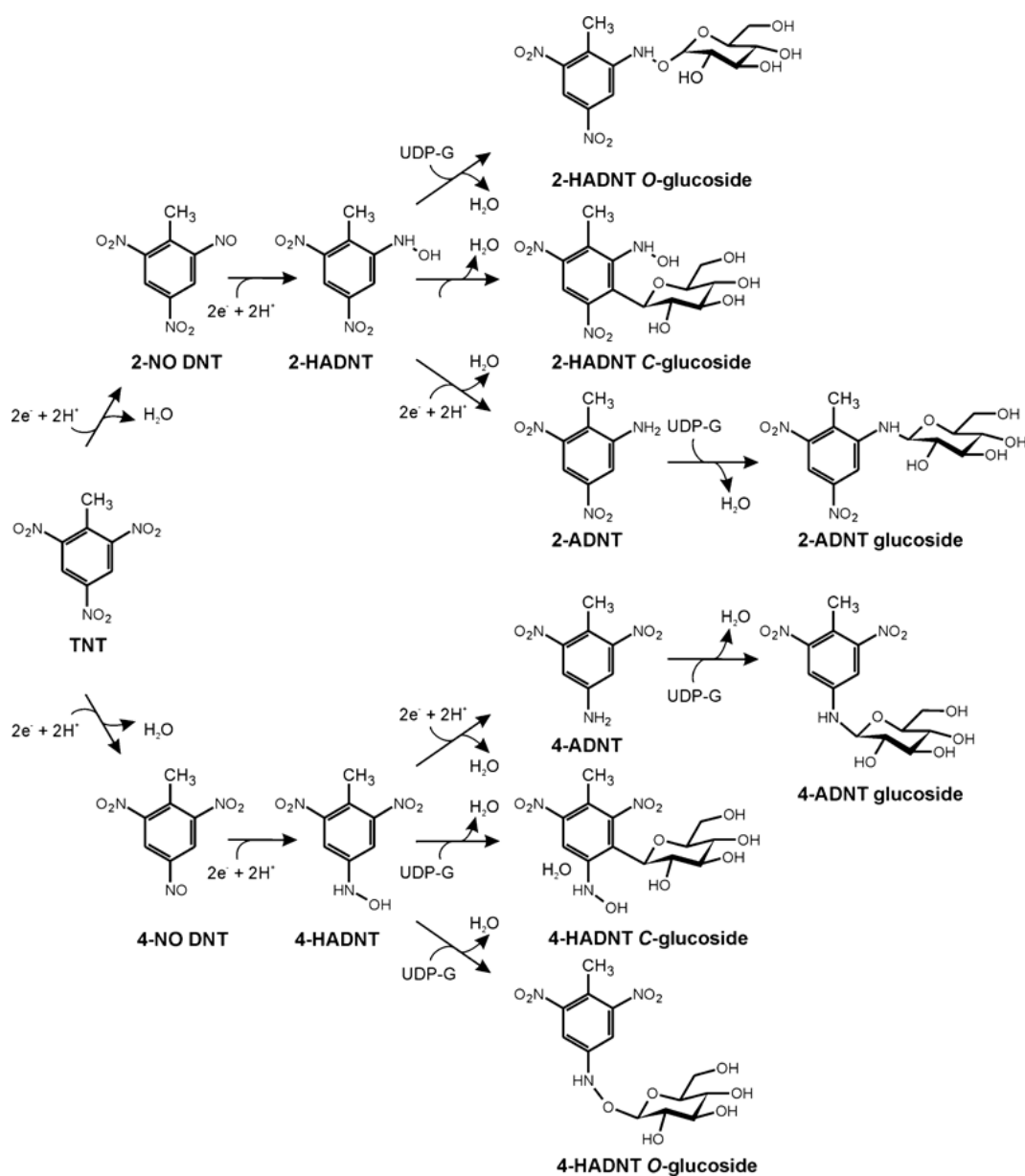


Figure 1.8: The proposed metabolic pathway for TNT in plants. Initially TNT is reduced by OPRs or other endogenous nitroreductases to HADNTs and ADNTs, which are subsequently conjugated to sugars by UGTs. The resulting conjugates are probably sequestered in the plant cell wall. Figure taken from Gandia-Herrero et al. [26].

The exact fate of the GSH-conjugates remains unknown. During compartmentation, TNT-derived conjugates are thought to be sequestered in the vacuole or the apoplast [6, 19, 58]. Various transporters that could be

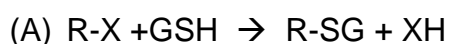
involved in the export of the conjugates from the cytosol to the vacuole have been found to be upregulated in response to TNT, including ABC transporters [21] such as the *Arabidopsis* multidrug resistance-associated proteins (*AtMRP1* & 2) [77]. In addition, cell-wall modification enzymes were upregulated in gene-expression studies from TNT-treated *Arabidopsis*, including, phenyl ammonium lyase, expansins, cinamin alcohol dehydrogenase, cinnamate 4-hydroxylase, 4-coumarate coenzyme A (coA) ligase, xyloglucan endotransglucosylase [75, 78]. This notion is supported by the identification of TNT metabolites in cell-wall fractions [24, 66, 67, 79-81].

1.5 Glutathione transferases

The glutathione transferases (GSTs) form an ancient family of catalytic and ligand binding enzymes that are encountered in all aerobic organisms, ranging from bacteria to humans [82]. From their first discovery in animals as drug metabolising enzymes in the 1960s [83], research regarding GSTs and consequently knowledge about them has increased enormously. A number of GSTs from a variety of species has been characterised, highlighting the abundance, divergence and variety of functions of its members. The first plant GST was identified in 1970 through its involvement in herbicide metabolism and ability to confer herbicide resistance to maize [83]. Plant GSTs have been found to be among the most responsive genes to both biotic and abiotic stress, exhibiting a range of catalytic and non-catalytic activities.

1.5.1 GST activities

The main activity of GSTs, although additional activities have been revealed (see section 1.5.6), is the transfer of the tripeptide glutathione (GSH; γ -Glu-Cys-Gly) to an electrophilic centre to form a polar glutathionylated conjugate. This is accomplished by either a substitution (A) or an addition (B) reaction:



This reaction reduces the hydrophobicity of the substrate and labels it for transportation. It is apparent through recent studies that GSTs are more complex than initially presumed and possess additional catalytic and non-catalytic functions [84, 85]. Eukaryotic GSTs are mainly cytosolic and in certain cases can constitute up to 2 % of the plant's soluble proteins [86]. In Arabidopsis, GSTs are relatively abundant and have been found to be associated with a number of subcellular compartments [87]. Though it is clear from an evolutionary perspective that GSTs were present long before xenobiotics and that they have an important role, their natural substrates are not yet fully characterised. It is possible that GSTs have evolved to detoxify endogenous toxic compounds. In studies, wheat and sorghum GSTs were able to detoxify 4-hydroxynonenal, a cytotoxic alkenal produced during oxidative damage [88]. In addition, certain plant GSTs were able to conjugate oxophytodienoic acid, a jasmonate synthesis intermediate, to glutathione [85, 87]. Anthocyanins, which require GST activity for their deposition in the vacuole, have also been proposed as endogenous substrates for maize (*Zea mays*) and petunia (*Petunia hybrida*) GSTs, on the premises that mutations of the respective GST genes disrupt the process and cause pigment accumulation in the cytosol [82].

1.5.2 Classification

Mammalian GSTs were the first to be thoroughly investigated and have since been categorised into eight classes: Alpha, Kappa, Mu, Pi, Theta Sigma, Zeta and Omega [82]. Plant GSTs were initially thought to be all closely linked to the mammalian Theta class of GSTs and were split into three groups based on their sequence identity [89]. As nucleotide and amino acid sequences were determined, significant differences among GSTs of the same group and between them and their mammalian counterparts were identified. As a result the classification scheme was refined and currently plant GSTs are divided into eight classes on the basis of gene organisation, nucleotide sequence similarity and conservation of specific residues in the protein. The eight classes are: Theta and Zeta which are also present in animals, the plant-

specific Phi and Tau, Lamda and dehydroascorbate reductase (DHAR) which are also plant specific, tetrachlorohydroquinone dehalogenase-like (TCHQD), and the membrane-associated proteins in eicosanoid and glutathione metabolism (MAPEG) [90]. The nomenclature is essentially an extension of the system used for mammalian GSTs. For each gene the initials of the species of origin are given in italic letters, followed by 'GST', a single letter indicating the class (F, Phi; U, Tau; Z, Zeta; T, Theta; L, Lamda) and a progressive number within that class, based on the gene's position in the genome [82, 84]. For example the 19th Tau class GST of *Arabidopsis thaliana* can be abbreviated as AtGSTU19.

1.5.3 Evolution of GSTs

Glutathione transferases share similar structure and sequence with other GSH- or cysteine-binding proteins that bear a thioredoxin-like fold, as well as with stress-related proteins from a variety of organisms [82]. This similarity led to the hypothesis that GSTs evolved originally in response to oxidative stress [91]. Based on the conservation of introns, active site residues, their function and their ubiquitous presence in organisms ranging from bacteria to higher eukaryotes, Theta and Zeta class GSTs are considered the predecessors of the GST superfamily, preceding the plant-animal separation in the evolutionary timeline [82]. According to phylogenetic analysis, plant GSTs have mainly evolved after the divergence of plants. The majority of the classes is small in size and contain one to four members. In *Arabidopsis*, the Phi and Tau class GSTs are the most populated classes with 13 and 28 members respectively (Figure 1.9) [84]. The unequal evolutionary rate of different GST classes is probably a consequence of their function and the fact that they are subjected to different selective pressures. Theta and Zeta class GSTs have roles revolving around primary cell metabolism so the need for divergence is low. On the other hand Phi and Tau class GSTs specialize in the detoxification of toxic compounds by GSH-conjugation. The adaptive advantage of this detoxification system and the capacity to cope with a wide range of toxic

compounds would be predicted to put strong selective pressure on these two classes accounting for the increased divergence [82, 92].

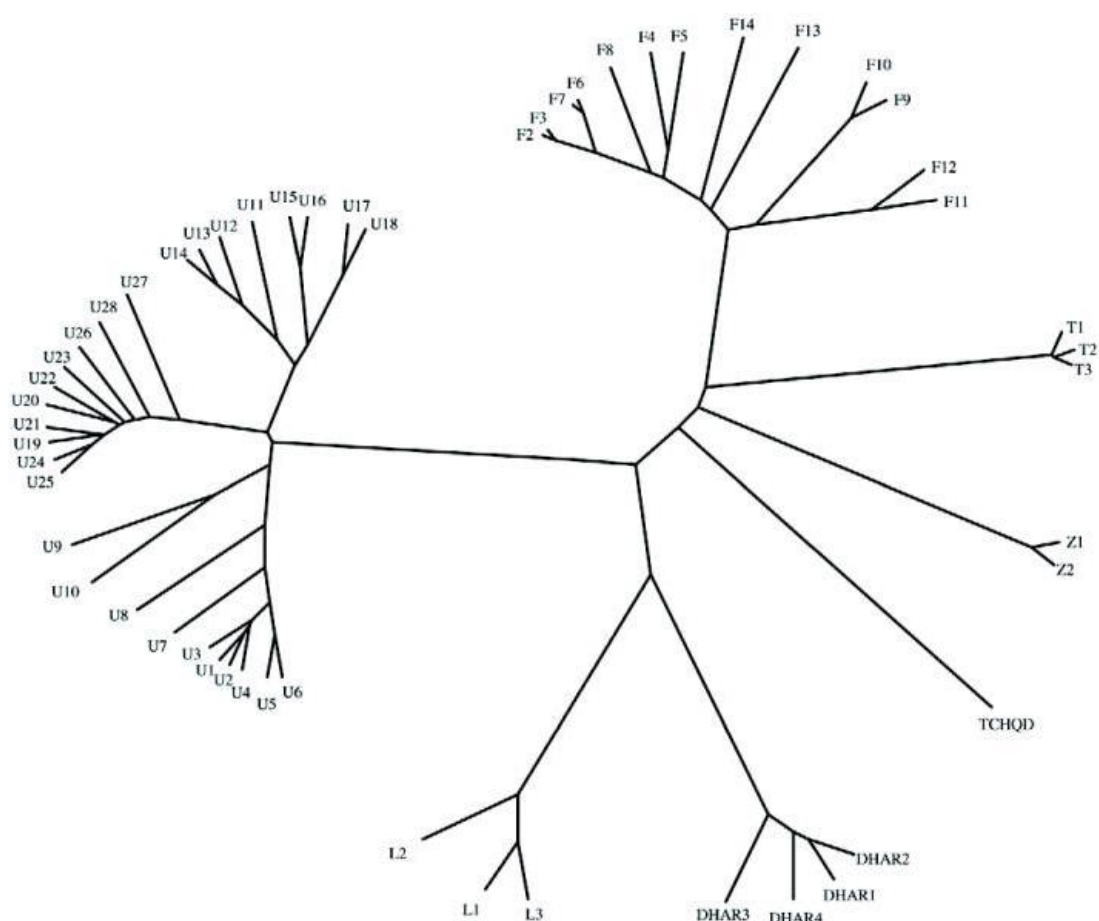


Figure 1.9: Phylogenetic tree illustrating the diversity of GSTs in Arabidopsis. Branch lengths are indicative of the evolutionary distance between protein sequences and different classes. U, Tau class; F, Phi class; Z, Zeta class; T, Theta class; L, Lambda class; DHAR, dehydroascorbate reductase class, TCHQD, tetrachlorohydroquinone dehalogenase-like class; Figure taken from Dixon and Edwards [84].

1.5.4 Gene organisation

The Arabidopsis genome contains 54 soluble GSTs and one membrane-associated GST, which are divided into eight distinct classes [84]. Of these, at least 52 are transcribed and 41 of the transcribed proteins possess GSH-dependent activities [83, 84]. The high number of Phi and Tau class GSTs along with the fact that these genes occur in clusters in the Arabidopsis genome (Figure 1.10) suggests that these classes have undergone repeated

gene duplication events [82]. In general the GST genes display a clustering tendency which is present, besides Arabidopsis, in the genome of rice and mammals indicating that this is a common organisational feature of the GST superfamily [82].

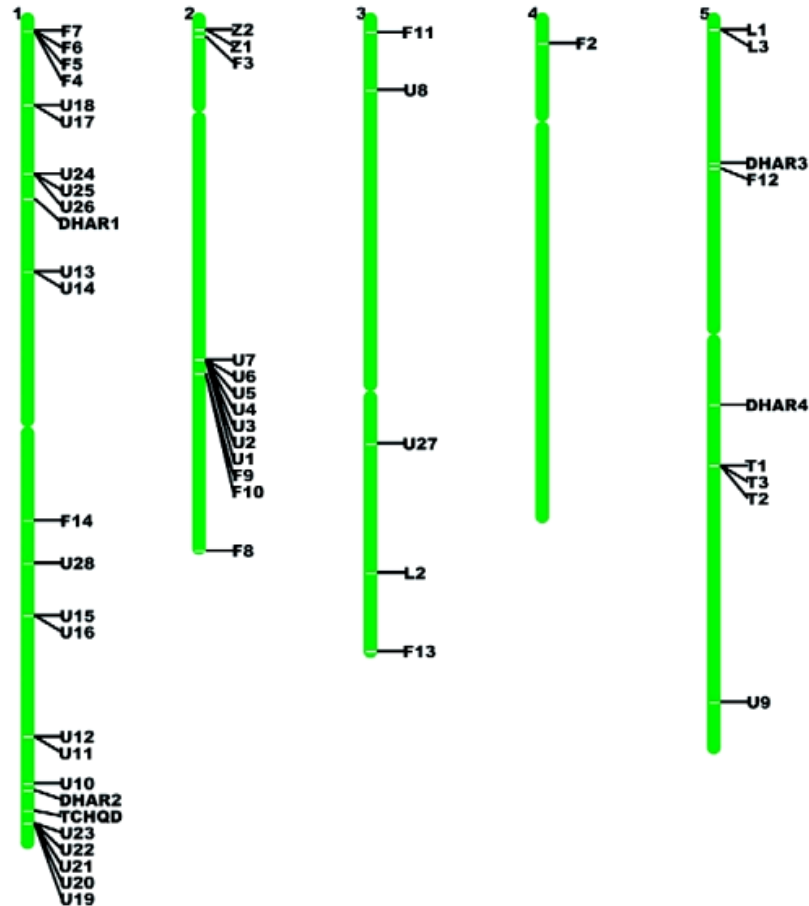


Figure 1.10: Distribution of GST genes in the Arabidopsis genome. U, Tau class; F, Phi class; T, Theta class GSTs; Z, Zeta class; L, Lambda class; DHAR, dehydroascorbate reductase class, TCHQD, tetrachlorohydroquinone dehalogenase-like class. Figure taken from Dixon & Edwards [84].

1.5.5 Structural features

To date, more than ten GSTs (two from Arabidopsis) have had their crystal structures solved. The sequence identity of GSTs of the same class averages at >40 % but can reach up to 98 % or as little as 17 % [93]. On the other hand the sequence identity of plant GSTs between different classes averages at <20 % [94]. The available GST crystal structures (the majority of which is

mammalian) have shown that GSTs share a very similar structure across species despite their significant sequence divergence.

Every soluble GST is encountered as a dimer [82], besides the lambda and DHAR class GSTs which appear to be monomeric according to gel filtration analysis [92]. Two subunits of approximately 26 kDa form a hydrophobic 50 kDa protein with an isoelectric point in the pH range of 4-5 [83]. The interactions on the subunit interfaces involve salt bridges, hydrogen bonds and hydrophobic interactions, including a lock-and-key motif that anchors the two subunits together [95]. The dimerisation is essential to the enzyme activity, even though the two subunits appear to be catalytically independent. GSTs are mainly encountered as homodimers; however, heterodimers can be formed by subunits of the same class. These heterodimers, as shown for GSTs active in herbicide metabolism, can contribute to the diversity of GSTs *in planta* [83]. The GST dimer possesses a central cleft with one catalytic site on each site. The catalytic site is composed of two components (Figure 1.11) [82, 83]. The first component is on the amino-terminal domain and is a highly conserved binding pocket that accepts only GSH (G-site) or closely related gamma-glutamyl peptides and has evolved from the thioredoxin fold. The second site is located on the carboxy-terminal domain and is much more structurally variable; it is often of hydrophobic nature, and binds the hydrophobic substrate (H-site). The H-site is adjacent to the G-site and is sufficiently open to be able to accommodate a wide range of substrates. Between the two domains there is located a short linker region of 5-10 residues that connects them [83].

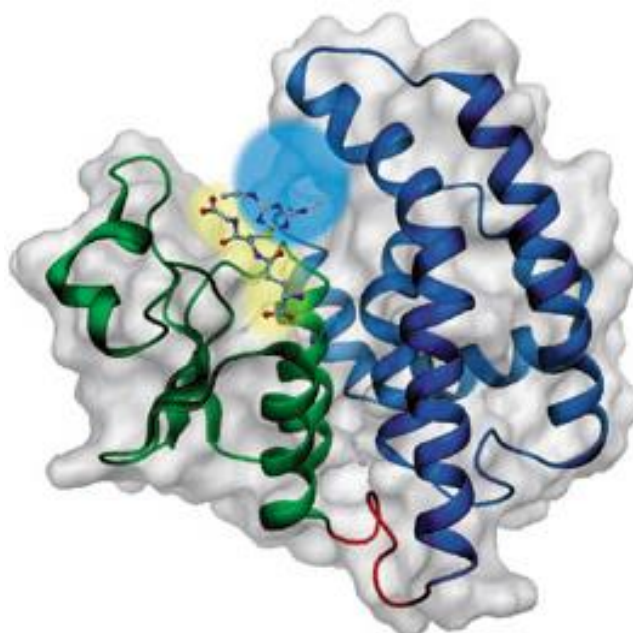


Figure 1.11: Overview of the GST structure. A typical GST subunit is represented as a ribbon-surface, with the amino-terminal domain (green), the carboxy-terminal domain (blue), the linker (red) and the protein surface (gray). The active site is composed of the H-site (yellow), where the hydrophobic substrate binds and the G-site (blue) where GSH binds. A glutathione-conjugate is given in ball-and-stick representation in the active site. Figure taken from Dixon et al. [83].

Catalysis depends on the stabilization of the reactive thiolate anion of GSH (GS^-). This sulphhydryl group has a pK_a of 9.4 [96]. In order to lower this value and assist the GS^- formation at physiological pH values, GSTs facilitate proton removal using an active residue located in the catalytic site. For mammalian GSTs that residue is tyrosine, while for plants it is a serine located near the N-terminus [97, 98]. Upon activation of the thiolate anion, GSH acts as a nucleophile and is available to react with electrophiles. The presence of a cysteine residue instead of a serine for Lamda and DHARs GSTs prevents the GS^- stabilization, and thus their conjugating activity, but allows the formation of disulphides with GSH [92].

Some GSTs carry non-active ligand-binding sites [99]. The presence of these sites could be of great significance; however, their main function remains elusive. Hypothesized functions include modulation of the GST activity by the ligand or simple transportation of the ligand by the GST [84, 100].

1.5.6 GST functions

The catalytic activity and hence function of GSTs varies a lot between classes, leading in certain cases to overlapping functions and effectively some redundancy. Besides the GSH conjugation activity the GST-associated activities include intracellular transport of molecules such as flavonoids, *cis-trans* isomerisation reactions, transient glutathione conjugation to protect reactive metabolites (e.g. oxylipins) and introduction of sulphur into secondary metabolites [84].

1.5.6.1 Zeta

The Zeta class of GSTs is highly conserved among all eukaryotes, indicative of their important function in cell metabolism. Two genes encoding Zeta class GSTs (*GST-Z1* & *GST-Z2*) have been identified in Arabidopsis, although only *GST-Z1* appears to be transcribed at a significant level [87]. This enzyme is known to catalyse the *cis-trans* isomerisation of maleylacetoacetate to fumarylacetoacetate, a step in the catabolism of tyrosine, and the GSH-dependent dehalogenation of dichloroacetic acid to glyoxylic acid [101].

1.5.6.2 DHAR

This is a plant specific GST class that catalyses the GSH-dependent reduction of dehydroascorbate to ascorbate. Members of the DHAR class are expressed as monomers and unlike most GSTs do not have the serine/tyrosine residue in their active site, but instead carry a cysteine [92]. As a consequence they are not able to stabilise the thiolate anion of GSH, but are able to form a mixed disulphide with GSH. Five DHAR-like genes have been identified in Arabidopsis, of which transcripts have been found for three (*DHAR1*, *DHAR2*, & *DHAR3*). DHAR GSTs are important to the ascorbate-glutathione cycle and thus should be localised in subcellular compartments where redox reactions are needed to maintain pools of reductants [102]. Consistent with such a role, DHARs have been reported in mitochondria, chloroplasts and peroxisomes and are hypothesised to have an important role during oxidative stress in plants [102, 103].

1.5.6.3 Lamda

Members of this class are very similar to the DHAR class. The Lamda class GSTs like the DHARs are expressed as monomers and carry a conserved cysteine residue in their active site. They cannot catalyse the typical GSH-conjugation GST reaction but can form mixed disulphides with GSH [92]. Three Lamda GSTs have been identified in Arabidopsis (*GST-L1*, *GST-L2*, & *GST-L3*). *GSTL1* and *GST-L3* are hypothesised to be cytosolic, while *GST-L2* is believed to be targeted in the chloroplast or peroxisome [87]. Relatively little is known about their natural substrates but they are presumed to act as reductases and catalyse the GSH-dependent reduction of small molecules.

1.5.6.4 Theta

This class of enzymes is conserved in both animals and plants. The plant members of the Theta class GSTs are localised mainly in the peroxisome and have high glutathione peroxidase activity (GPOX) that allows them to reduce organic hydroperoxides to their respective alcohols, using GSH [84, 85]. The GPOX reaction results in the release of water and glutathione disulfide (GSSG) [104].



Their activity and localisation suggests a role in the protection of the peroxisome from oxidative damage by detoxifying the lipid hydroperoxides that are formed in this highly oxidising compartment. Arabidopsis has three identified Theta GSTs (*GST-T1*, *GST-T2*, & *GST-T3*). Arabidopsis *GST-T3* is unusual as it can be transcribed as a fusion protein, with a C-terminal domain that resembles the Myb-like transcription factors, and is targeted in the nucleus. The significance of this fusion and localisation remains unclear. Roles in regulating gene expression under oxidative stress and detoxifying oxidatively damaged DNA have been suggested [87].

1.5.6.5 Phi

This is a large plant-specific class of enzymes, counting 13 members, with some apparent functional redundancy among them [105]. Information regarding the purpose of these enzymes in Arabidopsis is quite limited, although some of its members were among the first GSTs to be identified due to their herbicide detoxifying activity. Phi class enzymes are not strictly localized to the cytosol and can be also found in the chloroplast and plasma membrane [84, 87]. The lack of a distinct phenotype in knock-out lines suggests that individual enzymes are not essential to plant growth and primary metabolism [105]. Certain members of the family have been studied in more detail. GSTF2 is induced by oxidative stress and phyto-hormones; it is involved in flavonoid metabolism and can bind flavonoids as ligands [99]. The expression of GST-F8 is induced by hydrogen peroxide, pathogen infection and salicylic acid [106-108]. It also displays strong GSH-conjugation activity and the highest activity among all Phi class GSTs towards 1-chloro-2,4-dinitrobenzene (CDNB) [87]. GST-F12, which lacks the catalytic serine in the active site, has a role in the transportation of anthocyanins and proanthocyanidins from the cytosol to the vacuole [109, 110].

1.5.6.6 Tau

This plant specific class is the largest in Arabidopsis. As with the Phi class GSTs, relatively little is known about the individual functions of Tau-class enzymes. Some members of the Tau class have been identified as auxin-responsive genes, while almost all of them were found to selectively bind fatty acid derivatives [111]. The Arabidopsis GST-U19 is the best studied GST of this class. This enzyme displays strong GSH-conjugating activity towards CDBN and is induced by herbicide safeners [112]. GST-U20 has been found to interact with the far red insensitive protein FIN219, which is auxin-induced and is linked to phytochrome signaling [113]. GST-U24 is induced by a range of xenobiotics, including TNT [25], while GST-U25 displays high GSH-conjugating activity towards CDBN and particularly high GPOX activity towards cumene hydroperoxide [87].

1.5.6.7 TCHQD

Based on sequence homology with prokaryotic proteins, a single enzyme of this class has been identified in Arabidopsis (At1g77290). Apart from its localisation to the plasma membrane [87] and the presence of the highly conserved serine residue in the active site [84], suggesting that it is capable of the standard GST reactions, relatively little is known about this enzyme.

1.5.6.8 MAPEG

This is a non-soluble class of GSTs that is encountered in many eukaryotes and prokaryotes. In mammals these enzymes form membrane-bound trimers that possess GPOX and GSH-dependent activities. Based on sequence homology with mammalian proteins Arabidopsis has one MAPEG-like protein (At1g65820) [114].

1.6 Glutathione

The tripeptide glutathione (γ -glutamyl-cysteinyl-glycine) is the most abundant and principal form of organic sulphur in plants other than that incorporated into proteins. Some plant taxa contain GSH homologues that carry as a C-terminal residue an amino acid other than glycine. Such homologues are γ -glutamyl-cysteinyl- β -alanine [115] which is found in several legume species and γ -glutamyl-cysteinyl-serine and γ -glutamyl-cysteinyl-glutamate which have been identified in cereals [116].

The synthesis of GSH in plants is catalysed, as in other organisms, by two ATP-dependent enzymes [117]. γ -glutamyl-cysteine synthetase (γ -ECS) is encoded by *GSH1* and catalyses the ATP-dependent condensation of glutamate and cysteine to form the dipeptide γ -glutamyl-cysteine (γ -EC) the first and rate limiting step of GSH synthesis. The second step is catalysed by GSH synthetase (GSHS). This enzyme is encoded by *GSH2* and catalyses the ATP-dependent condensation of γ -glutamylcysteine and glycine to form GSH. In Arabidopsis the first step of GSH synthesis is restricted to the plastids (mainly chloroplasts), while the second step takes place in the cytosol [118].

The mechanism behind the regulation of the biosynthesis remains unknown. Many factors affect the GSH synthesis but the availability of cysteine and the activity of γ -ECS are considered to be the most important [119]. The main theories on γ -ECS regulation include regulation at the level of translation [120], and/or feedback inhibition by GSH and γ -EC [121-123].

The GSH: GSSG ratio acts as a redox buffer for the cell and subcellular compartments. Under normal conditions, most of the GSH is present in its reduced form with a small fraction present in its oxidized state (GSSG), whereas during oxidative stress high amounts of GSSG accumulate. While probably impossible to measure actual *in planta* levels, experiments indicate that under physiological conditions the GSH: GSSG ratio is maintained around 20:1 [124], by rapid recycling of the GSSG by a glutathione reductase (GR) in a NADPH-dependent reaction, with the ratio fluctuating in different tissues and subcellular compartments [125, 126]. The estimated subcellular distribution of GSH is similar among all dicotyledonous plant species [127]. Glutathione can be found in different concentrations among all cell compartments, with the vacuole and apoplast displaying significantly lower concentrations than the other compartments [117, 126]. In *Arabidopsis*, the GSH distribution differs also between tissues. In leaves, mitochondria display the highest levels of GSH, followed by the nucleus, cytosol and peroxisomes in that order [127, 128]. In the roots, mitochondria have the highest GSH abundance but the second highest concentration is found in the cytosol, followed by the nucleus and plastids [127].

Besides its roles as an antioxidant and in the detoxification of toxic electrophilic compounds, GSH is implicated in a number of important functions during plant development and metabolism that make it indispensable. The known functions include detoxification of 'heavy' metals, redox homeostasis, signaling agent, modulation of gene expression, roles in biosynthetic pathways and storage and transport of reduced sulphur (Figure 1.12) [117]. For example, GSH depletion in *Arabidopsis* mutants lacking the first enzyme of GSH synthesis causes embryo lethality [129]. Similarly, *Arabidopsis* mutants defective in GSHS display a seedling-lethal phenotype [122].

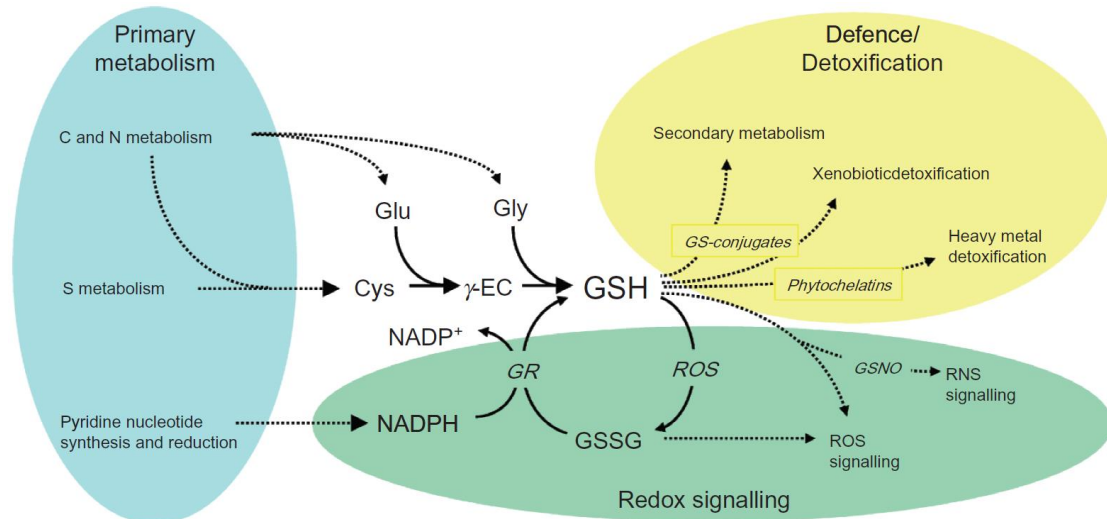


Figure 1.12: Overview of some of the most important GSH functions. GSSG, oxidized glutathione; GR, glutathione reductase; Cys, cysteine; Glu, glutamate; Gly, glycine; γ -EC, γ -glutamylcysteine; GS-conjugates, glutathione S-conjugates; ROS, reactive oxygen species. Figure from Noctor et al. [117].

Low levels of GSH have also been found to have a strong effect on root architecture, leading to significant decrease of the lateral root density relative to the wild type (WT) [130, 131]. Glutathione depletion seems to reduce root growth through inhibition of auxin transport, demonstrating a linear correlation between root growth and GSH content [132]. Glutathione is also important during pollen germination, with GSH depletion reducing germination rates by more than 65% in *Arabidopsis* [133]. The positioning of GSH between the reactive oxygen species and cellular reductants make it also ideal for signaling functions [117]. In accordance with the signaling function of GSH, depletion of GSH during oxidative stress has been found to alter the expression of genes encoding proteins in defense, cell signaling and stress tolerance in mammalian cells and in *Arabidopsis* [134, 135], demonstrating a possible signaling role for GSH in redox regulation. In addition, it has been demonstrated that GSH has an important role in the oxidant-dependent induction of jasmonic acid (JA) and salicylic acid (SA) signaling pathways [136].

1.7 Catabolism of glutathione conjugates

Once a xenobiotic compound is conjugated to GSH, its fate remains vague. Following glutathionylation, the GSH-derived conjugates are believed to be transported into the vacuole through the activity of multidrug resistance proteins (MRPs), a subfamily of the ATP-binding cassette (ABC) transporters [137, 138]. Studies on Arabidopsis root cells using monobromobimane (mBB), a compound which is conjugated to GSH and sequestered in the vacuole, revealed that there is further catabolism of these conjugates with two possible catabolic pathways. The catabolism of the GSH-conjugates can start either from the N-terminus by breaking the γ -glutamyl bond to produce Glu and Cys-Gly or the C-terminus to produce γ -EC and Gly, with no definite answer on which mechanism is prevalent.

C-terminal degradation is believed to be catalysed by phytochelatin synthase (PCS) and to result in the γ -Glu-Cys conjugate and release of Gly. Cell suspension cultures of bladder champion (*Silene vulgaris*) heterologously expressing an Arabidopsis cytosolic phytochelatin synthase, fed with mBB, were able to produce γ -Glu-Cys conjugates [139]. However, while the formation of γ -Glu-Cys conjugates proves that C-terminal degradation of GSH is possible in the Arabidopsis cytosol, studies in Arabidopsis showed that this activity is out-competed by vacuolar sequestration [140]. In addition, γ -Glu-Cys conjugates did not serve as suitable substrates to the transporters responsible for vacuolar sequestration [140]. Further characterisation of PCS proved that the enzyme is active only in the presence of sufficient concentration of 'heavy' metal ions [139, 140], weakening even more the hypothesis that degradation of GSH-conjugates starts in the cytosol from the C-terminus. These data, along with the fast and complete sequestration of the GSH-conjugates in the vacuole [140], indicate that the degradation of the conjugates is catalysed by a vacuolar enzyme rather than PCS in the cytosol. A barley vacuolar carboxypeptidase that cleaves alachlor GSH-conjugates C-terminally has been reported [141]. However, such an activity has not been identified in the vacuole of Arabidopsis, indicating that there are species differences.

The N-terminal degradation removes Glu to produce the Cys-Gly conjugate. The enzyme responsible for breaking the γ -glutamyl bond between Glu and Cys in GSH is γ -glutamyl transpeptidase (GGT). In Arabidopsis there are four genes homologous to mammalian *GGT*. They are named *GGT1* (At4g39640), *GGT2* (At4g39650), *GGT3* (At4g29210), *GGT4* (At1g69820) [142, 143]. *GGT1* and *GGT2* encode apoplastic proteins associated with the plasma membrane and/or cell wall, while *GGT3* encodes a protein associated with the endoplasmic system and targeted in the vacuole [143-145]. *GGT4* is a short gene fragment that probably derives from the C-terminal coding region of *GGT1* or *GGT2*, it is considered a pseudogene and does not produce any protein [144]. *GGT1*, 2 and 3 activities added together for each organ, account for the total GGT activities in wild-type plants [143]. In Arabidopsis root vacuoles the transpeptidation is catalysed by *GGT3*. Studies on *ggt3* mutants demonstrated that in the roots *GGT3* is responsible for the majority of the GSH-mBB-derived conjugates, while C-terminal degradation is insignificant. Wild-type plants fed with mBB were able to accumulate Cys-mBB with Cys-Gly-mBB as the confirmed intermediate, while disruption of *GGT3* activity in roots completely blocked GSH-mBB metabolism [143]. These results agree with the data published by a different group working on the same enzyme, suggesting that in Arabidopsis the degradation of GSH-conjugates strictly occurs by the ordered removal of Glu first and Gly second to yield the Cys conjugate [145]. The carboxypeptidase responsible for the hydrolysis of the Cys-Gly conjugates to Cys conjugates has not been identified. So far it remains unknown whether there is an advantage from salvaging Glu and Gly. By removing Glu from the GSH conjugates, the resulting Cys-Gly/Cys conjugates could be prevented from reverse transport back to the cytosol [143]. It is also possible that Cys conjugates are not the end-products and that this is an additional step before further metabolism occurs. Malonylcysteine derivatives are among the most abundant end-products in plants, while S-methyl derivatives have also been reported. The safener fenclorim was found to be glutathionylated and rapidly processed to its corresponding Cys conjugate in Arabidopsis. Downstream metabolism derivatives included among other, S-(4-chloro-2-phenylpyrimidyl)-6-N-malonylcysteine and 4-

chloro-6-(methylthio)-phenylpyrimidine [146]. These data together suggest that the sequential hydrolysis of GSH-conjugates in Arabidopsis is identical to that of mammals and starts with the removal of the γ -glutamyl residue [147].

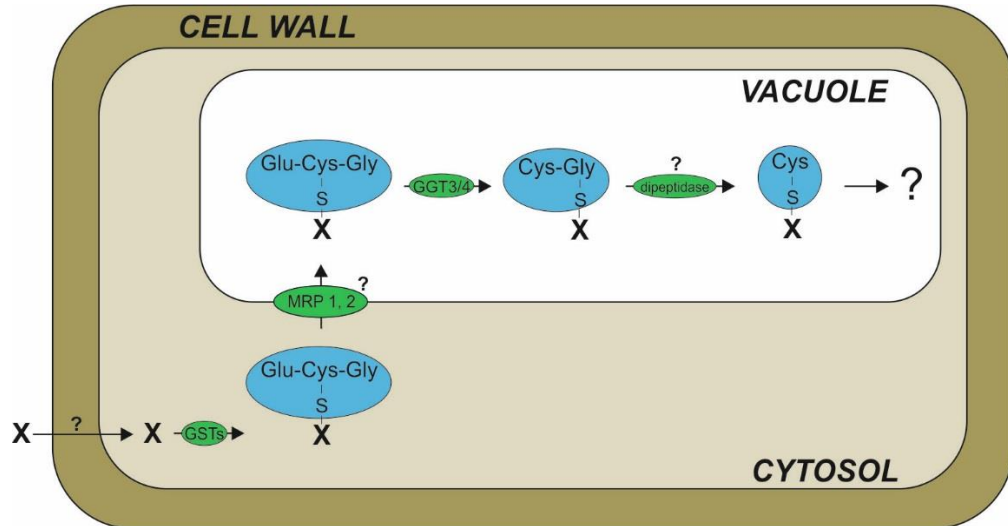


Figure 1.13: Schematic representation demonstrating the most likely catabolic pathway for the GSH-conjugates in Arabidopsis roots: X, xenobiotic compound; GSTs, glutathione transferases; MRP1,2, multidrug resistance-associated protein; GGT, γ -glutamyl transpeptidase. Question marks indicate unknown steps or steps where the protein catalysing it is unknown or hypothesized.

1.8 Current remediation strategies

The containment and clean-up of environmental pollutants is increasingly attracting attention and has become a legal requirement in many developed countries. The most efficient strategies currently employed for the remediation of TNT-contaminated soil can be summarised to the following:

1.8.1 Incineration

Incineration has been long considered the only viable strategy for the complete removal of TNT and its metabolites. It requires excavation and transportation of the soil to an incinerator, posing high costs and safety hazards. Early estimations (1992) report that incineration costs range from 800 to 1000 US dollars per ton depending on the size of the operation [148].

Incineration also has strong environmental repercussions, since it releases greenhouse emissions, such as CO₂ and NO_x, while the remaining ashes need to be treated as hazardous waste [4]. In addition, it destroys completely the physical structure of the soil, leaving it with little or no application for agriculture and cultivation.

1.8.2 Composting

In composting the soil is mixed (often on site) with degradable organic material (e.g. straw or woodchips), to stimulate the growth of microbes present that are able to transform TNT, and bulking material to increase aeration and moisture of the mixture [2, 149]. Composting can be effectively split into two categories, static pile and windrow composting, which are both performed off site. Static pile requires a costly, extensive internal ventilation system, while windrow requires regular turning and mixing of the soil. The best conditions for composting are those of windrow composting where alternate anaerobic and aerobic phases are used. In the first step (anaerobic) TNT is rapidly reduced and condensation of the amine derivatives to the soil humic fraction takes place. During the aerobic phase the products of the anaerobic treatment are further metabolized to non-toxic unknown products. Composting is a costly process. The costs for windrow composting range from 200 to 800 US dollars per ton [2]. In addition, it requires a large area.

1.8.3 Bioslurry

Formation of bioslurry is performed with the incubation of soil with water and nutrients, under optimal environmental conditions in a bioreactor [2, 150]. The results are similar to those of composting, since the aim in both cases is to stimulate microbial growth that can remediate the soil. Bioslurry is faster than composting but is more expensive since additional costs, such as soil excavation, sieving, transportation, bioreactor and maintenance need to be taken into account.

All of the methods listed above (incineration, composting and bioslurry) become prohibitively expensive when the scale of TNT contamination is taken into account. Phytoremediation may be the only cost-effective method.

1.8.4 Phytoremediation

Due to the high costs and limitations of the previously mentioned remediation strategies phytoremediation is currently being evaluated as an alternative and environmentally friendly solution. Phytoremediation is the use of plants to remove environmental pollution [63]. Phytoremediation utilises the innate ability of plants to absorb compounds from their surrounding environment. Along with the necessary nutrients they absorb natural and xenobiotic compounds for which they have developed specific detoxification mechanisms. Phytoremediation is an efficient clean-up technology. First developed for the remediation of heavy metals, phytoremediation has since proven to be an efficient remediation system for organic compounds such as polyaromatic hydrocarbons, chlorinated solvents and explosives [63, 71, 151]. Phytoremediation offers a range of advantages compared to the previously listed technologies (sections 1.8.1-1.8.3):

- Plants are a robust renewable source and are solar powered.
- They can generate large amounts of biomass compared to microbes.
- They can generate a dense and extensive root system, which promotes increased microbial activity in the rhizosphere.
- The plants can be easily monitored.
- Phytoremediation is performed *in situ*, therefore minimising the hazards associated with the transportation of toxic waste.
- In terms of cost, phytoremediation is significantly lower than both *in situ* and *ex situ* traditional processes, due to low installation and maintenance costs. On average, phytoremediation is ten-fold cheaper than engineering-based remediation strategies [63].
- It is a non-invasive and environmentally friendly solution.
- It is aesthetically pleasing with high public acceptance.

However, phytoremediation does have limitations as well [152]:

- Phytoremediation is limited by the root length of the plant to the surface area of the soil.
- It is a slow process, which can take up to years to significantly reduce contamination of a site.
- Incomplete metabolism of the pollutant can result in increased toxicity.
- The survival of the plant depends on the condition of the soil and the toxicity of the contaminant, with many plant species not able to tolerate the levels of contamination found in the field.
- It requires that the pollutant is bioavailable to facilitate uptake by the plant.
- Bio-accumulation of contaminants (e.g. heavy metals) in plants can pass into the food chain through consumption by animals.

Phytoremediation can be achieved through phytostimulation, phytoextraction, phytostabilisation, phytodegradation and phytovolatilisation (Figure 1.14) [63, 152, 153]. Optimal phytoremediation-specific species are considered to be fast growing, produce high biomass, high xenobiotic uptake and extensive root system.

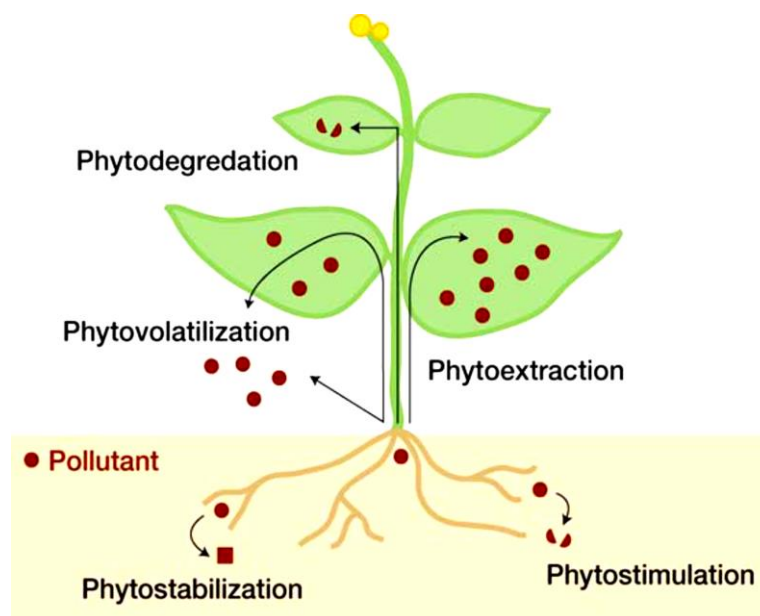


Figure 1.14: Main types of phytoremediation. The pollutant (represented as red circles) can be stabilised or degraded in the rhizosphere (yellow marked area), sequestered or degraded within the plant tissue, or in some cases be volatilised. Figure taken from Pilon-Smits [63].

Phytostimulation

This process relies on the release of exudates (e.g. amino acids, enzymes, sugars etc.) from the plant roots that will enhance microbial activity in the rhizosphere. The stimulated microorganisms are responsible for the degradation or transformation of the contaminant. It is usual that pollutants remediated this way are highly hydrophobic and thus unable to be taken up effectively by the plant. Phytostimulation has been successful in the remediation of chlorinated solvents and polyaromatic hydrocarbons (PAHs) [152].

Phytoextraction

Phytoextraction (otherwise known as phytoaccumulation) uses plants or algae to extract compounds from the surrounding environment (soil, sediments and water). The plants absorb the contaminants through their root system and accumulate them in harvestable plant biomass. Harvesting the plant tissue and allowing it to re-grow creates a continuing extraction system. The harvested plant material can be disposed (e.g. incineration), used for non-food purposes (e.g. cardboard) or in the case of valuable metals for recovery and recycle of the element, a process known as phytomining [154]. Depending on the level of contamination the growth/harvest cycle might have to be repeated several times to achieve significant removal of the contaminant. Plants that take up higher amounts of contaminants than most other species are known as hyperaccumulators. Phytoextraction has been used more for the remediation of 'heavy' metals than organic compounds. Phytoextraction has been successful in the remediation of arsenic, cadmium, zinc, lead, mercury, selenium and organic pollutants such as polychlorinated biphenyls (PCBs), using a variety of plant species which include among other, sunflower (*Helianthus annuus*), willow (*Salix sp.*), poplar (*Populus sp.*) and Indian mustard (*Brassica juncea*) [152].

Phytostabilisation

In phytostabilisation, contrary to phytoextraction, the aim is to sequester and immobilise the pollutants in the soil surrounding the roots and not to accumulate them in the plant tissue. The plant stabilises pollutants in the soil

by preventing erosion, leaching and runoff or by converting the pollutants into a less bioavailable form, thus reducing exposure of the pollutant to animals and humans. A combination of trees and grasses can be used for phytostabilisation. Trees such as poplar can prevent downward leaching due to their fast-transpiration and grasses are particularly suited to preventing erosion and runoff through extensive and dense root systems [63].

Phytodegradation

This approach harnesses the metabolic pathways of the plants to break down the pollutant within the plant tissue. Phytodegradation works well for organic compounds that are mobile within plants, such as herbicides and explosives [6, 63]. Degradation is usually the result of plant enzymatic activity, but in certain cases it can be the result of the activity of endophytic bacteria [155]. Due to their recalcitrant nature some compounds cannot achieve full mineralisation, and hence the term phytotransformation is used to better reflect their fate. The plant detoxification can be divided into three distinct phases (see section 1.4) that eventually result in the sequestration of the compound.

Phytovolatilisation

This is probably the most controversial of all the phytoremediation methods, as it utilises the plant's transpiration stream to release intact, or metabolically modified contaminants as gases into the atmosphere [152]. Phytovolatilisation has been successfully used for the removal of selenium and mercury [152, 156]. Arabidopsis has also been found to take up mercury in the form Hg (II), reduce it to Hg (0) and subsequently release it as gas [157, 158].

In order to further increase the remediation potential of plants, it is essential to understand the biological processes underpinning it. So far, despite the great promise, detoxification of organic pollutants using plants remains relatively slow, limited either by the respective enzymatic rates or by the accumulation of toxic compounds within the plant tissues.

1.9 Phytoremediation of TNT

Since TNT cannot be fully mineralised or released by the plant in the form of gas, phytotransformation is considered the best phytoremediation approach to tackle TNT pollution. Although it would still not fully mineralise TNT, phytotransformation allows for the transformation of TNT into less toxic products that can be sequestered within the plant tissue and away from soil. Most plants display moderate accumulation and detoxification of TNT that is not enough to remediate a contaminated site. Several studies have attempted to increase the phytotransformation of TNT by means of genetic engineering. Literature suggests that phase I reactions are the limiting step in the TNT detoxification pathway [69]. In accordance with this, plants recombinantly expressing bacterial nitroreductases with activity towards TNT demonstrate a strikingly enhanced ability to tolerate, take up and detoxify TNT [12, 159]. Transgenic tobacco plants expressing the bacterial PETNr from *E. cloacae* were able to tolerate TNT concentrations that inhibited the growth of untransformed tobacco plants [160]. Similarly transgenic expression of the bacterial reductases *nfsI* (*E. Cloacae*) and *nfsA* (*E. coli*) in tobacco and Arabidopsis respectively conferred increased TNT tolerance and uptake when compared to the untransformed plants [22, 69, 161]. Further experiments with a transgenic hybrid aspen (*Populus tremula* x *Populus tremuloides*) expressing the bacterial nitroreductase from *Pseudomonas putida*, PnrA, showed that the transgenic aspen was able to tolerate better the toxicity of TNT and remove higher amounts of TNT from contaminated water than untransformed plants [65]. Nonetheless, increased TNT tolerance and detoxification can also result from the over-expression of endogenous enzymes as proven by the over-expression of OPRs in Arabidopsis [27].

Besides phase I enzymes, attention has been also given to enzymes of the remaining phases of the detoxification process. Arabidopsis plants over-expressing the endogenous UGTs also exhibited increased transformation of TNT and an enhanced ability to tolerate the explosive [26], proving that identifying enzymes involved in the downstream conjugation steps could assist further in increasing the phytodetoxification of TNT. So far no effective

TNT degradation pathway that can lead to ring cleavage and subsequent mineralisation of TNT has been identified.

1.10 Aims of the current study

The present study builds on the work previously conducted in the Bruce laboratory. Dr Helen Sparrow and Dr Vanda Gunning have already shown in the past that two *Arabidopsis* GSTs upregulated in response to TNT treatment are able to conjugate TNT *in vitro* and produce three distinct conjugates (see section 3.1). This project aims to further explore the role and mechanisms of activity of glutathione transferases in detoxifying the pollutant TNT. In addition, genetic engineering approaches are explored to develop plant systems with an enhanced ability to remediate TNT contamination from explosives contaminated soil.

Chapter 2: General Materials and Methods

2.1 Consumables and reagents

Consumables and reagents were obtained from the following suppliers, unless stated otherwise in the text: Clontech Laboratories, Inc. (USA), Duchefa Biochemie (Netherlands), Expedeon (Swavesey, UK), Fisher Scientific Ltd (Loughborough, UK), Formedium (Hunstanton, UK), GE Healthcare (Little Chalfont, UK), Invitrogen (Paisley, UK), New England Biolabs Ltd (NEB) (Herts, UK), Promega (Southampton, UK), Qiagen (West Sussex, UK), Sigma-Aldrich Company Ltd. (Poole, UK), ThermoFisher Scientific (UK).

Primers were synthesised by IDT (Interleuvenlaan, Belgium) or Sigma-Aldrich and protein gel markers were obtained by NEB and Promega. In addition, DNA polymerases and restriction enzymes were purchased from NEB, Promega and Invitrogen. TNT was kindly donated by the Defence Science and Technology Laboratory (DSTL, Fort Halstead, UK) while the TNT derivatives, HADNT and ADNT, were obtained from Supelco Analytical (Bellefonte, US). Water was purified with the Elga Purelab Ultra water polisher (Elga Labwater, High Wycombe, UK).

2.2 Plasmids, bacteria and growth conditions

2.2.1 Plasmids

The plasmids used for gene cloning and enzyme expression are listed in table 2.1:

Table 2.1: Plasmids used for gene cloning and enzyme expression

Plasmid	Antibiotic resistance	Antibiotic concentration (µg/ml)	Source
pET-YSBLIC3C	Kanamycin	50	Bruce group stocks
pCR-Blunt II-TOPO	Kanamycin	50	Invitrogen (Paisley, UK)
pART7 ^[162]	Carbenicillin	50	Bruce group stocks
pART27 ^[162]	Spectinomycin	50	Bruce group stocks

2.2.2 Bacterial strains

The bacterial strains used in the present work are listed in table 2.2:

Table 2.2: Bacterial strains used for gene cloning and enzyme expression

Bacteria	Strain	Known resistance	Purpose	Source
<i>Escherichia coli</i>	DH5a	None	Cloning, plasmid prep and long term storage as glycerol stock (-80°C)	Bruce group stocks
<i>Escherichia coli</i>	BL21 (DE3)	None	Expression host	Bruce group stocks
<i>Agrobacterium tumefaciens</i>	GV3101	Gentamycin (50 µl/ml)	Transformation of Arabidopsis	Bruce group stocks

2.2.3 Preparation of high competency *Escherichia coli* cells

Cells of *E. coli* (DH5a or BL21 strain) were streaked on antibiotic-free LA plates (LB containing 15 g/L agar) and incubated O/N at 37 °C. Single colonies were picked up and inoculated in 5 ml LB medium at 37 °C with 200 rpm shaking for 2h. The cultures were then transferred in 2L flasks containing 250 ml super optimal broth (SOB) (Table 2.3) and were incubated at 18 °C with 180 rpm shaking until optical density (OD) reached 0.4-0.6 (~48h). Cells

were then transferred to suitable centrifuge bottles and were pelleted by centrifugation at 3000 rpm, 4 °C for 15 min in a Sorvall centrifuge. Pellets were re-suspended in 2/5 of the original volume (100 ml) TfbI solution (Table 2.4) and left on ice for 5 min. Cells were pelleted as before and were re-suspended in 1/25 of the original volume (10 ml) TfbII solution (Table 2.5) and left on ice for 5 min. Cells were split into 50 µl aliquots, snap frozen in liquid nitrogen and stored at -80 °C.

Table 2.3: The components of SOB (1L)

Tryptone	20 g
Yeast extract	5 g
NaCl	0.5 g
KCl	0.186 g
H ₂ O	1000 ml
2 M MgCl ₂ •6H ₂ O	4 ml
2 M MgSO ₄ •7H ₂ O	4 ml

Note: MgCl₂ & MgSO₄ solutions were filter-sterilised and added to the remaining solution once autoclaved. pH was adjusted to 7.6 with NaOH before autoclaving.

Table 2.4: The components of TfbI solution (100 ml)

K Acetate (30mM)	0.3 g
RbCl ₂ (100 mM)	1.2 g
CaCl ₂ •2H ₂ O (10 mM)	0.150 g
MnCl ₂ •4H ₂ O (50 mM)	0.99 g
H ₂ O	85 ml
Glycerol to 15%	15 ml

Note: pH to 5.8 with 10% acetic acid, sterilise by filtration.

Table 2.5: The components of TfbII solution (10 ml)

MOPS (10 mM)	0.02 g
CaCl ₂ •2H ₂ O (75 mM)	0.11 g
RbCl ₂ (10 mM)	0.012 g

H ₂ O	8.5 ml
Glycerol to 15%	1.5 ml

Note: pH to 6.5 with KOH, sterilise by filtration.

2.2.4 Transformation of chemically competent *Escherichia coli*

Aliquots of 50 µl of *E. coli* cells were allowed to thaw on ice for a few minutes. Subsequently, 1 µl of plasmid DNA was added to the cells and the cells were gently mixed. The mixture was incubated on ice for 30 min, heat shocked for 90 sec in a 42 °C water bath and returned on ice for an additional 2 min. Two hundred microliters of sterile LB were added to the cells in order to enhance recovery and cells were then incubated at 37 °C with 180 rpm shaking for 1 hr. After the incubation, 50 µl of the transformed cells were spread onto LA plates with the corresponding antibiotic (see Table 2.1). Plates were incubated at 37 °C overnight until colonies became visible.

2.2.5 Transformation of electro-competent *Agrobacterium tumefaciens*

Aliquots of 80 µl cells of *A. tumefaciens* were allowed to thaw on ice for a few minutes. Subsequently, 1 µl of undiluted plasmid DNA from the miniprep was added and the cells were gently mixed. The mixture was incubated on ice for 2 min and was then transferred to a 2 mm Electroporation Cuvette (Flowgen Bioscience Ltd, UK). A brief gene pulse was applied (~1 sec) using 2.5 kV, 400 Ω resistance and 25 µF capacitance on a BioRad MicroPulser. Eight hundred microliters of LB were added directly in the cuvette to assist the rapid recovery of the cells. The cells were then transferred to a 1.5 ml Eppendorf tube and were incubated at 30 °C with 180 rpm shaking for 3 hours. After the incubation 30 µl of the transformed cells were spread onto LA plates containing gentamycin (for *A. tumefaciens* selection) and a secondary antibiotic for plasmid selection (see Table 2.1). Plates were incubated at 30 °C for 2-3 days until colonies became visible.

2.2.6 Bacterial growth conditions

2.2.6.1 Growth conditions for liquid media

E. coli cultures were incubated in sterile LB media, with the appropriate antibiotics for plasmid selection (see Table 2.1), at 37 °C and 180 rpm shaking. *A. tumefaciens* cultures were incubated in LB with the appropriate antibiotics for selection of both strain and plasmid (see Table 2.1 & Table 2.2) at 30 °C and 180 rpm shaking.

2.2.6.2 Growth conditions for solid media

E. coli cultures were spread on sterile LA plates, with the appropriate antibiotics for plasmid selection (see Table 2.1), and incubated O/N at 37 °C before isolating single colonies. *A. tumefaciens* cultures were spread on sterile LA plates, with the appropriate antibiotics for selection of both strain and plasmid (see Table 2.1 & Table 2.2), at 30 °C for 3 days before isolating individual colonies.

2.3 Molecular biology techniques

2.3.1 Agarose gel electrophoresis

DNA fragments were separated according to their size on an agarose gel prepared with 1.2% (w/v) agarose and 0.6 µM ethidium bromide (Sigma-Aldrich Poole, UK) in 1x Tris-acetate-EDTA buffer (40 mM Tris-HCl, 18 mM glacial acetic acid and 1mM ethylenediaminetetraacetic acid (EDTA)). The DNA samples were diluted with a 5:1 ratio in loading dye (0.15% w/v bromophenol blue, 0.5% w/v sodium dodecyl sulphate (SDS), 0.15 mM EDTA and 60% w/v glycerol). Samples were run and separated at 120 V alongside a 1kb DNA ladder (Promega Southampton, UK), which was used as a molecular weight marker. Visualisation of ethidium bromide stained DNA was achieved through exposure to UV light.

2.3.2 Plasmid preparation

Extraction and purification of plasmid DNA was carried out using the “QIAprep Spin Miniprep kit” (Qiagen West Sussex, UK), according to the manufacturer’s instructions, for all bacterial strains used. DNA concentration and purity were determined on a Nanodrop Spectrophotometer (ThermoFisher Scientific, UK) by measuring the absorbance at 260 nm and the value A_{280}/A_{260} .

2.3.3 DNA fragment purification

For the purification of DNA fragments the “Wizard[®] SV Gel and PCR Clean-Up System” (Promega) was used according to the manufacturer’s instructions. For the purification of fragments generated by restriction digestion the samples were run on a 1.2% agarose gel (see section 2.3.1) and the bands of interest were excised from the gel prior to the purification using the PCR Clean-Up System.

2.3.4 Nucleotide sequencing and analysis

Sequencing was performed by GATC Biotech (London, UK). The DNA samples were diluted down to 80-100 ng/μl and 20-80 ng/μl for purified plasmid and PCR product respectively. The final sequencing sample consisted of 5 μl of the diluted DNA (plasmid or PCR product) mixed with 5 μl of 5 μM primer. For the sequencing of the pCR-Blunt II-TOPO vector M13 forward and reverse primers were used. For pET-YSBLIC3C T7 and T7term primers were used, while for the sequencing of pART7 and pART27 vectors, carrying the *DmGSTE6* gene, the gene-specific dGST-F114 and dGST-R613 primers were used. All primers are given in Table 2.6. Analysis of the sequencing results was performed with the following software packages: Sequence Scanner V1.0 (Applied Biosystems, U.S.A) and ClustalX V2.1 (online tool).

Table 2.6: Sequencing primers

Primer name	Sequence (5' -> 3')
M13 forward	GTAAAACGACGGCCAGTG
M13 reverse	GGAAACAGCTATGACCATG
T7	TTATACGACTCACTATAGGG
T7term	TATGCTAGTTATTGCTCAGCGGT
dGST-F114	ACCTATGAGTATGTTAACGTGGATATTGT
dGST-R613	TGTTCCAGCTTCTTGATCCAC

2.3.5 Polymerase chain reaction (PCR)

All primers were diluted in sterile dH₂O to create 100 µM stock solutions. These stocks were further diluted to create 10 µM working solutions. PCR amplifications were performed in a PTC-200 Thermal Cycler (MJ Research, U.S.A) at 50 µl volume and conditions suitable for the respective DNA polymerase according to the manufacturer. Phusion high-fidelity polymerase (NEB Herts, UK) was used during amplification for gene cloning or site-directed mutagenesis purposes. Taq DNA polymerase (NEB Herts, UK) was used for diagnostic purposes such as colony screening or confirmation of the presence of a gene in a purified vector. Details regarding the individual PCR conditions can be found in the relevant sections.

2.3.6 Restriction endonuclease digestion of DNA

Restriction endonuclease digestion was routinely performed at 37 °C for a total of 1-2 h, depending on the sample, with 1 U of restriction enzyme per µg of DNA and buffer at 10% of the reaction volume. Where double digestions were required an appropriate buffer compatible with both endonucleases was employed according to the manufacturer's instructions.

2.3.7 Dephosphorylation of a linearised vector

Prior to mixing with the insert/gene of interest for ligation the linearised vector was dephosphorylated with alkaline phosphatase FastAP (Fermentas). The final volume of the reaction was 350 µl, containing 2 µg of linearised vector,

20 U Fast AP and 10x FastAP buffer. The reaction was performed in a PTC-200 Thermal Cycler (MJ Research, U.S.A) at 37 °C for 15 min followed by an inactivation step at 65 °C for 5 min. The linearised-dephosphorylated vector was finally purified using the “Wizard[®] SV Gel and PCR Clean-Up System” (Promega) according to the manufacturer’s instructions.

2.3.8 DNA ligation

DNA ligation was performed with 100 ng of linearised-dephosphorylated vector and a ratio of vector to insert concentration ranging from 3:1 to 1:3. Ligations were performed with T4 DNA ligase (NEB) at a final reaction volume of 20 µl according to the manufacturer’s instructions. The reactions were incubated at room temperature for a minimum of 1h.

2.3.9 Blue/white colony screening

This technique was used to confirm successful cloning of a gene in the pART27 vector. Cells were transformed with the pART27 vector (see section 2.2.4) and were spread on LA plates containing spectinomycin and 80 µg/ml 5-bromo-4-chloro-3-indolylbeta-D-galactopyranoside (X-gal) (Promega).

2.4 Protein expression and purification

2.4.1 Protein expression

The pET-YSBLIC3C vector was used for the expression of all the proteins. Autotinduction (AI) medium (Table 2.7-2.8) was used for induction of expression. The vector containing the gene of interest was transformed (see section 2.2.4) into *E. coli* BL21 cells (DE3) and grown O/N at 37°C until colonies became visible. Starter cultures were set up in LB with 50 µg/ml kanamycin from single colonies and were incubated O/N at 37 °C with 180 rpm shaking. Starter cultures were then added to the AI medium in the ratio of 1ml starter culture per 1 L of AI and grown at 37 °C with 180 rpm shaking until

Chapter 2: General Materials and Methods

optical density (OD) of the solution reached 0.8-1.0 at 600 nm (~3-4 h). Then the cultures were cooled down and incubated at 20 °C with 180 rpm shaking for approximately 60 h (normally left over the weekend). After that period cultures were transferred into centrifuge bottles and cells were pelleted by centrifugation at 5000 rpm for 10 min in a Sorvall centrifuge.

Table 2.7: The components of AI medium (1L)

ZY solution (10 g/l tryptone, 5 g/l yeast extract)	928 ml
MgSO ₄ (1 M)	1 ml
1000 × metals solution	1 ml
50 × 5052 solution	20 ml
20 × NPS solution	50 ml

Table 2.8: Composition of stock solutions for AI medium

1000 x metals (100 ml)	0.1 M FeCl ₃ •6H ₂ O (in 0.1 M HCl)	50 ml
	1 M CaCl ₂	2 ml
	1 M MnCl ₂ •4H ₂ O	1 ml
	1 M ZnSO ₄ •7H ₂ O	1 ml
	0.2 M CoCl ₂ •6H ₂ O	1 ml
	0.1 M CuCl ₂ •2H ₂ O	2 ml
	0.2 M NiCl ₂ •6H ₂ O	1 ml
	0.1 M Na ₂ MoO ₄ •2H ₂ O	2 ml
	0.1 M Na ₂ SeO ₃ •5H ₂ O	2 ml
	0.1 M H ₃ BO ₃	2 ml
	H ₂ O	36 ml
50 x 5052 solution (100 ml)	Glycerol	25 g
	Glucose	2.5 g
	α-Lactose	10 g
	H ₂ O	73 ml
20 x NPS solution (100 ml)	Na ₂ SO ₄	3.6 g
	NH ₄ Cl	13.4 g
	KH ₂ PO ₄	17.0 g
	Na ₂ HPO ₄	17.7 g
	H ₂ O	90 ml

2.4.2 Cell lysis by sonication

Cell pellets were re-suspended to 1g/ml phosphate buffer saline pH 7.4 (PBS) (Table 2.9) plus 200 μ M phenylmethylsulfonyl fluoride (PMSF). Sonication was carried out on ice with an S-4000 Sonicator (Misonix) at 70% amplitude for a total of 4 min, with cycles of 3 s interrupted by 7 s cooling at 0 °C. Cell debris was removed through centrifugation at 17,500 x g, 4 °C for 30 min with a SS34 rotor in a Sorvall centrifuge. Supernatants were clarified through 0.45 μ m syringe filters before proceeding to the purification.

Table 2.9: The components of PBS (1L)

NaCl (140 mM)	8.2 g
KCl (2.7 mM)	201.2 mg
Na ₂ HPO ₄ (10 mM)	1.42 g
KH ₂ PO ₄ (1.8 mM)	245 mg
H ₂ O	1000 ml

2.4.3 Protein purification

Protein purification was carried out using the Glutathione Sepharose 4B (GE Healthcare, Little Chalfont, UK) according to the manufacturer's instructions. Cell lysate was incubated with the resin for 1 h at room temperature. Phosphate buffer saline (PBS) (see Table 2.9) was used for preparing the resin and three washes were performed to remove any residual unbound proteins after the incubation. Elution was carried out using 50 mM Tris-HCl, 10 mM reduced glutathione pH 8.0 (made on the day). Purification was confirmed via SDS-page electrophoresis and purified proteins were stored as 30 % (v/v) glycerol aliquots at -80 °C.

2.4.4 Protein visualisation

Protein visualisation was achieved via SDS-PAGE electrophoresis. Samples were solubilised in a 4x sample loading buffer (Table 2.10) containing 20 % (v/v) β -mercaptoethanol (added just prior to use). Samples were denatured by

incubation at 100 °C for 5 min. Gel assembly comprised of a 12 % (w/v) acrylamide separating gel and a 4% acrylamide stacking gel. Samples were run on 100 V whilst on the separating gel and 200 V whilst on the stacking gel. The “PageRuler™ Plus Prestained Protein Ladder” (ThermoFischer Scientific) was run alongside the samples to determine the molecular weight. The visualisation of the protein bands on the gel was done with “InstantBlue” according to the manufacturer’s instructions (Expedeon Swavesey, UK).

Table 2.10: The composition of 4x sample loading buffer

H ₂ O	1.2 ml
1 M Tris-HCl, pH 6.8	2 ml
Glycerol	3.2 ml
SDS	0.8 g
0.05% bromophenol blue (w/v)	8 mg
Total	8 ml

2.4.5 Protein quantification

Protein quantification was achieved through Bradford protein assay. 10 µl of each sample were added in 300 µl of Coomassie Plus reagent in the wells of a 96-well plate. Measurements were performed in triplicate for each sample. The plate was allowed to incubate for 10 min at room temperature and absorbance was then measured at 595 nm with a Sunrise™ Tecan plate reader. Samples were quantified against a standard curve made with diluted albumin (BSA) standards. Protein concentration can be calculated using the following equation: $c = (A - 0.0231)/0.0009$.

2.5 Plant methods

2.5.1 Seed sterilisation

Seeds were dry sterilised by chlorine gas (generated by the addition of 3 ml concentrated hydrochloric acid in 100 ml bleach) in an airtight container for 4

h. After sterilisation the lid of the container was opened in a flow hood for 10 min to remove any residual chlorine gas.

2.5.2 Stratification

Seeds were placed either on ½ MS agar (half strength Murashige and Skoog Basal Salt mixture, Duchefa Biochemie) plates or soil (F2 compost) and were imbibed in the dark (covered with foil) at 4 °C for a minimum of 72 h.

2.5.3 Growth conditions

2.5.3.1 Growth conditions for soil

The following conditions refer to plant grown in soil for generic purposes such as bulking up the seed stock, pushing plant generations forward and growing plants for floral dipping. In this case non-sterile seeds were evenly spread on top of either trays or pots (8 cm diameter), filled with F2 compost treated with the pesticide “Intercept” (active substance: imidacloprid), and stratified (see section 2.5.2). Plants were then allowed to propagate in the greenhouse. Plants grown in 3 inch pots for the purpose of floral dipping were weeded down to 10 plants per pot.

2.5.3.2 Growth conditions for solid media

The following conditions refer to seeds grown on ½ MS agar plates for the purpose of identification of successful transformants. In this case, chlorine-gas-sterilised seeds (see section 2.5.1) were spread on ½ MS agar plates supplemented with 20 mM sucrose and 50 µg/ml kanamycin. Resistant seedlings (putative transformants) were transplanted to soil for propagation and seed collection.

2.5.4 Genomic DNA isolation from plants

Plant tissue (normally a large leaf) was initially ground in a 1.5 ml Eppendorf tube. Immediately 500 µl of 2x CTAB buffer (Table 2.11) were added, the sample was mixed well and incubated at 65 °C for 30-60 min on a pre-heated

block. After the incubation 300 µl of chloroform: iso-amyl-alcohol (IAA) (24:1) were added and the sample was vortexed. The sample was then centrifuged at maximum speed on a tabletop centrifuge for 5 min and 300 µl of the top aqueous layer were transferred into a clean 1.5 ml Eppendorf tube. Then 960 µl of ethanol and 40 µl of sodium acetate (to reduce ionic tension) were added, the sample was mixed and left overnight at 4 °C to precipitate genomic DNA. The following day the sample was centrifuged at 4 °C and maximum speed on a tabletop centrifuge for 15 min. The supernatant was discarded and the pellet was rinsed with 70% ethanol before being centrifuged again for 5 min. The ethanol was removed with a pipette and the pellet was dried in a Savant™ DNA110 SpeedVac at high temperature for 15 min to remove any residual ethanol. The pellet was re-suspended in 50-100 µl of H₂O.

Table 2.11: The composition of 2x CTAB buffer (100 ml)

Cetyltrimethyl ammonium bromide (CTAB)	2 g
NaCl (1.4 M)	8.2 g
100 mM Tris-HCl pH 8	10 ml of 1 M stock solution
Disodium EDTA (20 mM)	0.74 g
H ₂ O	90 ml

2.6 Statistical analysis

Data were analysed for statistical significance using analysis of variance (ANOVA), with post-hoc Tukey's honestly significant difference and the SPSS 22.0 software.

Chapter 3: *At*GSTU24 and *At*GSTU25 over-expressing Arabidopsis lines

3.1 Introduction

As part of the phase I reactions of the detoxification mechanism, TNT is reduced by nitroreductases to HADNTs, and then further reduced to ADNTs [6, 26, 72, 163]. In *Arabidopsis thaliana* (Arabidopsis) it has been reported that these steps are catalysed by oxophytodione reductases (OPRs), which are able to produce both HADNTs and ADNTs [27], without excluding the possibility of other contributing nitroreductases. The phase I reactions are believed to be the limiting step in the TNT detoxification pathway [22, 69, 73]. In accordance with this, plants recombinantly expressing bacterial nitroreductases with activity towards TNT demonstrate a strikingly enhanced ability to tolerate, take up and detoxify TNT [22, 69]. Following from this, identifying and increasing the activity of enzymes involved in the downstream conjugation steps should assist further in increasing the detoxification of TNT and the remediation potential of plants.

The conjugation of HADNTs and ADNTs produced during phase II reactions has been well characterised. In the past, six recombinantly expressed uridine diphosphate (UDP)-glycosyltransferases (UGTs) from Arabidopsis that exhibited increased transcript levels of between 14- and 173-fold in response to TNT treatment were shown to conjugate HADNTs and ADNTs, with the conjugates subsequently incorporated into the plant biomass [26]. Over-expression of two of these UGTs (UGT743B4 and UGT73C1) in Arabidopsis resulted in increased conjugate production and enhanced seedling root growth in the presence of TNT with the conjugates being isolated *in planta* [26]. Conjugation to other sugar molecules and organic acids may also occur. Mammalian GSTs have been shown to have activity towards TNT [76]. Further expression studies have identified GSTs that are highly upregulated in the response to TNT in *Populus trichocarpa* (poplar) [76, 164] and Arabidopsis

[25, 75], suggesting GSTs as an alternative phase II enzyme family with a role in the detoxification of TNT. However, even though the two GSTs upregulated in poplar demonstrated activity towards TNT, the activity was deemed too low for efficient detoxification [164] and a direct correlation between GSTs and TNT detoxification remains to be established.

Previously in Neil Bruce's laboratory a microarray analysis of cDNA from 14-day-old Arabidopsis seedlings treated with 60 μ M TNT for 6 h was conducted in order to identify genes which could be involved in the detoxification of TNT [26]. Several genes were upregulated in response to TNT including a wide range of phase I and II detoxification enzymes. Among the phase II enzymes upregulated were members of the Tau class GST family. This enzyme family displayed some of the most highly upregulated enzymes of the microarray analysis. As demonstrated by Dr Helen Sparrow, out of the eight Tau class GSTs significantly upregulated (>8-fold) in the presence of TNT (Figure 3.1) [26] two of them, *At*GSTU24 (GST-U24) and *At*GSTU25 (GST-U25), have activity towards TNT *in vitro* [165, 166].

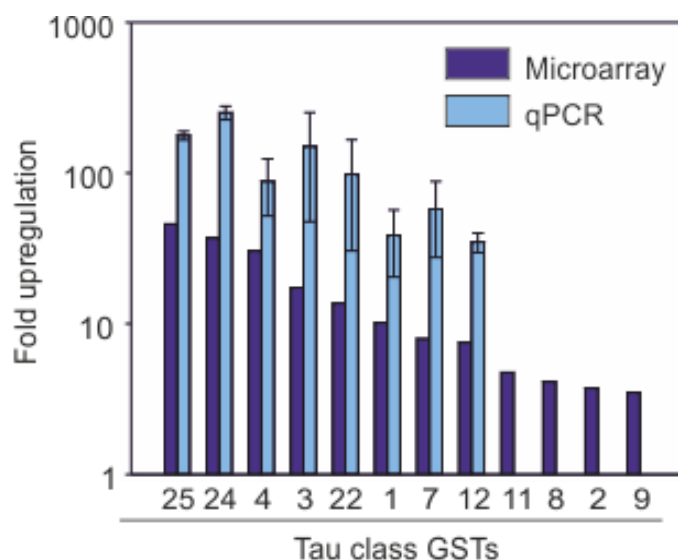


Figure 3.1: Microarray and qPCR data showing Arabidopsis Tau class GSTs upregulated more than 2 fold following TNT treatment. Eight GSTs are upregulated more than 8-fold. Out of those eight, GST-U24 and GST-U25 demonstrated activity towards TNT *in vitro*.

Following affinity chromatography, purification and characterisation of recombinant forms of the enzymes it was shown that both GST-U24 and GST-U25 have the ability to conjugate TNT directly in its original form without the

need for any prior reduction of the compound [165, 166]. This activity offers a potential advantage of skipping the phase I reactions which are believed to contain the rate limiting step in the detoxification process [22, 69, 73].

Subsequent HPLC-based assays, mass spectrometry and NMR spectroscopy, conducted by Dr Vanda Gunning (Bruce laboratory), proved that TNT-glutathione conjugation results in three distinct conjugates (Figure 3.2) [165]. Two of the resulting conjugates, C-glutathionylated-4-hydroxylaminodinitrotoluene and C-glutathionylated-2-hydroxylaminodinitrotoluene (conjugates 1 and 2 respectively) are isomers. Both conjugates share a molecular mass of 518 and the GSH conjugation occurs via the methyl group of TNT. Subsequent reduction of a nitro group at position 2/6 gives conjugates 1, while reduction of the nitro group at position 4 results in conjugate 2. The remaining conjugate, 2-glutathionyl-4,6-dinitrotoluene (conjugate 3) occurs via substitution of a nitro group at the 2/6 position, and results in concurrent release of nitrite (Figure 3.2) [165]. Conjugate 3 could be more chemically labile than the original TNT structure as one of the nitro groups is removed and restores (at least partially) the electron density of the aromatic ring. This conjugate is, therefore, potentially more amenable to biodegradation. Further studies revealed that whilst GST-U24 produces predominantly conjugate 2, with trace amounts of conjugates 1 and 3, GST-U25 is able to produce all three conjugates dependent on pH [165]. At pH 6.5-7.0, which is closer to the physiological pH of the Arabidopsis cytosol [167-170], GST-U25 produces almost exclusively conjugate 3 with only traces of the remaining conjugates being produced. Besides their glutathione conjugating activity, GST-U24 and GST-U25 are also able to exhibit GPOX activity [87].

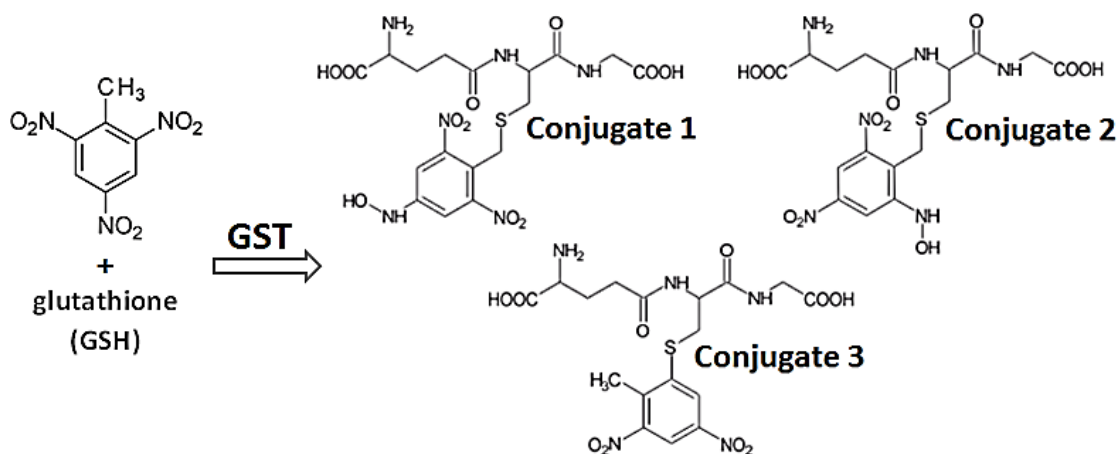


Figure 3.2: Glutathionylation of TNT (catalysed by GST-U24 or -U25) can result into three distinct conjugates. Conjugates 1 & 2 are isomers and the glutathionylation takes place on the methyl group at the top of the aromatic ring, leaving the nitro groups untouched. Conjugate 3 is produced by nucleophilic substitution of a NO₂⁻ by GSH and results in concurrent release of nitrite.

To investigate whether increasing the levels of GST-U24 and GST-U25 could confer increased ability to detoxify TNT *in planta* the cDNAs of both enzymes were cloned into plant expression vectors under the control of the CaMV 35S promoter and several 35S-GST over-expression (OE) Arabidopsis (Columbia 0 ecotype) lines were generated by Dr Helen Sparrow in the Bruce lab [166]. Assays, using 1-chloro-2,4-dinitrobenzene (CDNB) as a substrate, on protein extracts from rosette leaves of the GST-U24 and GST-U25 OE lines, demonstrated that GST-U24 and GST-U25 have activity towards CDNB and that the GST OE lines had higher conjugation activities than the WT [165]. Subsequent studies, by Dr Vanda Gunning, revealed that the Arabidopsis OE lines of GST-U24 and GST-U25 were more resistant towards TNT and displayed longer roots, relative to wild type seedlings, when grown on agar plates containing TNT (Figure 3.3) [165]. Additional experiments showed that the OE lines were able to remove more TNT from liquid media during hydroponic cultures [165]. Following from this work, this chapter investigates the performance and detoxification abilities of these lines in soil, to establish a direct correlation between GSTs and TNT detoxification.

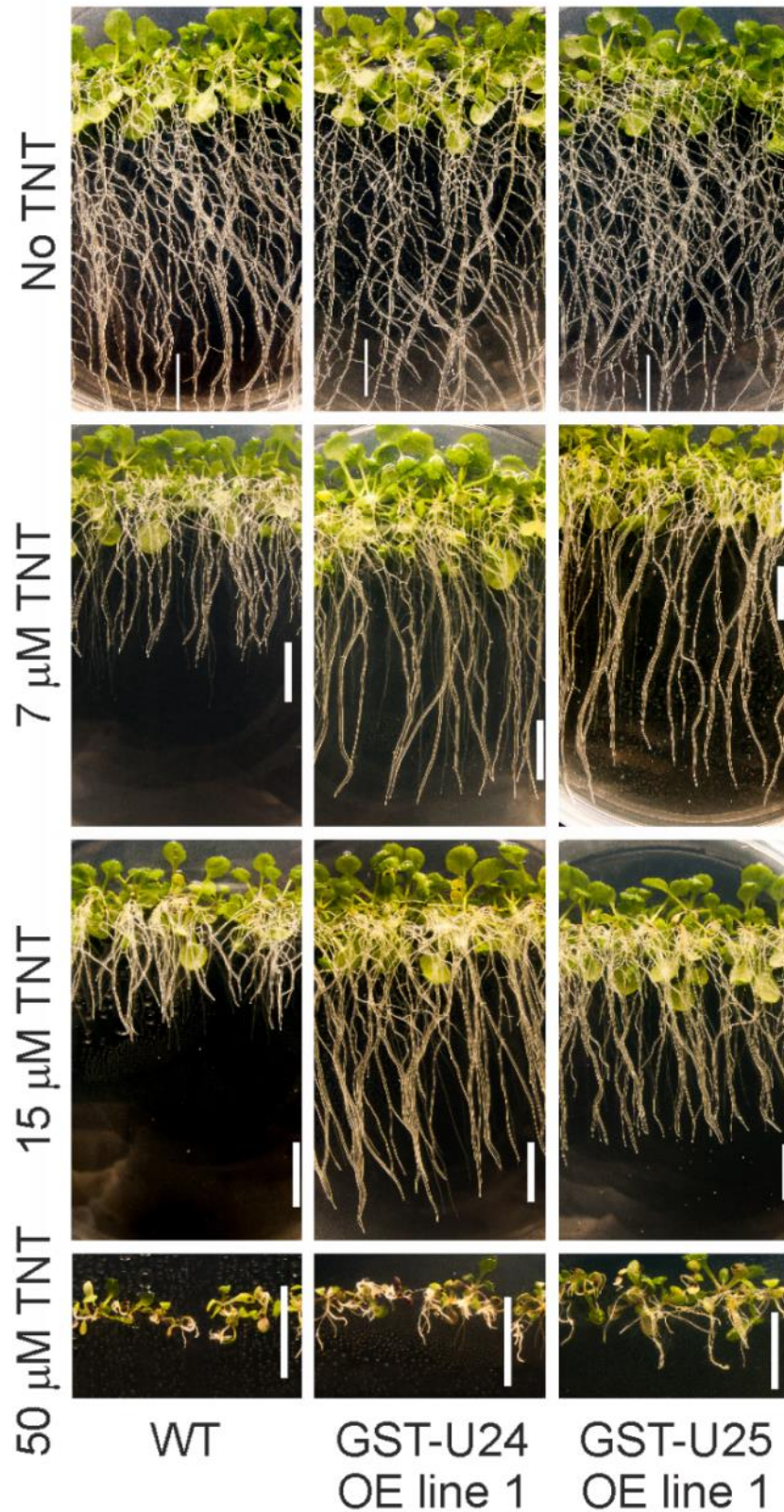


Figure 3.3: Appearance of 20-day-old Arabidopsis seedlings, wild-type (WT) and GST over-expressing (OE) lines, grown vertically on agar plates containing $\frac{1}{2}$ MS medium and a range of TNT concentrations. White bars = 1 cm. Figure adapted from Dr V. Gunning's PhD thesis [165].

3.2 Methods

3.2.1 Protein extraction from plant tissue

Seeds were sterilised, stratified and placed in a single row on ½ MS plus 20 mM sucrose plates. The plates were grown vertically until the roots reached the bottom of the plate (approximately two weeks). Plant tissue was harvested and 50 mg of tissue were grinded in 500 µl of ice-cold protein extraction buffer (100 mM Tricine, 1 mM EDTA, 20% glycerol (v/v), 5% PVP-40 (w/v) and 2 mM DTT (added just prior to use)) [171], using a bead mill. Samples were centrifuged at 13,000 rpm and 4 °C for 10 min. Supernatants were transferred to clean Eppendorf tubes and kept on ice until assaying.

3.2.2 CDNB activity assay on plant protein extracts

The GST generic substrate 1-chloro-2,4-dinitrobenzene (CDNB) was used to measure the conjugating activity of plant protein extracts. The CDNB assay was originally developed as a simple colorimetric assay to measure mammalian GST activity [172]. Glutathione transferases catalyse the removal of a proton from GSH to generate the thiolate anion GS^- , which is more reactive than GSH. Conjugation of CDNB with the thiolate anion occurs at carbon 1 where the chloride is bound, producing a Meisenheimer complex. The complex is unstable and the chloride dissociates releasing glutathionyl-dinitrobenzene (Figure 3.4) [98]. Upon conjugation of the thiol group of GSH to the CDNB substrate, there is an increase in the absorbance at 340 nm [172], which allows the measurement of the reaction rate spectrophotometrically.

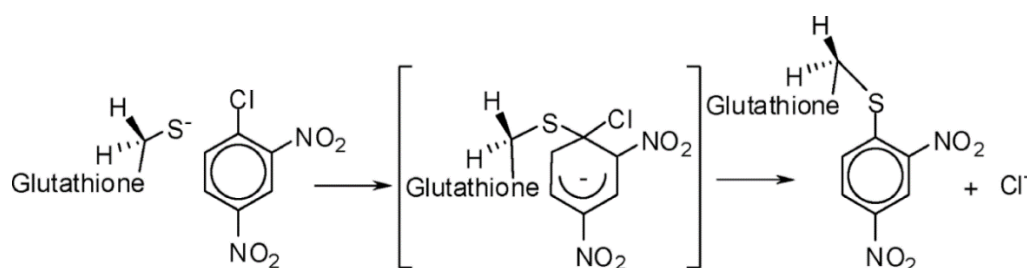


Figure 3.4: GST catalysed conjugation of CDNB with glutathione via a Meisenheimer complex. Figure from [98].

To measure the CDNB conjugation activity of plant protein extracts, plants were grown for two weeks vertically on ½ MS agar plates. After that period plant tissue was harvested, proteins were extracted (see section 3.2.1) and their respective conjugation activities were determined. The reaction was performed at 25 °C in 1 ml cuvettes with a Varian Carry® 50 Bio UV-Vis Spectrophotometer. The reaction mix consisted of 100 mM potassium phosphate buffer pH 6.5, 5 mM GSH, 50 µl of plant protein extract and 1 mM CDNB. The reaction was initiated with the addition of CDNB and the increase in A_{340} was monitored over a minute. Each reaction was performed in triplicate. Results were normalised according to root fresh weight.

3.2.3 TNT-containing soil preparation

The protocol for the TNT-containing soil preparation was based on a published method [159]. Initially a 20 mg/ml TNT solution in acetone was prepared. Following that, 65 g of dry sand were weighed in 2-L polypropylene tubs. The TNT in acetone solution was added onto the sand and the acetone was allowed to evaporate. For the TNT-free soil, a volume of acetone equivalent to that used for soil containing the highest level of TNT was applied. A 35-mm glass marble was added to each tub and the tubs were then mixed in a rotating mixer for a minimum of 20 min. After mixing Levington's F2 compost was added and water content was standardised to 40.5% water and a final weight of 465 g. Finally, soil and sand were mixed on the rotating mixer once more for a minimum of 1 h. Sealed tubs were then stored at 4 °C.

3.2.4 Soil studies

Soil studies were based on a previously described protocol [159]. Seeds were stratified and germinated on TNT-free soil (Levington's F2 compost). Five one-week-old seedlings were then transferred to a pot containing 18 g of TNT-containing soil. Plants were grown for six weeks in a controlled environment (Sanyo growth cabinets), under $180 \mu\text{mol m}^{-2} \text{s}^{-1}$ light with a 12-h photoperiod, 21 °C day and 18 °C night temperatures to ensure uniform plant quality, and between-experiment reproducibility. After six weeks plant material was

harvested to determine root and shoot dry weight (dried O/N at 60 °C). Dry weight was chosen contrary to fresh weight because it removes the water content, which could impair the weight of the samples, and is therefore a direct measurement of biomass.

3.2.5 Extraction of TNT and derivatives from soil

The method for the extraction of nitrotoluenes from soil was based on the U.S. Environmental Protection Agency (EPA) method 8330 [173, 174]. The only modifications comparing to the original method were the absence of CaCl₂ addition and filtration steps. This avoided dilution of the samples and any contact between nitrotoluenes and plastic. Centrifugation was used instead of filtration to remove soil debris, while samples were concentrated by 10-fold to produce more clear peaks during HPLC analysis. In summary, nitrotoluenes were extracted from 2 g of dry (dried O/N at 60 °C) ground soil by mixing in a glass tube with 10 ml of acetonitrile in a cooled (4 °C) ultrasonic bath for 18h. Following centrifugation at maximum speed in a Sorvall centrifuge, 5 ml of supernatant were transferred to a fresh glass tube, evaporated, and then re-suspended to 1/10 of the original volume (500 µl) of 50: 50 H₂O: acetonitrile prior to HPLC analysis. During HPLC analysis 50 µl of sample were run on a 50: 50 H₂O: methanol isocratic method with a Waters X-Bridge C18 column (250 X 4.6 mm, 5 µm). The respective retention times for TNT and ADNTs were 12.6 and 14.8 min. Integration was performed at 230 nm with Empower Pro Software. Quantification of the samples was done using a standard curve produced with 0-200 µM pure TNT and ADNTs standards.

3.2.6 LC/MS analysis of soil extraction products

The mass spectrometry analysis of TNT and derivatives extracted from soil was performed using a Finnigan Surveyor Autosampler Plus, Finnigan Surveyor LC pump Plus, Finnigan Surveyor PDA Plus detector and an LCQ detector Finnigan MAT 2.0 (all from Thermo Electron Corporation). A Waters X-Bridge C18 column (250 x 4.6 mm, 5 µM) and a 50: 50 H₂O: methanol isocratic method, with a 20 µl injection volume was used for the LC analysis.

Electrospray Ionisation (ESI) was used for the production of ions in negative mode with mass range 100-1000. Data were analysed and integrated with Excalibur 2.0 SUR 1 software.

3.2.7 Glutathione measurements

Glutathione measurement was based on a previously described plate-reader-based protocol [175], modified for assaying on a spectrophotometer. Plant tissue was harvested and homogenised in 1ml of 0.2 N HCl per 100 mg of fresh tissue using a bead mill. Beads were removed and samples were centrifuged at 13,000 rpm for 10 min at 4 °C. After centrifugation 800 µl of supernatant were transferred to a clean Eppendorf tube and were complemented with 80 µl of 0.2 M NaH₂PO₄ and 640 µl of 0.2 M NaOH (pH at this stage should be in the range of 5-6). This neutralised sample was used for determining the abundance of total GSH. For the determination of oxidised glutathione (GSSG) 400 µl of the neutralised sample were mixed with 2 µl of 2-vinylpyridine (VPD) at room temperature for 30 min, to complex reduced glutathione and remove it from the assay. The sample was then centrifuged at 13,000 rpm for 15 min and 250 µl of the supernatant were transferred into a clean Eppendorf tube. This sample was used for the GSSG measurements. The measurements on the spectrophotometer were performed as follows:

Master-mix for 200 assays:

- 100 ml 0.2 M NaH₂PO₄ (pH 7.5) 10 mM EDTA
- 10 ml of 12 mM DTNB
- 60 ml of sdH₂O

In a 1ml cuvette:

- 850 µl master-mix for total GSH (or 800 for measuring GSSG)
- 50 µl sample for total GSH (or 100 µl for measuring GSSG)
- 50 µl 10 mM NADPH
- 50 µl glutathione reductase (in 0.2 M NaH₂PO₄ (pH 7.5) 10 mM EDTA)

The rate of 5,5'-dithiobis(2-nitrobenzoic acid) (DTNB) reduction to thionitrobenzoic acid by GSH was monitored by following the increase in A_{412} and corrected by mean value of assay with 0 GSH standard. An overview of

the process is given in Figure 3.5. Levels of GSSG were deduced from total GSH levels to calculate the amount of reduced GSH. Quantification of GSSG and GSH levels relied on standard curves created with fresh standards prepared on the day of the assay.

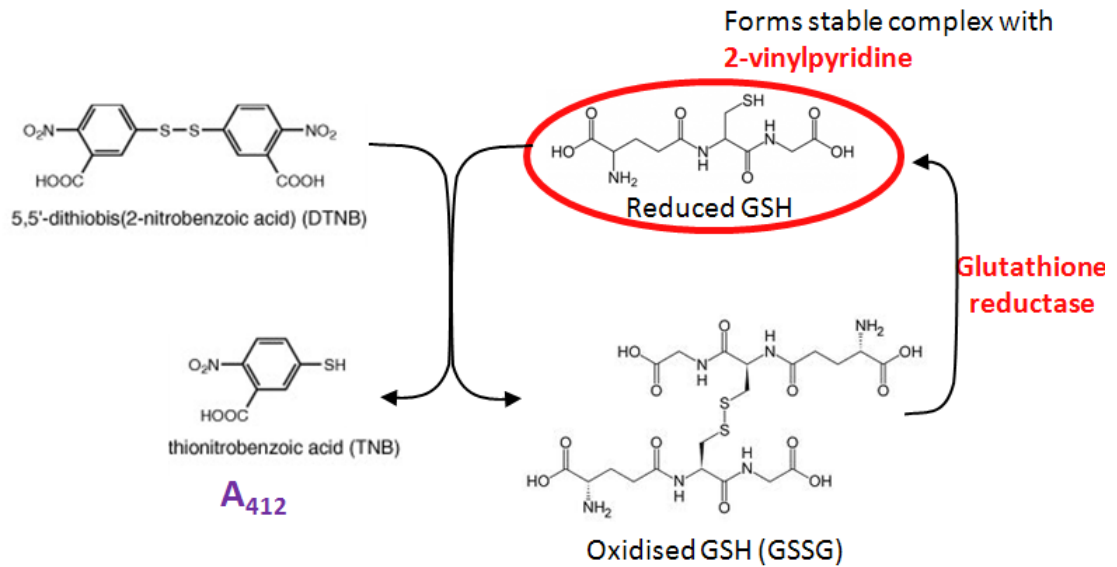


Figure 3.5: Overview of the process employed to determine the abundance of reduced and oxidised glutathione.

3.2.8 GPOX assay

The glutathione peroxidase (GPOX) activity was measured indirectly through a coupled reaction with glutathione reductase (GR). Reduction of hydroperoxides by GPOX-activity-possessing enzymes leads to production of GSSG which is subsequently recycled to GSH by GR and NADPH (Figure 3.6). The oxidation of NADPH to NADP⁺ is accompanied by a decrease in absorbance at 340 nm. Therefore GPOX activity can be determined spectrophotometrically.

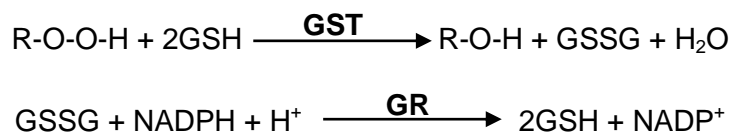


Figure 3.6: Overview of the hydroperoxide reduction reaction catalysed by a glutathione S-transferase (GST) and the recycling of GSSG to GSH catalysed by glutathione reductase (GR).

To assay GPOX activity with purified GST-U24 and GST-U25, cumene hydroperoxide was used as substrate. The assay was based on a previously described method by Edwards and Dixon (2005) [176] with the following modifications. The reactions were conducted in 50 mM Tris-HCl, pH 6.5, 0.5 mM EDTA, with 5 mM GSH, 0.25 mM NADPH, 0.6 U/ml GR, 5-1,500 μ M cumene hydroperoxide, 2.5-10 μ M TNT, and 30 and 5 μ g of GST-U24 and GST-U25 respectively, in a final volume of 190 μ l per well on a 96-well-plate. The reaction was initiated with the addition of cumene hydroperoxide and the decrease in A_{340} was monitored spectrophotometrically over a minute on a POLARstar OPTIMA plate reader (BMG laboratories). The K_m and V_{max} Michaelis-Menten parameters were calculated using Sigma Plot 12.0.

3.3 Results

3.3.1 CDNB activity of plant protein extract

The GSH-conjugating activity of root protein extracts of the GST over-expressing (OE) lines, grown for two weeks vertically on $\frac{1}{2}$ MS agar plates (Figure 3.7A), was assessed spectrophotometrically using the generic substrate CDNB.

Results confirmed that the GST OE lines had higher conjugation activities than WT plants. All of the GST-U24 and GST-U25 plant lines displayed higher conjugating activities than WT, with GST-U25 OE lines achieving the highest activity (Figure 3.7B). The GST-U25 OE lines higher activity can be attributed to the higher affinity that GST-U25 displays towards CDNB, comparing to GST-U24. The enzymes shared similar V_{max} (38.9 ± 2.0 nkat mg^{-1} and 28.1 ± 0.6 nkat mg^{-1} for GST-U24 and GST-U25 respectively), while their K_m values were significantly different ($K_m = 954.9 \pm 119.6$ μM and 30.6 ± 3.1 μM for GST-U24 and GST-U25 respectively).

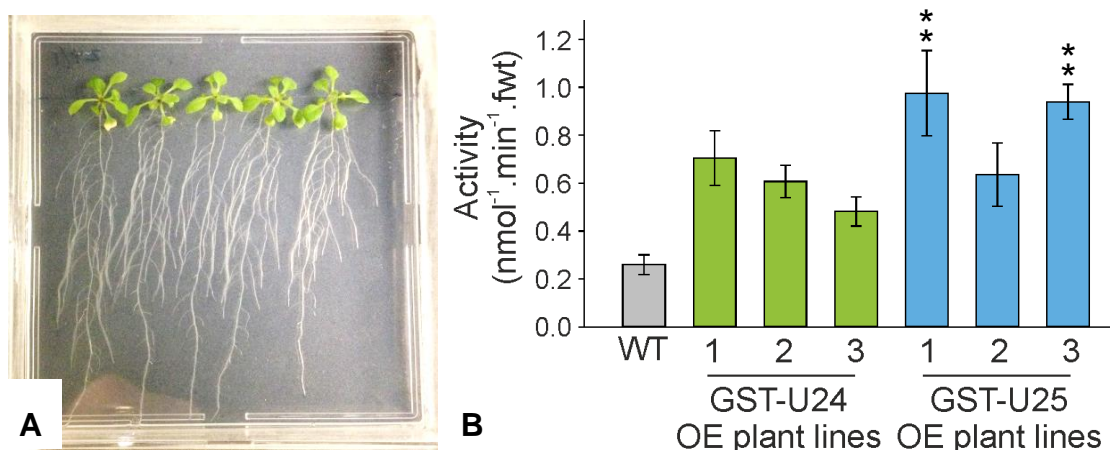


Figure 3.7: (A) Appearance of two-week-old plants grown vertically on agar plates of TNT-free, $\frac{1}{2}$ MS medium. (B) Conjugation activities in root protein extracts from Arabidopsis wild type (WT) and GST over-expressing two-week-old plants. Plants were assayed using CDNB as the substrate. Rate of conjugate production was determined spectrophotometrically over 1 min at 340 nm. Results were standardised according to root fresh weight. Results are means of five biological measurements \pm se. Asterisks denote statistically significant from the WT: ** $P < 0.01$.

3.3.2 Biomass of GST-U24 and U25 OE Arabidopsis lines

To test the detoxification abilities of the GST-U24 and GST-U25 OE lines, the plants were grown on TNT-free soil, and soil containing 25, 50 and 100 mg kg⁻¹ TNT. These concentrations allow unmodified (wild type; WT) Arabidopsis plants to germinate, while at the same time TNT levels remain close to those found at contaminated sites.

During the first three weeks of growth the plants did not display any significant differences in appearance (Figure 3.8A). After six weeks of growth in soil, shoots and roots of the GST OE lines appeared smaller than those of unmodified plants when grown in TNT-free soil (Figure 3.8B). Dry weight measurements confirmed that amounts of both shoots and roots were significantly lower ($P < 0.05$) for GST-U24 and -U25 lines (Figure 3.9A, B), with the effect being stronger on the GST-U24 lines. As TNT concentration increased to 25 mg kg⁻¹ the biomass of the shoots remained similar to that of the TNT-free soil for all plant lines. On the contrary, at the root level the WT plants exhibited 1/3 of the biomass recorded in the TNT-free soil (Figure 3.9B). At this concentration almost all of the OE lines remained unaffected in terms of root biomass and achieved higher amounts of biomass than WT plants. At the higher TNT concentrations (50 and 100 mg kg⁻¹) most of the OE lines displayed higher TNT tolerance and produced significantly more biomass than WT plants. At 50 mg kg⁻¹ TNT all of the OE lines displayed higher root biomass than the WT plants, while at 100 mg kg⁻¹ the difference increased even more, with the most successful OE lines displaying more than 7-fold higher root biomass than WT (Figure 3.9A, B).

To account for the reduced biomass displayed by the OE lines in the TNT-free soil, the data were normalised by calculating the biomass on soil containing TNT to that of TNT-free soil for each line and TNT concentration, relative to WT (Figure 3.9C). Overall at 100 mg kg⁻¹ TNT (the concentration that the highest difference was recorded) the combined mean for the shoots and roots was 6.4 and 7.7-fold higher than the WT for GST-U24 lines and 2.9 and 6.4-fold respectively for the GST-U25 lines (Figure 3.9C).

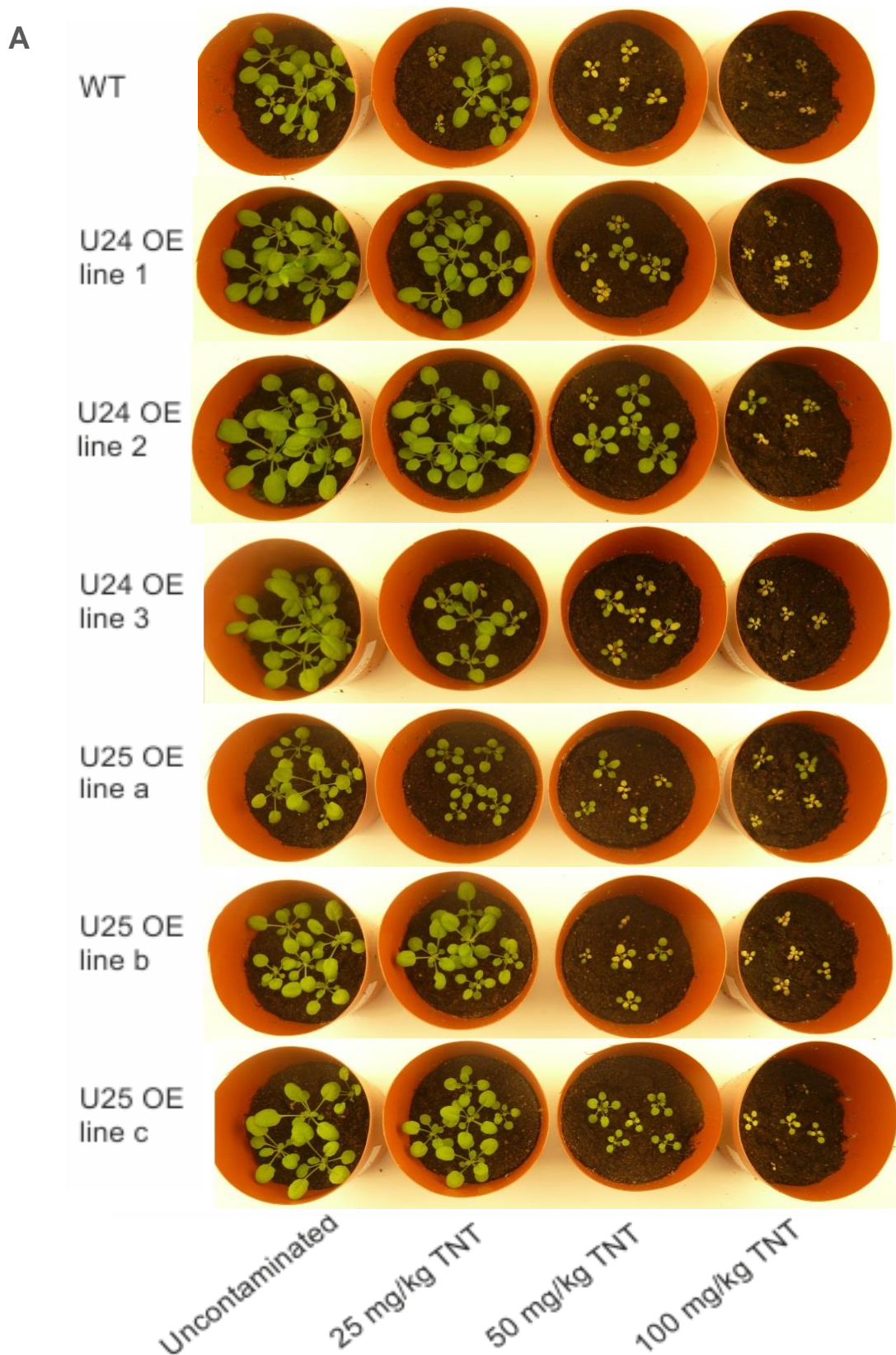


Figure 3.8: Appearance of Arabidopsis seedlings grown for (A) three weeks and (B) six weeks (following page) in soil containing a range of TNT concentrations. WT, untransformed plants; GST-U24 OE, independent GST-U24 over-expressing lines; GST-U25 OE, independent GST-U25 over-expressing lines.



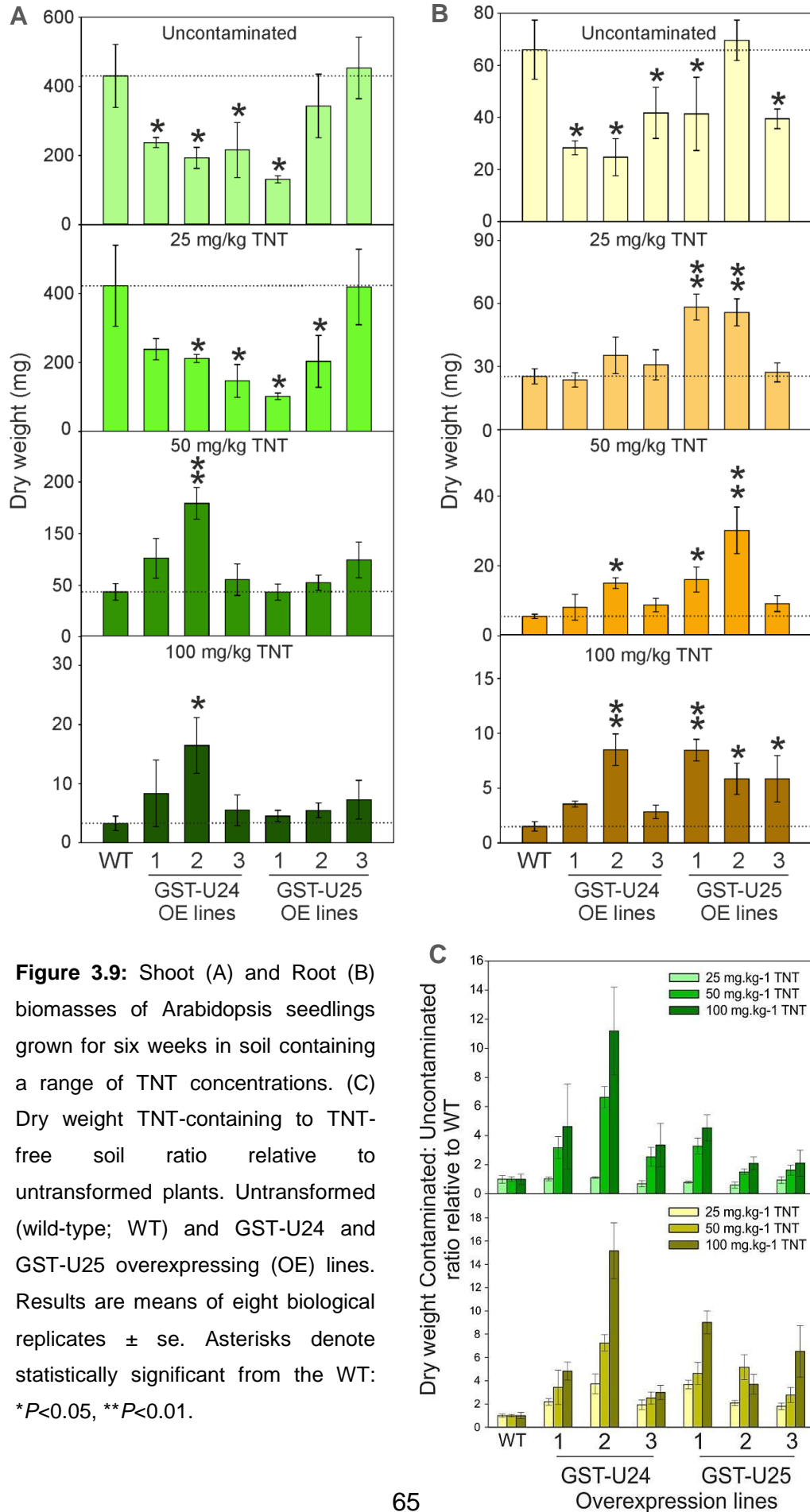


Figure 3.9: Shoot (A) and Root (B) biomasses of Arabidopsis seedlings grown for six weeks in soil containing a range of TNT concentrations. (C) Dry weight TNT-containing to TNT-free soil ratio relative to untransformed plants. Untransformed (wild-type; WT) and GST-U24 and GST-U25 overexpressing (OE) lines. Results are means of eight biological replicates \pm se. Asterisks denote statistically significant from the WT: * $P < 0.05$, ** $P < 0.01$.

3.3.3 TNT uptake from soil

To determine whether the GST OE lines take up more TNT than WT plants, the OE lines were grown alongside WT plants in soil of 25 and 50 mg kg⁻¹ TNT concentration as done previously for the biomass measurement (see section 3.3.2), in order to extract TNT and derivatives remaining in soil. At these TNT concentrations WT and GST OE lines display differences with regards to their biomass, while at the same time all plant lines develop a significant amount of roots that ensure a strong uptake of the TNT found in soil.

The HPLC analysis of extracted samples revealed two peaks with retention times of 12.6 min and 14.8 min (Figure 3.10). The UV absorption spectra, compared to authentic standards, suggested that the former peak was TNT and the latter peak was 2-amino-dinitrotoluene (2-ADNT) and 4-amino-dinitrotoluene (4-ADNT) co-eluting (Figure 3.10). Subsequent LC/MS analysis confirmed the identity of the peaks as TNT and ADNTs. The 12.6 min peak gave in negative mode, an [M-H]⁻ ion of 226.11, consistent with the TNT molar mass (227.12). The 14.8 min peak gave an [M-H]⁻ ion of 196.07 confirming the peak as ADNT, with a mass of 197.14 (Figure 3.11).

At both TNT concentrations, the GST OE lines removed more TNT from the soil than the WT plants, with the most active lines exhibiting up to 21 % higher TNT uptake (Figure 3.12). Analysis of the TNT and derivatives suggested that most of the TNT remaining in soil was found in the form of ADNTs (Figure 3.12). Furthermore, the ratio of TNT to ADNT was lower in the soil of the GST OE lines than that of WT indicating that the OE lines remove TNT in preference to ADNT. At 25 mg kg⁻¹ TNT concentration the TNT: ADNT ratio was for WT 0.35; for GST-U24 lines 0.35, 0.08 and 0.11 respectively; and for GST-U25 lines 0.21, 0.26 and 0.05 respectively.

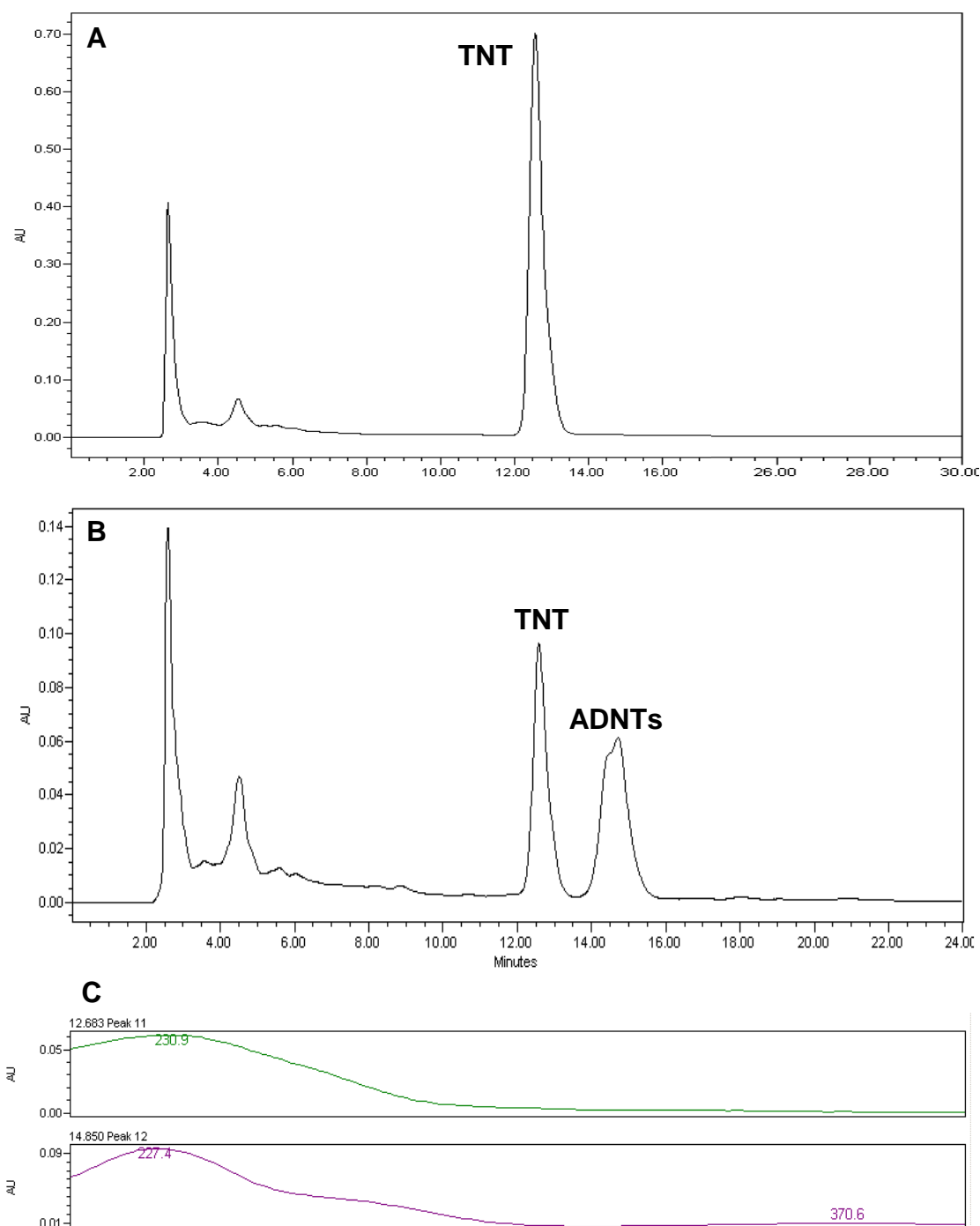


Figure 3.10: HPLC chromatograms for (A) a soil sample spiked with 50 mg kg^{-1} TNT just prior to the extraction and (B) a soil sample on which plants were grown for six weeks. (C) UV absorption spectra traces and absorption maxima for TNT (green) and ADNTs (purple). TNT elutes at 12.6 min and ADNTs co-elute in a single peak at 14.8 min.

Chapter 3: AtGSTU24 and AtGSTU25 over-expressing Arabidopsis lines

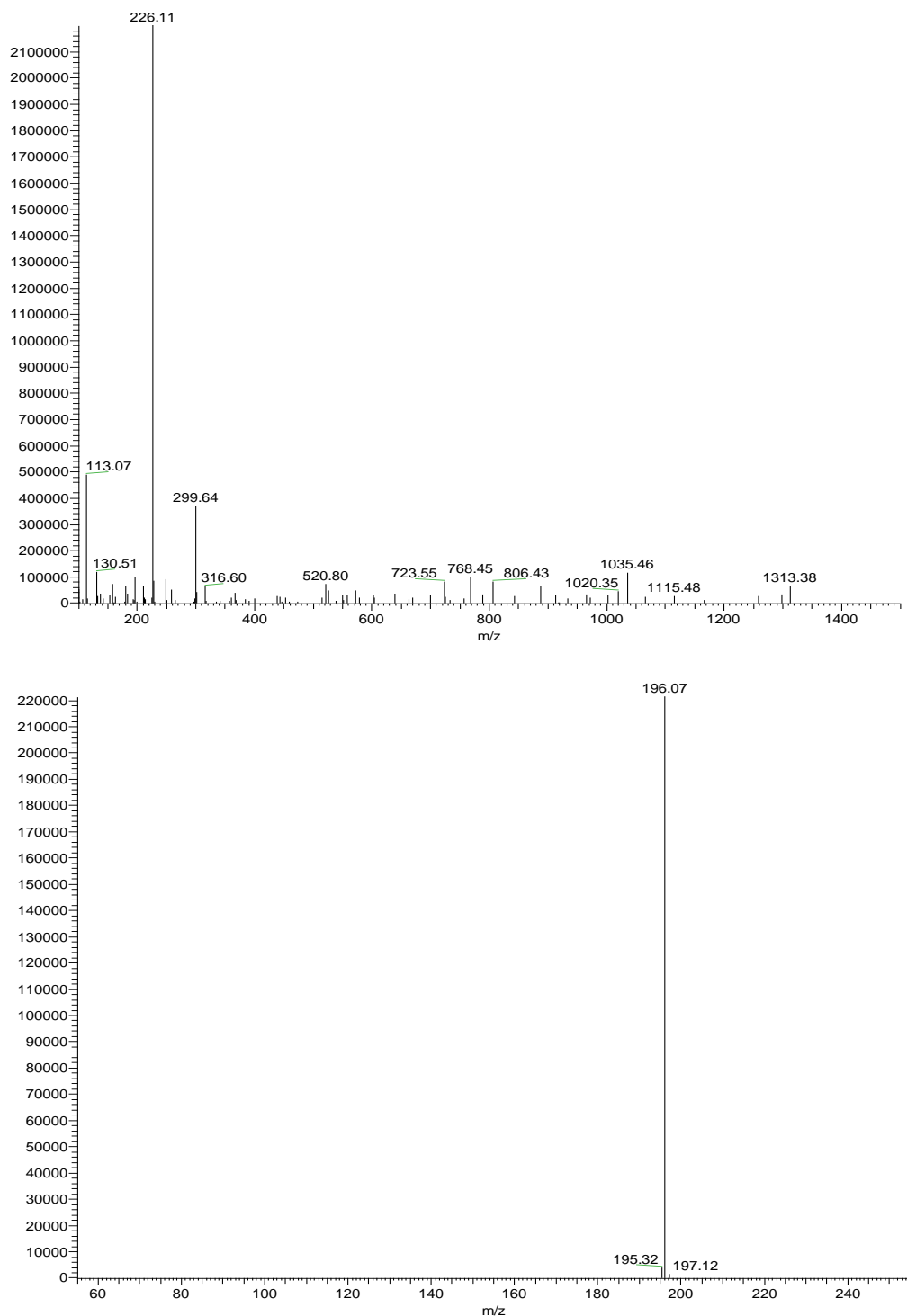


Figure 3.11: Mass spectrometry data as identified by LC/MS analysis of the samples extracted from soil. (Top) Mass spectrum for the peak eluting at 12.6 min in negative mode, giving an $[M-H]^-$ ion of 226.11 and mass of 227.12, confirming the peak as TNT. (Bottom) Mass spectrum for the peak eluting at 14.8 min in negative mode, giving an $[M-H]^-$ ion of 196.07 and mass of 197.14, confirming the peak as ADNT.

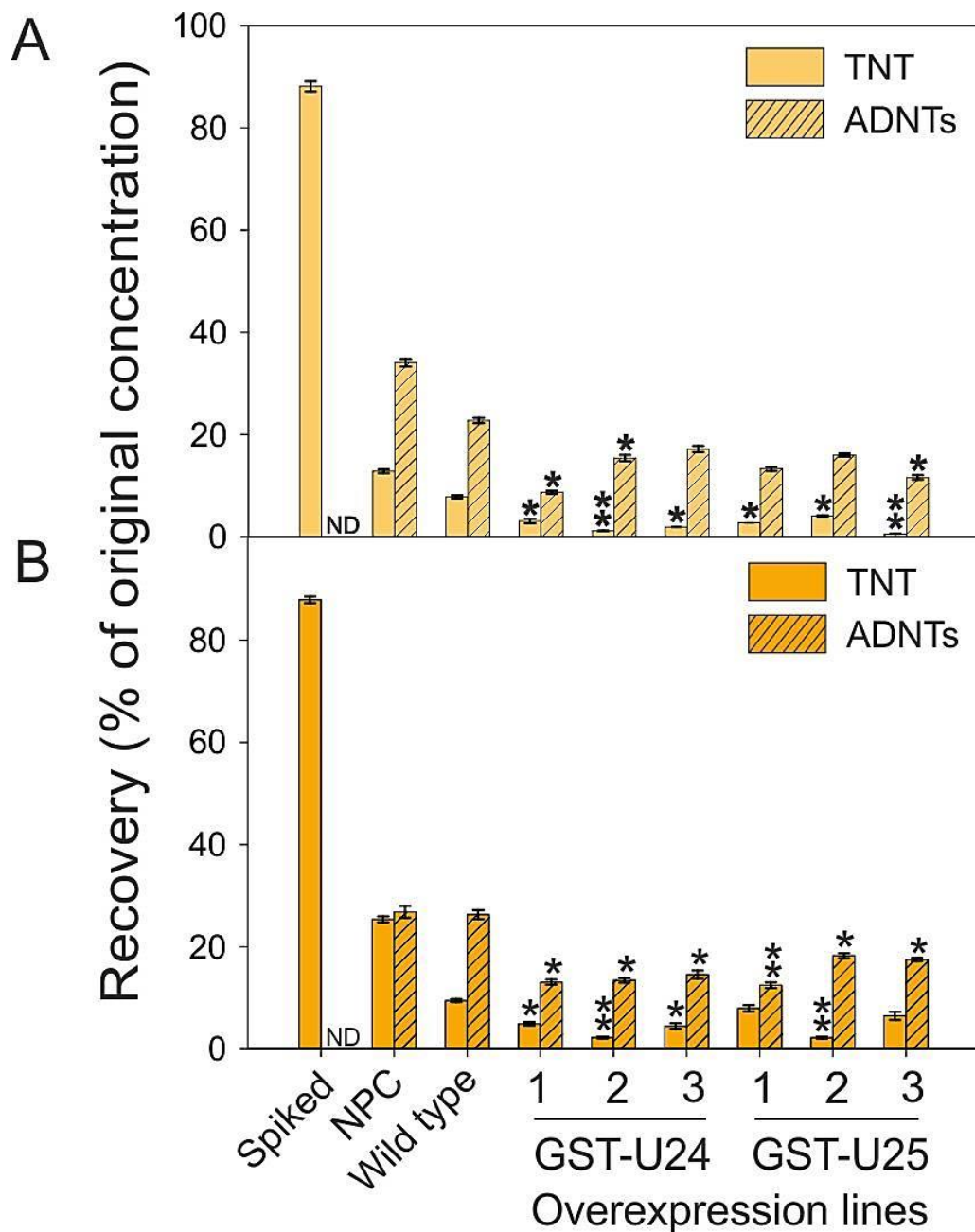


Figure 3.12: Levels of nitrotoluenes recovered from TNT-containing soil. Arabidopsis plants were grown on 25 mg kg⁻¹ (A) and 50 mg kg⁻¹ (B) TNT for six weeks. Spiked, soil dosed with TNT right before extraction to assess the extraction efficiency; NPC, no plant control; WT, untransformed plants; GST-U24 OE, independent GST-U24 over-expressing lines; GST-U25 OE, independent GST-U25 over-expressing lines; ND, not detected. Results are mean of eight biological measurements \pm se. Asterisks denote statistically significant from the WT: * $P < 0.05$, ** $P < 0.01$.

3.3.4 Glutathione abundance

As the GST over-expressing plant lines removed more TNT from soil than wild type plants, GSH levels were measured to see if there was a corresponding decrease in GSH pools resulting from the formation of TNT-GSH conjugates. GSH measurements were also carried out to ascertain whether the poor growth of the GST over-expressing lines grown in the TNT-free soil could be attributed to severe GSH depletion.

Levels of GSH were measured in the rosette leaves of plants grown in soil without TNT and in soil containing 50 mg kg⁻¹ TNT. Due to the difficulty of extracting GSH from soil-grown roots, levels of GSH in roots were determined from two-week old plants grown vertically on agar plates of TNT-free, ½ MS medium. Glutathione levels were assayed spectrophotometrically using a plate-reader protocol as described previously by Queval and Noctor [175] (see section 3.2.7).

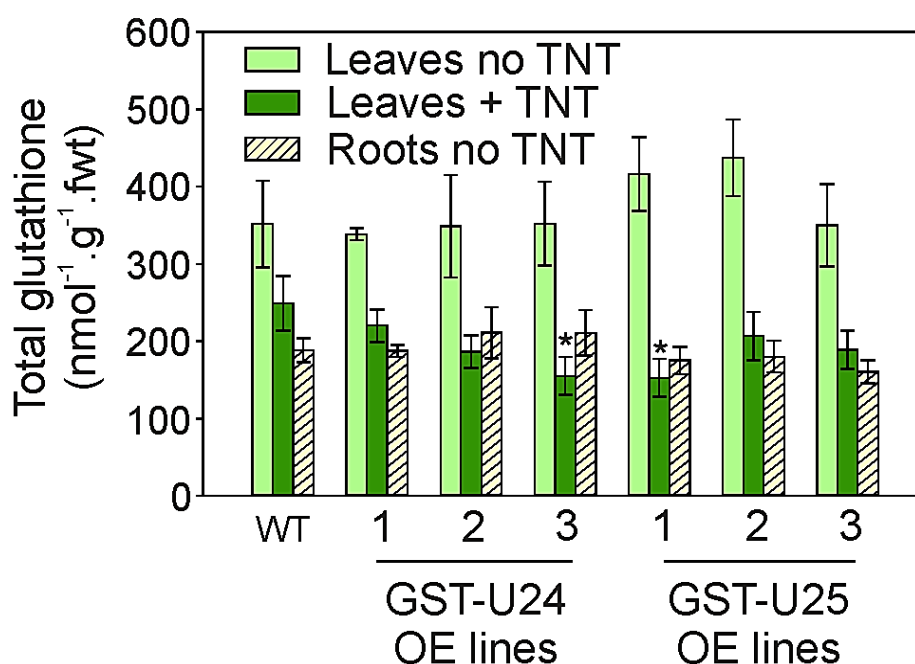


Figure 3.13: Total glutathione levels in Arabidopsis leaves and roots. Rosette leaves were from plants grown in soil without TNT, or soil containing 50 mg kg⁻¹ TNT for six weeks. Roots were from two-week old plants grown on ½ MS plus agar plates. Wild type (WT), GST-U24 and GST-U25 over-expressing (OE) lines, fresh weight (fwt). Results are means of eight biological replica \pm SD. Asterisk denotes statistically significant from the WT: * $P < 0.05$.

The results showed that when grown on agar plates without TNT, the levels of total GSH in the roots of all plant lines (including wild type) were 30-50 % lower to those in the leaves (Figure 3.13). Additionally, leaves from plants grown in TNT-containing soil had lower levels of total GSH than leaves from plants grown in TNT-free soil (Figure 3.13). Furthermore, the decrease in GSH in aerial tissues grown in TNT-containing soil relative to TNT-free soil, were all greater in the GST-U24 and GST-U25 lines (for GST-U24 lines, 35, 46 and 47 %, respectively; and for GST-U25 lines, 53, 56 and 65 % respectively) than in wild type plants (29 %).

Glutathione levels correspond to the increased conjugating activity of the GST over-expressing lines and appear to be lower than those of wild type plants. However, none of the over-expressing lines displayed severe depletion of their GSH levels. The GSH levels from plants grown on plates without TNT were comparable to those of wild type plants and were not related to the poor 'performance' of the over-expressing lines in the absence of TNT. In addition, no significant difference in the levels of GSSG or in the ratios of GSH to GSSG, in leaves or roots of the over-expressing lines was recorded when compared to wild type plants (Figure 3.14).

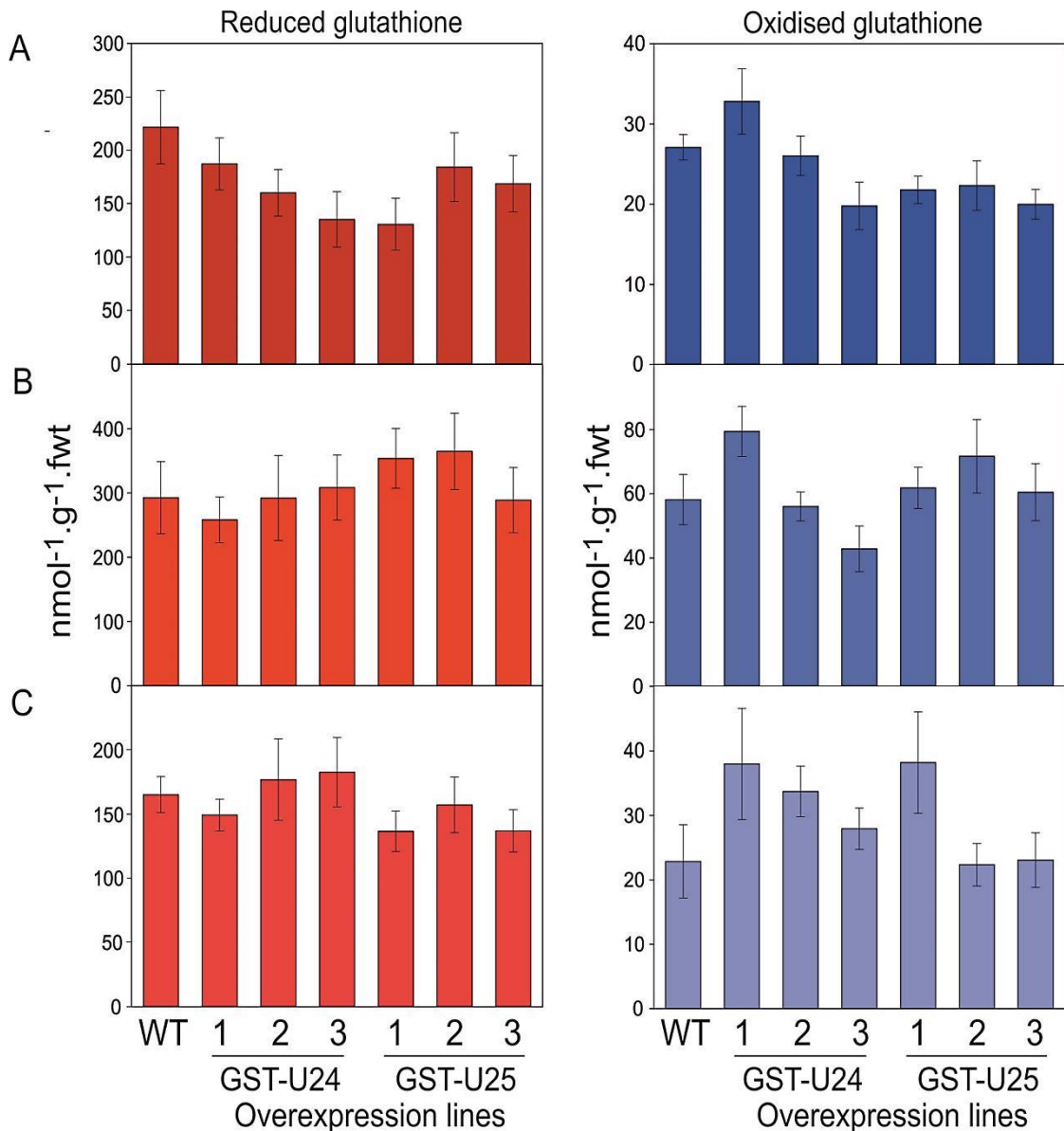


Figure 3.14: Reduced and oxidised glutathione levels in (A) rosette leaves from plants grown in soil containing 50 mg kg⁻¹ TNT. (B) Rosette leaves and (C) Roots from plants grown on TNT-free soil and TNT-free ½ MS agar plates respectively. WT, untransformed plants; GST-U24 OE, independent GST-U24 over-expressing lines; GST-U25 OE, independent GST-U25 over-expressing lines. Results are mean of eight biological measurements ± se. The data were tested for statistical significance but none of the GST-U24/U25 lines displayed GSH levels, reduced or oxidised, statistically significant from the WT.

3.3.5 GPOX activity

Substrate competition studies were conducted with purified GST-U24 and GST-U25, to compare conjugating and GPOX activity using TNT and cumene hydroperoxide as substrates respectively. Enzymes were recombinantly expressed and purified through affinity chromatography (Figure 3.15) as described in section 2.4.

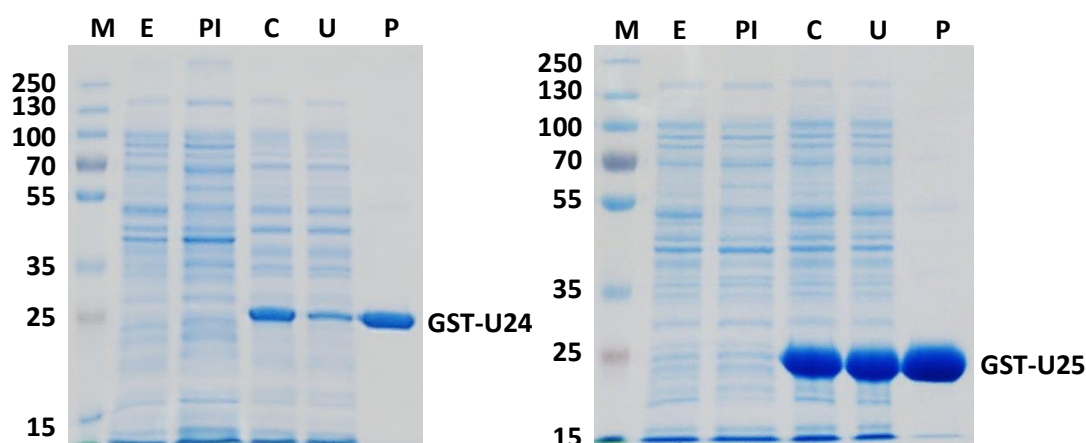
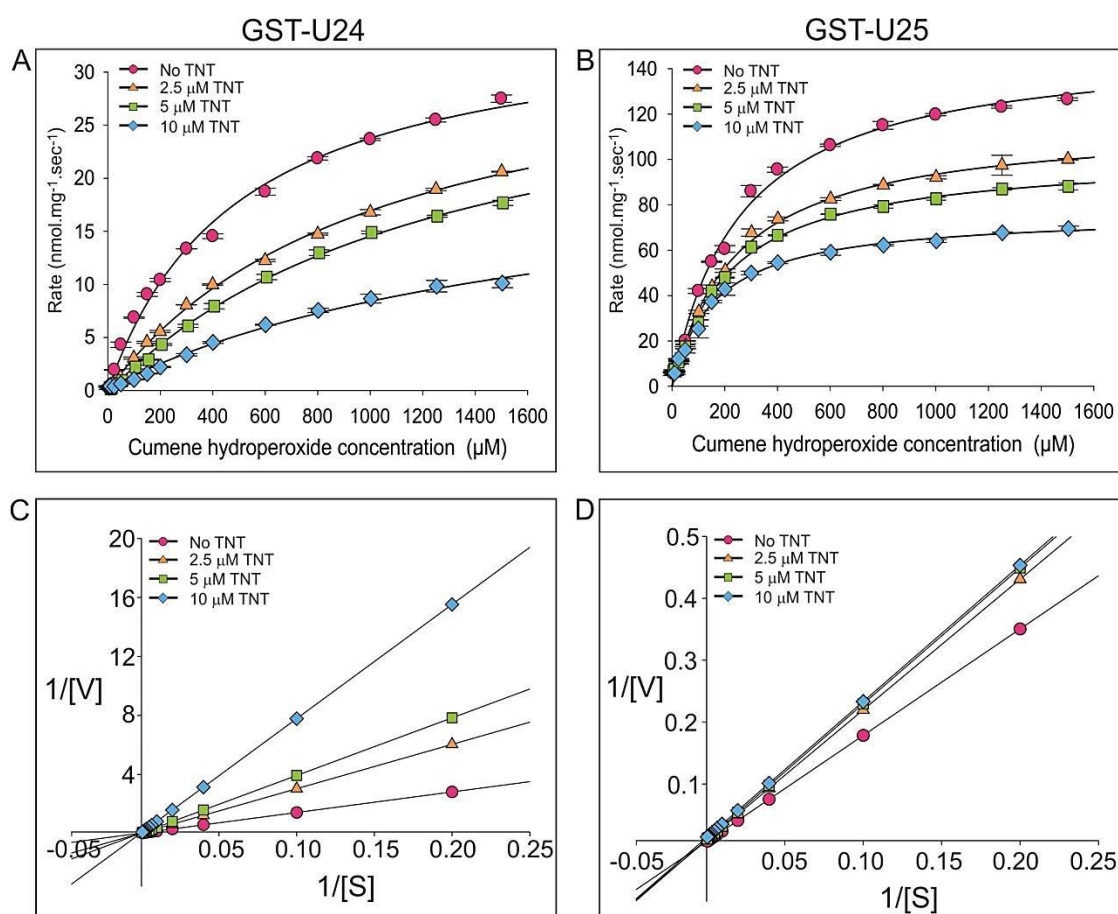


Figure 3.15: SDS-PAGE analysis of the expression and purification of (A) GST-U24 and (B) GST-U25. M, molecular weight marker (kDa); EV, crude protein extract from *E. coli* (BL21) cells transformed with empty vector; PI, crude protein extract from *E. coli* (BL21) cells cultures with optical density 0.8-1 at 600 nm prior to induction; C, crude protein extract from *E. coli* (BL21) cells after induction and ~60 h of expression; U, unbound fraction of the purification process; P, purified protein.

The results, shown in Table 3.1, revealed GPOX activities similar to those reported by Dixon et al. (2009) [87], with GST-U25 exhibiting a 2-fold lower K_m and 4-fold higher V_{max} than GST-U24. To measure the effect of TNT on GPOX activity in GST-U24 and GST-U25, GPOX activity was measured with increasing concentrations of TNT. The resulting Lineweaver-Burk double reciprocal plots demonstrate that for both enzymes, V_{max} decreases with increasing TNT concentrations (Figure 3.16C, D). For GST-U25, the K_m also decreases, while the calculated K_m values for GST-U24 increase with increasing TNT concentration.

Table 3.1: Kinetic analysis of glutathione peroxidase (GPOX) activity by GST-U24 and GST-U25 using cumene hydroperoxide as substrate.

GST	TNT concentration (μM)	K_m (μM)	V_{\max} (nkat.mg^{-1})
GST-U24	0	495.8 ± 23.8	35.5 ± 0.7
	2.5	1036.1 ± 34.5	34.5 ± 0.6
	5.0	1322.9 ± 63.5	33.9 ± 0.9
	10	1733.0 ± 221.5	22.4 ± 1.8
GST-U25	0	259.6 ± 10.4	150.9 ± 1.9
	2.5	244.0 ± 10.2	115.5 ± 1.5
	5.0	222.3 ± 8.9	101.2 ± 1.2
	10	167.0 ± 10.0	75.87 ± 1.2

**Figure 3.16:** Enzyme kinetic data for purified GST-U24 and GST-U25. Michaelis-Menten plots for (A) GST-U24 and (B) GST-U25. Lineweaver-Burk double reciprocal plots for (C) GST-U24 and (D) GST-U25 with cumene hydroperoxide as substrate. Glutathione peroxidase activity was monitored spectrophotometrically using an NADPH-linked assay. Results are means of three technical replica \pm se.

3.4 Discussion

The data presented in this chapter show that GSTs contribute to the TNT detoxification pathway in Arabidopsis, while over-expression of plant GSTs confers enhanced resistance to TNT, along with an increased ability to detoxify this environmental pollutant. The GST over-expressing lines displayed higher shoot and root biomasses than untransformed plants when grown in the presence of TNT. The reduced biomass of the GST over-expressing lines when grown in soil without TNT was unexpected and has not been previously reported. This yield drag could be the result of deleterious conjugation and/or GPOX activity. In the absence of TNT, GPOX activity could be employed to reduce organic hydroperoxides to their respective alcohols. It is also possible that the negative effects on biomass derive from depletion in the short-chain hydroxylated acid pools. Previous studies reported accumulation of short-chain hydroxylated glutathione conjugates by GST-U25 when recombinantly expressed in *E. coli* and transiently expressed in tobacco [111]. Besides their conjugation activity, GSTs have been found to selectively bind and stabilise or transport key pathway intermediates [110, 177, 178]. Since GST-U24 and GST-U25 are endogenous to Arabidopsis they could be able to bind essential internal metabolites and interfere with key pathways.

Besides the biomass measurements it was important to determine the difference in TNT uptake by the OE lines and WT plants. Higher biomass of the GST OE lines when grown in the presence of TNT suggests higher detoxification ability and further supports the involvement of GSTs in the TNT detoxification pathway, but it does not necessarily improve the TNT uptake by the plants, which is a main objective of the present study. Nitrotoluenes were extracted from soil in which GST OE lines had been grown to evaluate the remediation potential of plants. An alternative way to determine TNT uptake would be to grind the plant tissue and try to extract TNT-conjugates. However, the fact that TNT is mainly localised in the roots [65-69], glutathione conjugates are further catabolised [143, 146], and potentially incorporated in the plant biomass [26, 179] made it a more technically-challenging approach. The GST over-expression resulted in an increased ability to remove TNT from

soil, but not ADNTs, since plants appear to remove TNT preferably to ADNTs. This is in agreement with previous studies, using purified enzymes, showing that GSTs do not have activity towards the reduced derivatives of TNT [76, 165]. The recovery of most of the initial TNT concentration in the form of ADNTs is not surprising as soil-based microbial populations are well documented to reduce TNT via endogenous nitroreductases [37, 180-184]. This is further supported by the fact that no ADNTs were recovered from spiked samples (soil dosed with TNT just prior to extraction), indicating that ADNTs were created gradually over the six weeks of the experiment. Absence of HADNTs can be attributed to their low stability and further reduction to ADNTs [72, 183-185]. Since the GST OE lines remove more TNT, there is less TNT to be converted to ADNTs, which explains why ADNT levels, also, appear lower in the soil of GST OE lines than that of WT.

Nonetheless, another issue is the overall low recovery of nitrotoluenes from soil (<50 % recovery of initial amount of TNT) even in the case of the no plant controls (NPC). This could be attributed either to the fact that both TNT and ADNTs are known to bind strongly to soil organic matter [180, 186, 187] or to the soil spiking process. A study using a similar TNT spiking process to the one used in the present work (see section 3.2.3), reports recoveries from soil of 31% and 48% of the nominal TNT dose for 25 and 50 mg kg⁻¹ concentrations respectively [23]. The authors attribute most of the loss to the spiking process (dissolving TNT in acetone and evaporating in order to absorb TNT to sand). However, this claim is weakened by the fact that they did not conduct any extraction from aged soil and also previous studies used alternative spiking methods [70]. Reports where TNT-contaminated soil is directly from the field [180] also describe low TNT recoveries. The spiked samples used here (soil dosed with TNT just prior to extraction), were mainly employed to validate the efficiency of the extraction method and their 88 % recovery agrees with previous findings that 10 % of the initial TNT in soil is lost upon dosing and is no longer extractable [180, 185]. Experiments by Singh et al. (2008) [180] proved that TNT sorption to organic matter increases with time. Soil containing TNT at levels comparable to those of the present study (31 and 54 mg kg⁻¹) showed that only 30-50 % of the initial amount of

TNT was extractable after 30 days of incubation, with the recovery decreasing to 20-30% after 60 days [180]. In addition, Conder et al. (2004) [185] report a recovery of only 25-40 % of the nominal TNT dose from soil aged for 57 days. Taking into account the results presented here and the literature, it is possible to conclude that the low recovery of TNT and derivatives is a direct result of the increasing sorption of nitrotoluenes to the soil organic matter with time.

Following from the soil studies, GSH measurements showed that the GST over-expressing lines removed more TNT from soil than WT plants, with a corresponding decrease in total GSH levels. However, none of the over-expressing lines displayed severe depletion of their GSH levels; probably because glutathione reductases (GR), which are involved in sustaining GSH pools, are upregulated in response to TNT treatment [75]. As far as the GSH level measurements are concerned, the levels of total GSH recovered were in the range of ~200-500 nmol⁻¹ g⁻¹ fwt for all plant lines. Glutathione levels in unstressed wild type plants are species and tissue dependent and vary between ~300 to 1000 nmol⁻¹ g⁻¹ fwt [188-190]. In Arabidopsis, GSH levels have been found to be in the range of ~400-600 nmol⁻¹ g⁻¹ fwt for whole plant measurements [189] and in the range of ~800-1000 nmol⁻¹ g⁻¹ fwt for Arabidopsis cell suspension cultures [190]. The values in the range of 400-600 nmol⁻¹ g⁻¹ fwt are in agreement with those reported here and confirm the validity of the assay. On the other hand, the values in the range of 800-1000 nmol⁻¹ g⁻¹ fwt, reported by Meyer et al. (2001) [190] deviate significantly. This can be explained by the method utilised in that work to determine GSH levels, where a fluorescent method of labelling GSH was used, allowing quantitation of GSH *in vivo* and thus avoiding any loss of GSH that might occur during the extraction process [190]. In addition, GSH abundance was measured in suspension-culture cells during exponential growth, which are claimed to contain higher GSH levels [190].

The GPOX activity exhibited by GST-U24 and GST-U25, along with the fact that previous attempts to extract a significant amount of TNT-GST conjugates from the over-expressing lines failed [166], poses the question of whether the enhanced resistance to TNT displayed by the GST OE lines derives from the

conjugating activity or the GPOX activity of the GSTs. Glutathione abundance, on its own, cannot serve as a good indicator, since it is utilised by both activities. Substrate competition studies *in vitro* showed that TNT significantly inhibits GPOX activity for both GST-U24 and GST-U25. For GST-U25, the K_m also decreases, indicative of uncompetitive inhibition. In the case of GST-U24, the calculated K_m values increase with increasing TNT concentration. While this result is difficult to explain, it infers that TNT inhibits GST-U24 GPOX activity in a different, possibly non-competitive, way than it does for GST-U25. In addition to the inhibition of GPOX activity, the observed decrease in GSH levels in the presence of TNT derives mainly from decline in the levels of reduced GSH. The levels of GSSG (oxidised glutathione) remain relatively unaffected since GSTs can utilise only the reduced form of glutathione for conjugation. Had the GPOX activity been the primary catalytic activity of the over-expressed GSTs, and the main reason of the enhanced tolerance towards TNT, the levels of total GSH should have remained relatively stable with a corresponding change in the GSH: GSSG ratio in favour of the oxidised levels. Together, these findings indicate that the enhanced TNT tolerance observed in the over-expressing lines derives from the direct glutathionylation of TNT rather than the enhanced GPOX activity.

Studies with knockout (KO) lines would be interesting and could further support the involvement of GSTs in the detoxification of TNT, but it is highly likely that they would not display any significant difference to WT plants. In the past, root length studies with GST-U24 KO lines displayed no difference to WT plants in the presence of TNT [191]. The high number of endogenous GSTs and their wide substrate specificity make overlapping *in vivo* activity towards TNT very likely. Besides GST-U24 and GST-U25, additional GSTs have been found to be upregulated in response to TNT (GST-U19) [75], suggesting that other GSTs could have activity towards the explosive. The upregulated GST-U19 shares 76 and 72% homology with GST-U25 and GST-U24 respectively. This homology is higher than all of the GSTs that were found to be upregulated in response to TNT by the microarray analysis in our laboratory, suggesting that GST-U19 could have activity towards TNT.

Finally, over-expression of plant GSTs has been found to confer resistance to a number of biotic and abiotic stresses [84, 85]. With that said, it is possible that GST-U24 and GST-U25 over-expressing lines also have resistance against other xenobiotics, and this should be tested. Member of the Tau class GSTs are particularly associated with herbicide detoxification [84].

Chapter 4: Biochemical characterisation of a TNT detoxifying *Drosophila* GST and recombinant expression in *Arabidopsis*

4.1 Introduction

This chapter describes the characterisation of a *Drosophila melanogaster* GST (*DmGSTE6*) that was known to have activity towards TNT (Professor Bengt Mannervik, University of Stockholm, pers. comm.) and the subsequent engineering of transgenic *Arabidopsis* plants. The GST belongs to the Epsilon class and shares only 24 and 23 % protein sequence identity to GST-U24 and GST-U25 respectively.

The *D. melanogaster* GST superfamily has been annotated, identifying 36 genes, of which four undergo alternative splicing, to yield a total of 41 GST proteins [192]. These proteins are encountered, as with plant GSTs, as homo- or hetero-dimers with monomers of approximately 25 kDa in size [193]. The *D. melanogaster* GSTs can be split into seven distinct classes, Theta, Omega, Sigma, Zeta, Delta and Epsilon. The relatively high degree of conservation of GST genes belonging to Zeta, Theta, and Omega classes across taxa suggests that they play essential roles in conserved physiological pathways. The Delta and Epsilon class GSTs are the most closely related, and the most numerous, with a total of 25 genes for the two classes combined. These two classes appear to be present mainly in insects and other arthropods [194-198]. One apparent function of Delta and Epsilon classes in *Dipteran* organisms is to confer resistance to insecticides [193, 199]. In addition, enzymes of these two classes were able to conjugate a variety of physiological substrates [192]. Their catalytic diversity and overlapping

substrate specificities suggest that enzymes from these classes would have major roles in detoxification [192].

The *D. melanogaster* Epsilon class genes (14 in number) are all located on chromosome 2R, with most of them in close proximity, indicating that the cluster was probably formed by repeated duplication events [192, 200]. The *DmGSTE5* and *DmGSTE6* genes are located next to each other and are the two GSTs that diverged most recently on an evolutionary time scale according to phylogenetic analysis [200].

Epsilon class GSTs, with the exception of *DmGSTE8*, are expressed in soluble forms as shown by heterologous expression in *E. coli* [192]. All 14 members of this class are able to catalyse the conjugation of the generic GST substrate 1-chloro-2,4-dinitrobenzene (CDNB), with *DmGSTE6* exhibiting the third highest conjugation activity [192]. Assays for glutathione peroxidase activity (GPOX), using arachidonic acid 5-hydroperoxide (5S)-HpETE, showed that most Epsilon class GSTs are not capable of GPOX activity, or in the case of *DmGSTE6*, exhibit very low activities [192]. This chapter focuses on the biochemical characterisation of *DmGSTE6* and its value for the phytoremediation of TNT.

4.2 Methods

4.2.1 Cloning of *Dm*GSTE6 in pET-YSBLIC3C

For the expression of *Dm*GSTE6, a variant of the LIC vector based on the Novagen plasmid pET-28a, named pET-YSBLIC3C [201] was employed. The gene sequence was amplified through PCR from the pJexpress401:69884 vector using the primer set given in Table 4.1. The PCR amplification was performed with a PCR cycle of 98 °C for 30 s, and 32 cycles of 90 °C for 15 sec, 52 °C for 30 s and 72 °C for 1 min followed by a final extension at 72 °C for 10 min. A PCR aliquot was run on a 1.2 % (w/v) agarose gel to confirm the success of the amplification, while the remaining PCR product was purified using Wizard® SV Gel and PCR Clean-Up System (Promega) according to the manufacturer's instructions.

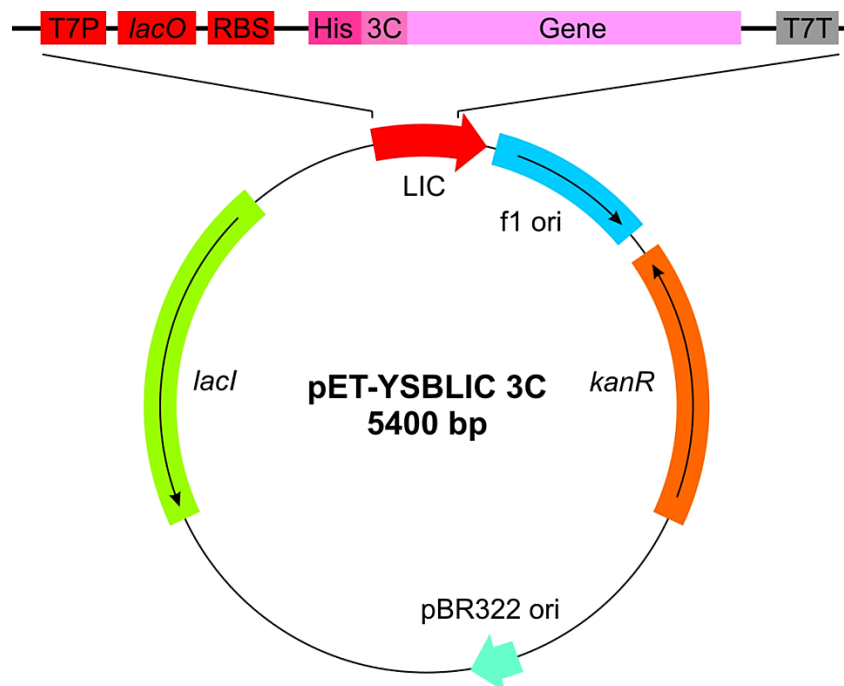


Figure 4.1: Vector map of the pET-YSBLIC 3C plasmid bearing the gene insert. The plasmid has two origins of replication (f1 ori and pBR322 ori), a kanamycin resistance gene (*kanR*), and a repressor gene (*lacI*) for IPTG induction. The cloning site comprises a T7 promoter (T7P) and a T7 terminator (T7T), a Lac operator (*lacO*), a ribosome binding site (RBS) and a 6x His-tag (His) which can be cleaved at the HRV 3C protease site (3C).

Table 4.1: Primers for cloning *DmGSTE6* in pET-YSBLIC3C. Red colour indicates the vector specific sequence of the primer; black colour indicates the gene specific sequence of the primer.

Primer name	Sequence (5' -> 3')
dGST_LICF1 (forward)	CCAGGGACCAGCAATGGTTAAACTGACTTTGTACGGTCTGGAC
dGST_LICR1 (reverse)	GAGGAGAAGGCGCGTTATCATTAAAGCCTCAAACGTAAAGTTCGTT

The pET-YSBLIC3C vector was linearised by digestion with the *BseRI* restriction enzyme. The digestion was carried out with 5 µg of vector, 20 U of *BseRI* (New England Biolabs) and 1x NEB buffer 2 in a final volume of 100 µl for 3 h at 37 °C. After digestion, the linearised vector was run on a 1 % (w/v) agarose gel and gel purified using the Wizard® SV Gel and PCR Clean-Up System (Promega). The purified PCR product was cloned into the purified, linearised pET-YSBLIC3C vector using the In-Fusion Cloning Kit (Clontech) according to the manufacturer's instructions. The cloning reaction was then transformed into *E.coli* cells (see section 2.2.4), the cells were spread on LB-agar plates containing kanamycin (50 µg/ml) and incubated at 37 °C O/N. Liquid cultures containing kanamycin were set up the following day from individual colonies and were incubated at 37 °C O/N. Cells were then pelleted by centrifugation at 5,000 rpm for 10 min and plasmid preparation was done using the QIAprep Spin Miniprep kit (Qiagen), according to the manufacturer's instructions. Successful cloning was confirmed by sequencing of the purified plasmid (see section 2.3.4).

4.2.2 Expression and purification of *DmGSTE6*

Expression, purification and quantification of *DmGSTE6* were conducted as previously described in section 2.4.

4.2.3 Kinetic assay with CDNB

The conjugating activity of purified recombinant *DmGSTE6*, was assayed using CDNB. The resulting conjugate, CDNB-GS, absorbs at 340 nm, allowing

monitoring of the reaction spectrophotometrically. The reaction was performed at 25 °C in 1 ml cuvettes with a Varian Carry[®] 50 Bio UV-Vis Spectrophotometer. The reaction mix consisted of 100 mM potassium phosphate buffer pH 6.5, 5 mM GSH, 500 ng of purified *DmGSTE6* and 0-1250 µM CDNB. The reaction was initiated by the addition of CDNB and monitored over a minute. Each reaction was performed in triplicate. The K_m and V_{max} Michaelis-Menten parameters were calculated using Sigma Plot 12.0.

4.2.4 TNT activity assay

Since the solubility limit of TNT in aqueous solutions is approximately 512 µM [202] at 20 °C, to ensure complete solubilisation of TNT, 200 µM was chosen as concentration for the reaction. Potassium phosphate buffer was used since it was shown in the past that it does not impair the activity of the enzyme and produces consistent results [166]. To establish the rate of non-enzymatic conjugation, a control reaction containing enzyme denatured by heating to 95 °C for 5 min (boiled control) was included. Preliminary assays to establish the optimal amount of enzyme for all reactions showed that 10 µg of enzyme produced consistently detectable levels of conjugate products. Reactions to assay pH and temperature optima for *DmGSTE6* were set as follows. For the pH screening the assay was performed in 100 mM potassium phosphate buffer pH 5.5-9.5 at room temperature, with 10 µg of enzyme and 5 mM GSH in a final volume of 250 µl. The temperature screening assay was performed as for the pH assay but using 100 mM potassium phosphate buffer pH 9.0 and temperatures from 4 -60 °C. Reactions, initiated by the addition of TNT, were performed in triplicate and run for 0, 10, 30, 45 and 60 min, then stopped by the addition of TCA to a final concentration of 10% (v/v), to precipitate the protein and terminate the reaction. After centrifugation at 13,000 rpm for 10 min, samples of the reactions were analysed by HPLC using a Waters Alliance 2695 separation module with a Waters 2996 photodiode array detector, according to the method and conditions given in Table 4.2. The expected retention times are the following: TNT- 30.9 min, Conjugate 1- 16.7 min, Conjugate 2- 20.2 min, Conjugate 3- 21.0 min. Integration was

performed at 250 nm with Empower Pro Software. Total conjugate concentration was plotted against time and the rate of each reaction was calculated from the slope of the curve ($y = ax$).

Table 4.2: HPLC conditions optimised for Waters X-Bridge C18 column

Sample temperature: 25 °C		
Column temperature: 25 °C		
Injection volume: 40 µl		
Mobile phase A: acetonitrile		
Mobile phase B: H ₂ O + 0.1 % formic acid		
HPLC gradient: 0 min	5 % A	95 % B
5 min	5 % A	95 % B
25 min	40 % A	60 % B
30 min	100 % A	0 % B
35 min	5 % A	95 % B

4.2.5 Kinetic assay with TNT

Contrary to the kinetic analysis of *Dm*GSTE6 with CDNB, there are currently no methods to measure spectrophotometrically the conjugation of TNT to GSH, thus for the kinetic assay with TNT, HPLC analysis was employed as described in section 4.2.4. Reactions were carried out at the optimal conditions for *Dm*GSTE6 activity as identified by the pH and temperature screening (100 mM potassium phosphate buffer pH 9.0 at 30 °C with 10 µg of enzyme, 10-3000 µM TNT, and 5-45 mM GSH in a final volume of 250 µl). To ensure complete solubility of TNT in the reaction, stock TNT concentrations were prepared in DMSO and consistently 5% of the TNT stock solution was added to the final volume of the reaction, as this volume was found not to affect the activity of the enzyme [166]. Reactions were performed in triplicate, terminated using TCA, and TNT conjugates quantified using HPLC as described in section 4.2.4. The K_m and V_{max} Michaelis-Menten parameters were calculated using Sigma Plot 12.0.

Purified recombinant GST-U25 was used as a positive control in the experiment since it is able to produce all three conjugates. The GST-U25 reactions were performed at 30 °C in 100 mM potassium phosphate buffer pH 7.0 with 150 µg GST-U25, 200 µM TNT and 5 mM GSH in a final volume of 250 µl.

4.2.6 LC-MS analysis of conjugation products

Mass spectrometry analysis of TNT and derivatives was performed using a Finnigan Surveyor Autosampler Plus, Finnigan Surveyor LC pump Plus, Finnigan Surveyor PDA Plus detector, an LCQ detector Finnigan MAT 2.0 (all from Thermo Electron Corporation) and a Waters X-Bridge C18 column (250 x 4.6 mm, 5 µM). Electrospray Ionisation (ESI) was used for the production of ions in negative mode with mass range 100-1000. Data were analysed and integrated with Excalibur 2.0 SUR 1 software. For the LC analysis, a 50: 50 H₂O: methanol isocratic method, with a 20 µl injection volume was used for samples extracted from soil, and a 48: 52 H₂O: methanol isocratic method, with a 20 µl injection volume for samples from hydroponic cultures.

4.2.7 HADNTs and ADNTs activity assay

To test the activity of *Dm*GSTE6 towards HADNTs, assays were performed in 100 mM potassium phosphate buffer pH 7.0 or 9.0 at 30 °C, with 10 µg of enzyme, and 5 mM GSH in a final volume of 250 µl. Reactions were initiated by the addition of either 50 µM 2/4-HADNT or 200 µM 2/4-ADNT, terminated using TCA and TNT conjugates quantified using HPLC as described in section 4.2.4. The concentration of HADNTs used was lower than the ADNTs due to expense and supply limitations. The expected retention times are the following: HADNTs- 30.2 min, ADNTs- 29.2 min.

4.2.8 GPOX activity

The GPOX assay was performed as described in section 3.2.8 with 10-150 µg of enzyme.

4.2.9 Expression of *DmGSTE6* in *Arabidopsis*

Agrobacterium mediated transformation was used to transform *Arabidopsis thaliana* (*Arabidopsis*) plants. *Agrobacterium tumefaciens* GV3101 was transformed with the binary vector pART27, carrying the *DmGSTE6* gene, through electroporation (see section 2.2.5). Following transformation, 20 µl of the cells were spread on LB agar plates, containing gentamycin and spectinomycin (50 µg/ml) and were incubated at 30 °C for 3 days. Colony PCR was carried out to further confirm the presence of the gene. Single colonies were then inoculated in 10 ml LB with gentamycin and spectinomycin, at the same concentrations as before, at 30 °C with 180 rpm shaking for 2 days. The 10 ml cultures were transferred in 2 L flasks containing 500 ml of LB (with both antibiotics) and were grown O/N at 30 °C with 180 rpm shaking. Cultures were transferred to centrifuge bottles and centrifuged in a Sorvall centrifuge at 5000 rpm for 10 min. Supernatant was discarded and pellets were re-suspended in the same volume (500 ml) of 5% sucrose plus 0.05% Silwet surfactant (Helena chemicals) solution (or 1% Triton X-100 surfactant). The flowers of 10 pots (10 seedlings per pot) were dipped into the *A. tumefaciens* solution for approximately 30 s before being put on a tray, covered with an autoclave bag (to prevent *agrobacterium* from spreading to other plants) and taken to the growth rooms. The following day the autoclave bag was removed and the plants were transferred to the greenhouse in order to grow. In due time seeds were collected and successful transformants were selected on ½ MS plates with kanamycin (see section 2.5.3.2).

4.2.10 Protein extraction from plant tissue

Protein extraction from plant tissues was conducted as previously described in section 3.2.1.

4.2.11 CDNB activity assay on plant protein extract

The CDNB activity assay on plant protein extract was conducted as previously described in section 3.2.2.

4.2.12 Griess assay

The Griess assay is a colorimetric assay which detects the presence of free nitrite produced during a reaction. The assay relies on a diazotization reaction, first described by Griess in 1879 [203]. During the reaction, free nitrite reacts, under acidic conditions, with sulfanilamide to form a diazonium cation which subsequently couples to the aromatic amine N-(1-naphthyl)ethylenediamine (NED) to produce a red-violet coloured, water-soluble azo dye with a maximum absorbance at ~540 nm (Figure 4.2) [204]. The change in absorbance allows the quantification of free nitrite, and thus conjugate 3 production, spectrophotometrically.

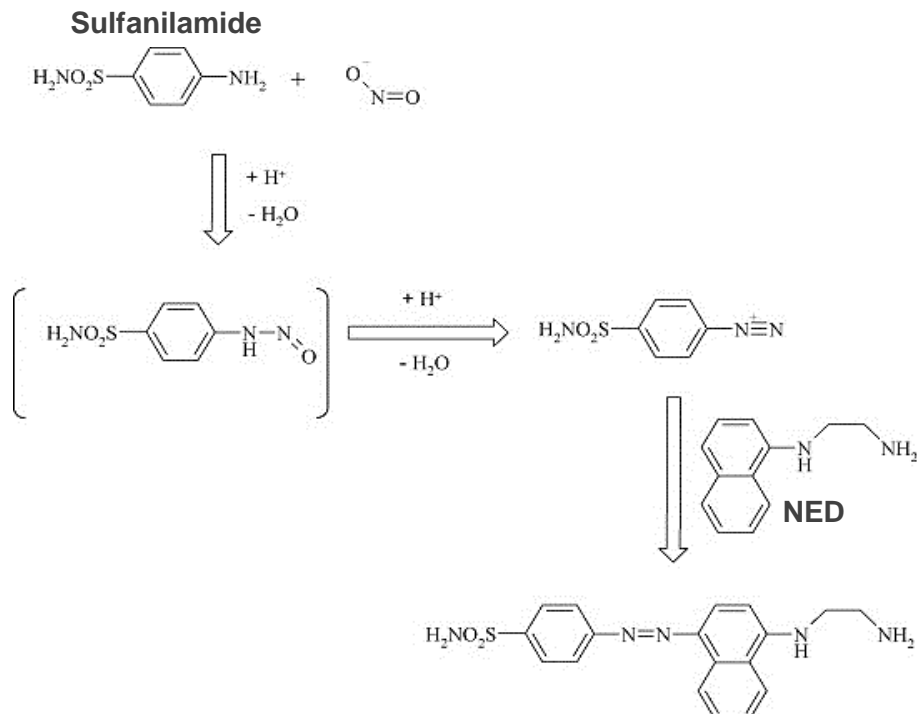


Figure 4.2: The chemical reactions of Griess assay. Free nitrite reacts with the amino group of sulfanilamide, under acidic conditions, to form the diazonium cation, which couples to N-(1-naphthyl)ethylenediamine (NED) in *para*-position to form the corresponding azo dye [204].

The assay was used to determine the amount of conjugate 3 produced during nucleophilic substitution of a NO_2^- group from TNT by GSH, as shown in Figure 3.2. The TNT conjugation reactions were performed in triplicate on a 96-well-plate for 3 h at 20 °C in 100 mM phosphate buffer (pH 6.5, 8 and 9.5), with 5mM GSH in a total volume of 180 μl . The corresponding enzyme concentrations were 300 μg for GST-U24 and GST-U25, and 10 μg for *DmGST*E6. Reactions were initiated by the addition of 500 μM TNT and stopped by the addition of TCA to a final concentration of 10% (v/v). The TNT concentration of 500 μM was chosen this time in order to compare with published data and ensure there was enough TNT present to give strong coloration. After the reaction was stopped, 50 μl of acidified sulfanilamide were added to the solution and the samples incubated at room temperature, in the dark, for 10 min. After that period 20 μl of half-strength N-(1-naphthanyl)ethylenediamine (NED) solution were added and the solution incubated at room temperature for a further 10 min. The amount of free nitrite was measured spectrophotometrically at 540 nm on a Sunrise™ Tecan plate reader. Quantification of the samples was done using a standard curve produced with 0-100 μM NaNO_2 (Figure 4.3). Nitrite concentration can be calculated from the absorbance at 540 nm using the following equation: $c = (A-0.0171)/0.0213$.

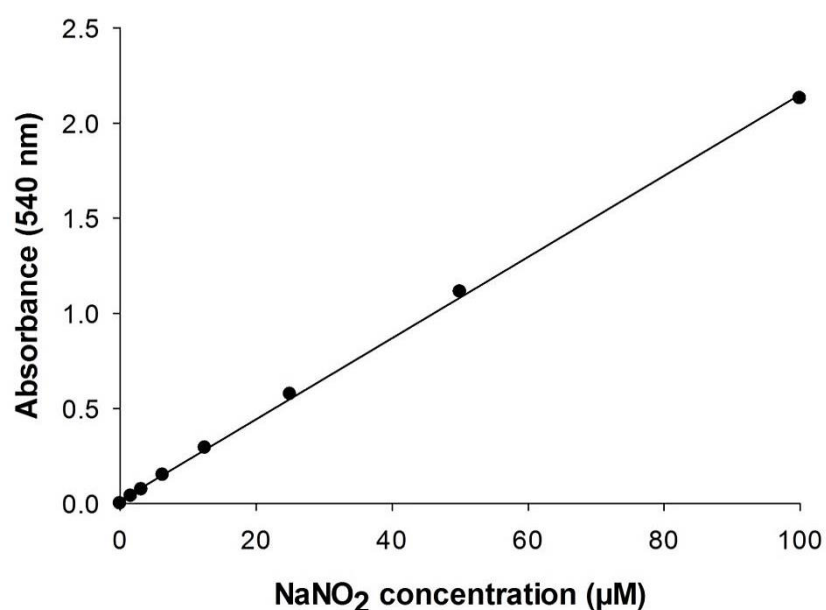


Figure 4.3: Standard curve of nitrite concentration versus absorbance at 540 nm.

Plant protein extracts were assayed in a similar manner, using 50 µl of plant protein extract from two-week-old plants grown on TNT-free ½ MS agar plates, in a total volume of 180 µl.

4.2.13 RT-PCR

Independent T3 generation plants transformed with *DmGSTE6* were grown on soil alongside WT plants for three weeks. Leaf tissue was ground in liquid nitrogen and total RNA was extracted using the Isolate II RNA plant kit (Bioline), according to the manufacturer's instructions. The extracted RNA was reverse transcribed to cDNA with SuperScript II Reverse transcriptase (RT) (Life technologies) according to the manufacturer's instructions, using oligo(dT)₁₂₋₁₈ primers. Once cDNA concentrations had been determined, an efficiency test was performed with 4 logs of cDNA concentration (0.04, 0.4, 4, 40 ng) to test that the designed primers for the real-time (RT) PCR were suitable, and to determine the appropriate cDNA concentration for the assay. The primers for *DmGSTE6* were designed based on the published *DmGSTE6* cDNA sequence and are given in Table 4.3. The RT PCR reactions were performed in 96 well plates with five biological replicates and three technical replicates for each plant line. The reaction was conducted in nuclease free water with 4 ng of cDNA, 0.2 µM of forward and reverse primer, 10 µL Power SYBR Green Mix (Applied Biosystems) in a final volume of 20 µl. Plates were briefly centrifuged (2 min) at 5000 x g before being placed in a 7000 sequence detection system RT-PCR machine (Applied Biosystems). Cycle conditions were 20 sec at 95 °C, then 40 cycles of 3 sec at 95 °C, followed by 30 sec at 60 °C and a melt curve stage at 95 °C for 15 sec, then 60 °C for 1 min and 95 °C for 15 sec. The results were normalized against the values obtained for the *ACTIN2* gene (At3g18780), conventionally used as the endogenous control.

Table 4.3: Primers used for RT-PCR. Amplification of *DmGSTE6* with the primers given below, gives a product of 139 bp.

Primer name	Sequence (5' -> 3')
dqPCR1_F (forward)	GGACGACGGTCACTACATCT
dqPCR1_R (reverse)	GCCGCTTTCAAATGCAGAC
qActinF (forward)	TACAGTGTCTGGATCGGTGGTT

qActinR (reverse)	CGGCCTTGGAGATCCACAT
-------------------	---------------------

4.2.14 Root length studies and analysis

In order to measure the effect of TNT on *Arabidopsis* root length, approximately 20 sterile seeds were placed in single rows on ½ MS agar plates containing a range of TNT concentrations (dissolved in DMSO; final DMSO concentration 0.05% (v/v)). The seeds were stratified as described in section 2.5.2, germinated and then grown vertically for twenty days. Photographs of the seedlings were taken normally after 10 and 20 days unless stated otherwise in the text. Quantification of these results was carried out by ImageJ software for up to 10-day-old seedlings (results expressed as root length in mm) and Adobe Photoshop software was used for 10 to 20-day-old seedlings (results expressed as root surface area in pixels). For the analysis with ImageJ (1.48v), image spatial calibrations were provided by a ruler included in each picture (calibrated over 50 mm of the ruler). For the analysis with Adobe Photoshop, pre-analysis processing of the pictures with Camera Raw 6.0 software was required to isolate the roots and remove any reflections/background, using the following parameters:

Exposure: +0.46
Fill light: 36
Black: 59
Contrast: +2
Clarity: +38

4.2.15 TNT-containing soil preparation

The TNT-containing soil preparation was conducted as previously described in section 3.2.3.

4.2.16 Soil studies

The TNT-containing soil studies were conducted as previously described in section 3.2.4.

4.2.17 Extraction of TNT and derivatives from soil

The TNT and derivatives extraction from soil was conducted as previously described in section 3.2.5.

4.2.18 Hydroponic culture setup

The axenic hydroponic culture setup was based on the method of Kumari et al. [205] with the following modifications: Rafts composed of lightweight plastic, 70 mm in diameter and 6 mm thick, bearing approximately 100 holes (3-4 mm in diameter). The holes of the rafts were filled with $\frac{1}{2}$ MS agar, and then ten seeds were pipetted onto the holes of each raft. The seeded rafts were subsequently stratified for 3 days at 4 °C and placed inside sterile jars containing 150 ml $\frac{1}{2}$ MS medium. The plants were grown for 20 days under $100 \mu\text{mol m}^{-2} \text{s}^{-1}$ light with a 16 h photoperiod, with 21 °C and 18 °C day and night temperatures respectively. After that period the medium was replaced with 60 ml of $\frac{1}{2}$ MS medium containing 50 μM TNT. Samples were collected at regular time-points and analysed by HPLC. The method employed was an isocratic method of 48:52 H₂O: Methanol, with a runtime of 15 min per sample and TNT eluting at 11.5 min.

4.2.19 Liquid culture setup

Seeds were sterilised and stratified on $\frac{1}{2}$ MS agar plates. Plates were then moved to the growth rooms where they were allowed to germinate and grow for one week. Eight one-week-old seedlings were transferred into 100 ml conical flasks containing 20 ml $\frac{1}{2}$ MS medium plus 20 mM sucrose. Plants were grown for an additional 14 days under $20 \mu\text{mol m}^{-2} \text{s}^{-1}$ light on a rotary shaker with approximately 130 rpm shaking. After that period the medium was replaced with 20 ml $\frac{1}{2}$ MS plus 20 mM sucrose medium containing 250 μM TNT and a range of GSH concentrations (0, 100, 250, 1000 μM). Samples were collected at regular time-points and analysed by HPLC, as described in Table 4.4. The development of this method was based on previously published methods that separate efficiently GSH and GSSG [206, 207]. The

expected retention times were: TNT-17.3 min, GSH-4.9 min, GSSG-8.9 min, 2-ADNT-16.4 min, 4-ADNT-16.5 min. Integration was performed at 215 nm for GSH and GSSG and at 254 nm for TNT and ADNTs with Empower Pro software.

Table 4.4: HPLC conditions optimised for Waters X-Bridge C18 column

Sample temperature: 25 °C

Column temperature: 40 °C

Injection volume: 40 µl

Mobile phase A: acetonitrile

Mobile phase B: 50 mM NaH₂PO₄, pH 2.7 (with 85% phosphoric acid)

HPLC gradient: 0 min	0 % A	100 % B
6 min	0 % A	100 % B
11 min	50 % A	50 % B
25 min	100 % A	0 % B
30 min	0 % A	100 % B
38 min	0 % A	100 % B

4.2.20 Chlorophyll measurement

Chlorophyll was extracted by solubilisation in 80% acetone (v/v) and quantified by measurement of the absorbance at the absorption maxima for chlorophylls *a* and *b* (663 and 645 nm respectively), as based on the method of Arnon. [208]. The following equation was then used to relate absorbance to the amount of chlorophyll in the acetone extract:

$$\text{Chlorophyll conc. } (\mu\text{g/ml}) = 20.2 (A_{645}) + 8.02 (A_{663})$$

In more detail, 100 mg of fresh tissue were grinded in 500 µl of 80% acetone using pestle and mortar. Throughout the procedure, where possible, the samples were kept chilled and in the dark. After grinding samples were

centrifuged at 14,000 rpm for 2 min at 4 °C in a tabletop centrifuge. The supernatant was assayed spectrophotometrically.

4.2.21 Glutathione measurements

Glutathione measurements were conducted as previously described in section 3.2.7.

4.2.22 Glutathione depletion studies

Ten seeds of each plant line were sterilised and placed in a single row on ½ MS agar plates containing 0-1000 µM buthionine sulfoximine (BSO) dissolved in water, and plates containing 0-1000 µM BSO plus 7 µM TNT. Seeds were subsequently stratified for three days, then germinated and seedlings grown vertically for one week. Photographs of the seedlings were taken after that period. Quantification of the root length for each line was carried out as described in section 4.2.14.

4.2.23 *ggt3/1* knockout lines grown on TNT-containing media

Seeds of *ggt1-1*, *ggt3-1* and *ggt1-1/ggt3-1* knockout mutant lines (Landsberg background) [143, 144] were germinated and grown on ½ MS agar plates of 7 µM TNT concentration as described in section 4.2.21. Photographs of the seedlings were taken after 9 and 20 days. Quantification of root length and root surface was carried out as described in section 4.2.14.

4.3 Results

4.3.1 Cloning, expression and purification of *DmGSTE6*

The *DmGSTE6* gene was sub-cloned from pJexpress401:69884 into pET-YSBLIC3C to ensure a reliable and high yield expression system and that the same expression system was used for GST-U24/U25 and *DmGSTE6*. Following expression in *E. coli* and purification through affinity chromatography, the purified protein was analysed by SDS-PAGE to determine the purity of the enzyme. Results showed that *DmGSTE6*, with an expected size of ~25 kDa, was successfully expressed and purified (Figure 4.4).

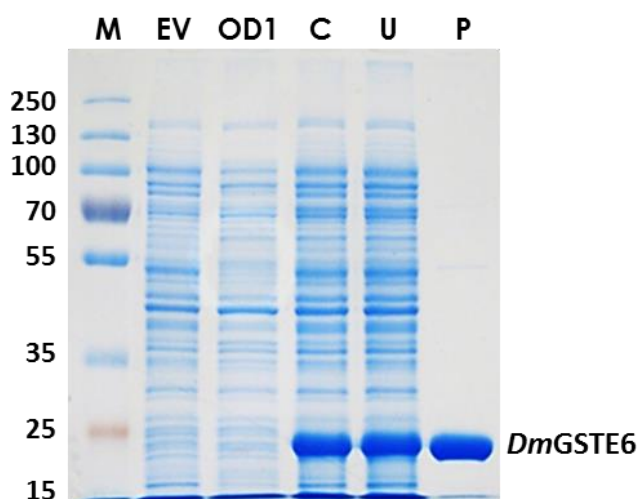


Figure 4.4: Instant *Blue* Coomassie - stained SDS-PAGE gel showing the expression and purification of *DmGSTE6*. M, molecular weight marker (kDa); EV, protein extract from cells transformed with the empty vector; OD1, protein extract from cultures with optical density 0.8-1 at 600 nm before the induction of the protein expression; C, crude protein extract from cells after the 60 h period of expression; U, unbound fraction of the purification process; P, purified protein.

4.3.2 Kinetic analysis of *DmGSTE6* with CDNB

The *DmGSTE6* K_m and V_{max} parameters, using CDNB as substrate were calculated from the Michaelis-Menten plot shown in Figure 4.5 and are given in Table 4.2. The K_m value agrees with the K_m value of 130 μ M for *DmGSTE6*

as reported by Saisawang et al [192], however, the V_{max} calculated here is more than 2-fold higher than the V_{max} calculated in that study ($208 \pm 9.21 \mu\text{mol}\cdot\text{min}^{-1}\cdot\text{mg}^{-1}$), which is unexpected result considering that the assay was executed in the same way.

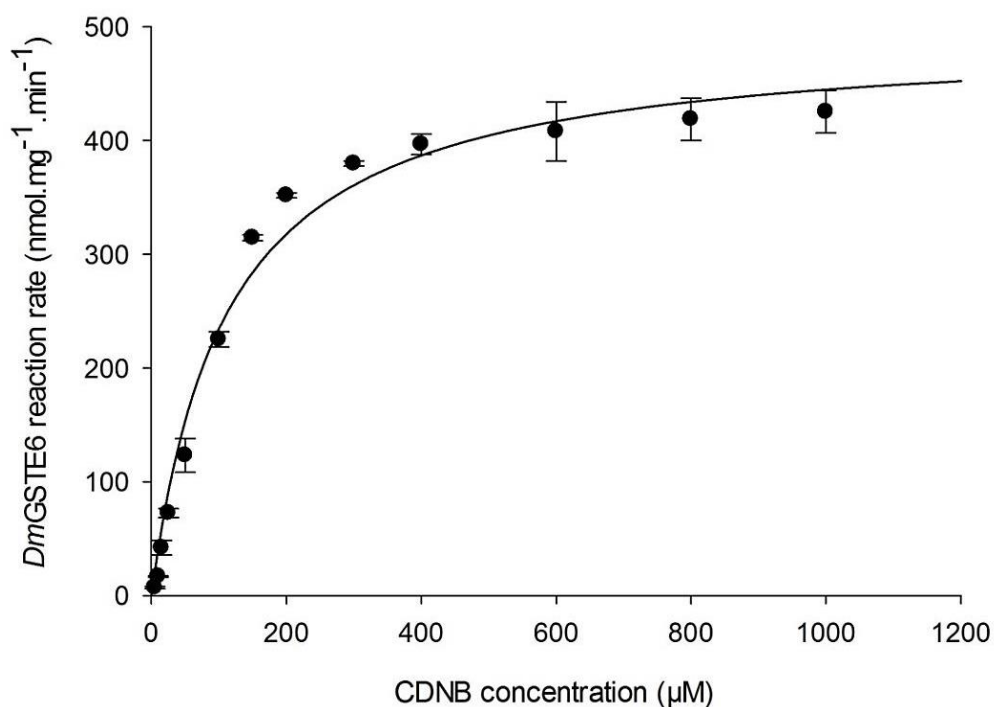


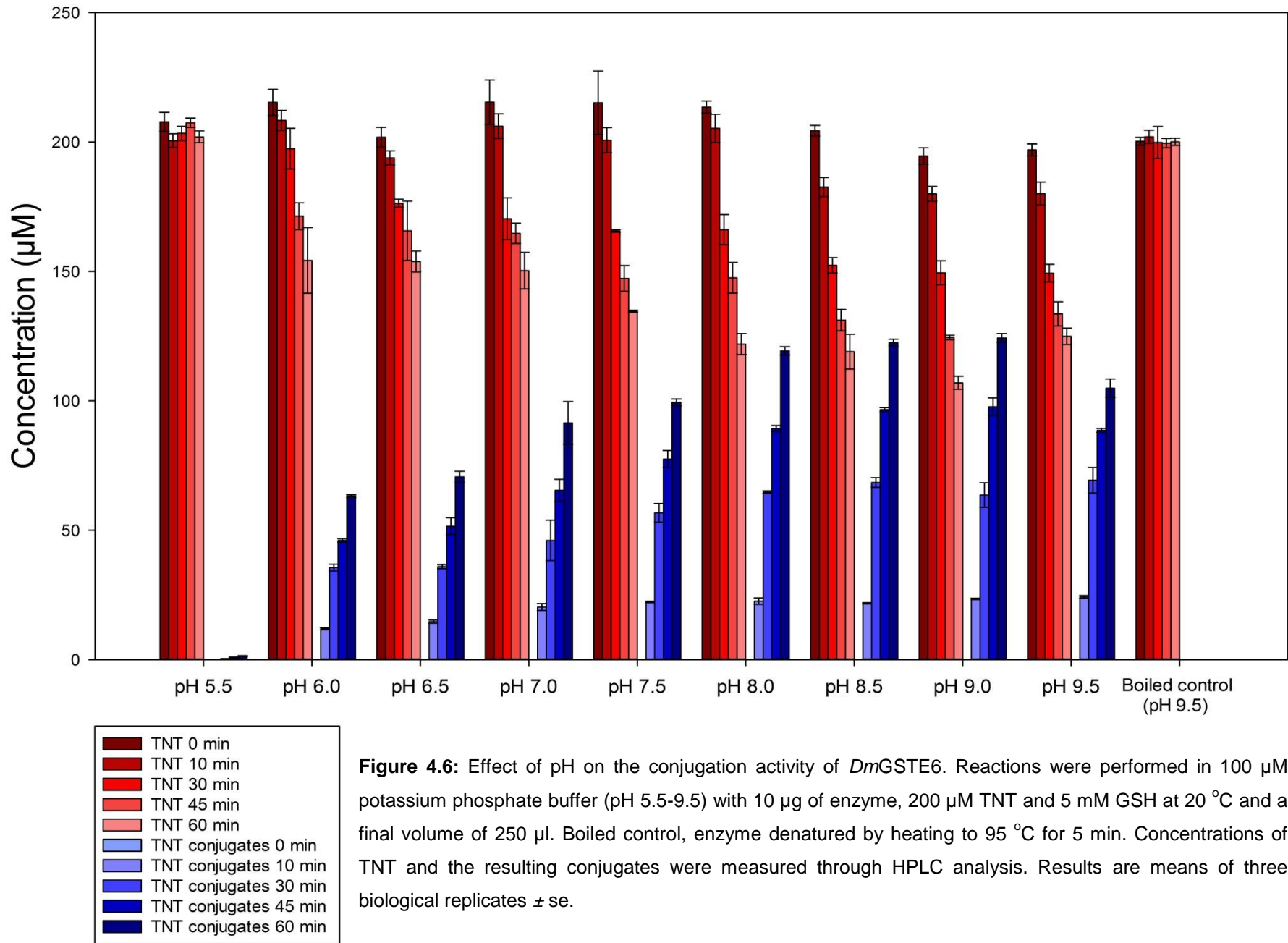
Figure 4.5: Michaelis-Menten plot of *DmGSTE6* with CDNB. Rate of conjugate production was measured spectrophotometrically at 340 nm. Reactions were performed at room temperature with 0.5 μg of purified enzyme, 5-1000 μM CDNB and 5 mM GSH in 100 mM of phosphate buffer pH 6.5 and a total volume of 1 ml. Values represent the mean of the reactions performed in triplicate \pm se.

Table 4.5: Kinetic analysis of CDNB-conjugating activity by *DmGSTE6*, GST-U24 and GST-U25.

Enzyme	V_{max} ($\text{nmol}\cdot\text{min}^{-1}\cdot\text{mg}^{-1}$)	K_m (μM)
<i>DmGSTE6</i>	494 ± 13.6	110.6 ± 10.7
GST-U24	38.9 ± 2.0	954.9 ± 119.6
GST-U25	28.1 ± 0.6	30.5 ± 3.1

4.3.3 Effect of pH on GST activity

The conjugating activity of *DmGSTE6* to TNT is shown in Figure 4.6. Activity increased with increasing pH, with the highest activity recorded at pH 9.0 where almost 50 % of the initial TNT was conjugated within 60 min. At higher pH values the activity started to decrease. At pH values lower than 6.0 the enzyme also displayed a strong decrease in activity. At pH 5.5 the enzyme exhibits ~1 % of the activity at pH 9.0 (Table 4.6). Of the three TNT-GSH conjugates identified, *DmGSTE6* produced almost exclusively conjugate 3 across the pH range tested (Figure 4.7). Small amounts of conjugate 2 were produced at pH 8.0 and above, while conjugate 1 was not detected. No significant changes were observed in the TNT concentration of the boiled control reactions, confirming the absence of non-enzymatic conjugation and the stability of TNT at the different pH values tested.



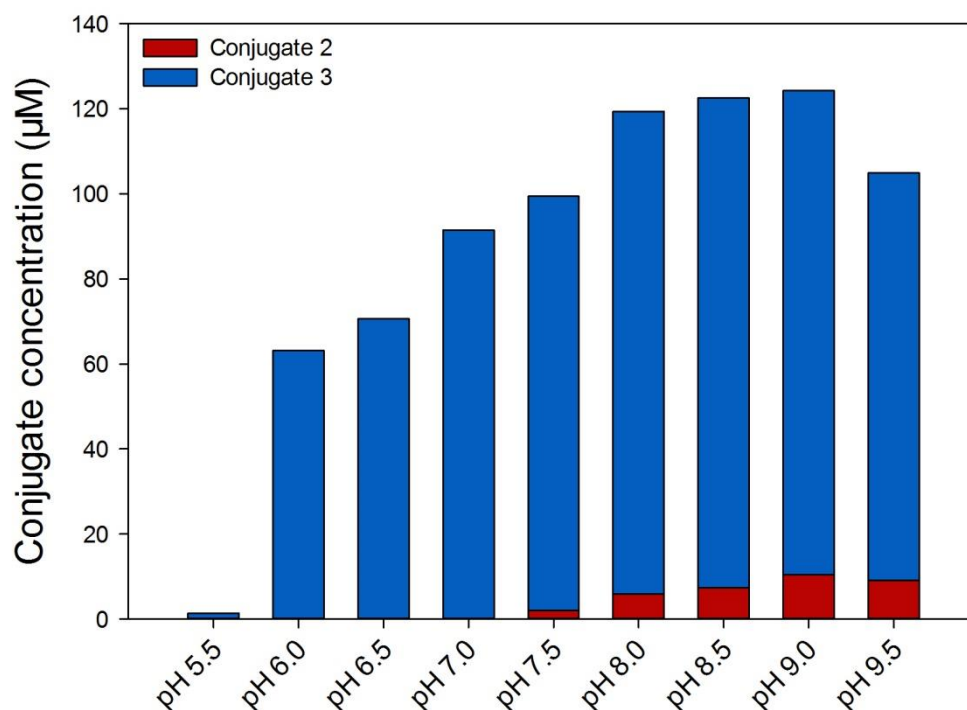


Figure 4.7: Conjugate production profile for *DmGSTE6* after 60 min incubation. Reactions were performed in 100 µM potassium phosphate buffer (pH 5.5-9.5) with 10 µg of enzyme, 200 µM TNT and 5 mM GSH at 20 °C and a final volume of 250 µl. Concentrations of TNT and the resulting conjugates were calculated through HPLC analysis. Results are means of three biological replicates \pm se.

Table 4.6: Activity of *DmGSTE6* towards TNT across the range of pH values tested. Highlighted in green is the highest activity, observed at pH 9.0.

pH	Activity (nmol.min ⁻¹ .mg ⁻¹)
pH 5.5	0.5 \pm 0.03
pH 6.0	26.6 \pm 0.14
pH 6.5	29.3 \pm 1.05
pH 7.0	37.8 \pm 2.26
pH 7.5	42.9 \pm 0.53
pH 8.0	50.3 \pm 0.34
pH 8.5	52.7 \pm 0.58
pH 9.0	52.8 \pm 1.25
pH 9.5	47.5 \pm 0.83

4.3.4 Effect of temperature on GST activity

To determine the effect of temperature and the optimum temperature for the conjugation activity of *DmGSTE6* with TNT, a range of temperatures was screened. A similar approach with the pH screening was employed, at pH 9.0, and variable temperature from 4 to 60 °C.

Results of HPLC analysis (Figure 4.8) showed that the enzyme remained active across a wide range of temperatures; at both 4 and 50 °C *DmGSTE6* was able to conjugate ~10 % of the initial TNT concentration within 60 min. Activity increased linearly to 30 °C with this temperature achieving the highest reaction rate (Table 4.7). At higher temperatures denaturation of the enzyme resulted in gradual loss of activity.

As with pH, across all temperatures tested, *DmGSTE6* produced almost entirely conjugate 3, with conjugate 2 being significantly produced at 20 to 42 °C (Figure 4.9). The increased conjugate 2 production could have been the result of the increased activity at these temperatures. However, increasing the activity at higher temperatures does not affect both conjugates equally. The conjugate 3: conjugate 2 ratio was not constant, with conjugate 2 being produced at higher amounts as temperature increased. The conjugate 3: conjugate 2 ratios for 4, 10, 20, 30, 37, 42, 50 and 60 °C were 11.2, 9.48, 6.3, 5.3, 4.75, 3.83, 3.72 and 1.64 respectively.

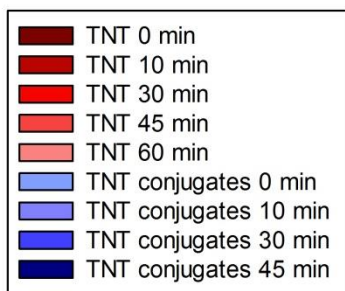
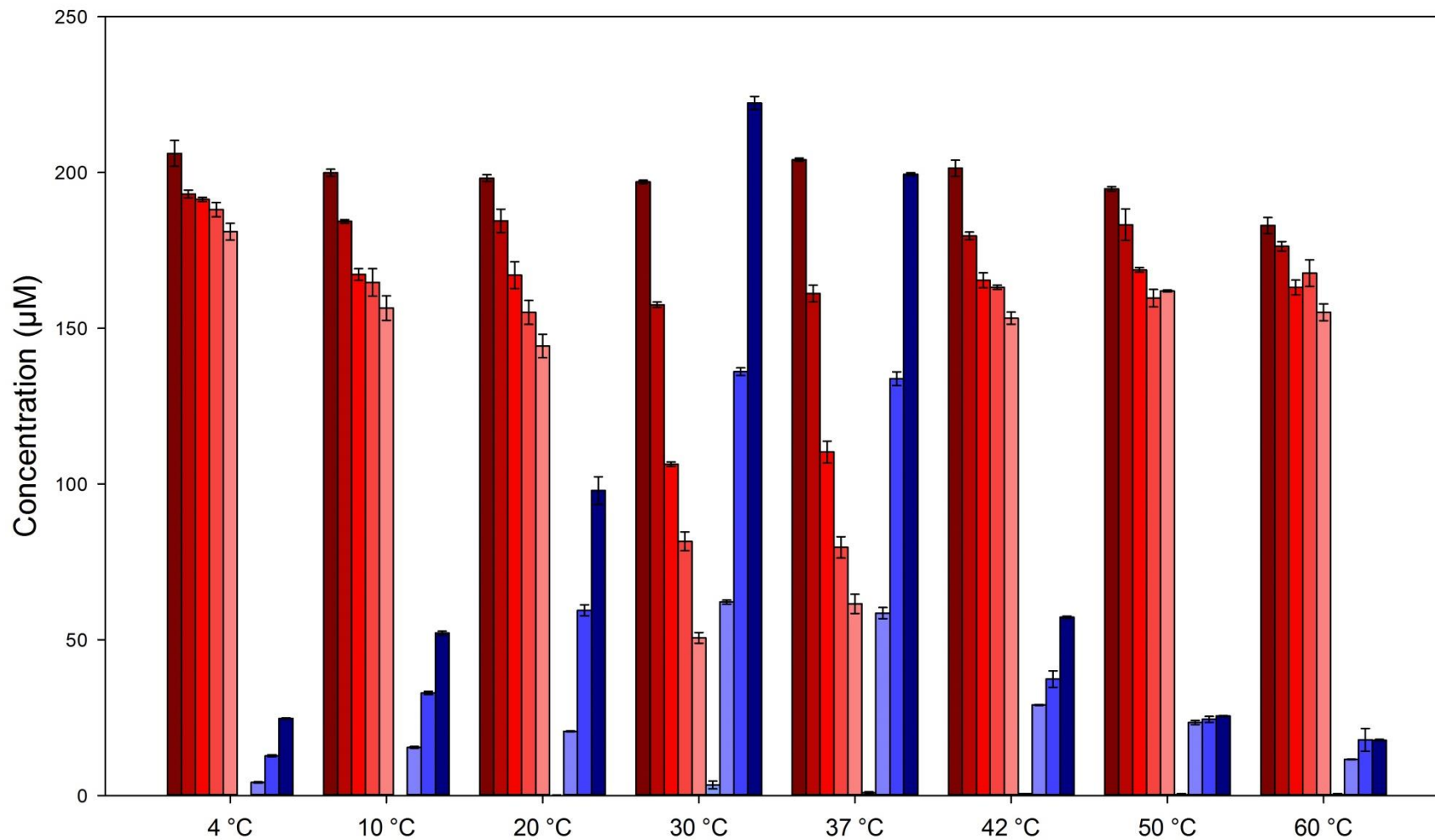


Figure 4.8: Effect of temperature on the conjugation activity of *DmGSTE6*. Reactions were performed in 100 μM potassium phosphate buffer pH 9.0 with 10 μg of enzyme, 200 μM TNT and 5 mM GSH at temperatures ranging from 4 to 60 $^{\circ}\text{C}$ and a final volume of 250 μl . Concentrations of TNT and the resulting conjugates were measured through HPLC analysis. Results are means of three biological replicates \pm se.

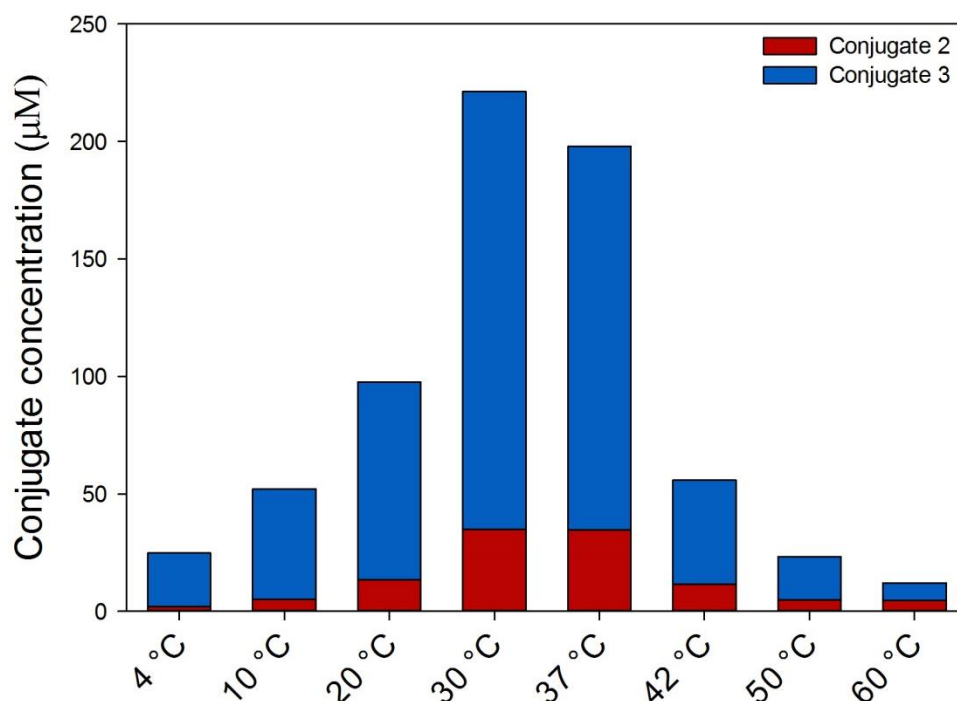


Figure 4.9: Conjugate production profile for *DmGSTE6* after 60 min incubation. Reactions were performed in 100 µM potassium phosphate buffer pH 9.0 with 10 µg of enzyme, 200 µM TNT and 5 mM GSH at temperatures ranging from 4 to 60 °C and a final volume of 250 µl. Concentrations of TNT and the resulting conjugates were calculated through HPLC analysis. Results are means of three biological replicates \pm se.

Table 4.7: Activity of *DmGSTE6* towards TNT across the range of temperatures tested. Highlighted in green is the highest activity, observed at 30 °C.

pH	Activity (nmol.min ⁻¹ .mg ⁻¹)
4 °C	10.5 \pm 0.16
10 °C	23.4 \pm 0.47
20 °C	43.1 \pm 1.01
30 °C	98.5 \pm 0.85
37 °C	91.4 \pm 0.75
42 °C	25.3 \pm 0.23
50 °C	13.5 \pm 0.55
60 °C	6.7 \pm 0.41

4.3.5 Kinetic analysis with TNT

Kinetic analysis with TNT was performed at the conditions optimal for enzyme activity, as identified by the pH and temperature screening tests (pH 9.0, 30 °C), with TNT concentrations ranging from 10-3000 μM . The resulting Michaelis-Menten plot (Figure 4.10) was used to calculate the K_m and V_{max} values shown in Table 4.8. The K_m and V_{max} parameters of GST-U24 and GST-U25 for TNT have been calculated in the past [209]. The kinetic data obtained show that *DmGSTE6* has a 2.4-fold higher V_{max} than GST-U24 and GST-U25, and a 4.5 to 6.1-fold lower K_m respectively (Table 4.8).

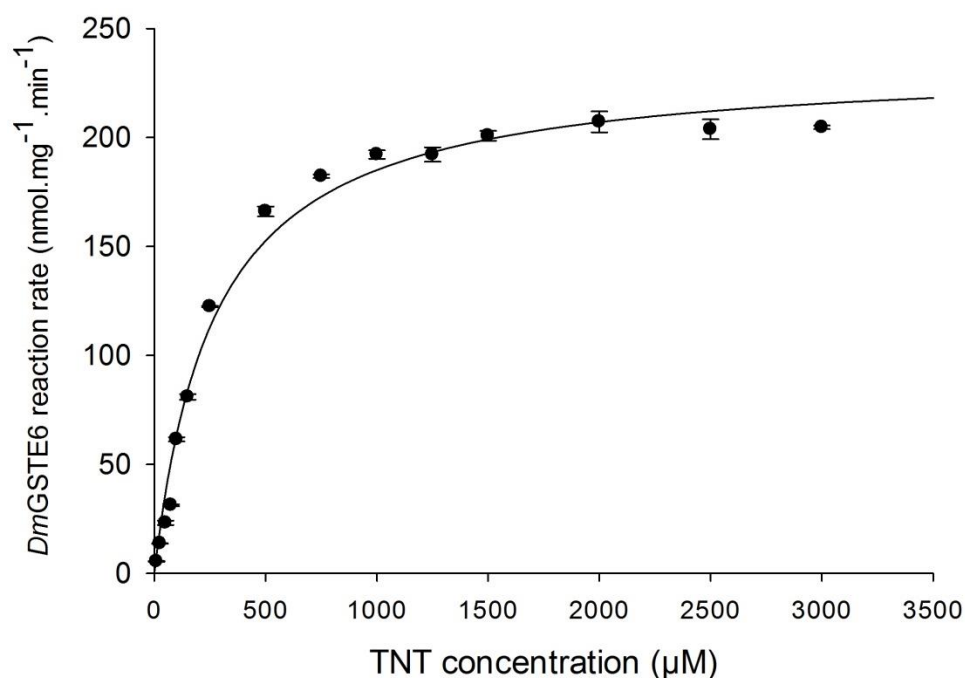


Figure 4.10: Michaelis-Menten plot of *DmGSTE6* with TNT. Rate of conjugate production was determined by HPLC analysis. Reactions were performed at 30 °C with 10 μg of purified enzyme, 10-3000 μM TNT and 5-45 mM GSH in 100 mM of phosphate buffer pH 9.0 and a total volume of 250 μl . Values represent the mean of the reactions performed in triplicate \pm se.

Table 4.8: Kinetic analysis of TNT-conjugating activity by *DmGSTE6*, GST-U24 and GST-U25.

Enzyme	V_{max} ($\text{nmol.min}^{-1}.\text{mg}^{-1}$)	K_m (μM)
<i>DmGSTE6</i>	235 ± 3.9	269.5 ± 17.5
GST-U24	92.3 ± 2.6	1644 ± 113.2
GST-U25	98.39 ± 3	1210 ± 85.7

4.3.6 Griess assay

Griess assays were performed to obtain data on the conjugation of GSH by nucleophilic substitution of a nitro group of TNT (conjugate 3) and further confirm the conjugate production profile observed during the pH and temperature screenings. Results of the assay (Figure 4.11) confirmed that GST-U24 was unable to produce conjugate 3. GST-U25 was able to produce conjugate 3, with lower pH values favouring conjugate 3 over the other conjugates. *DmGSTE6* produced significantly higher amounts of conjugate 3 than GST-U25, with higher amounts of nitrite recorded at higher pH values, in accordance with the results of the pH screening (see section 4.3.3). Interestingly, some nitrite release was observed in the “No GSH” controls. Nitrite release was not observed from the boiled enzyme control, suggesting an enzyme-related release of nitrite from TNT without the formation of a GST-TNT conjugate.

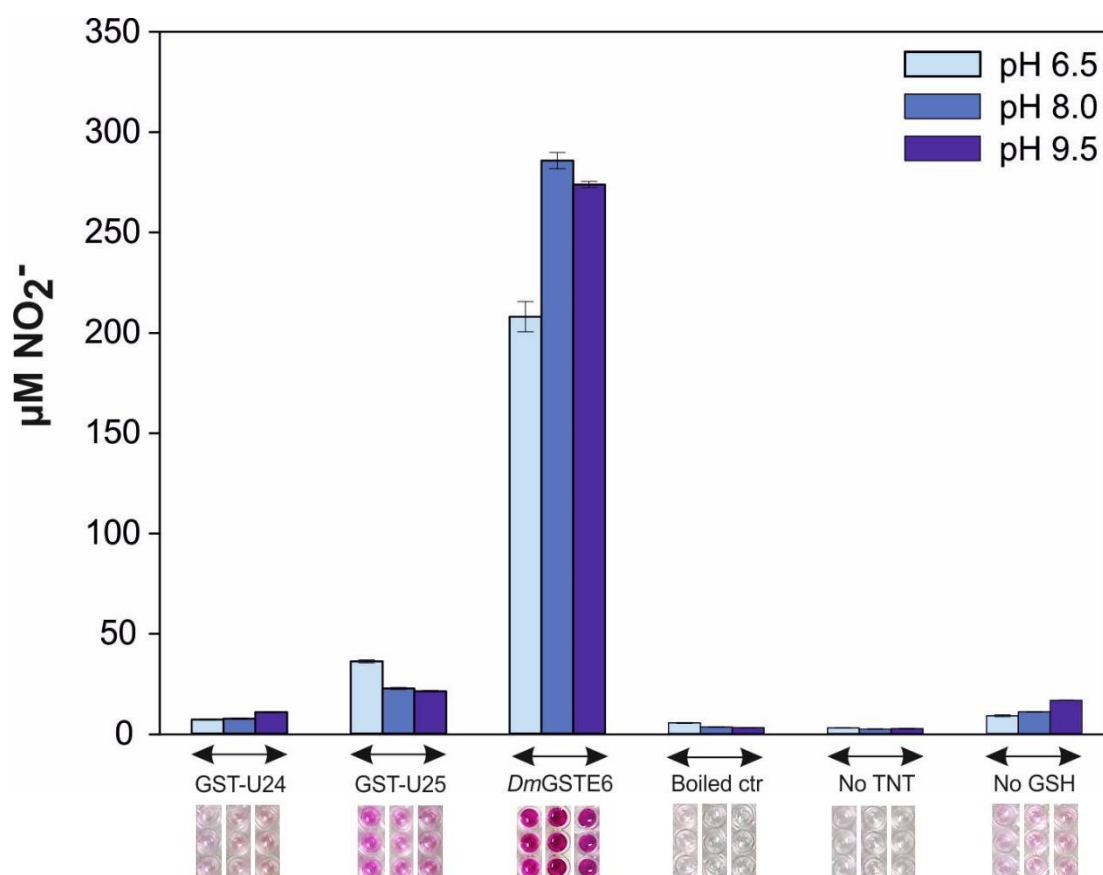


Figure 4.11: Levels of nitrite as measured by the Griess assay after 3 h, along with an image of the colouration achieved by each sample. Boiled control, *DmGSTE6* denatured by heating to 95 °C for 5 min; No TNT, control reactions with *DmGSTE6* were TNT was omitted; No GSH, control reactions with *DmGSTE6* were GSH was omitted. Amount of free nitrite was measured spectrophotometrically at 540 nm. Quantification of the samples was performed according to a standard curve produced with 0-100 µM NaNO₂. Results are means of five biological replica ± se.

4.3.7 Activity towards ADNTs and HADNTs

The activity of *DmGSTE6* towards HADNTs and ADNTs was assayed at pH 7.0 and 9.0, and 30 °C. HPLC analysis showed no detectable conjugation with HADNTs or ADNTs (Figure 4.12) and substrate levels did not diminish suggesting that, as seen with GST-U24 and GST-U25, HADNTs and ADNTs do not serve as substrates for *DmGSTE6*.

Chapter 4: Biochemical characterisation of a TNT detoxifying *Drosophila* GST

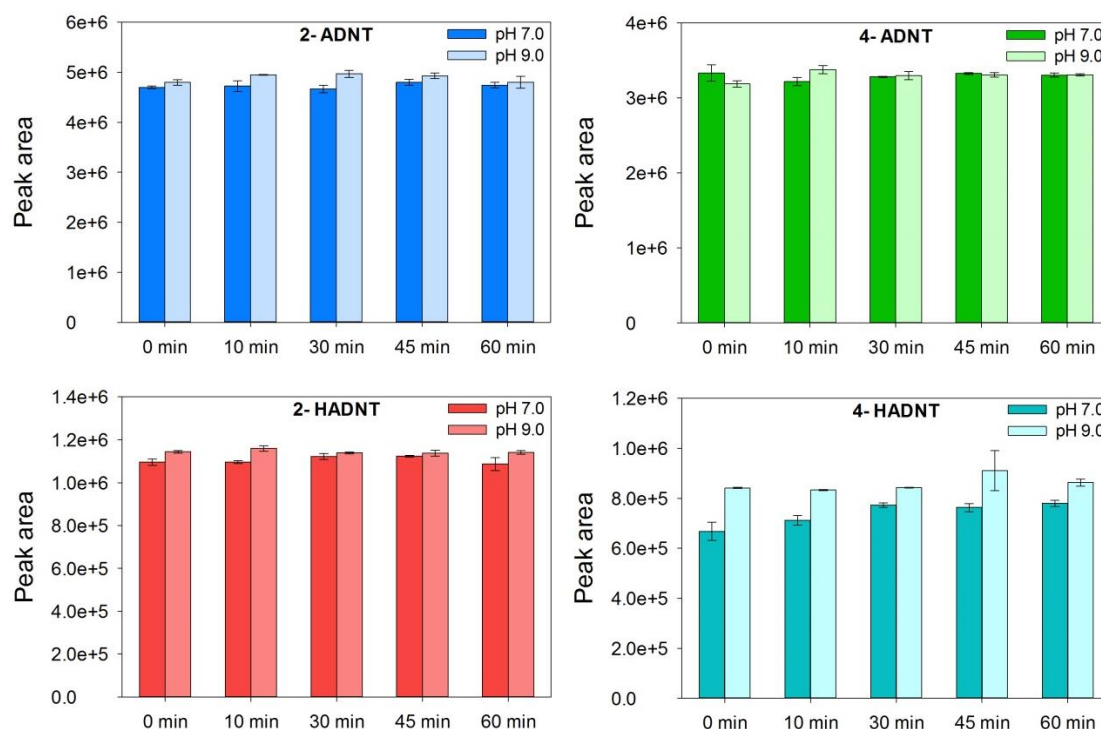


Figure 4.12: Levels of HADNTs and ADNTS during one hour of incubation with *DmGSTE6* at 30 °C. Results are means of three biological replicates \pm se.

4.3.8 GPOX activity

DmGSTE6 was assayed for GPOX activity using the same conditions as described previously for GST-U24 and GST-U25 (see section 3.3.5). The purified GST-U25 which has measurable GPOX activity served as a positive control for the assay.

Results showed that under the conditions tested, GPOX activity was not observed for *DmGSTE6* (Figure 4.13). Increasing the concentration of the enzyme up to 150 μ g made no difference, indicating that *DmGSTE6* either is not capable of GPOX activity or that, under the conditions tested, the activity is below the detection limit. This result is in agreement with the previously reported GPOX activity for *DmGSTE6*, using (5*S*)-HpETE as the substrate [192].

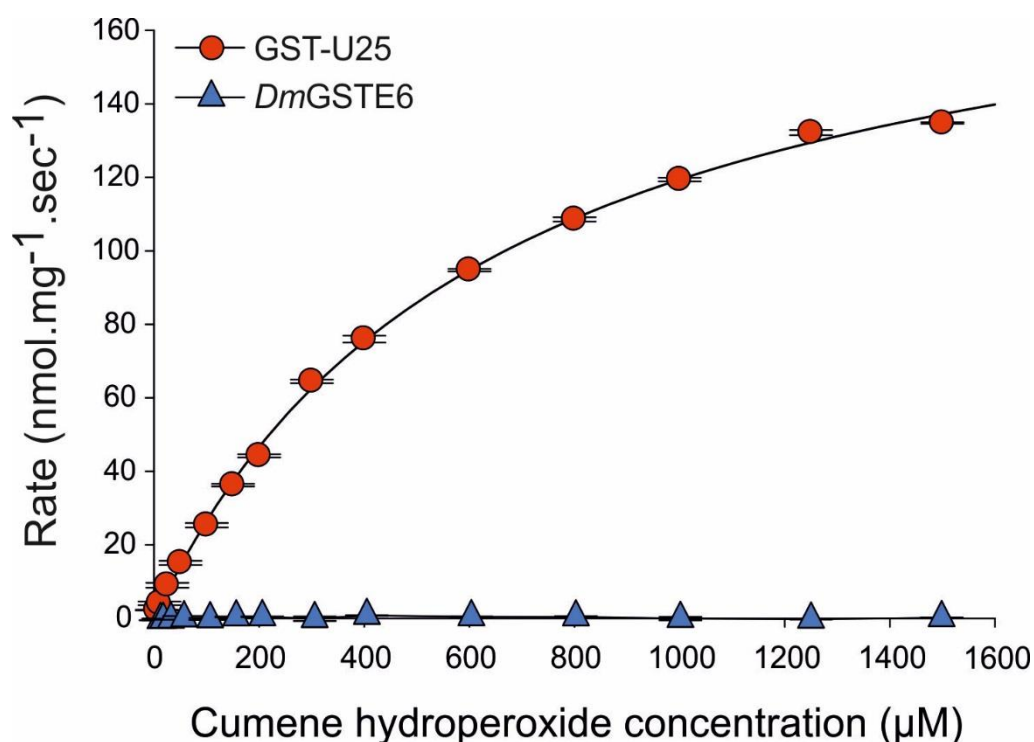


Figure 4.13: Enzyme kinetic data for purified GST-U25 (5 µg) and *DmGSTE6* (150 µg, highest amount of enzyme assayed) with cumene hydroperoxide as substrate. Glutathione peroxidase activity was monitored spectrophotometrically using an NADPH-linked assay. Results are means of three technical replicates ± se.

4.3.9 Recombinant expression of *DmGSTE6* in *Arabidopsis*

The *DmGSTE6* gene was PCR amplified from the pJexpress401:69884 vector and cloned into the pCRTM-Blunt II-TOPO[®] vector using the Zero Blunt[®] TOPO[®] PCR Cloning Kit (Invitrogen). Subsequently, the gene was cut and ligated into the pART7 plasmid [162], excised with the restriction endonuclease *NotI* (Figure 4.14A) and then ligated into pART27 [162]. Diagnostic digestions with *NotI* (Figure 4.14B) and sequencing confirmed the successful cloning into pART27. Finally, *Arabidopsis* Col 0 plants were transformed through *Agrobacterium* mediated transformation. Resistance to kanamycin along with PCR on genomic DNA extracted from heterozygous resistant seedlings (Figure 4.15) confirmed the successful transformation of *Arabidopsis* with *DmGSTE6*.

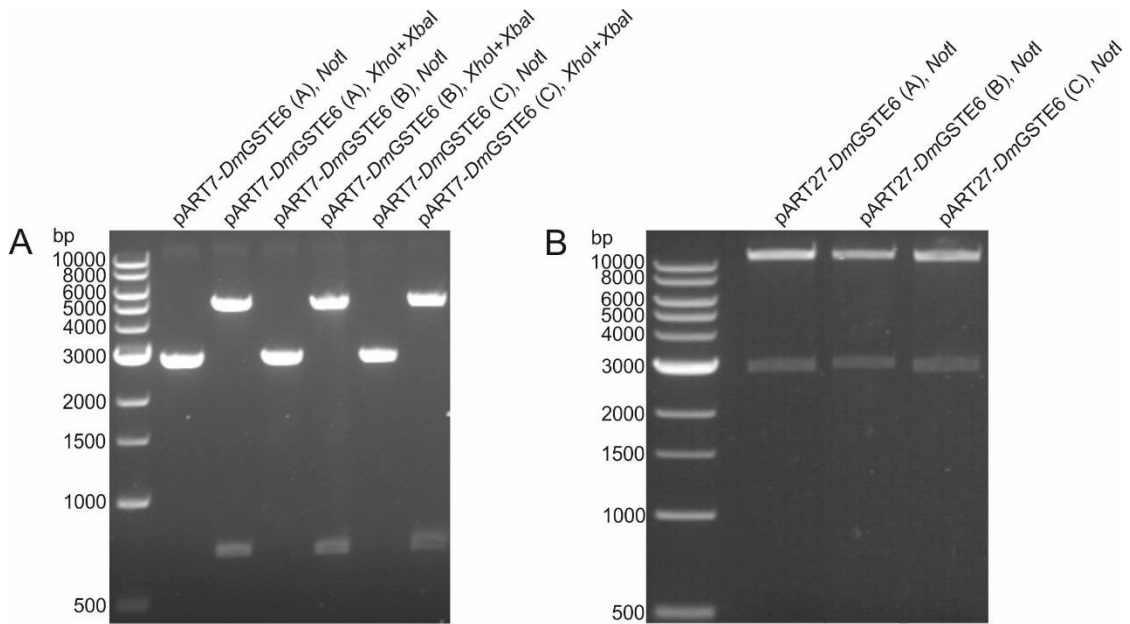


Figure 4.14: Confirmation of cloning *DmGSTE6* into (A) pART7 and (B) pART27. Digesting pART7 containing the *DmGSTE6* gene with the restriction endonuclease *NotI* should yield a single band at ~2.8 kb (vector backbone and expression cassette have the same size). Digestion of pART7 containing the *DmGSTE6* gene with the restriction endonucleases *XhoI* and *XbaI* should release the gene and yield a band at 714 bp. Digestion of pART27 containing the *DmGSTE6* with the restriction endonuclease *NotI* should release the expression cassette with a size at ~2.8 kb. The larger band in all the lanes, besides the pART7-*DmGSTE6* digested with *NotI*, corresponds to the backbone of the respective vector.

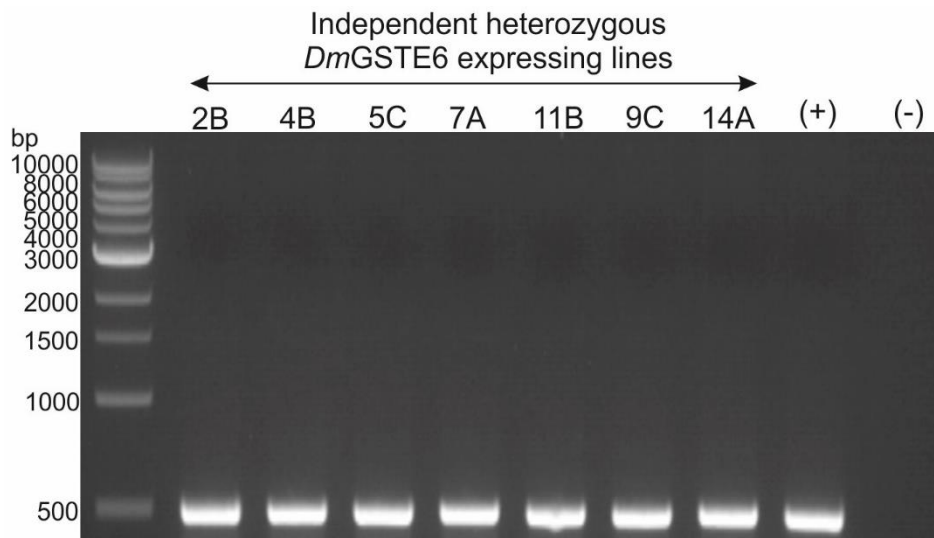


Figure 4.15: Diagnostic PCR on whole genome extracted from plants transformed with the pART27-*DmGSTE6* construct. Presence of a band at ~ 500 bp indicates successful insertion of the *DmGSTE6* in the plant genome. (+), purified pART7-*DmGSTE6* used as a positive control; (-), genome extracted from untransformed plants used as a negative control.

4.3.10 Preliminary screening of the *DmGSTE6* transgenic *Arabidopsis* lines

4.3.10.1 Preliminary screening of *DmGSTE6* expressing *Arabidopsis*

To identify the best performing lines, seven T3 homozygous *DmGSTE6* expressing lines, containing single T-DNA insertional events (as identified by their segregation ratios on kanamycin) were grown in the presence of TNT. The concentration of 30 μM TNT was chosen as high enough for the plants to display stunting of their roots, but not too high to completely arrest their growth [165].

The preliminary screening confirmed that the plants expressing the *DmGSTE6* had increased tolerance towards TNT, and that tolerance was higher than observed for the GST-U24/U25 OE lines. All of the *DmGSTE6* expressing lines had roots of equal or higher length than that achieved by WT and GST-U24/U25 OE lines (Figure 4.16). Of the seven *DmGSTE6* expressing lines 14A5, 2C4 and 11B2 displayed the longest roots. Among the WT and GST-U24/U25 OE lines, the GST-U24 OE line displayed the highest root length, in agreement with previous findings by Dr Vanda Gunning [165].

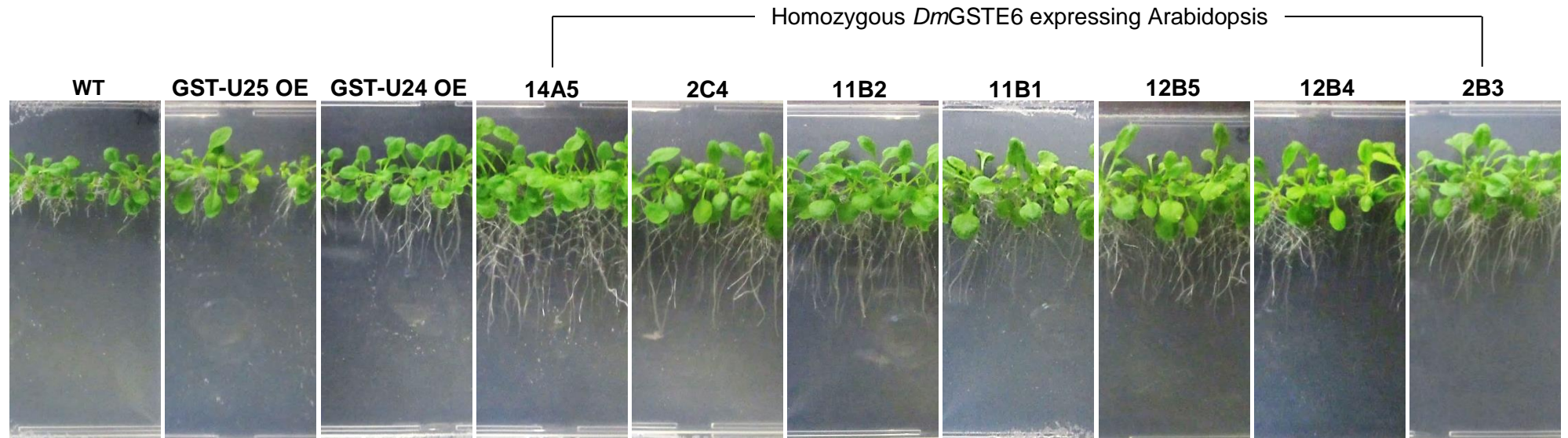


Figure 4.16: Preliminary screening of the *DmGSTE6* expressing lines detoxification abilities. Homozygous *DmGSTE6* expressing Arabidopsis were grown, alongside untransformed (WT) and the best performing GST-U24/U25 over-expressing (OE) plants, vertically on 1/2 MS agar plates contaminated with 30 μM TNT for twenty days.

4.3.10.2 CDNB activity of plant protein extracts

Plants were assayed for GST activity using CDNB as a substrate to test whether the higher activity of the *DmGSTE6* observed *in vitro* correlated with increased tolerance towards TNT *in vivo*. Root and leaf protein extract from untransformed (WT), GST-U24/U25 OE lines and *DmGSTE6* expressing lines grown on TNT-free ½ MS agar plates, were used for the CDNB assays. The data were normalised against a no-enzyme control.

Results showed that the protein extracts from the selected *DmGSTE6* transgenic lines displayed higher activity towards CDNB when compared to WT and GST-U24 OE lines with both root and leaf protein extract but lower CDNB activity than GST-U25 OE lines (Figure 4.17). The GST-U25 OE lines displayed higher activity than all the *DmGSTE6* transgenic lines in leaves (Figure 4.17). A similar trend was observed for the roots, but the difference was not significant. From the *DmGSTE6* expressing lines given in Figure 4.17, lines 14A5, 2C4, 11B2 and 11B1 displayed the highest conjugation activities. Since 11B2 and 11B1 come from the same T2 plant and independent homozygous lines are preferable, 14A5, 2C4 and 11B2 lines were brought forward for the remaining experiments. These lines will be referred to as dGST/1, dGST/2, dGST/3 respectively.

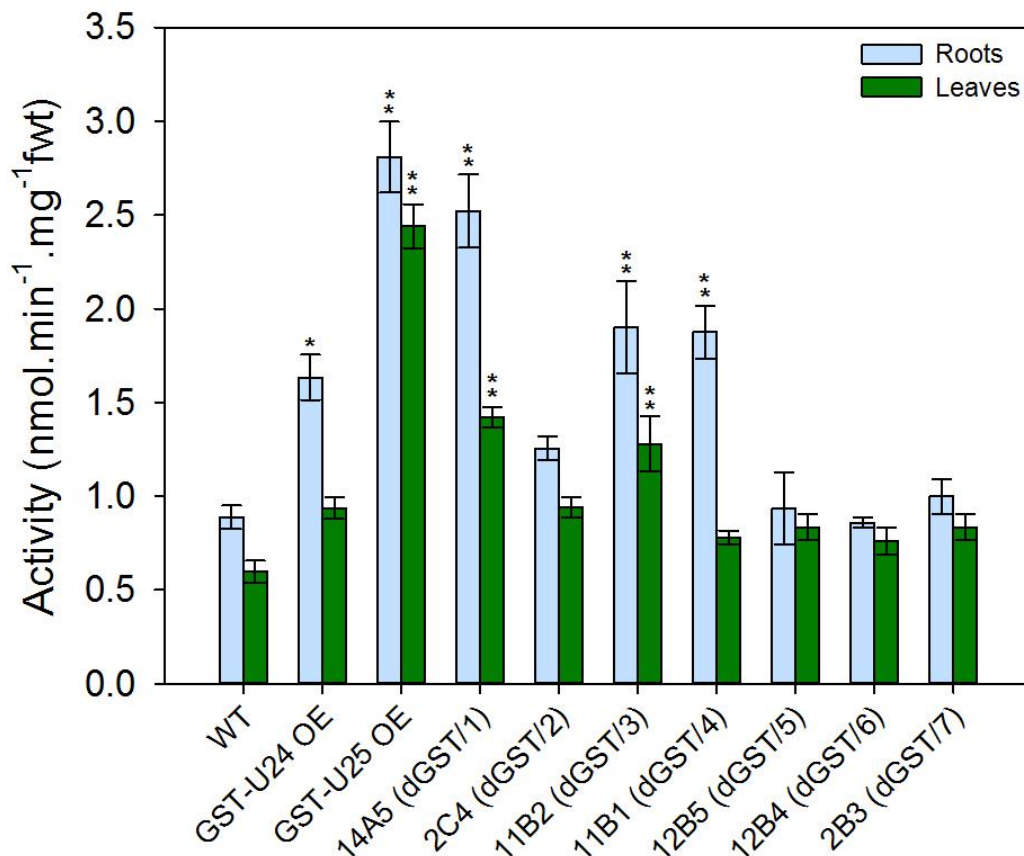


Figure 4.17: Rate of CDNB-conjugate production by root and leaf protein extract from two-week old plants grown vertically on agar plates containing $\frac{1}{2}$ MS medium. Rate of conjugate production was determined spectrophotometrically over 1 min at 340 nm. Reactions were performed with 50 μ l of extract, 1 mM CDNB and 5 mM GSH in 100 mM of phosphate buffer pH 6.5 and a total volume of 1 ml. Results were standardised according to fresh weight. Absorbance values represent the mean of five biological measurements \pm se. Asterisks denote statistically significant from the WT: * $P < 0.05$, ** $P < 0.01$

4.3.10.3 RT-PCR on *DmGSTE6* expressing *Arabidopsis* lines

To establish if expression levels of *DmGSTE6* relate to increased conjugation activity in the three independent dGST lines, the plants were subjected to RT-PCR analysis. The observed transcript levels confirmed that the *DmGSTE6* is expressed in the three dGST lines, while the absence of detectable transcripts for the WT confirmed the validity of the assay (Figure 4.18). Furthermore, the expression levels of *DmGSTE6* transcript among the three transgenic lines agreed with the activity profiles observed for the CDNB activity assay discussed in the previous section, where dGST/1 and dGST/3 gave comparable and higher activities than dGST/2.

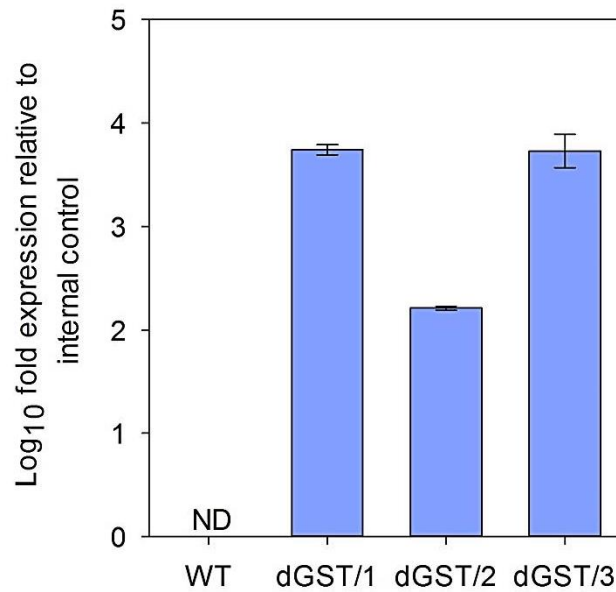


Figure 4.18: RT-PCR results from cDNA of 14-day-old *Arabidopsis* grown on soil without TNT. WT, untransformed plants; dGST/1-3, independent *DmGSTE6* expressing lines; ND, not detected. Results are means of five biological replicates \pm se.

4.3.10.4 Griess assay of plant protein extracts

To establish whether the dGST lines have a higher relevant conjugation activity than the GST-U25 OE lines, an assay examining the *in vivo* activity towards TNT was necessary. The GST conjugating activity in root protein extracts was assessed using the Griess assay, with WT and GST-U24 OE plants included as controls. The results given in Figure 4.19 demonstrated that all of the dGST lines produced higher amounts of free nitrite than the GST-U25 OE, and thus more conjugate 3. Protein extracts from WT and GST-U24 OE lines generated amounts of free nitrite close to those of the GST-U25 OE lines. This is probably the result of endogenous GST-U25 in those samples (GST-U25 is still expressed albeit at lower levels in WT and GST-U24 OE plants) and/or the presence of other enzymes that might also have activity towards TNT. Finally, the conjugation activity of the three independent *DmGSTE6* expressing lines (dGST/1-3) was in agreement with that observed for CDNB and with the RT-PCR results, as dGST/1 and dGST/3 displayed similar and higher conjugation activities than dGST/2.

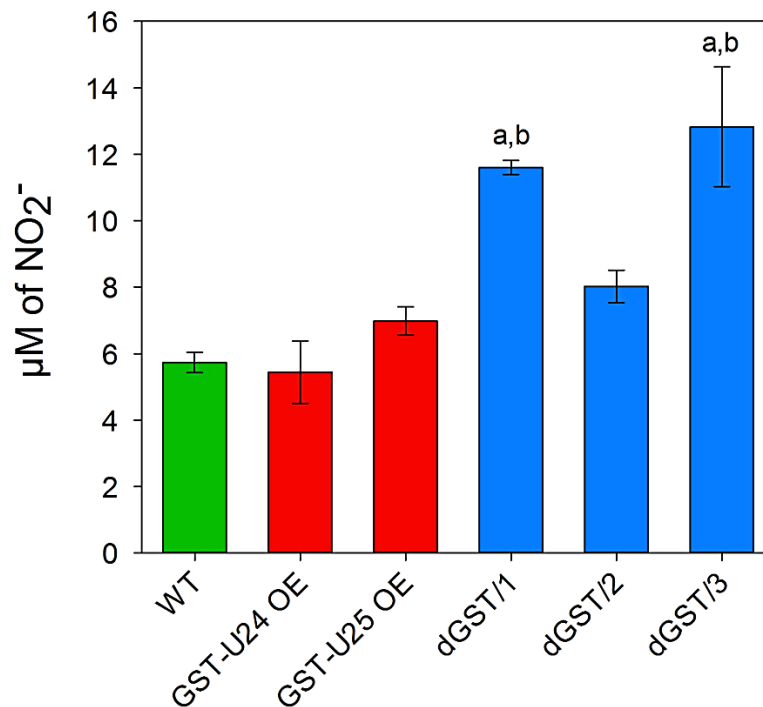


Figure 4.19: Levels of nitrite as measured by the Griess assay after 3 h. WT, untransformed plants; GST-U24 OE, best performing GST-U24 over-expressing line; GST-U25 OE, best performing GST-U25 over-expressing line; dGST/1-3, independent *DmGSTE6* expressing lines. Amount of free nitrite was measured spectrophotometrically at 540 nm. Quantification of the samples was performed according to a standard curve produced with 0-100 µM NaNO₂. Results are means of five biological replicates ± se. a, b denote statistically significant from the WT ($P < 0.01$) and the GST-U24/U25 OE lines ($P < 0.05$) respectively.

4.3.11 Root length studies

In order to compare TNT tolerance of the dGST plant lines to that of the GST-U24/U25 OE lines, the plants were grown for twenty days on ½ MS agar plates containing a range of TNT concentrations, alongside WT and the selected GST-U24/U25 OE lines, as identified by the previous experiments described in Chapter 3. The appearance of the plants at the end of the experiment is shown in Figure 4.20. The TNT present in the medium had a severe effect on the root growth of all plant lines (Table 4.9 & Table 4.10).

After ten days of growth the GST-U24/U25 OE plants displayed small differences in terms of root length compared to the WT, across the range of TNT concentrations tested (Figure 4.21A). The dGST plant lines displayed no significant differences to WT or GST-U24/U25 OE lines at TNT concentrations

up to 7 μM but at higher concentrations the dGST lines displayed significantly greater root lengths than either WT or GST-U24/U25 OE lines (Figure 4.21A). At 15 and 30 μM the dGST plants exhibited on average 1.5-fold greater root length than WT and 1.2-fold greater root length than the greatest achieved by the GST-U24/U25 OE lines.

After twenty days of growth the difference between the plant lines became more apparent. Concentrations of TNT up to 7 μM were probably not toxic enough, since no significant differences were recorded among the different plant lines (Figure 4.21B). However, at higher TNT concentrations, all of the dGST lines displayed greater root surface area than both WT and the GST-U24/U25 OE lines, suggesting that expression of *DmGSTE6* could further enhance TNT tolerance comparing to GST-U24/U25 OE lines. In more detail, at 30 μM TNT the best 'performing' dGST line (dGST/3) displayed 4.4-fold greater root surface area than WT and could only be compared with the GST-U24 OE lines (Figure 4.21B). At the highest TNT concentration tested (50 μM) WT and GST-U25 OE plants appeared dead, with < 40% of the GST-U24 OE seedlings surviving (Figure 4.20). At 50 μM TNT, the dGST lines, even though they suffered severe stunning of their growth, were still able to germinate and achieve a 1.6-fold higher root surface area than that of the GST-U24 OE plants.

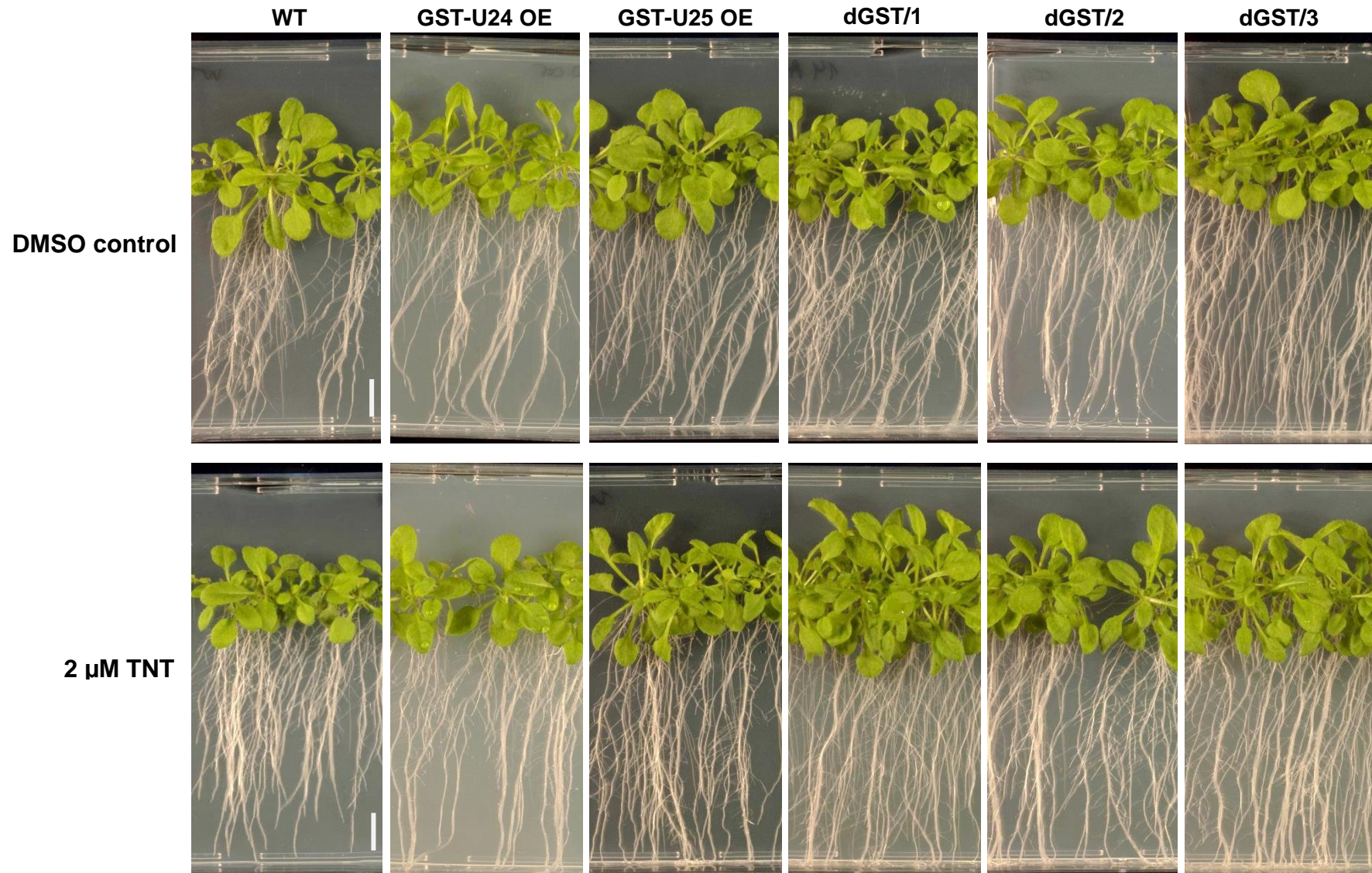
Table 4.9: Root length in mm (A) and ratio to WT (B) of 10-day-old plants grown vertically on ½ MS agar plates containing 0-50 µM TNT. Results are mean of 3 biological replicates or ~ 60 seedlings for each plant line.

A	WT	GST-U24 OE	GST-U25 OE	dGST/1	dGST/2	dGST/3
DMSO ctr	24.4 ± 0.79	18.9 ± 0.43	25.8 ± 1.6	26.4 ± 0.7	20.0 ± 1.5	30.3 ± 1.0
2 µM	16.1 ± 0.62	17.9 ± 0.91	18.7 ± 1.0	20.3 ± 1.8	18.3 ± 2.6	19.6 ± 0.8
7 µM	7.1 ± 1.92	10.2 ± 1.2	5.5 ± 0.3	8.6 ± 1.0	9.0 ± 0.8	7.6 ± 1.2
15 µM	3.5 ± 0.44	4.4 ± 0.13	3.3 ± 0.3	5.7 ± 0.7	4.9 ± 0.1	4.9 ± 0.2
30 µM	1.9 ± 0.07	2.5 ± 0.20	1.9 ± 0.1	3.6 ± 0.1	3.6 ± 0.3	3.9 ± 0.4
50 µM	1.6 ± 0.14	1.6 ± 0.15	1.6 ± 0.07	2.5 ± 0.07	2.1 ± 0.1	2.8 ± 0.3
B	WT	GST-U24 OE	GST-U25 OE	dGST/1	dGST/2	dGST/3
DMSO ctr	1.0 ± 0.03	0.77 ± 0.02	1.06 ± 0.07	1.08 ± 0.03	0.82 ± 0.06	1.24 ± 0.04
2 µM	1.0 ± 0.04	1.11 ± 0.06	1.16 ± 0.06	1.26 ± 0.11	1.14 ± 0.17	1.22 ± 0.05
7 µM	1.0 ± 0.27	1.43 ± 0.17	0.77 ± 0.04	1.21 ± 0.14	1.26 ± 0.11	1.07 ± 0.16
15 µM	1.0 ± 0.12	1.25 ± 0.04	0.94 ± 0.10	1.61 ± 0.20	1.38 ± 0.04	1.40 ± 0.07
30 µM	1.0 ± 0.04	1.34 ± 0.10	1.03 ± 0.05	1.89 ± 0.07	1.89 ± 0.17	2.03 ± 0.19
50 µM	1.0 ± 0.09	0.95 ± 0.09	0.99 ± 0.04	1.51 ± 0.04	1.27 ± 0.09	1.70 ± 0.17

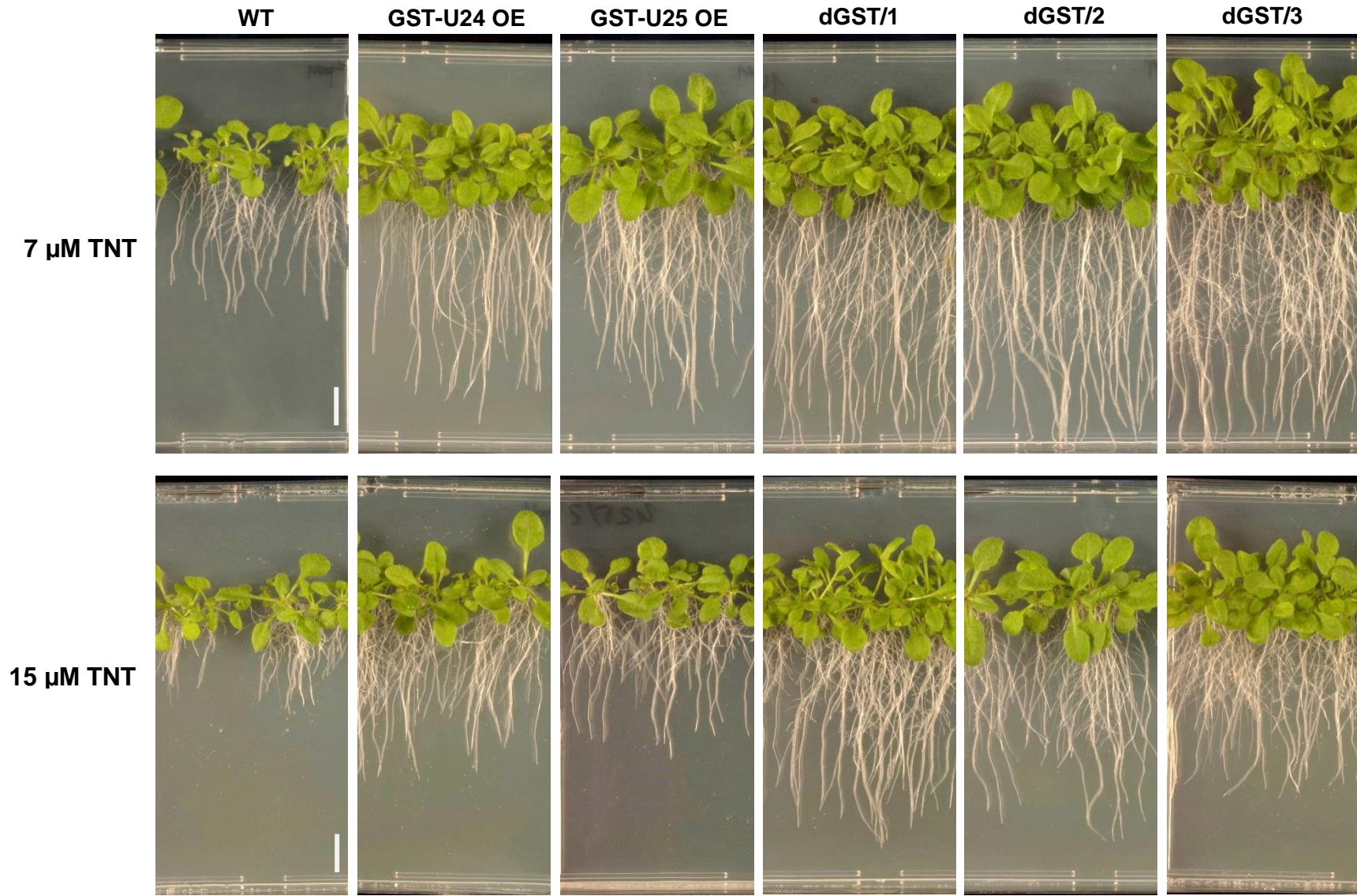
Table 4.10: Root surface area expressed as pixels (A) and ratio to WT (B) of 20-day-old plants grown vertically on ½ MS agar plates containing 0-50 µM TNT. Results are mean of 3 biological replicates or ~ 60 seedlings for each plant line.

A	WT	GST-U24 OE	GST-U25 OE	dGST/1	dGST/2	dGST/3
DMSO ctr	13498 ± 1414	12654 ± 1082	12127 ± 497	13569 ± 3792	14600 ± 1992	16505 ± 2431
2 µM	15143 ± 1844	16708 ± 2132	13528 ± 866	16479 ± 1164	23813 ± 3141	16187 ± 2043
7 µM	8947 ± 456	13262 ± 2078	13635 ± 1139	16375 ± 1077	18639 ± 2243	15352 ± 701
15 µM	6355 ± 1554	11907 ± 3453	9116 ± 969	14802 ± 1239	14006 ± 3795	13559 ± 467
30 µM	1810 ± 205	6669 ± 337	1659 ± 210	7712 ± 445	7241 ± 254	7948 ± 346
50 µM	1427 ± 104	2956 ± 170	1454 ± 55	4656 ± 265	4418 ± 267	4766 ± 836
B	WT	GST-U24 OE	GST-U25 OE	dGST/1	dGST/2	dGST/3
DMSO ctr	1.0 ± 0.10	0.94 ± 0.08	0.90 ± 0.03	1.01 ± 0.28	1.08 ± 0.15	1.22 ± 0.18
2 µM	1.0 ± 0.12	1.10 ± 0.14	0.88 ± 0.06	1.09 ± 0.08	1.57 ± 0.20	1.07 ± 0.13
7 µM	1.0 ± 0.05	1.48 ± 0.23	1.52 ± 0.13	1.83 ± 0.12	2.08 ± 0.25	1.72 ± 0.08
15 µM	1.0 ± 0.24	1.87 ± 0.54	1.43 ± 0.15	2.33 ± 0.19	2.20 ± 0.60	2.13 ± 0.07
30 µM	1.0 ± 0.11	3.68 ± 0.19	0.92 ± 0.12	4.26 ± 0.24	1.00 ± 0.14	4.39 ± 0.19
50 µM	1.0 ± 0.07	2.07 ± 0.12	1.02 ± 0.04	3.26 ± 0.19	3.1 ± 0.19	3.34 ± 0.59

Chapter 4: Biochemical characterisation of a TNT detoxifying Drosophila GST



Chapter 4: Biochemical characterisation of a TNT detoxifying *Drosophila* GST



Chapter 4: Biochemical characterisation of a TNT detoxifying *Drosophila* GST

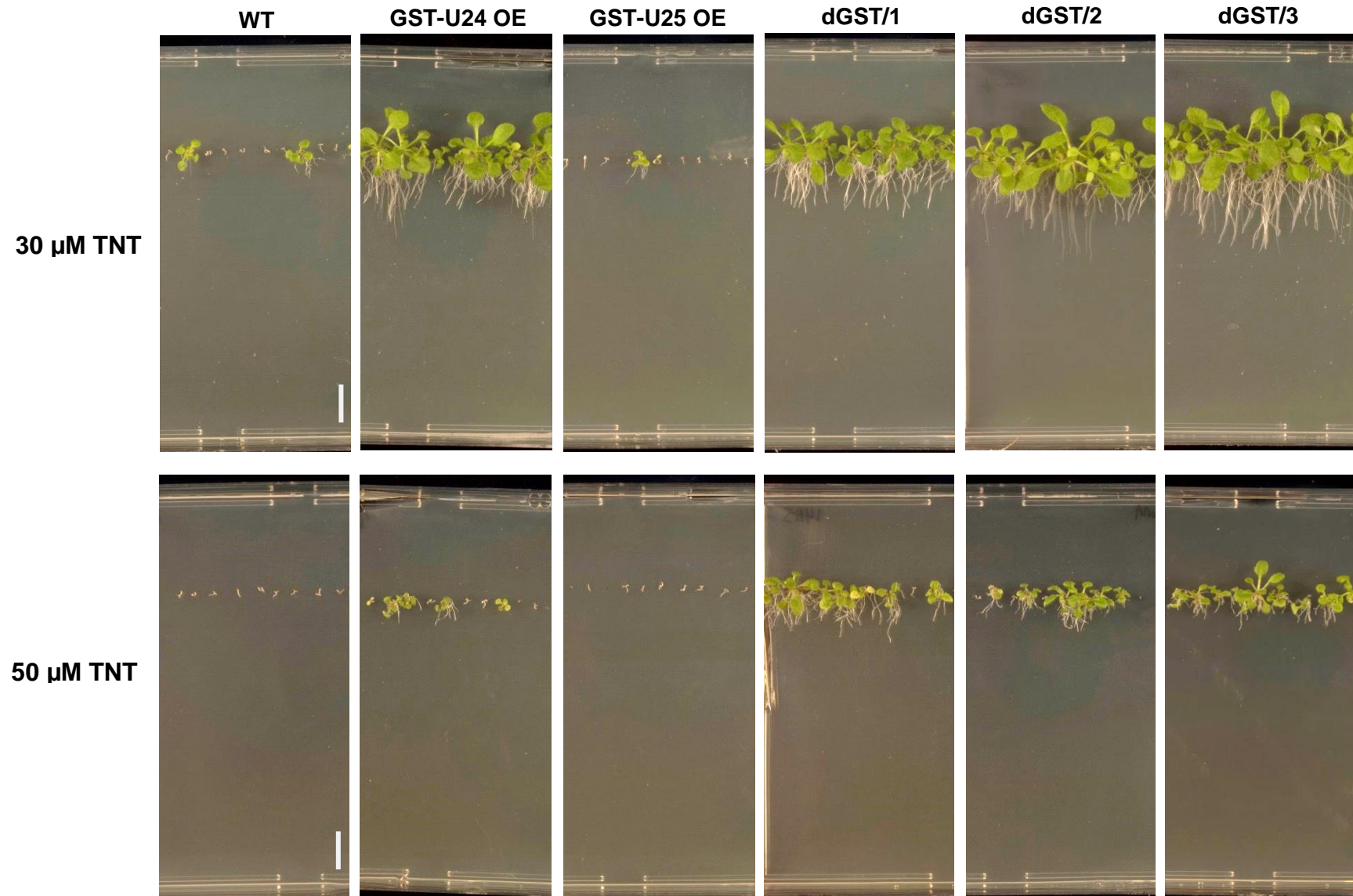


Figure 4.20: Effect of TNT on root growth of *Arabidopsis* seedlings. Photographs of 20-day-old seedlings grown vertically on $\frac{1}{2}$ MS agar plates with a range of TNT concentrations. WT, untransformed plants; GST-U24/U25, over-expressing (OE) lines; dGST/1-3, independent homozygous lines expressing *DmGSTE6*. White scale bar is 1 cm long.

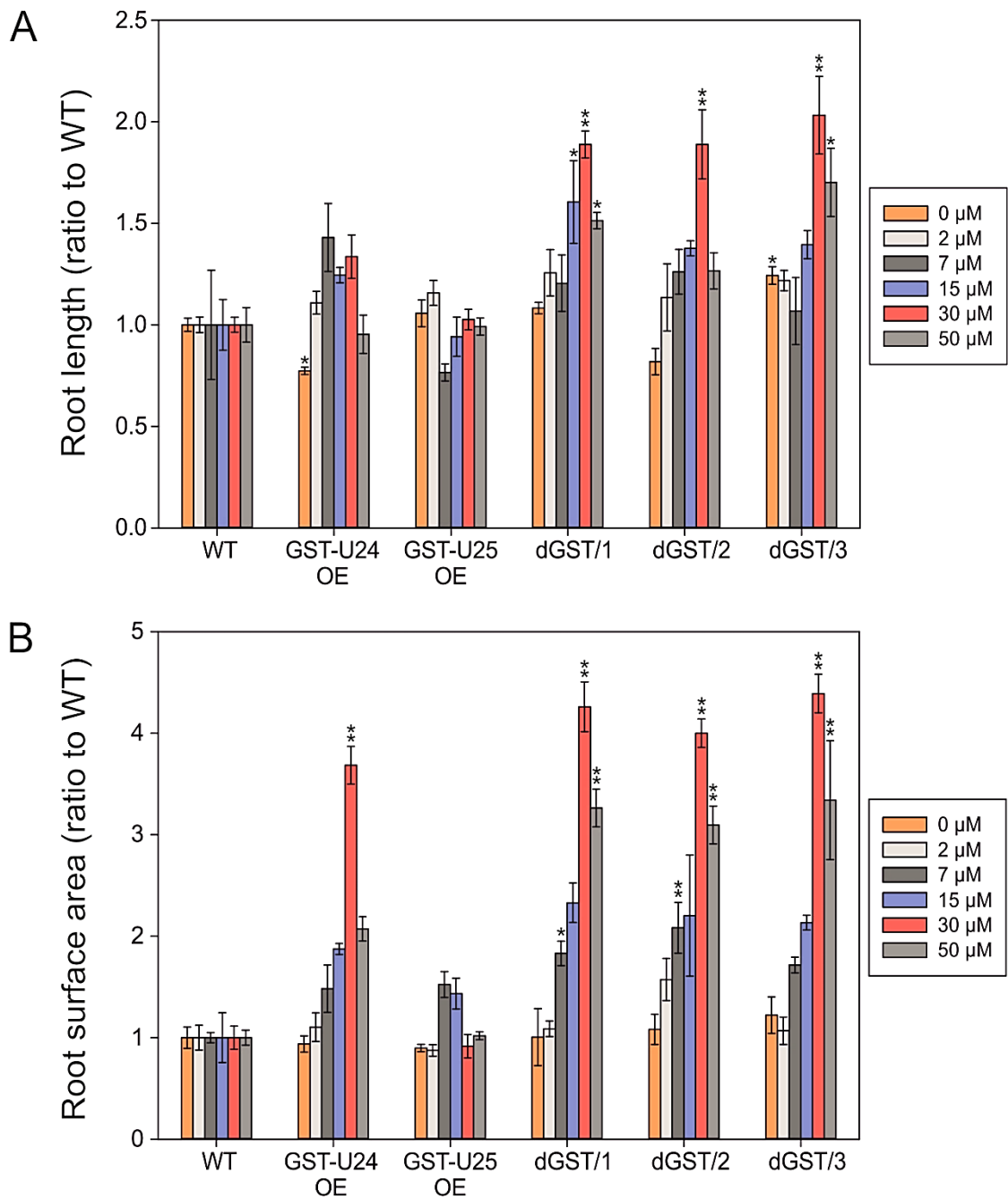


Figure 4.21: Ratio to WT of (A) root length (mm) of plants grown for ten days vertically on $\frac{1}{2}$ MS agar plates containing a range of TNT concentrations and (B) root surface area (pixels) of plants grown for twenty days vertically on $\frac{1}{2}$ MS agar plates containing a range of TNT concentrations. WT, untransformed plants; GST-U24/U25, over-expressing (OE) lines; dGST/1-3, independent homozygous lines expressing *DmGSTE6*. Results are means of three biological replicates or ~ 60 seedlings for each plant line \pm se. Asterisks denote statistically significant from the WT at that concentration: * $P < 0.05$, ** $P < 0.01$.

4.3.12 Biomass of transgenic lines grown on TNT-containing soil

Once the increased tolerance of the dGST lines compared to both WT and GST-U24/U25 OE lines was established, the next step was to assess the detoxification abilities of these lines. To test the detoxification abilities in conditions that resemble those encountered in the field, the dGST lines were grown on soil without TNT and soil of 50, 100 and 200 mg kg⁻¹ TNT concentrations. The concentration of 25 mg kg⁻¹ TNT, used in the soil studies of the previous chapter, was omitted since at this concentration plants did not display major changes in terms of biomass comparing to the TNT-free soil.

The appearance of the lines during the experiment is shown in Figure 4.22. As expected, at TNT concentrations higher than 50 mg/kg WT plants appeared chlorotic and suffered severe stunting of their growth. On the contrary, the dGST lines did not appear chlorotic and their growth was less stunted, with the most successful lines being able to continue growing at 200 mg/kg, a concentration found to completely inhibit growth for both WT and GST-U24/U25 OE lines in a previous study (Dr V. Gunning, personal communication). In more detail, at 50 mg kg⁻¹ the best 'performing' dGST line (dGST/1) exhibited up to 1.2-fold higher shoot and 1.8-fold higher root biomass when compared to WT (Figure 4.23). Increasing TNT concentration further enhanced the difference with the shoot and root biomasses being 2.4-fold and 3.2-fold higher than WT at 100 mg kg⁻¹, and 2.8-fold and 4.8-fold higher at 200 mg kg⁻¹ respectively (Figure 4.23).

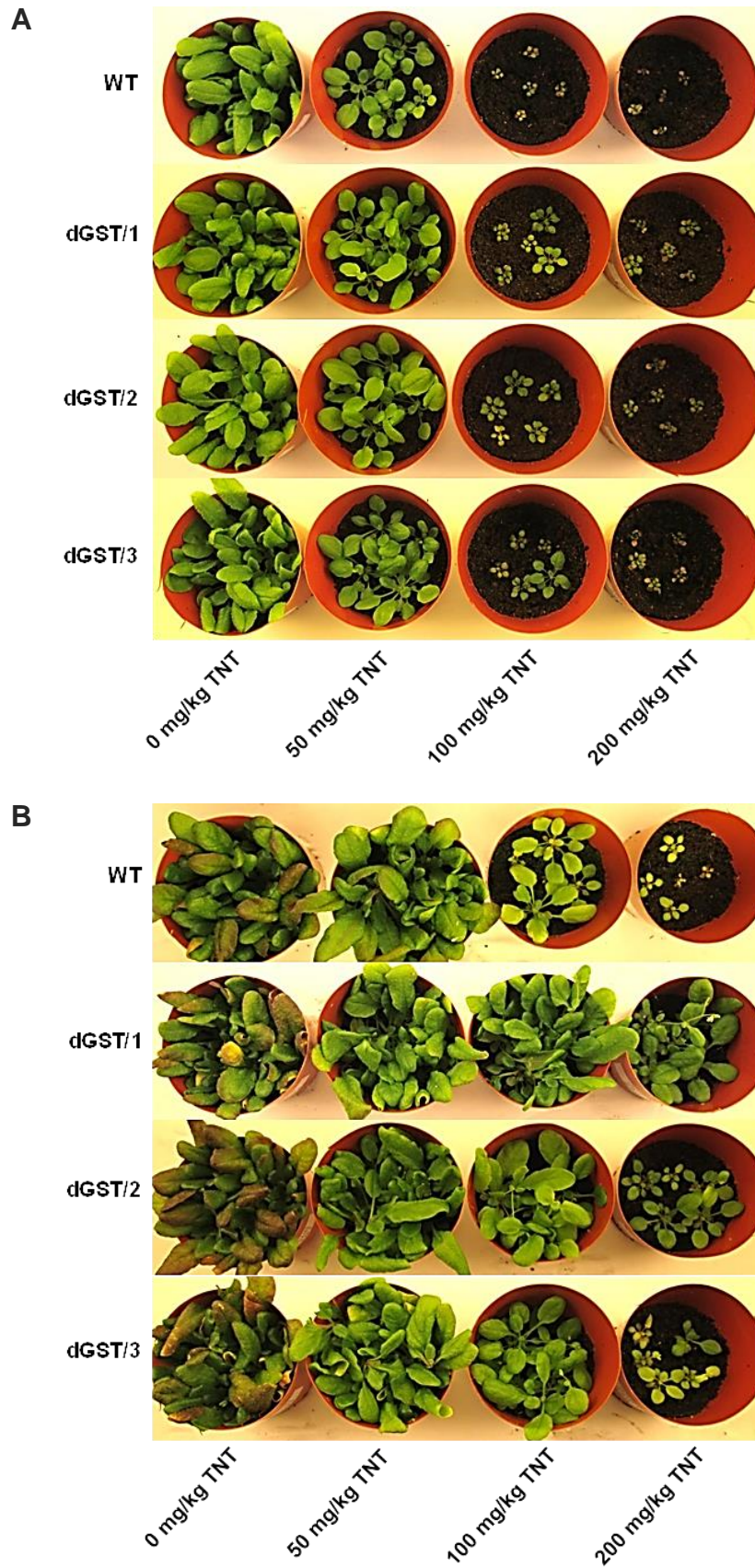


Figure 4.22: Appearance of one-week-old *Arabidopsis* seedlings grown for (A) three weeks and (B) six weeks in soil containing a range of TNT concentrations. WT, untransformed plants; dGST/1-3, independent homozygous lines expressing *DmGSTE6*.

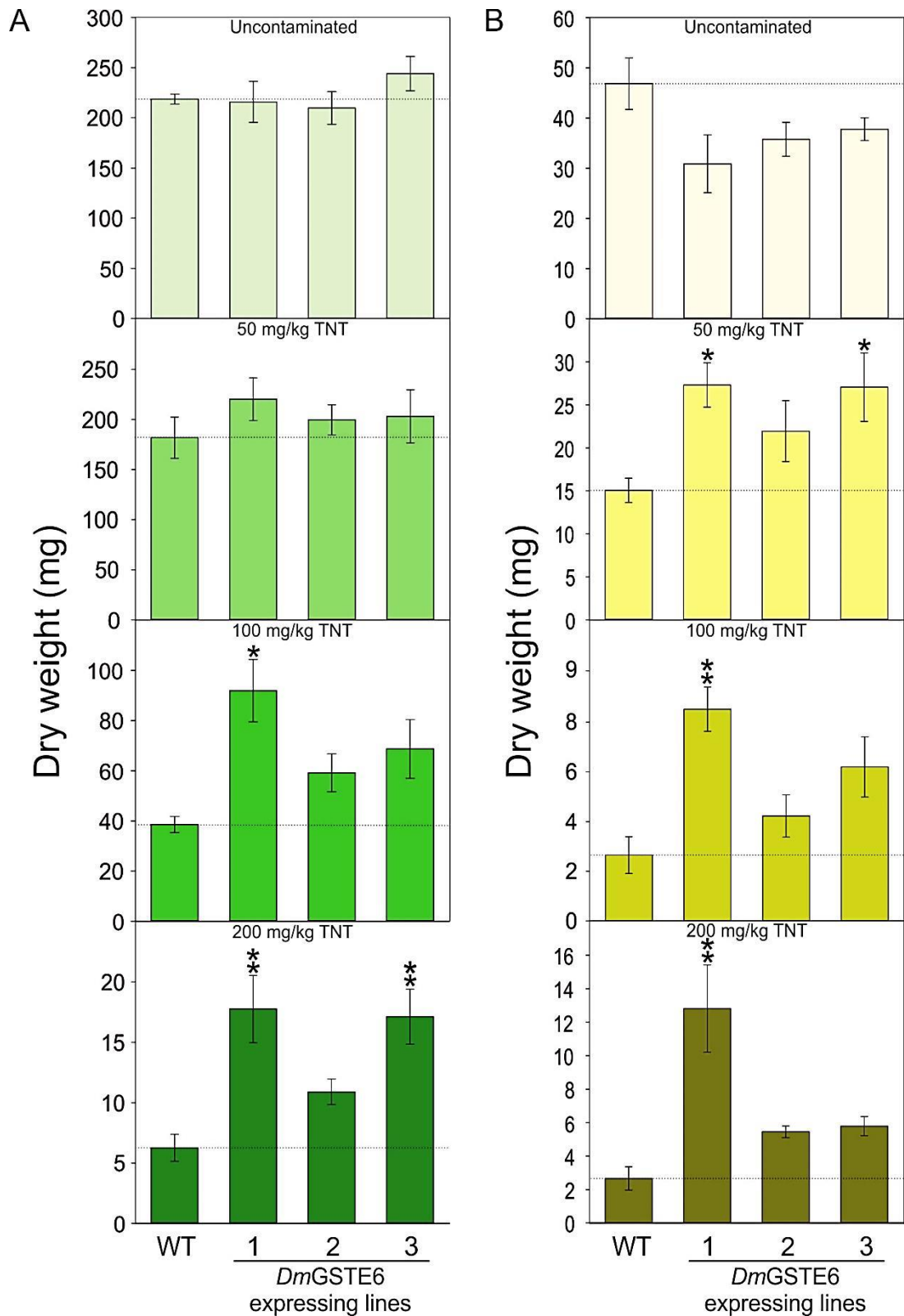


Figure 4.23: Shoot (A) and Root (B) biomasses of one-week-old *Arabidopsis* seedlings grown for six weeks in soil containing a range of TNT concentrations. WT, untransformed; dGST/1-3, independent homozygous lines expressing *DmGSTE6*. Results are means of eight biological replicates \pm se. Asterisks denote statistically significant from the WT: * $P < 0.05$, ** $P < 0.01$.

Some variation between the soil experiment conducted here and that previously done with the GST-U24/U25 OE lines (see section 3.3.2) was observed as WT plants performed better at 100 mg kg⁻¹ TNT than the previous experiment. This is not surprising as small deviations in factors such as initial water content of the soil or watering patterns can directly affect the concentration and thus phytotoxicity of TNT.

4.3.13 TNT uptake by the transgenic lines from soil

After harvesting the plants and determining the biomass during the previous experiment, the soil from the pots containing 50 mg kg⁻¹ TNT was collected and TNT and TNT-derivatives extracted. At this concentration growth was sufficient to ensure roots were distributed throughout the pot, while biomass differences were still observed.

The HPLC analysis of the TNT and TNT-derivatives proved that most of the extractable TNT remaining in soil was recovered in the form of the reduced derivatives of TNT, ADNTs. Results suggest that all of the dGST lines take up more TNT than the untransformed plants, with some transgenic lines taking up to 25% more TNT than WT (Figure 4.24). This uptake rate is very similar to that displayed by the GST-U24/U25 OE lines (≈21% higher than WT plants). Further interpretation of these findings is complicated by the lack of a no-plant-control.

The ratio of TNT to ADNTs recovered from soil after six weeks (duration of the previous experiment) was 0.36, 0.32, 0.33 and 0.31 for WT, dGST/1, dGST/2 and dGST/3 respectively.

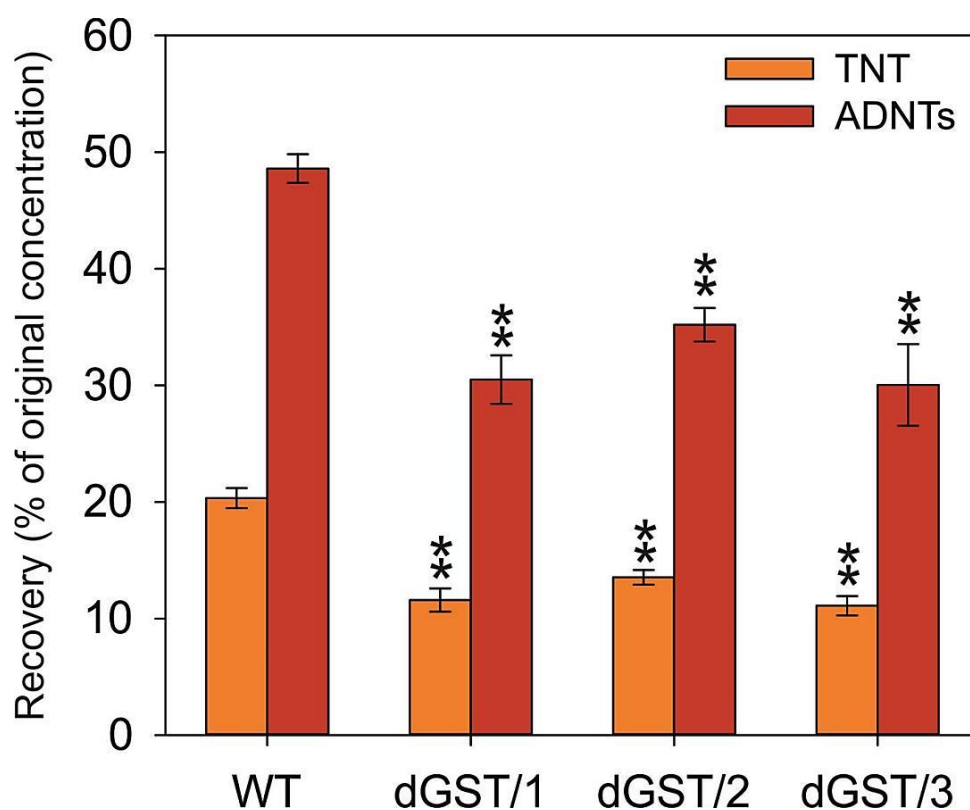


Figure 4.24: Levels of nitrotoluenes recovered from TNT-containing soil. Arabidopsis plants were grown on 50 mg kg⁻¹ TNT for six weeks. WT, untransformed plants; dGST/1-3, independent homozygous lines expressing *DmGSTE6*. Results are mean of eight biological measurements \pm se. Asterisks denote statistically significant from the WT: ** $P < 0.01$.

4.3.14 Hydroponic cultures

To investigate further the TNT uptake by the dGST lines and directly compare it to that of the GST-U24/U25 OE lines, plants were grown hydroponically on plastic rafts containing drilled holes that allowed only the roots to be exposed to the liquid media. This experimental set-up, shown in Figure 4.25, has the advantage of delivering a known concentration of TNT specifically to the roots. The leaf and shoot is not submerged and are more akin to soil-grown plants than the submerged liquid culture grown plants.



Figure 4.25: Hydroponic culture assembly of *Arabidopsis* seedlings. Plants growing on rafts in sterile jars with only their roots exposed to liquid $\frac{1}{2}$ MS medium. Rafts were made from circular lightweight plastic, 70 mm on diameter and 6 mm thick, with approximately 100 holes (3-4 mm diameter) drilled into each disk. Sterile *Arabidopsis* seeds (ten per raft) were pipetted onto the holes filled with $\frac{1}{2}$ MS agar.

All the GST-U24/U25 OE lines and dGST lines removed TNT from the medium faster than WT plants. Almost 30 % of the initial amount of TNT was removed by all plant lines within the first 4 h (Figure 4.26). After that and for the next week the TNT remaining in solution decreases almost linearly with time. After seven days ~30 % of the initial TNT amount remained in the media containing the WT plants, while the GST lines (GST-U24/U25 OE and dGST) displayed lower, but almost identical recovery, or ~24 % of the initial TNT amount (Figure 4.26).

The difference between the WT and the GST lines increased with time. At the end of the experiment only 7.2-10.2 % of the initial TNT amount remained in solution for the GST lines contrary to 19 % for the WT plants (Figure 4.26). The difference between WT plants and the GST lines was statistically significant at 120 h and 168 h (at $P < 0.05$) and statistically significant at $P < 0.01$ after 240 h (last time point collected). The difference in removal was not as big as that of the soil experiment, probably because the TNT concentration used during this experiment was lower.

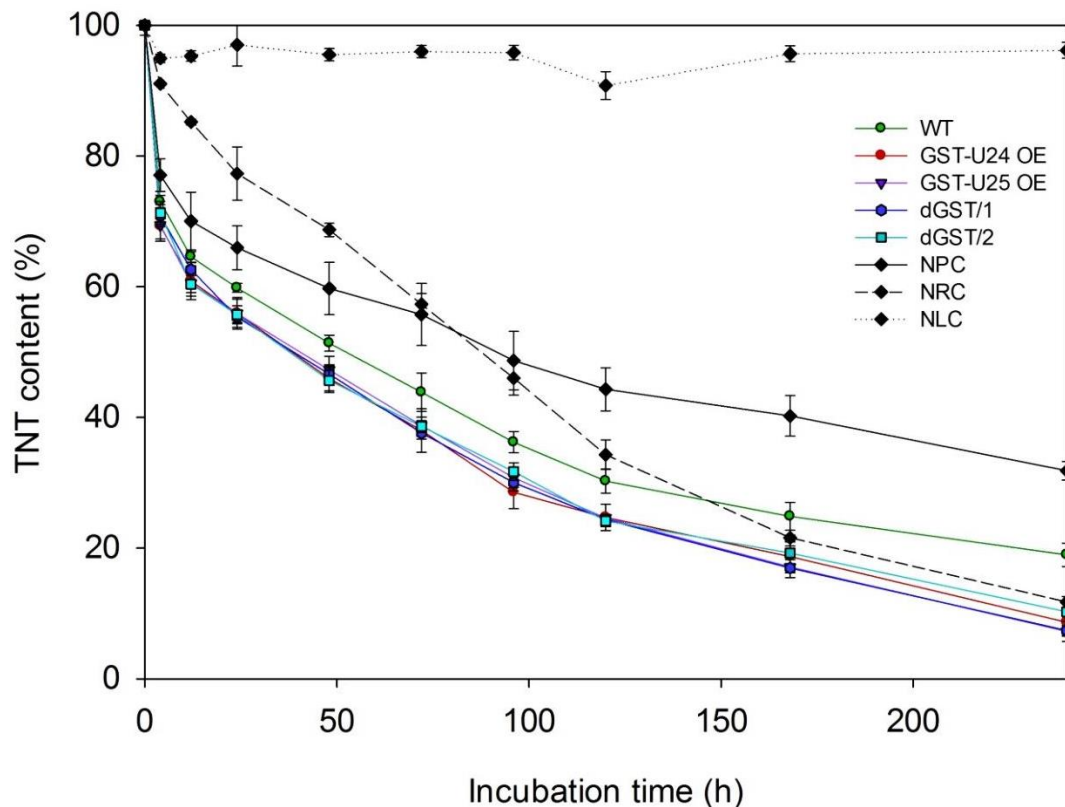


Figure 4.26: TNT uptake from hydroponic cultures. Ten 21-day-old seedlings were grown hydroponically for ten days in jars containing 60 ml of $\frac{1}{2}$ MS with 50 μ M TNT. Samples of the medium were taken from the flasks at regular time points and analysed by HPLC. WT, untransformed plants; GST-U24 OE, GST-U24 over-expressing line; GST-U25, GST-U25 over-expressing line; dGST/1-2, independent homozygous *DmGSTE6* expressing lines NPC, no plant control (to measure the absorption of TNT by the plastic rafts); NRC, no plant control without a raft (to measure the photo-degradation of TNT); NLC, no plant control without raft and light. Results are means of 4 - 5 biological replicates \pm se.

Following analysis of the data it became apparent through the control samples that TNT underwent significant photo-degradation during the course of the experiment. After ten days, a distinct pink coloration of the solution was displayed in the no plant/no raft control (NRC) and to a lesser extent in the no plant control (NPC) (Figure 4.27A). In addition, the intact TNT remaining in solution for the NRC control was at levels comparable to those of the GST-U24/U25 OE and dGST lines. Analysis by HPLC revealed unknown peaks, with retention times at 4.6, 16.2 and 7.5 min, in the NRC and NPC controls that were absent from the remaining samples and that probably corresponded to photo-degradation products (Figure 4.27B).

Chapter 4: Biochemical characterisation of a TNT detoxifying *Drosophila* GST

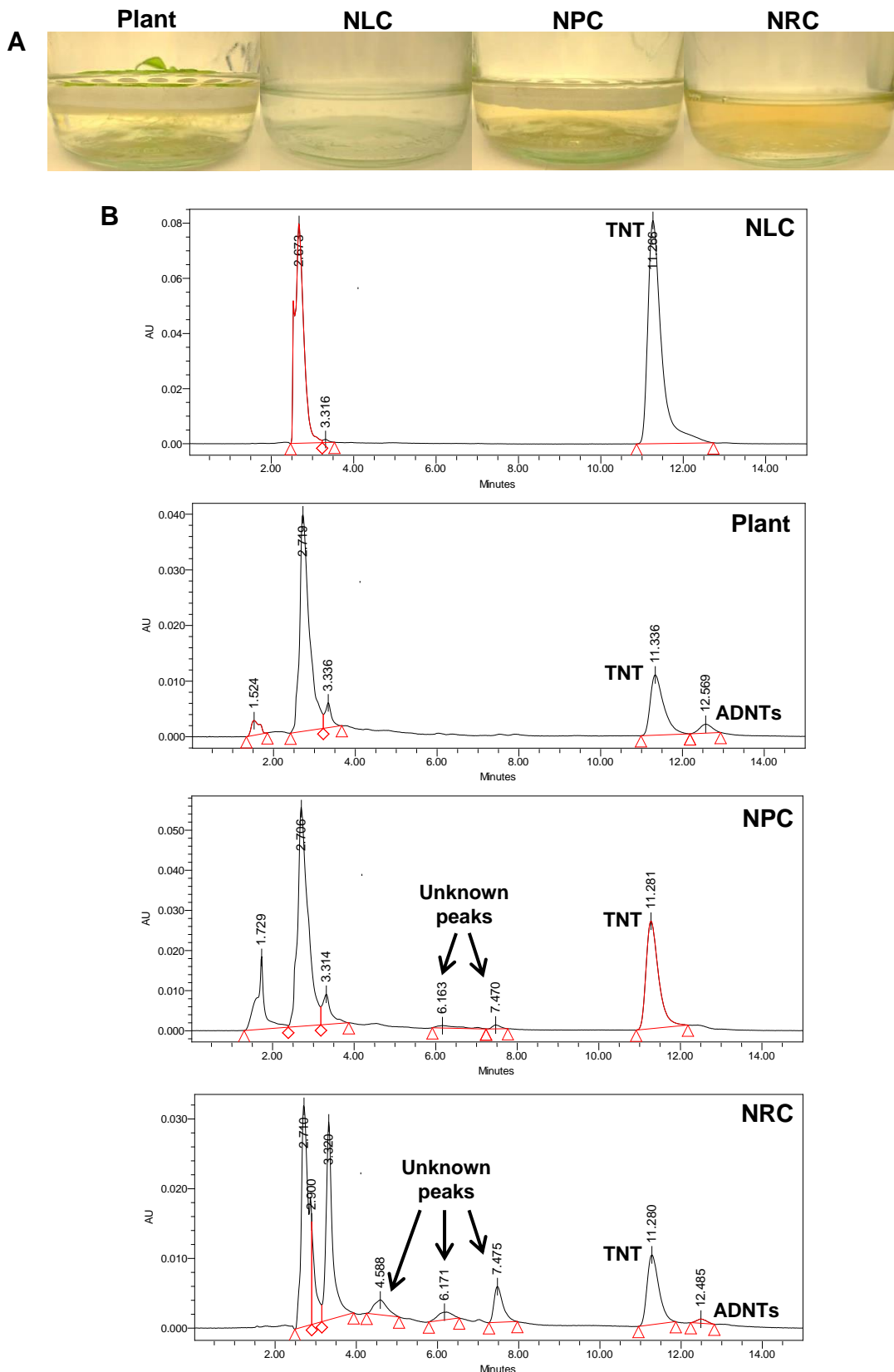
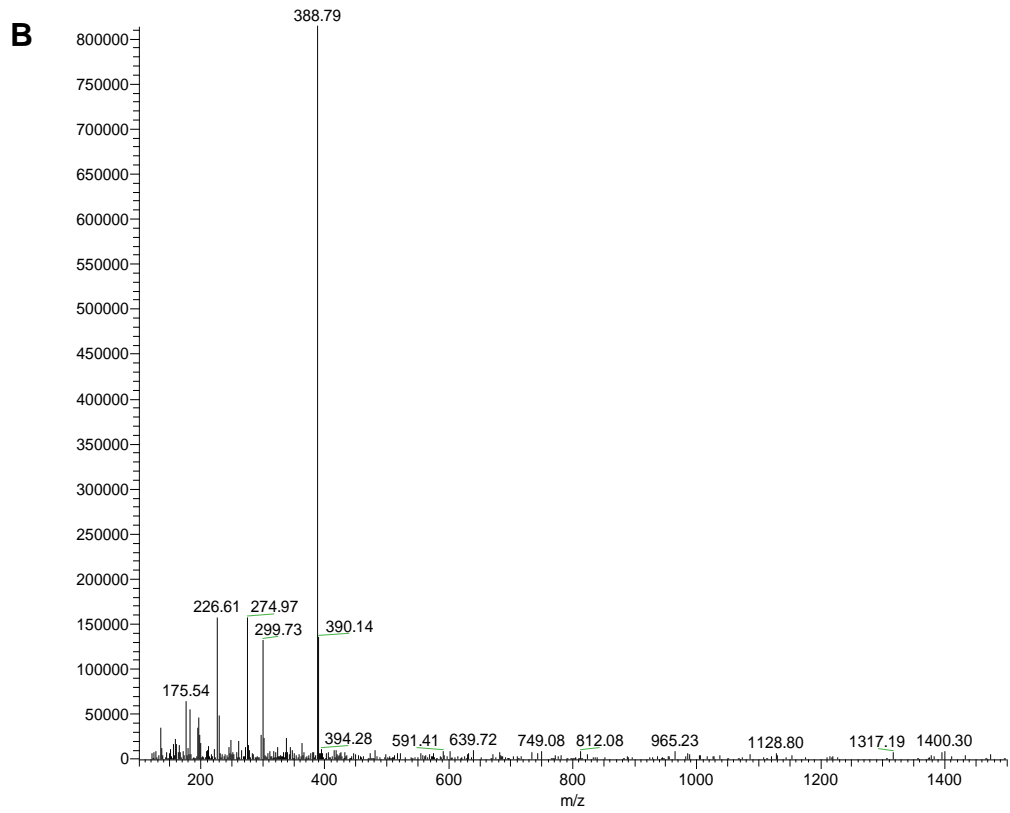
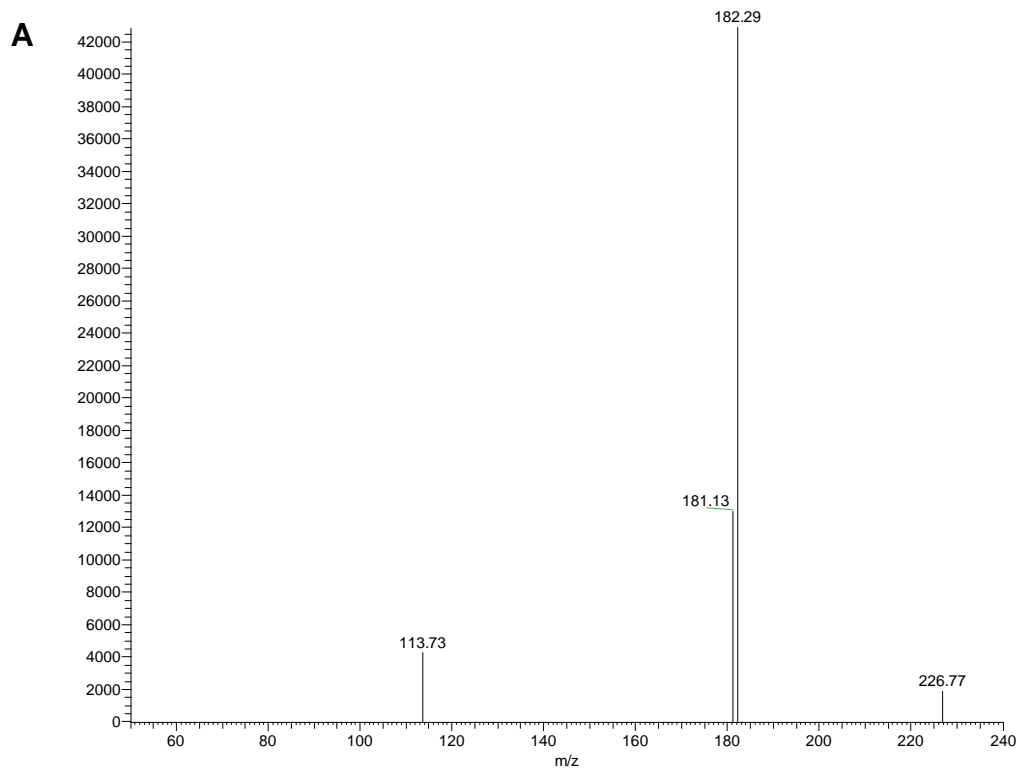


Figure 4.27: (A) Coloration of the $\frac{1}{2}$ MS liquid medium containing $50 \mu\text{M}$ TNT after ten days of incubation. (B) HPLC chromatograms of samples collected after ten days of incubation in $\frac{1}{2}$ MS liquid medium containing $50 \mu\text{M}$ TNT. Plant, jars where untransformed or GST plants were grown; NPC, no plant control; NRC, no plant and no raft control; NLC, no plant, no raft and no light control.

Chapter 4: Biochemical characterisation of a TNT detoxifying *Drosophila* GST



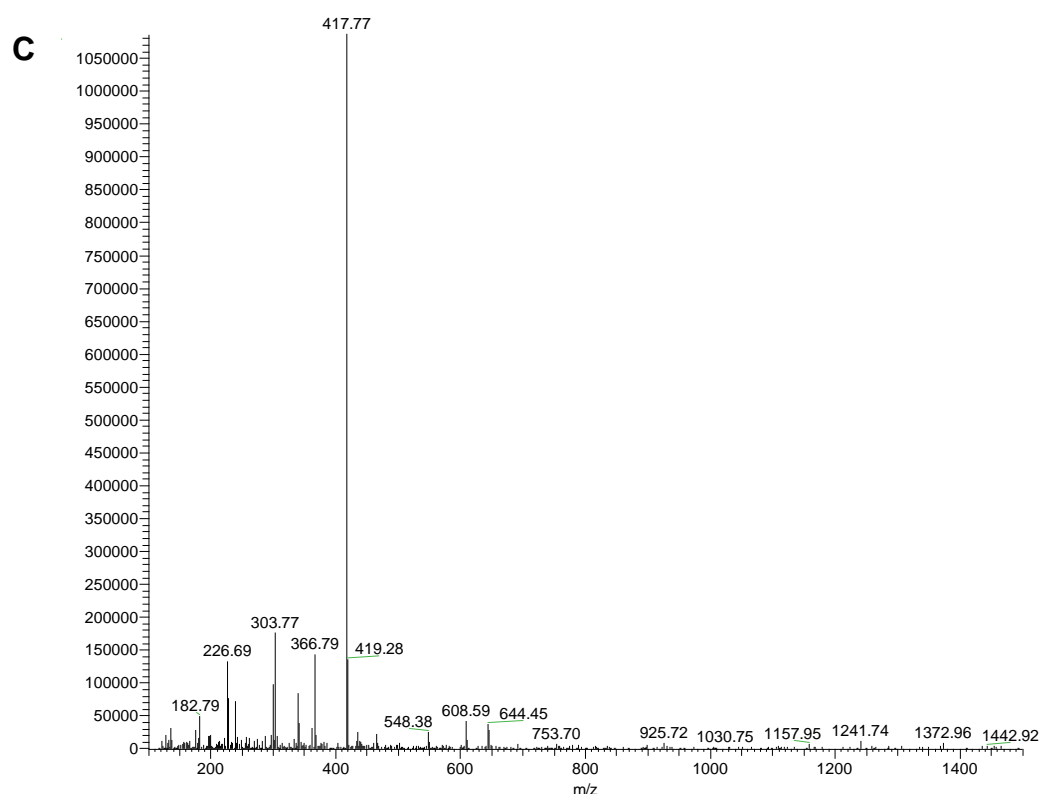
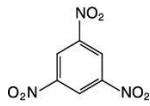
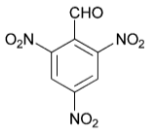
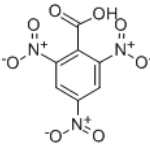
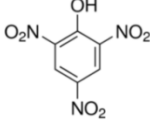
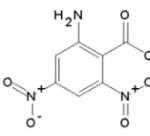
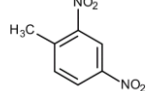
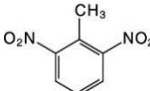
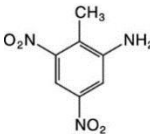
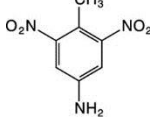
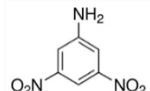


Figure 4.28: Mass spectrometry data as identified by LC/MS analysis of the unidentified peaks with retention times (A) 4.6 min, (B) 6.2 min and (C) 7.5 min. The three peaks give in negative mode an $[M-H]^-$ ion of 182.29, 388.79 and 417.77 respectively.

The no light control (NLC) displayed no fluctuation in the TNT levels throughout the experiment confirming that light was responsible for the degradation of TNT (Figure 4.26). Subsequent LC/MS analysis showed that the unidentified products with retention times 4.6, 6.2 and 7.5 min, gave in negative mode an $[M-H]^-$ ion of 182.29, 388.79 and 417.77 respectively (Figure 4.28). Besides the product eluting at 4.9 min which could potentially be identified as 2,4- or 2,6-dinitrotoluene the mass of the other two products did not match any of the common TNT photo-degradation products as suggested by the literature (Table 4.11). Previously, mass spectrometric analysis of TNT metabolites from plants grown in liquid cultures revealed molecular masses higher than that of TNT and ADNTs, ranging from 238 to 488 [81]. The authors suggest that these metabolites are downstream conjugates of TNT, however, the possibility of these compounds being generated in the medium abiotically and subsequently being taken up by the plant should not be

excluded. Along those lines 4,4',6,6'-tetranitro-2,2'-azoxytoluene and 2,2',6,6'-tetranitro-4,4'-azoxytoluene, the result of condensation of partially reduced TNT intermediates, with a molecular mass of 406.2 have been found to be taken up effectively by plants [72].

Table 4.11: Possible TNT photo-degradation products.

#	Name	MW (g/mol)	Chemical formula	References
1	1,3,5-trinitrobenzene (1,3,5-TNB)	213.11		[210-212]
2	2,4,6-trinitrobenzaldehyde	241.12		[213]
3	2,4,6-trinitrobenzoic acid	257.11		[213, 214]
4	2,4,6-trinitrophenol (picric acid)	229.10		[214]
5	2-amino-4,6-dinitrobenzoic acid	227.13		[210]
6	2,4-Dinitrotoluene (2,4-DNT)	182.13		[210]
7	2,6-Dinitrotoluene (2,6-DNT)	182.13		[210]
8	2-Amino-4,6-dinitrotoluene (2-ADNT)	197.15		[210, 215]
9	4-Amino-2,6-dinitrotoluene (4-ADNT)	197.15		[210, 215]
10	3,5-dinitroaniline (3,5-DNA)	183.12		[211, 215]

4.3.15 Liquid cultures supplemented with TNT and GSH

As GSH is a substrate for *DmGSTE6* it is possible that GSH levels become depleted in the *DmGSTE6* lines, and perhaps more so in the presence of TNT, as a result of conjugation. To test whether the application of exogenous GSH could enhance a potentially limiting supply of endogenous GSH, plants were grown in liquid cultures supplemented with TNT and a range of GSH concentrations for one week. Glutathione has been previously found to be taken up by seedlings, embryos and pollen grains of *Arabidopsis* [129, 132, 133, 189].

GSH was successfully taken up from the media by the plants and had a direct effect on the uptake and detoxification of TNT. In the absence of GSH, the *dGST/1* lines, as expected, displayed a statistically significant (at $P < 0.05$) higher TNT uptake rate than WT plants, with 67 and 49% respectively of the TNT removed after 24 hours (Figure 4.29). When 100 μM of GSH was present in the media, the rate of TNT uptake increased for both WT and *dGST/1* plants; after 24 hours, 83 and 64 % of the TNT had been removed by the *dGST/1* and wild-type lines respectively with that difference being statistically significant at $P < 0.01$. Increasing the GSH concentration to 250 μM enhanced the uptake only slightly in *dGST/1* plants and did not enhance at all the uptake in wild-type plants, which displayed a lower TNT uptake rate than that observed in the absence of GSH.

At 1000 μM GSH a strong toxic effect was observed on the plants which became chlorotic (Figure 4.30). Glutathione concentrations up to 250 μM had visible toxic effects on the plants after five days of incubation, with the *dGST/1* plants being more tolerant than WT plants. The highest GSH concentration used (1000 μM) was lethal for both plant lines, with the plant lines displaying strong chlorosis after only two days of incubation and appearing necrotic after five (Figure 4.30). The toxic effect of GSH on the plants was confirmed by measuring the chlorophyll content of the plants at the end of the experiment. Chlorophyll was found to reduce in both plant lines in a dose-dependent manner with increasing concentrations of GSH (Figure 4.31).

The GSH levels in solution were monitored throughout the experiment. The GSH levels decreased after the first 24 h in all samples (Figure 4.32), indicating successful uptake by the plants, however, reduced GSH in the remaining samples was not measured. While the method enabled the simultaneous detection of both GSH and TNT metabolites, it was not optimised for GSH. During HPLC analysis there were problems with the GSH peak detection and due to time constraints the experiment was not repeated. The levels of GSSG are given in Figure 4.33. In general, liquid media supplemented with up to 250 μM did not display any significant levels of GSSG, probably because most of the GSH was taken up by the plants and as a result less GSH remained in solution to be oxidised. The samples supplemented with 1000 μM GSH displayed elevated levels of GSSG in solution that followed the same formation pattern for both plant lines, reaching a maximum after 2-3 days, and decreasing in tandem with the plants becoming necrotic at day 5.

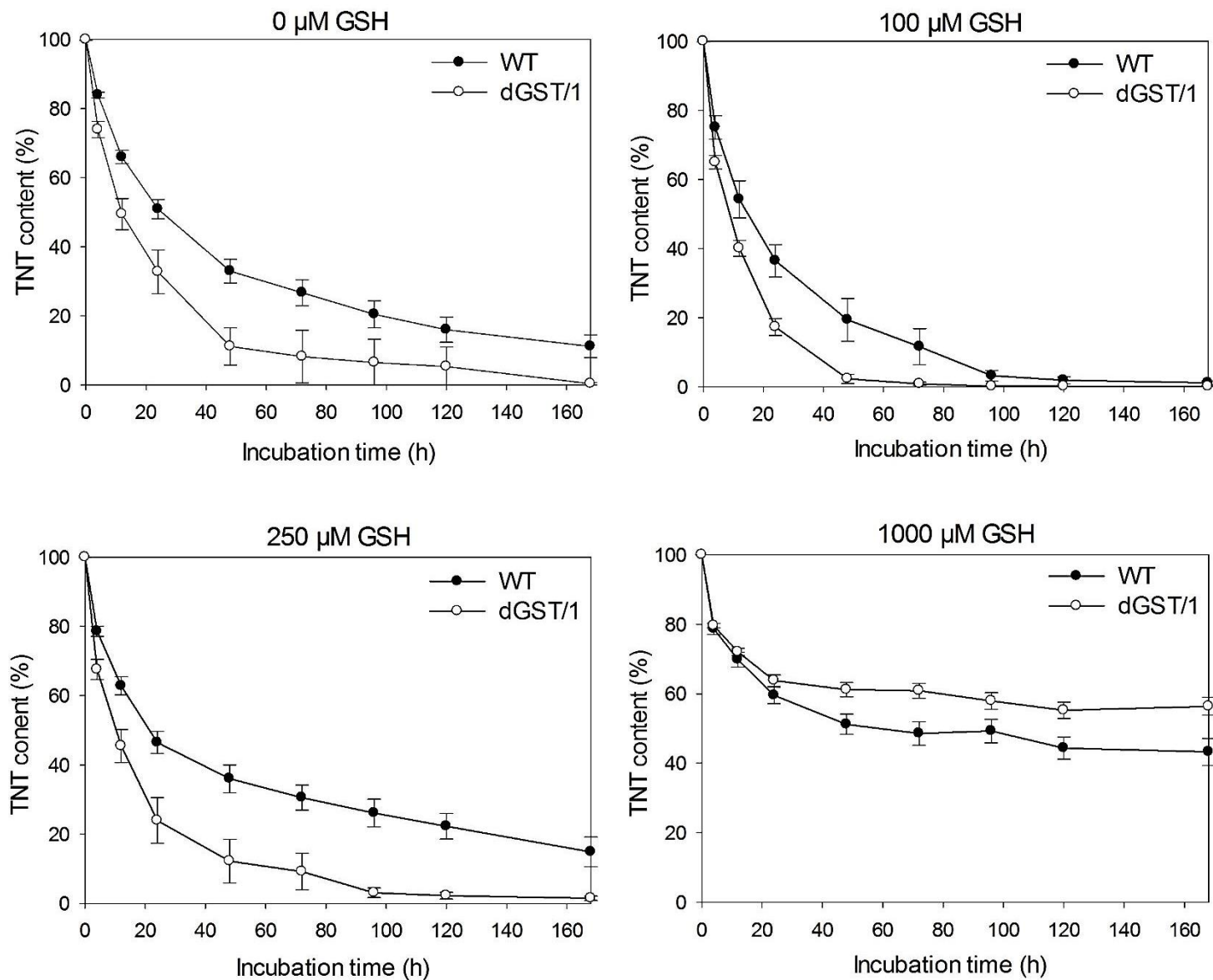


Figure 4.29: TNT remaining in solution expressed as percentage of initial concentration. Plants were grown for a week in ½ MS liquid media containing 250 μM TNT and a range of GSH concentrations. WT, untransformed plants; dGST/1, best performing *DmGSTE6* expressing line. Results are means of 5-6 biological replicates ± se.

Chapter 4: Biochemical characterisation of a TNT detoxifying *Drosophila* GST

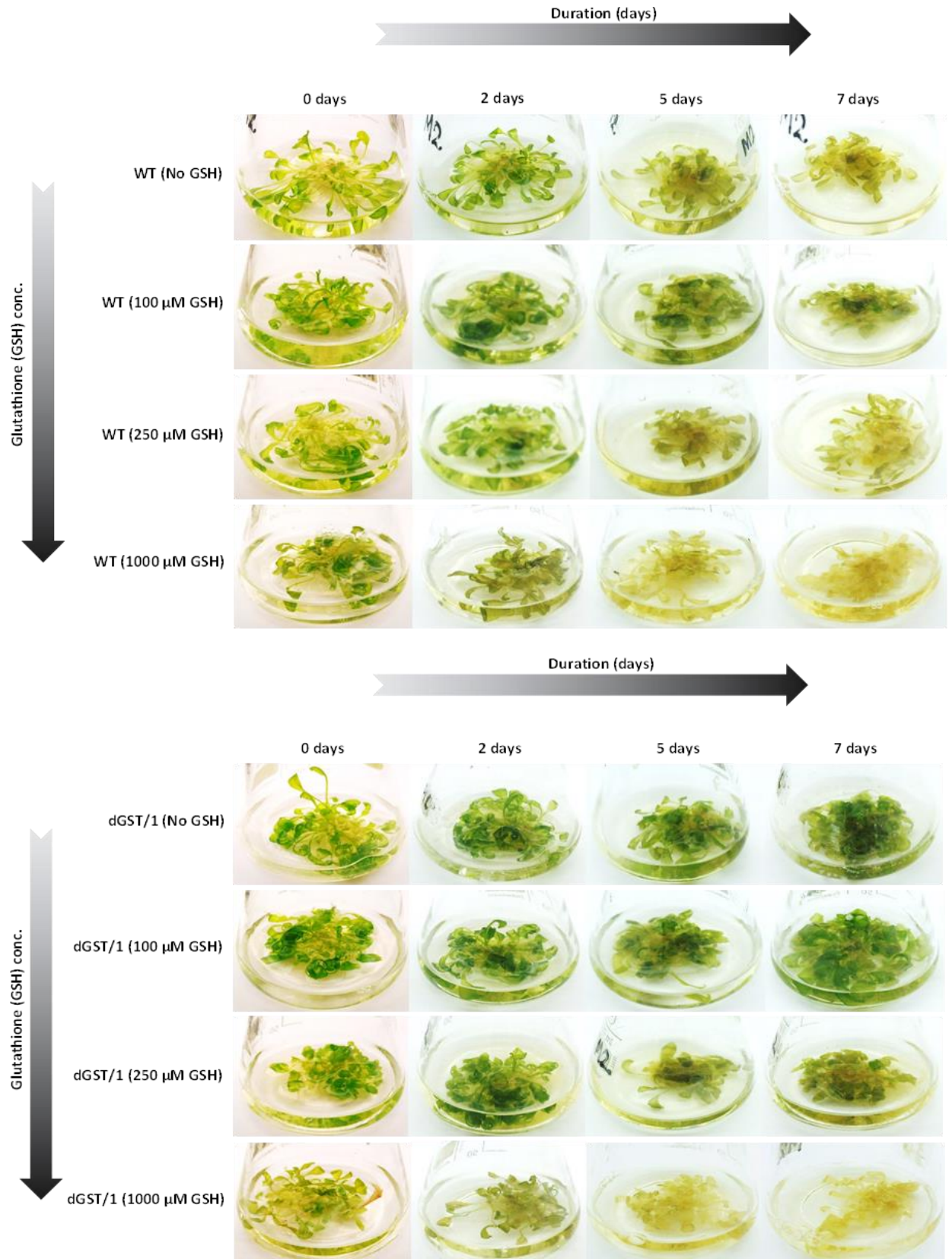


Figure 4.30: Appearance of untransformed (WT) (above) and the best performing *DmGSTE6* expressing line (dGST/1) (below) grown for one week in $\frac{1}{2}$ MS liquid media containing 250 μM of TNT and a range of GSH concentrations.

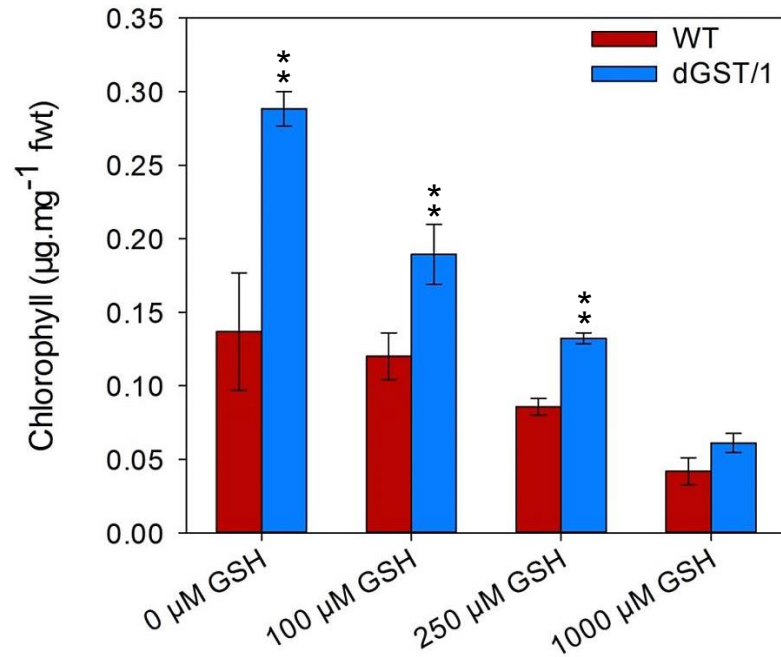


Figure 4.31: Chlorophyll content of plants grown after one week of incubation in ½ MS liquid media supplemented with 250 µM TNT and a range of GSH concentrations. WT, untransformed plants; dGST/1, best performing *DmGSTE6* expressing line. Results are means of 5-6 biological replicates ± se. Asterisks denote statistically significant from the WT: ***P*<0.01.

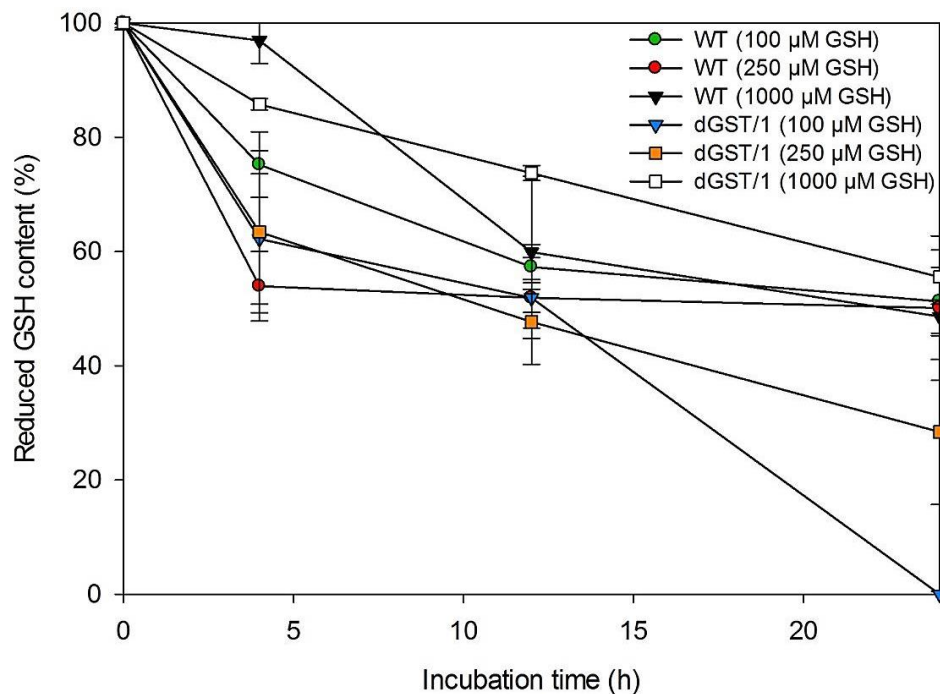


Figure 4.32: Levels of GSH in ½ MS liquid media supplemented with 250 µM TNT and a range of GSH concentrations. Plants were grown in the liquid media for one week. WT, untransformed plants; dGST/1, best performing *DmGSTE6* expressing line. Results are means of 5-6 biological replicates ± se.

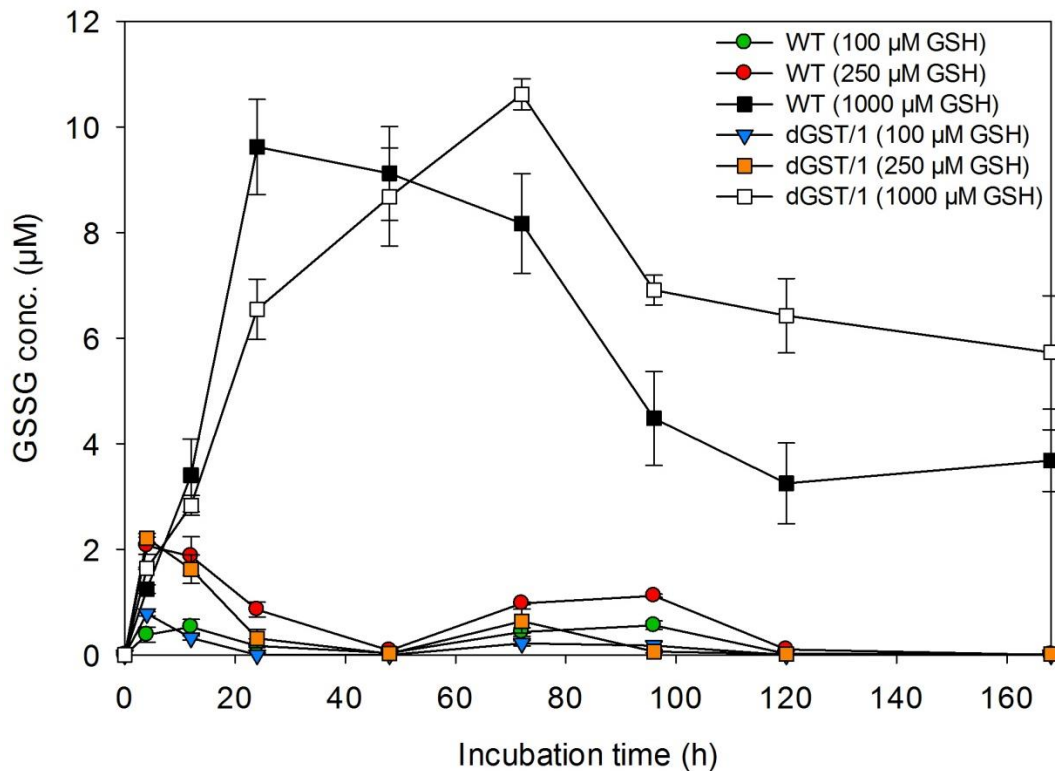


Figure 4.33: Levels of GSSG in $\frac{1}{2}$ MS liquid media supplemented with 250 μ M TNT and a range of GSH concentrations. Plants were grown in the liquid media for one week. WT, untransformed plants; dGST/1, best performing *DmGSTE6* expressing line. Results are means of 5-6 biological replicates \pm se.

4.3.15.1 Effect of exogenous GSH on internal levels of GSH

To investigate whether the exogenous GSH is efficiently taken up by the plants and that the internal levels of GSH correspond to this uptake, WT and dGST/1 plants were grown for 24 h in $\frac{1}{2}$ MS liquid media, supplemented with either 250 μ M TNT, 100 μ M GSH, or both. After 24 h, plants were harvested and GSH levels were determined. Results are given in Figure 4.34. As expected, levels of GSH in WT plants increased beyond that found in the TNT-only plants when GSH was supplied exogenously. The WT plants grown in the medium containing both TNT and GSH displayed levels of GSH intermediate between those of the TNT only and GSH-only plants. This pattern, however, was not followed by the dGST/1 plants which displayed higher GSH levels than WT plants in TNT only medium. In addition, the dGST/1 GSH levels were unaffected by the exogenous GSH supplied. The levels of oxidised glutathione were comparable between WT and dGST/1,

showing that the main difference between the two plant lines derived from the levels of reduced glutathione. Nevertheless, further interpretation of these results was hindered by the lack of a 'No TNT/GSH' control.

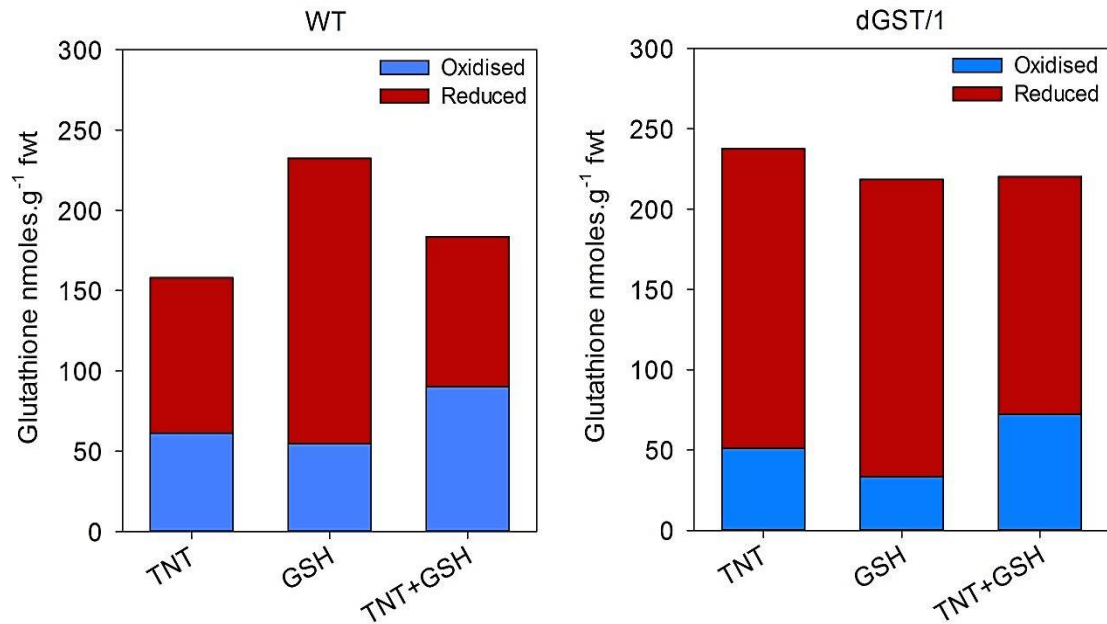


Figure 4.34: Internal GSH levels of plants grown for 24 h in ½ MS liquid media supplemented with 250 µM TNT, 100 µM GSH, or both. WT, untransformed plants; dGST/1, *DmGSTE6* expressing line. Results are means of six biological replicates ± se.

4.3.16 Glutathione depletion studies

Results so far indicate that GSH supply could be a limiting factor in TNT detoxification by GSTs. To test the effect of GSH depletion on the growth and detoxification abilities of the dGST lines, the plants were grown on ½ MS agar plates with no TNT and plates containing 7 µM TNT in the presence of increasing concentrations of the GSH synthesis inhibitor buthionine sulfoximine (BSO). Buthionine sulfoximine is a non-toxic inhibitor of the rate-limiting enzyme of GSH synthesis, γ-glutamylcysteine synthase (γ-ECS) [130, 132, 133, 216]. Results are given in Figure 4.35.

In the absence of TNT, across the increasing BSO concentrations the dGST lines displayed consistently higher root growth than WT plants (Figure 4.35A, B). BSO concentrations of up to 100 µM had a strong effect on the plant growth of WT plants but not on the dGST lines. At 50 and 100 µM BSO the dGST lines displayed on average 2.1 and 3.2-fold longer root lengths than WT respectively. At 500 and 1000 µM BSO, amounts that have been reported to reduce GSH levels by up to 90 % [122, 130], all plants suffered severe stunting of their growth. At 1000 µM WT, dGST/1 and dGST/3 plants displayed 0.09, 0.15 and 0.13-fold of the root length achieved at 0 µM BSO. Nevertheless, at 1000 µM BSO the dGST lines had on average 1.6-fold greater root length than WT (Figure 4.34A). The presence of TNT in addition to the GSH depletion had a negative effect on root growth, as all plant lines exhibited reduced root growth when compared to growth on plates containing only BSO (Figure 4.35C). The dGST lines displayed longer roots than WT in the presence of TNT, reaching on average 1.4, 4.3 and 2.3-fold greater root length than WT at 0, 50 and 100 µM BSO respectively. The increased difference between WT and dGST lines in the presence of TNT reflects the superior TNT detoxification abilities of the dGST lines. Higher BSO concentrations reduced the root length of all plant lines to levels similar to those of the TNT-free plates (Figure 4.35C, D).

Chapter 4: Biochemical characterisation of a TNT detoxifying *Drosophila* GST

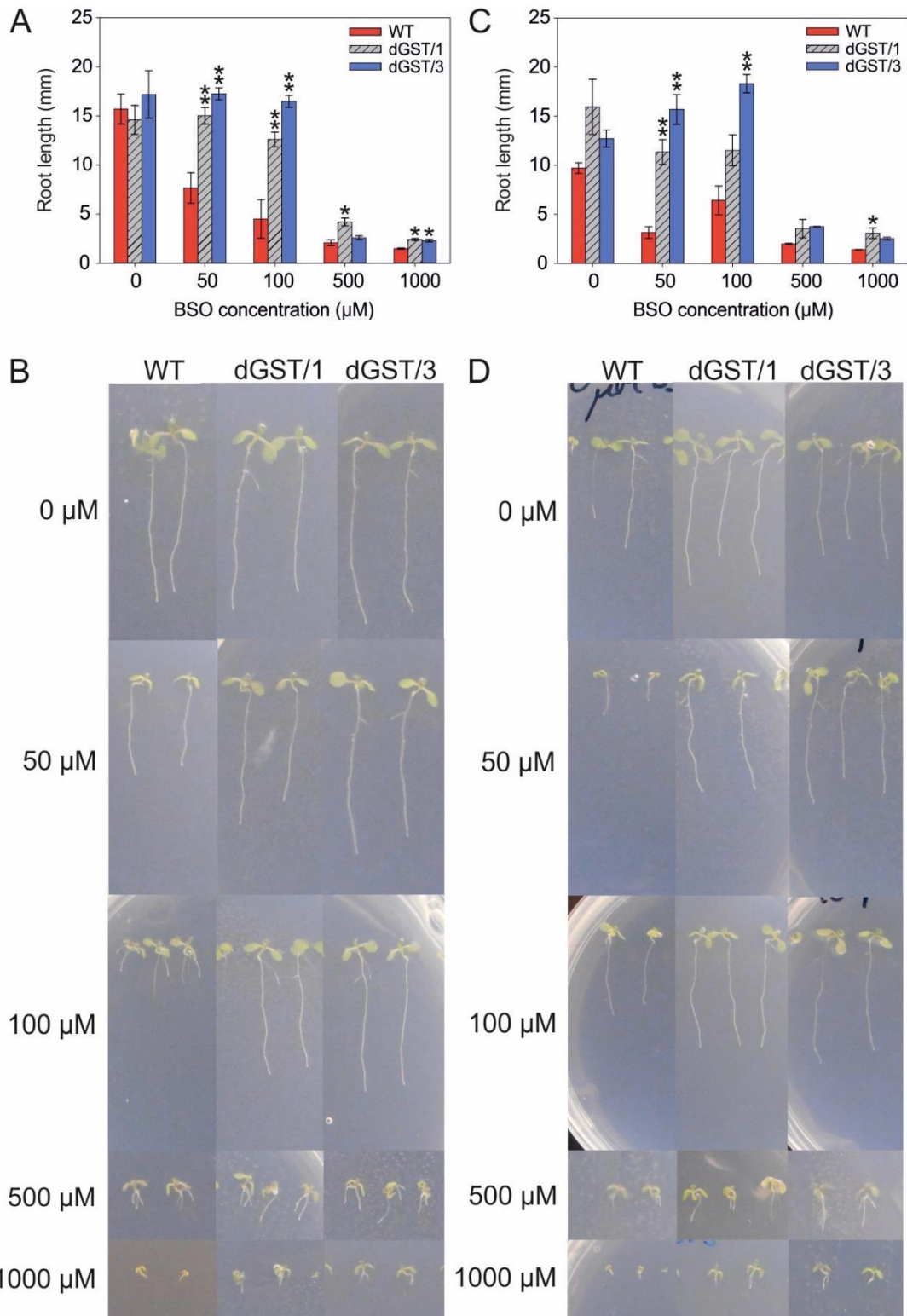


Figure 4.35: Root length (A) and appearance of plants (B) grown vertically for one week on ½ MS agar plates with a range of BSO concentrations. (C, D) Root length and appearance of plants grown vertically for one week on ½ MS agar plates containing 7 µM TNT and a range of BSO concentrations. WT, untransformed plants; dGST/1-3, independent homozygous *DmGSTE6* expressing lines. Results are means of 3 biological replicates ± se. Asterisks denote statistically significant from the WT: * $P < 0.05$, ** $P < 0.01$.

4.3.17 GGT1 and GGT3 involvement in the catabolism of TNT-GSH conjugates

The enzymes GGT1 and GGT3 are the two γ -glutamyl transpeptidases that account for the total GGT activity in the roots of *Arabidopsis*. To test whether GGT1 and GGT3 could be involved in the catabolism of the TNT-derived conjugates, knockout (KO) plant lines for GGT1 (*ggt1-1*), GGT3 (*ggt3-1*) and double mutants (*ggt1-1/ggt3-1*) were grown alongside WT plants in the presence of TNT. The plants were monitored over a twenty-day period.

Analysis of the root lengths showed that after nine days, both *ggt1-1* and *ggt3-1* seedlings displayed shorter roots than WT plants, independently of the presence of TNT. Between the two single KO lines the *ggt3-1* mutants were more affected by the toxicity of TNT, displaying the shortest roots among all plant lines at the highest TNT concentration tested (15 μ M TNT). On the other hand, the double KO lines *ggt1-1/ggt3-1* were less affected than the single KO plants, achieving similar or higher root length than the WT plants across all TNT concentrations.

After twenty days of incubation, calculation of the root surface area showed that the plants did not follow the same trend as with the nine-day analysis. With few exceptions most of the KO lines had comparable root surface area to WT, or even higher. The *ggt1-1* mutant displayed higher root surface than WT at 15 μ M TNT concentration, a result that contradicts that observed during the nine-day analysis, whereas the *ggt1-1/ggt3-1* double mutant exhibited root surface area higher than WT at 2 and 15 μ M TNT. The only observation that agrees between the nine and twenty-day analysis is that at the highest TNT concentration tested the *ggt3-1* mutant displayed the shorter roots or smaller root surface area among all the plants lines.

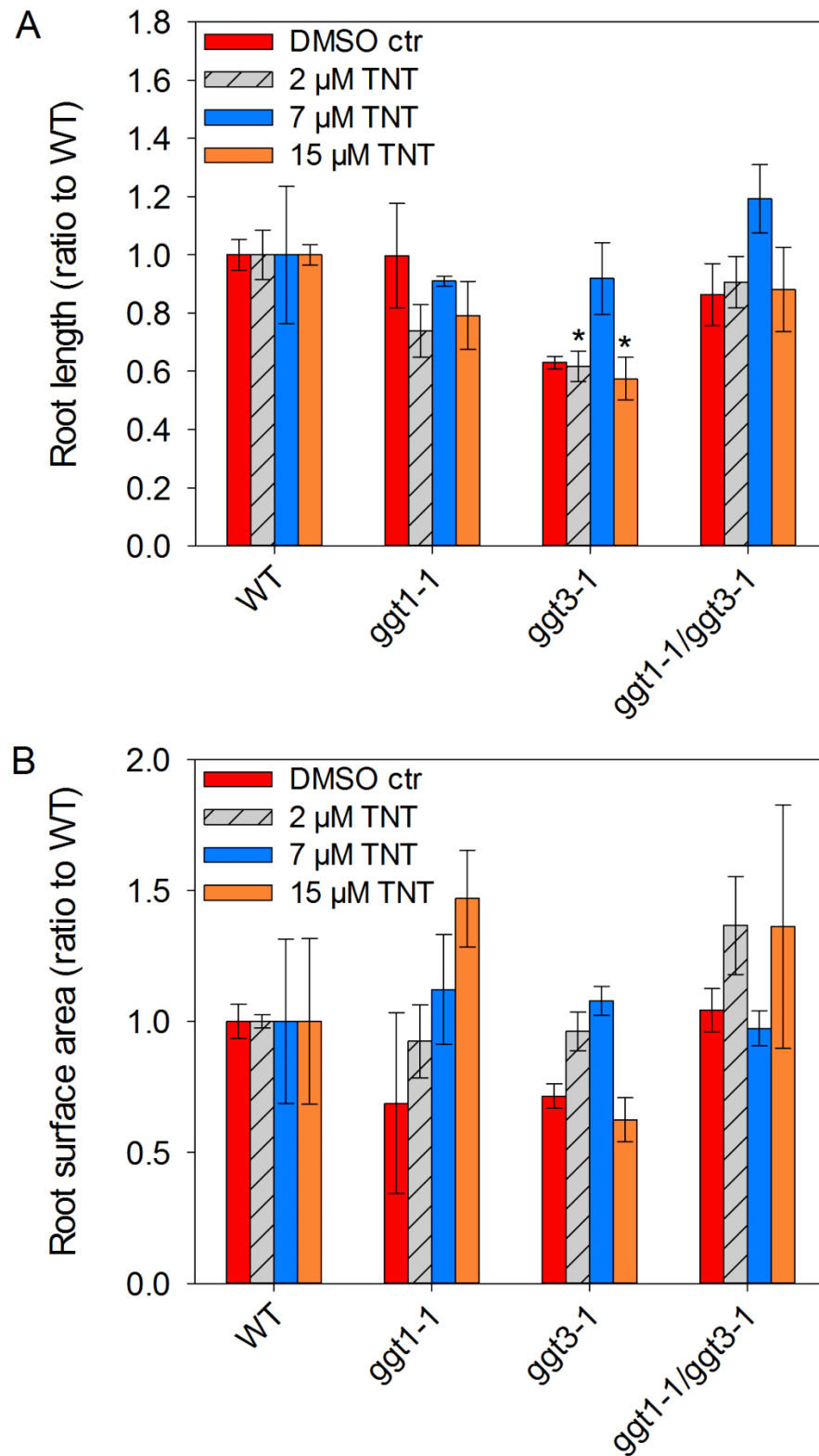


Figure 4.36: Root length (mm) of plants grown for 9 days (A) and root surface area (pixels) of plants grown for 20 days (B) on agar plates containing a range of TNT concentrations. All plants used were of Landsberg background. WT, untransformed plants; ggt1/3, single and double knockout lines for GGT1 and GGT3 γ -glutamyl transpeptidase. Results are means of three biological replicates \pm se. Asterisks denote statistically significant from the WT: * P <0.05.

4.4 Discussion

The *D. melanogaster* Epsilon class GST, *DmGSTE6*, was previously shown to have activity towards TNT (Professor Bengt Mannervik, University of Stockholm, pers. comm.). As a result, *DmGSTE6* was characterised and recombinantly expressed in *Arabidopsis* to evaluate its potential for the phytoremediation of TNT. Kinetic analysis with CDNB was performed to test the activity and functionality of the purified *DmGSTE6*. Although many GSTs are not active with this xenobiotic substrate, Delta and Epsilon class GSTs from insects were previously found to catalyse the conjugation of CDNB [200, 217]. The kinetic analysis of GST-U24 and GST-U25 with CDNB had already been carried out in the past in the Bruce laboratory [165, 166]. Comparing to GST-U24 and GST-U25, *DmGSTE6* displayed significantly higher activity towards CDNB but lower affinity towards this substrate. While the K_m value calculated here agrees with the previously published data of Saisawang et al. [192] for *DmGSTE6*, the V_{max} value displayed significant deviation. As the authors do not mention the temperature used in their assay description it is possible that the difference in the V_{max} value is the result of different assay temperatures. Different temperatures can result in different V_{max} values while the K_m value remains unaffected.

The *DmGSTE6* was found to catalyse the conjugation of TNT to GSH, but had no activity towards the reduced derivatives, HADNTs and ADNTs, as previously shown for GST-U24 and GST-U25 [165]. In addition, significant levels of GPOX activity were not detected. The conjugation of TNT with GSH results almost exclusively in conjugate 3 production with concurrent nitrite release, as confirmed by the results of the pH and temperature screening, and the Griess assay. Increasing temperature resulted in higher activity of the enzyme along with an increased production of conjugate 2. The ratio of conjugate 3: conjugate 2 decreased at increasing temperatures in a temperature dependent manner. Different temperatures can affect the thermostability of the enzyme and cause conformational changes to the enzyme [218, 219], directly affecting the active site, and thus could account for the increased conjugate 2 production at higher temperatures. Screening of

different pH values revealed that the activity of *DmGSTE6* increased with pH, with the optimum pH at pH 9.0. This is in agreement with the pH optimum of between 9.0 and 9.5 observed for both GST-U24 and GST-U25 [165]. This high catalytic activity at higher pH values can be attributed to the sulfhydryl group of GSH which has a pKa of 9.4, making the reactive thiolate anion more stable at higher pH values [84]. There are only a few studies that have investigated the pH optima of plant GSTs, nonetheless, their findings agree with the high pH optima of 9.0 observed here. A purified maize GST was found to have a broad pH optimum of between 7 and 8 using metolachlor as a substrate [220], while another purified maize GST isozyme displayed a pH optimum of 8 to 8.5, using atrazine as the substrate [221]. The Griess assay of the purified enzymes showed that at higher pH values nitrite release from non-TNT conjugating activity occurs. Since the amount of nitrite increased with increasing values of pH, it can be assumed that this is probably the result of alkaline hydrolysis. Qasim et al. have reported that significant amounts of nitrite resulted from the alkaline hydrolysis of TNT in aqueous solutions of high pH values [17]. Under such alkaline conditions polymerisation reactions can also occur between the TNT molecules [17], reducing the number of exposed nitro groups. In such a case the presence of enzyme could reduce polymerisation by binding TNT molecules in the active site or in non-catalytic ligand binding sites that have been previously identified in plant GSTs [100], allowing alkaline hydrolysis to proceed. This hypothesis can explain the non-conjugating enzyme-related nitrite release, and the absence of nitrite release in the boiled enzyme control samples.

The high K_m values of GST-U24 and GST-U25 towards TNT (1.6 and 1.2 mM respectively) indicate that TNT needs to be present in the cytosol at levels that are toxic when supplied exogenously, before it can be optimally detoxified by these enzymes. On the other hand, the significantly higher V_{max} of *DmGSTE6* compared to that of GST-U24 and GST-U25, along with an increased affinity towards TNT (4.5 and 6.1-fold lower K_m than GST-U24 and GST-U25 respectively), would allow the *DmGSTE6* to detoxify TNT more efficiently, and possibly before the cytosolic concentration reaches toxic levels.

DmGSTE6 was expressed in *Arabidopsis* under the control of the near-constitutively expressing CaMV 35S promoter. The activity of protein plant extracts towards CDNB showed that the dGST lines had higher activity than WT and GST-U24 OE lines but not GST-U25 OE lines. The increased activity of the GST-U25 lines can be explained by the use of CDNB as substrate. Although CDNB is a near-universal substrate for GSTs, the significantly different affinities displayed by GST-U25 and *DmGSTE6* towards this substrate made it not suitable for comparing the *in vivo* conjugation activities of GST-U25 OE and the dGST transgenic lines. The results of the Griess assay confirmed the higher conjugation activity of the dGST plants when compared to both WT and GST-U24/U25 OE lines. The Griess assay was chosen since it can indirectly measure the amount of conjugate 3 produced by monitoring levels of nitrite. At pH values of 6.5-7.0 both GST-U25 and *DmGSTE6* produced almost exclusively conjugate 3. Within the roots, the site of detoxification in dicot and grass species [66-68], the pH of the cytosol is estimated to be within the range of 6.5 to 7.9 [167-170]. As a result, measurement of the amount of conjugate 3 produced at such pH values directly compared the *in vivo* activities of the two enzymes and confirmed the higher GST activity of the dGST lines comparing to the GST-U25 OE lines.

Expression of *DmGSTE6* in *Arabidopsis* conferred increased tolerance to TNT compared to WT and GST-U24/U25 OE lines. The plants were able to generate more biomass in soil studies and when grown on ½ MS agar plates. The previously observed yield drag for the GST-U24/U25 OE lines was not observed for the dGST lines. Across the experiments performed with growth on agar plates, the dGST lines did not display any decrease of their root growth compared to untransformed plants when grown on media without TNT. In soil studies, dGST plants grown on soil without TNT achieved the same shoot biomass as WT plants but displayed lower root biomass. Although this effect was not statistically significant and did not appear in any of the remaining experiments, there was a trend across the dGST lines for lower root biomass than WT that was specific to the soil studies and limited to the roots when grown in TNT-free soil. Since the *DmGSTE6* does not possess any significant GPOX activity and the trend appears only in the soil studies, it

could be hypothesised that the yield drag could be the result of deleterious conjugation or stabilisation of a compound present in the soil.

Extraction of nitrotoluenes from TNT-containing soil in which the dGST lines had been grown revealed that the enhanced TNT tolerance of the dGST lines compared to that of the GST-U24/U25 OE lines, and the increased specific activity of the *DmGSTE6* recorded *in vitro*, does not translate into a higher TNT uptake. One obvious reason for this result could be between experiments variation. Since the GST-U24 and GST-U25 OE lines were not included in this specific experiment it could be argued that the conditions of the individual experiments were responsible for the similar TNT uptake rates. Nevertheless, attempts were made to standardise the soil experiment (equal soil water contents when dosing, same growth cabinet) and wild type plants were grown in both experiments. In any case, the results of the hydroponic cultures disprove that claim. Although the hydroponic system proved to be not an optimal system, due to significant TNT photo-degradation, the results confirmed a similar TNT uptake rate by the dGST and GST-U24/U25 OE lines. The levels of TNT remaining in solution for all the GST lines were lower than those of the WT, but when compared to each other GST-U24/U25 OE and dGST plants displayed almost indistinguishable TNT uptake rates throughout the hydroponic experiment. The GSH concentration is, therefore, likely to be limiting the conjugation reaction. The GSH abundance in the *Arabidopsis* cytosol is predicted to be in the range of 1 to 3 mM [190, 222], a concentration high enough to detoxify efficiently TNT in the presence of sufficient GST activity. However, it is possible that GSH levels are limited because GSH is utilised by other biochemical processes, because they are compartmentalised to secure the GSH levels of specific organelles or because the actual GSH levels are lower than those reported. Glutathione is implicated in important biochemical processes and can move between subcellular compartments [117]. Despite the lack of evidence for GSH synthesis, high GSH concentrations have been reported in the mitochondria [128], while García-Giménez et al. (2013) showed that GSH can accumulate in the nucleus against a concentration gradient [223]. In addition, the first putative plant GSH transporters have been cloned and functionally characterised, as the *OsGST1*

transporter from rice (*Oryza sativa*) was shown to transport exogenous GSH, GSSG and GS-conjugates across the plasma membrane [224]. Supplementing the medium with GSH increased the ability of both WT and dGST plants to remove TNT from media. The greatest GSH-supplemented increase in TNT uptake was seen for the dGST line. This is presumably because the dGST line had more GST activity to conjugate excess GSH to TNT. This result further supports the hypothesis that GSH abundance is limiting the reaction. However, at the higher concentrations tested, the exogenously supplied GSH exhibited strong toxic effects on the plants. The GSH:GSSG ratio acts as a homeostatic redox buffer and is strictly regulated, contributing to the maintenance of the cellular redox balance [225]. Under physiological conditions, leaves (no data are available for the roots), maintain on average a GSH:GSSG ratio of 20:1, with ratios fluctuating between subcellular compartments and different tissues [124, 126]. The exogenous GSH absorbed by the plant cells could alter the GSH: GSSG ratio significantly, disturbing the redox status of the cells and thus accounting for the toxicity [226, 227]. Concentrations of GSH up to 1 mM (the highest GSH concentration used here) have been used in previous studies with *Arabidopsis*, without any toxic effects for the plants being reported. This lack of toxicity can be explained by the conditions used in those experiments. All of the plants/seeds in those studies supplemented with GSH concentrations of up to 1 mM had deprived GSH levels due to the use of BSO or a mutation in the GSH1 gene blocking GSH synthesis. As a result, even after taking up GSH supplemented in the medium, the internal GSH concentration in the plant tissues is likely to have been lower than the one reported here. These findings, along with the results presented in this chapter suggest the existence of a threshold for GSH concentration that, once exceeded, becomes toxic to the plant. This is in agreement with the findings of Zechman et al. [133] who reported that poor germination rates due to GSH depletion by BSO could be restored by the addition of 1 mM GSH in the growth media without any toxic effects. However, further increase of the GSH concentration to values higher than 3 mM exhibited strong toxic effects, reducing germination to only 12 %.

The studies using BSO along with the measurement of plant GSH levels in the liquid cultures supplemented with GSH suggest that the dGST lines are either more resistant to GSH depletion by BSO or have higher levels of GSH than WT plants. Although elevated levels of GSH in response to recombinant expression of a GST have not been reported before, it is possible that increased conjugation of TNT or, in the absence of it, of a cell metabolite could decrease GSH levels, triggering GSH synthesis, and resulting in the elevated levels of GSH. The γ -ECS which catalyses the first and rate limiting step of GSH has been found to be regulated by feedback inhibition by GSH [122, 123].

Analysis of the effect of GGT3 and GGT1 on the performance of plants grown in the presence of TNT, did not yield any strong indication that these enzymes are directly involved in the catabolism of the TNT-GSH conjugates. Besides the shorter roots and smaller root surface area displayed by the *ggt3-1*, that could suggest the importance of the GGT3 enzyme for the metabolism of the TNT-GSH conjugates, the results after nine and twenty days were contradictory, whilst the higher root growth of double KO lines comparing to single KO plants was also unexpected. It is possible that the absence of sufficient TNT-GSH conjugate flux did not stress the plants enough to display any significant differences. In addition, no genotyping was carried out to confirm the mutations due to time constraints, and although this is an unlikely cause for the results, it should still be confirmed. At this point the data collected are inconclusive and further investigation is required. Crossing or transforming the *ggt1/3* KO plants with *DmGSTE6* would demonstrate whether the absence of GGT1 and GGT3 affects the plant in terms of increased TNT-conjugate production.

Chapter 5: Site-directed-mutagenesis on *AtGSTU24* & *U25*

5.1 Introduction

Nitro-substituted organic compounds, such as TNT, pose a distinct challenge to plant and bacterial degradation. TNT is particularly recalcitrant to degradation, when compared to other nitroaromatic compounds, due to the electron-withdrawing properties of the nitro groups that delocalize electrons of the aromatic ring to such an extent, that the aromatic carbons are no longer available for electrophilic attack by oxygenases [17, 18]. Biodegradation of aromatic compounds by aerobic bacteria begins with the initial oxidation of the substrate by dioxygenases. Dioxygenases attack aromatic compounds (e.g. dinitrotoluene) and catalyse the addition of two hydroxyl groups, in order to form unstable intermediates that are subsequently cleaved by ring cleavage enzymes (Figure 5.1) [16, 228, 229].

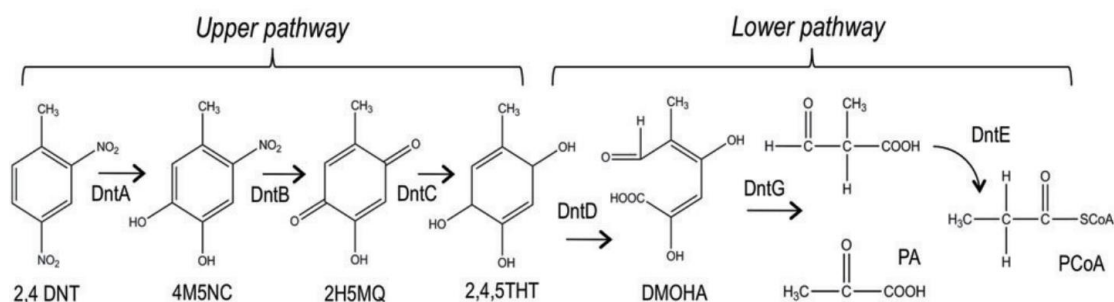


Figure 5.1: Degradation of 2,4-dinitrotoluene (2,4-DNT) by *Burkholderia* sp. DNT, through oxygenase attack at the aromatic ring. DntA, multicomponent DNT dioxygenase; DntB, 4M5NC mono-oxygenase; DntC, unidentified endogenous reductase; DntD, 2,4,5-THT oxygenase; DntG, DMOHA isomerase/4-hydroxy-2-keto-5-methyl-6-oxo-3-hexenoate hydrolase; DntE, a methylmalonate semialdehyde dehydrogenase; 4M5NC, 4-methyl-5-nitrocatechol; 2H5MQ, 2-hydroxy-5-methylquinone; 2,4,5-THT, 2,4,5-trihydroxytoluene; DMOHA, 2,4-dihydroxy-5-methyl-6-oxo-2,4-hexadienoic acid; PA, pyruvic acid; PCoA, propionyl-CoA. Figure adapted from de las Heras et al. [230].

Exposure of microbes to nitro-substituted compounds is likely to have been limited since there are only a few occurring naturally. Nitroarenes can result from photochemical transformation of polyaromatic hydrocarbons in the atmosphere [231], while *Pseudomonas* spp. and *Streptomyces* spp. produce pyrrolnitrin and chloramphenicol, two nitroaromatic antibiotics [232, 233] (Figure 5.2).

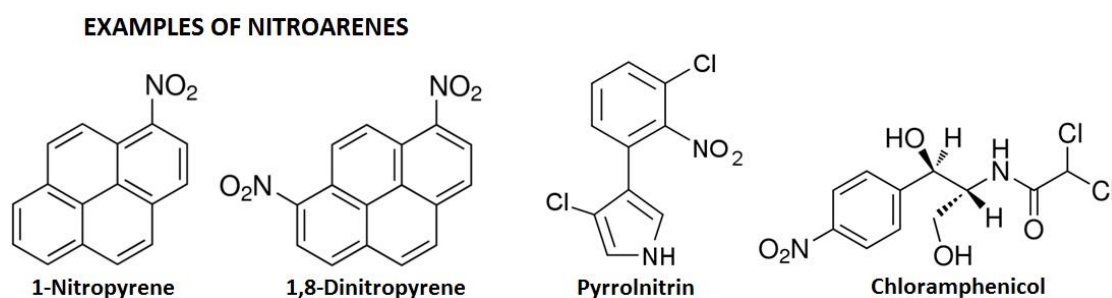


Figure 5.2: Chemical structures of the naturally occurring nitro-substituted compounds.

In sections 3.1 and 4.3.3 it was described how the GSTs investigated in this study (GST-U24, GST-U25 and *Dm*GSTE6) conjugate TNT to produce three distinct TNT-GSH conjugates. Conjugate 3 (1-glutathionyl-2-hydroxylamino, 4,6-dinitrotoluene) is the result of conjugation of GSH to TNT by nucleophilic substitution of a nitro group and is particularly interesting as this substitution destabilises the aromatic ring and could potentially make it more amenable to cleavage by microbial dioxygenases, and hence lead to degradation.

The information in the literature regarding the structural features and the residues that contribute to the catalytic activity of the plant specific, Tau class GSTs is quite limited. Looking beyond the structures of Arabidopsis GSTs, the large number of solved crystals shows that despite their diversity in primary sequence, GSTs are all remarkably similar in structure. Most cytosolic GSTs are encountered as dimers. Each subunit has a kinetically independent active site comprising a GSH binding site (G-site) and a binding site for the hydrophobic substrate (H-site). Each subunit folds to form two spatially distinct domains [82]: (a) the highly conserved N-terminal domain that consists of α -

helices and β -strands, with a $\beta\alpha\beta\alpha\beta\alpha$ topological arrangement similar to the thioredoxin fold that carries the G-site (see figure 5.5), and (b) a more variable C-terminal domain composed entirely of helices of variable number (5-9) depending on the enzyme, that carries the H-site. Although a significant amount of research has focused on the highly conserved G-site [97, 234-237], relatively little is known about the H-site. The H-site is formed mainly by residues with non-polar side chains that provide a hydrophobic character, essential for the binding of hydrophobic electrophiles [82]. The H-site is variable in both sequence and topology and is responsible for the ample and distinct substrate specificities among Tau and Phi class GSTs. It consists of residues that are not conserved among different classes and modulate substrate specificity by affecting the size, shape and the binding characteristics of the H-site [95].

To investigate this matter further, and to identify key amino acid residues that are involved in conjugate specificity and activity towards TNT, a site-directed mutagenesis approach was adopted. Tau is the most numerous class of GSTs in *Arabidopsis* and its members are suggested to be involved in the detoxification of a range of toxic compounds based on their activity and gene expression studies. The GST-U19, GST-U24 and GST-U25 all display strong conjugating activity with the generic substrate CDNB [87], while GST-U24 is induced by a range of xenobiotics [25].

Between the three enzymes studied here, GST-U24 and GST-U25 share a higher degree of protein identity (79%) than they do with *Dm*GSTE6, as demonstrated by the multiple sequence alignment of the amino residues of the GSTs given in Figure 5.3. The GST-U24 and GST-U25 are 1.3 kb apart on chromosome I, probably the result of a recent duplication event, and yet GST-U24 makes almost exclusively conjugate 2, whereas GST-U25 can catalyse the production of all three conjugates dependent upon the pH, with lower pH values favouring conjugate 3. The high identity between GST-U24 and GST-U25, along with their different conjugate production profiles made these two enzymes attractive targets for site-directed mutagenesis to establish the key

residues associated with the specificity of the conjugation reaction of TNT with GSH.

```

GST-U24      MADEVILLDFWASMFGRTRIALAEKRVKYDHREEDLWNK---SSLLEMPVHKKIPVL 57
GST-U25      MADEVILLDFWPSMFGMRTRIALEEKNVKFDYREQDLWNK---SPILLEMPVHKKIPVL 57
DmGSTE6      -MVKLTLYGLDPPPVRAVKLTLAALNLTYEYVNVDIVARAQLSPEYLEKNPQHT-VPTL 58
              :: * .: .*      .:::*      .::: : * : * . ** ** * . :*,*

GST-U24      IHNGKPVCESLIQIEYIDETWPDNPLLPSDPYKRAHAKFWADFIDKKVNVT-----AR 111
GST-U25      IHNGNPVCESLIQIEYIDEVWPSKTPLLPSDPYQRAQAKFWGDFIDKKVYAS-----AR 111
DmGSTE6      EDDGHYIWDSHAI IAYLVSKYADSDALYPKDPLKRAVVDQRLHFESGVVFANGIRSISKS 118
              .:*: : :* * *: . :... .* ** ** :** .. .* . * ..

GST-U24      RIWAVKGEEQAAK-ELIEILKTLESELGDKKYFGDETFGYVDIALIGFHSWFVAYEKFG 170
GST-U25      LIWGAKGEEHEAGKKEFIEILKTLESELGDKTYFGGETFGYVDIALIGFYSWFEAYEKFG 171
DmGSTE6      VLFQGQTKVPKERYDAIIEIYDFVETFLKGQDYIAGNQLTIADFSLVSSVASLEAFVALD 178
              :: : : :      :*** . :*: * .: * :... : .*:*: . : : .: .:

GST-U24      NVSIESECSKLVAVAKRCLERESVAKALPESEKVVITFISERRKKLGLG-- 218
GST-U25      SFSIEAECPKLIAMGKRCVERESVAKSLPDSEKIIKFVPELRKKLGLGIEIE 221
DmGSTE6      ----TTKYPRIGAWIKKLEQLPYEEANGKGVRLVAIFKKTN-FTFEA- 222
              :: .: : ** *: :      : : .. : : : : : : : *
    
```

Figure 5.3: Protein sequence alignment of GSTs. The GST-U24 and GST-U25 were aligned with the *Dm*GSTE6 using ClustalW. Asterisks (*) indicate identical residues.

5.2 Methods

5.2.1 Generation, expression and purification of the mutants

The generation of the mutants was based on the protocol of the QuickChange II Site-Directed Mutagenesis Kit (Agilent Technologies). The procedure utilises a double-stranded DNA (dsDNA) (vector), with an insert (gene to be mutated) and two synthetic oligonucleotide primers, both containing the desired mutation. The oligonucleotide primers are complementary to opposite strands of the vector and are extended by a high fidelity polymerase to amplify the whole vector. The details of the procedure are given below:

PCR reaction mix:

- 30-35 ng of dsDNA (pET-YSBLIC3C vector carrying GST-U24 or GST-U25)
- 1 µl of 10 µM forward primer
- 1 µl of 10 µM reverse primer
- 1 µl of 10 mM dNTPs
- 1 µl of *Pfu* HF DNA polymerase (2.5 U/µl)
- 5 µl of 10x reaction buffer
- x µl of H₂O up to 50 µl

PCR conditions:

98 °C for 1 min
14 cycles of
 98 °C for 30 sec
 60 °C for 1 min
 72 °C for 4 min
and
 4 °C on hold

All primers used are given in Table 5.1. At the end of the PCR reaction, each reaction was mixed with 1 µl of the endonuclease *Dpn* I (10 U/µl) and incubated at 37 °C for one hour. DNA isolated from almost all *E. coli* strains is methylated and therefore susceptible to *Dpn* I digestion. The *Dpn* I endonuclease targets methylated DNA and was used to digest the parental DNA template (pET-YSBLIC3C with original GST-U24/U25) and select for the, mutation-containing, newly synthesised DNA. Following digestion, *E. coli* (DH5a) cells were transformed with 1 µl of PCR reaction mix and spread onto LB-agar plates containing 50 µg/ml kanamycin. The following day liquid

cultures were set up from individual colonies and were incubated for ~20 h at 37 °C. Plasmids were then isolated from those cultures and send for sequencing to confirm the mutations. Successfully mutated plasmids were transformed into *E. coli* (BL21) cells, and the mutated protein was expressed and purified as previously described in section 2.4.

Table 5.1: Primes used for the site-directed mutagenesis of GST-U24 and GST-U25

GST-U24		
Mutation	Primer set	Primer sequence (5'→3')
Ala12Pro	U24-A12P-F	GGCAGATGAGGTGATTCTTCTGGATTTCTGGCCGAGTATGTTTGGG
	U24-A12P-R	GCCAGAGCAATTCTGTCTCATCCCAAACATACTCGGCCAGAAATC
Asn107Tyr	U24-N107Y-F	CTGGGCCGACTTCATCGACAAAAGGTGTATGTTACGGCGAG
	U24-N107Y-R	GACCGCCCAAATCCTTCTCGCCGTAACATACACCTTTTTGTCTG
Ala115Gly	U24-A115G-F	GGTGAATGTTACGGCGAGAAGGATTTGGGGGGTCAAAGG
	U24-A115G-R	GCTGCTTCTGCTCCTCACCTTTGACCCCAAATCC
Ala115Gly*	U24-A115Gb-F	GGTGTATGTTACGGCGAGAAGGATTTGGGGGGTCAAAGG
	U24-A115Gb-R	<i>same as U24-A115G-R</i>
Ile208Val	U24-I208V-F	GCCCTGCCTGAGTCAGAGAAGGTCATTACATTCGTTTCCGAACG
	U24-I208V-R	CTCCAACCCAAGTTTCTTCTACGTTCCGAAACGAATGTAATG
Arg211Leu	U24-R211L-F	GGTCATTACATTCATTTCCGAAGTTAGGAAGAAACTTGGGTTGG
	U24-R211L-R	CTCCAACCCAAGTTTCTTCTAAGTTCCGAAATGAATGTAATGACC
Arg211Leu*	U24-R211Lb-F	GGTCATTACATTCGTTTCCGAAGTTAGGAAGAAACTTGGGTTGG
	U24-R211Lb-R	CTCCAACCCAAGTTTCTTCTAAGTTCCGAAACGAATGTAATGACC
GST-U25		
Mutation	Primer set	Primer sequence (5'→3')
Pro12Ala	U25-P12A-F	GGCAGACGAGGTGATTCTTCTTGATTTCTGGGCGAGCATG
	U25-P12A-R	GCAATCCTCGTCTCATTCCAAACATGCTCGCCAGAAATC
Tyr107Asn	U25-Y107N-F	GGCCAAATTTTGGGGAGATTTATTGATAAGAAGGTGAATGCTTCAGC
	U25-Y107N-R	GCTCCCAAATCAACCTCGCTGAAGCATTACCTTCTTATC
Gly115Ala	U25-G115A-F	GGTGTATGCTTCAGCGAGGTTGATTTGGGCAGCTAAAGGC
	U25-G115A-R	CGCCTCATGCTTTCGCCTTAGCTGCCCAAATCAACCT
Gly115Ala*	U25-G115Ab-F	GGTGAATGCTTCAGCGAGGTTGATTTGGGCAGCTAAAGGC
	U25-G115Ab-R	<i>same as U25-G115A-R</i>
Val209Ile	U25-V209I-F	GTCTCTTCTGATTCCGAGAAGATCATTAAAGTTATTCTGAGC
	U25-V209I-R	CCCAAGTTTTTCTTAGCTCAGGAATGAACTTAATGATCTTCTCCG
Leu212Arg	U25-L212R-F	CGGAGAAGATCATTAAAGTTCTGTTCTGAGCGAAGGAAAAAAC
	U25-L212R-R	CTATTGATTTTCGATCCCAAGTTTTTCTTCTGCTCAGGAACG
Leu212Arg*	U25-L212Rb-F	CGGAGAAGATCATTAAAGTTATTCTGAGCGAAGGAAAAAAC
	U25-L212Rb-R	CTATTGATTTTCGATCCCAAGTTTTTCTTCTGCTCAGGAATG

Note: The asterisks (*) mark primer sets that were designed for the generation of sequential mutations and carry in their sequence the previous mutation, e.g. the Ala115Gly* primer set is designed to insert the Ala115Gly mutation into a sequence that already has the Asn107Tyr mutation.

5.2.2 Homology modelling

Searching the Protein Data Bank (PDB) (<http://www.rcsb.org/pdb/home/home.do>) with the protein sequences of GST-U24 and GST-U25 identified a Tau class GST from *Glycine max* (PDB accession code: 2VO4) [95, 237] with 67 and 69 % identity to GST-U24 and GST-U25 respectively. The crystal structure of the *G. max* GST was used as a template for constructing the models of GST-U24 and GST-U25. The amino acid sequences of the proteins were aligned using the HH-pred Bioinformatics Toolkit from the Max-Planck Institute (<http://toolkit.tuebingen.mpg.de/hhpred>). Modeller software [238] was used to generate the models and the PyMOL Molecular Graphics System (v1.3 Schrödinger, LLC.) was used for the analysis, visualisation and refinement of the models.

5.2.3 Activity assays towards TNT

The assay was performed in 100 mM potassium phosphate buffer pH 7.0 at 20 °C, with 300 µg of enzyme, 200 µM TNT and 5 mM GSH in a final volume of 250 µl. Reactions were performed in triplicate and run for 60 min before stopped with the addition of 10% TCA to precipitate the protein and terminate the reaction. After centrifugation at 13,000 rpm for 10 min samples of the reactions were analysed by HPLC using a Waters Alliance 2695 separation module with a Waters 2996 photodiode array detector, according to the method and conditions given in Table 5.2. The expected retention times are the following: TNT-30.9 min, Conjugate 1-16.7 min, Conjugate 2-20.2 min, Conjugate 3-21.0 min. Integration was performed at 250 nm with Empower Pro Software. Total conjugate concentration was plotted against time and the rate of each reaction was calculated from the slope of the curve ($y = ax$).

Table 5.2: HPLC conditions optimised for Waters X-Bridge C18 column

Sample temperature: 25 °C

Column temperature: 25 °C

Injection volume: 40 µl

Mobile phase A: acetonitrile

Mobile phase B: water + 0.1 % formic acid

HPLC gradient: 0 min	5 % A	95 % B
5 min	5 % A	95 % B
25 min	40 % A	60 % B
30 min	100 % A	0 % B
35 min	5 % A	95 % B

5.2.4 Activity assays towards CDNB

The CDNB conjugation assay was performed at 25 °C with a POLARstar OPTIMA plate reader (BMG laboratories). The reaction mix consisted of 100 mM potassium phosphate buffer pH 7.0, 5 mM GSH, 5 µg of enzyme and 1 mM CDNB, in a final volume of 200 µl per well on a 96-well-plate. The reaction was initiated by the addition of CDNB and the increase in A_{340} was monitored over one minute. Each reaction was performed in triplicate.

5.2.5 ANS binding assays

The 1-anilino-8-naphthalene-sulfonate (ANS) binding assay was based on the previously published protocol by Yang et al [239]. ANS has a low fluorescence yield in aqueous solution, which is enhanced when it is bound to the hydrophobic sites of proteins. Upon binding to the hydrophobic site, a unique fluorescence-emission spectrum is generated. Any conformational changes affecting the hydrophobic site of the protein affect the binding of ANS and thus generate a different fluorescence-emission spectrum [240, 241]. The assay was performed in a 1 ml cuvette with 100 µl of 2 mM ANS, 50 µg of enzyme and 100 mM potassium phosphate buffer pH 6.5. The fluorescence emission was monitored using a FluoroMax[®]-4 Spectrofluorometer (Horiba Scientific). A total of three technical replicates (three scans) for each blank and sample were recorded and averaged.

5.3 Results

5.3.1 Selection and production of GST-U24 and GST-U25 mutants

Alignment of GST-U24 and GST-U25 with a Tau class GST from wheat (*TaGSTU4-4*) and a Tau class GST from soybean (*GmGSTU4-4*) whose structures have already been solved, highlighted the amino acid residues that are involved in the formation of the hydrophobic H-site and are most likely important to the substrate specificity of the Tau class GSTs (Figure 5.4). The structure of *TaGSTU4-4* has been determined in complex with *S*-hexylglutathione [242], while *GmGSTU4-4* structure has been determined in complex with *S*-(*p*-nitrobenzyl)-glutathione, a compound with a nitro-substituted aromatic ring [95].

TaGSTU4-4	MAGGDDLKLLGAMPSPFVTRVKLALALKGLSYEDVEEDLYKKSELLLSNPVHKKIPVLI	60
GmGSTU4-4	--MQDEVVLLDFWSPFGMRVRIALAEKGIKYEYKEEDLRNKSPLLLQMPVHKKIPVLI	58
GST-U24	--MADEVILLDFWSPFGMRTRIALAEKRVKYDHREEDLWNKSSLLLEMNPVHKKIPVLI	58
GST-U25	--MADEVILLDFWSPFGMRTRIALEEKNVKFDYREQDLWKNSPILLEMNPVHKKIPVLI	58
	*: : ** * * * * : : * * : : : * : * : * : * : * : * : * : *	
TaGSTU4-4	HNGAPVCESMIILQYIDEVFASTGPSLLPADPYERAIARFWAVYVDDKLYAPWRQWLRGK	120
GmGSTU4-4	HNGKPICESLIAVQYIEEVWNRNP--LLSPDPYQRAQTRFWADYVDDKIIYDLGRKIINTSK	117
GST-U24	HNGKPVCESLIQIEYIDETWPDNNP--LLSPDPYKRAHAKFWADFIDKKVIVTARRIIVAVK	117
GST-U25	HNGNPVCESLIQIEYIDEVWPSKTP--LLSPDPYQRAQAKFWGDFIDKKVASARLIIVGAK	117
	*** : * : * : * : * : * : * : * : * : * : * : * : * : * : * : *	
TaGSTU4-4	TEEEKSEGKKQAFAAVGVLEGALRECSKGGGFGGDGVGLVDVALGGVLSIMKVTEALSG	180
GmGSTU4-4	G-EEKEAAKKEFIEALKLLEEQL----GDKTYFGDNLGFVDIALVPPFYTFKAYETFGT	172
GST-U24	G-EEQEAA-KELIEILKLTLESEL----GDKKYFGDETFGYVDIALIGFHSIVFAVEKFGN	171
GST-U25	G-EEHEAGKKEFIEILKLTLESEL----GDKTYFGGETFGYVDIALIGFYSIVFEAYEKFGS	172
	* : . * : : * * * : : * : * : * : * : * : * : * : * : * : *	
TaGSTU4-4	DKIFDAAKTPLLAAWVERFIELDAAKALPDVGRLLLEFAKAREAAAAASK-	230
GmGSTU4-4	LNI--ESECPKFIWAKRCLQKESVAKSLPDQKQVYEFIMDLRKKLGIE--	219
GST-U24	VSI--ESECskLVAWAKRCLERESVAKALPESEKVIIFISERRKKLGLE--	218
GST-U25	FSI--EAECPKLIWAGKRCVERESVAKSLPDSEKIIEVPELRKKLGIEIE	221
	. * : : : * * * : : : : * : * : * : * : * : * : *	

- Ser13 catalytic residue
- Residues important to substrate specificity in Tau class GSTs
- Residues forming the hydrophobic H-site in Tau class GSTs

Figure 5.4: Protein sequence alignment of GSTs. The GST-U24 and GST-U25 were aligned with *TaGSTU4-4* and *GmGSTU4-4*, whose structures have been solved, using ClustalW. Asterisks (*) indicate identical residues.

Of the amino acid residues contributing to the substrate specificity of Tau class GSTs, the residue at position 107 was targeted for mutagenesis since it was the only one that was not identical between GST-U24 and GST-U25 (Asn for GST-U24, Tyr for GST-U25) and could possibly account for the altered conjugate production profile. Subsequent homology modeling using the published structure of *GmGSTU4-4* [95], which shares high protein sequence identity (>60%) to GST-U24 and GST-U25, as template, demonstrated that amino acid residues at positions 12, 115, 208 (209 for GST-U25) and 211 (212 for GST-U25), which form part of the H-site, are oriented towards the centre of the active site and could be involved in the binding of the hydrophobic substrate (Figure 5.5). As a result these four residues were also targeted for site-directed-mutagenesis.

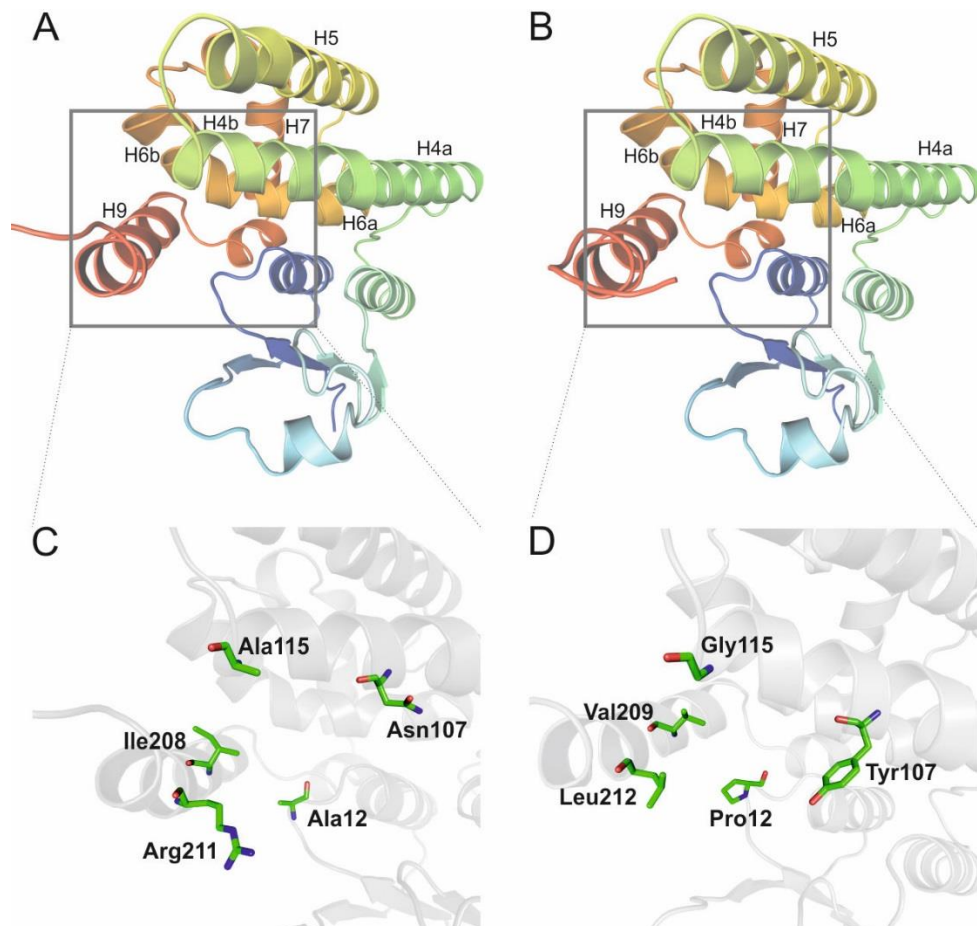


Figure 5.5: Models of monomeric forms of GST-U24 (A) and GST-U25 (B) based on homology modelling using the crystal structure of *Glycine max GmGSTU4-4* (PDB accession code: 2VO4) as template. The helices that compose the C-terminal domain of each enzyme are annotated. The active site of GST-U24 (C) and GST-U25 (D) with the five amino acids targeted for mutagenesis shown.

The amino acid residues targeted for mutagenesis and the resulting mutants are given in Table 5.3 and Figure 5.5C, D. From this point forward the mutants will be referred to with their single letter identifier (A-J). Mutants bearing sequential mutations will carry all the mutation identifiers, e.g. A+B+E. The mutations are essentially exchanging the amino acid residues between GST-U24 and GST-U25 to investigate whether the respective conjugate production profiles could be manipulated. The A+B+C+D+E mutant should engineer the near complete active site of GST-U25 into GST-U24 and should, at least theoretically, alter the conjugate production profile of GST-U24, allowing the production of conjugate 3.

Table 5.3: The GST-U24 and GST-U25 mutants

Enzyme	Mutation identifier	Substitution
GST-U24	A	Ala12Pro
	B	Asn107Tyr
	C	Ala115Gly
	D	Ile208Val
	E	Arg211Leu
GST-U25	F	Pro12Ala
	G	Tyr107Asn
	H	Gly115Ala
	I	Val209Ile
	J	Leu212Arg

5.3.2 Activity of GST-U24 and GST-U25 mutants towards TNT

The purified mutated proteins were assayed for activity towards TNT. The results for GST-U24 showed that mutations B, B+C+D and A+B+C+D reduced the overall activity to 55-80% of the wild-type GST-U24, with B+C+D exhibiting the lowest activity (Figure 5.6). All three mutants were able to produce conjugate 1; this is in contrast to GST-U24 which produces only conjugates 2 and 3. The ratios of the three conjugates were similar in the three mutants.

Mutations A+B and A+B+C+D+E displayed up to 66% higher activity than the original GST-U24 and were both able to produce conjugate 1, as seen with the previous mutants. The mutant A+B+C+D+E was distinct among the others as it displayed the highest conjugating activity. It was also able to produce significantly higher amounts of conjugate 3 than GST-U24 and the other mutants, and produced all three conjugates in almost equimolar concentrations (Figure 5.6).

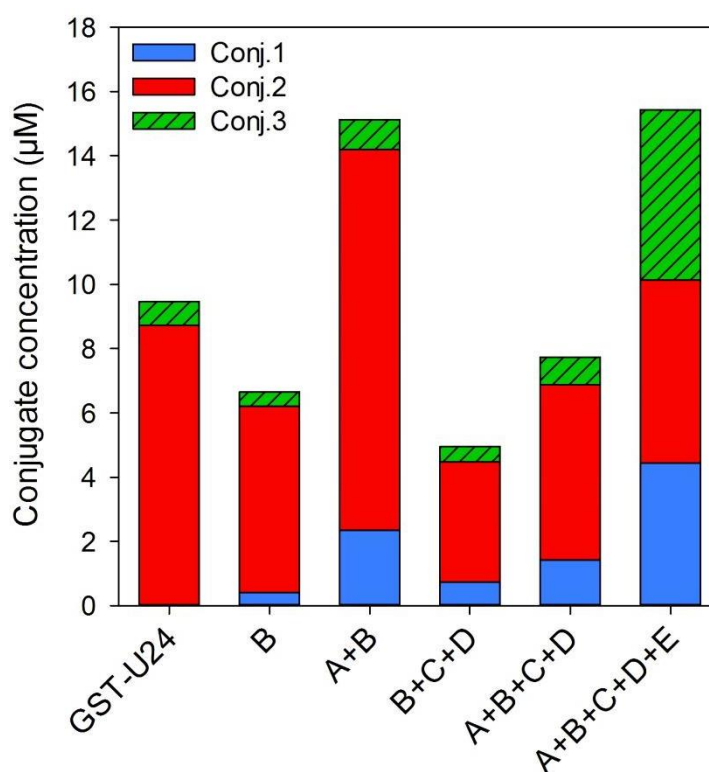


Figure 5.6: Activity towards TNT and conjugate production profile of GST-U24 and its respective mutants, after 1 h incubation with 200 µM TNT at 20 °C. Results are means of three technical replicates.

In the case of GST-U25, mutants G and F+G exhibited a dramatic decrease from the original GST-U25 activity. The reduced activity of these mutants affected mainly the levels of conjugate 3 and conjugate 1 production, leaving the levels of conjugate 2 relatively unaffected (Figure 5.7). Mutant G+H+I showed a slightly increased activity comparing to wild-type GST-U25 and an altered conjugate production profile producing more conjugate 2 and less conjugate 1 and 3 (Figure 5.7). Finally, mutant F+G+H+I displayed almost

identical total activity to that of GST-U25, but with an increased production of conjugate 2 at the expense of mainly conjugate 1.

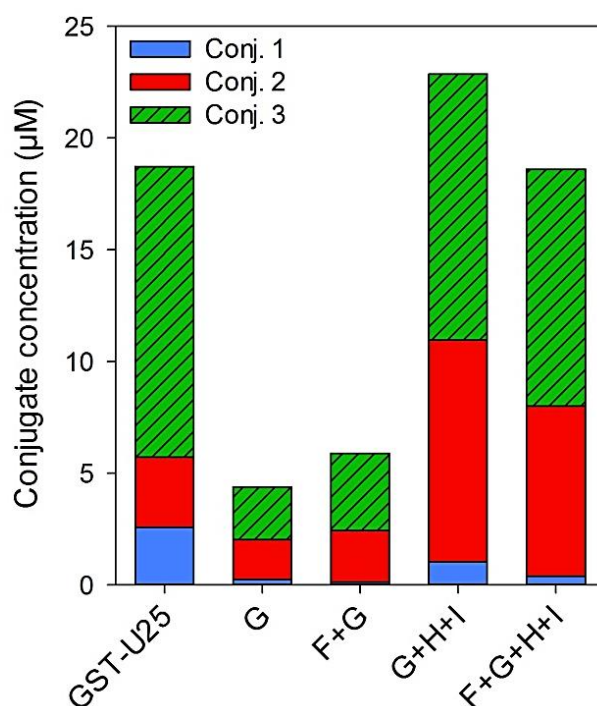


Figure 5.7: Activity towards TNT and conjugate production profile of GST-U25 and its respective mutants, after 1 h incubation with 200 µM TNT at 20 °C. Results are means of three technical replicates.

5.3.3 Activity of GST-U24 and GST-U25 mutants towards CDNB

The effect of the different mutations on the conjugating activity of GST-U24 and GST-U25 towards the generic GST substrate CDNB was tested.

For GST-U24, mutant A+B reduced the original activity of GST-U24 by 60%. (Figure 5.8A). Mutants A+B+C+D+E, A+B+C+D and B+C+D increased the activity towards CDNB by 100, 31 and 59% respectively. Mutant B had similar activity to that of GST-U24. In the case of GST-U25, the mutations displayed a mild effect on the activity towards CDNB. Besides mutant G, which displayed a 35% decrease in activity, the remaining mutants exhibited levels of activity similar to those of wild-type GST-U25 (Figure 5.8B).

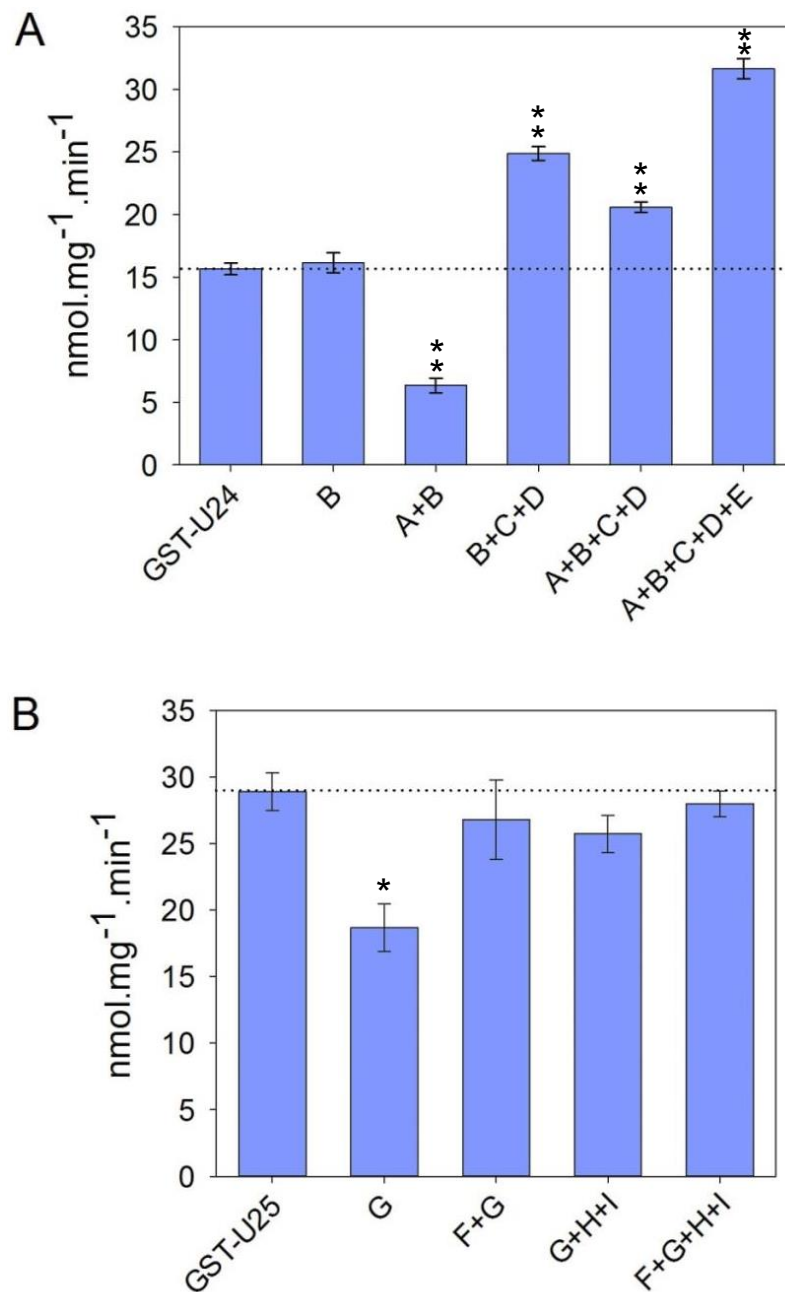


Figure 5.8: Activity towards CDNB of (A) GST-U24 and its respective mutants and (B) GST-U25 and its respective mutants. Results are means of three technical replicates \pm se. Asterisks denote statistically significant from GST-U24 and GST-U25 respectively: * P <0.05, ** P <0.01.

5.3.4 Probing the GST-U24 and GST-U25 mutants for conformational changes

To identify any conformational changes that might be caused by the mutations, the mutants were probed with ANS and the spectra measured. A valuable probe widely used for probing structural changes in proteins [240, 241], ANS has been successfully used in the past to probe a Tau class glutathione transferase from rice [239].

When proteins were added to the mixture and ANS bound to them, the fluorescence intensity was enhanced and accompanied by a shift in the fluorescence emission maximum from 520 nm (free ANS in buffer) to 500 nm (Figure 5.9), as previously described for GST-U19 of rice and its respective mutant [239]. Both GST-U24 and GST-U25 are predicted to share a similar structure in the hydrophobic site (Figure 5.9A). Among the different GST-U24 mutants, only the A+B+C+D+E mutant generated a significantly different fluorescence spectrum, indicative of a change in conformation (Figure 5.9B). The fluorescence spectra of the different GST-U25 mutants, varied slightly to one another, but none of them suggested a significant conformational change had occurred (Figure 5.9C).

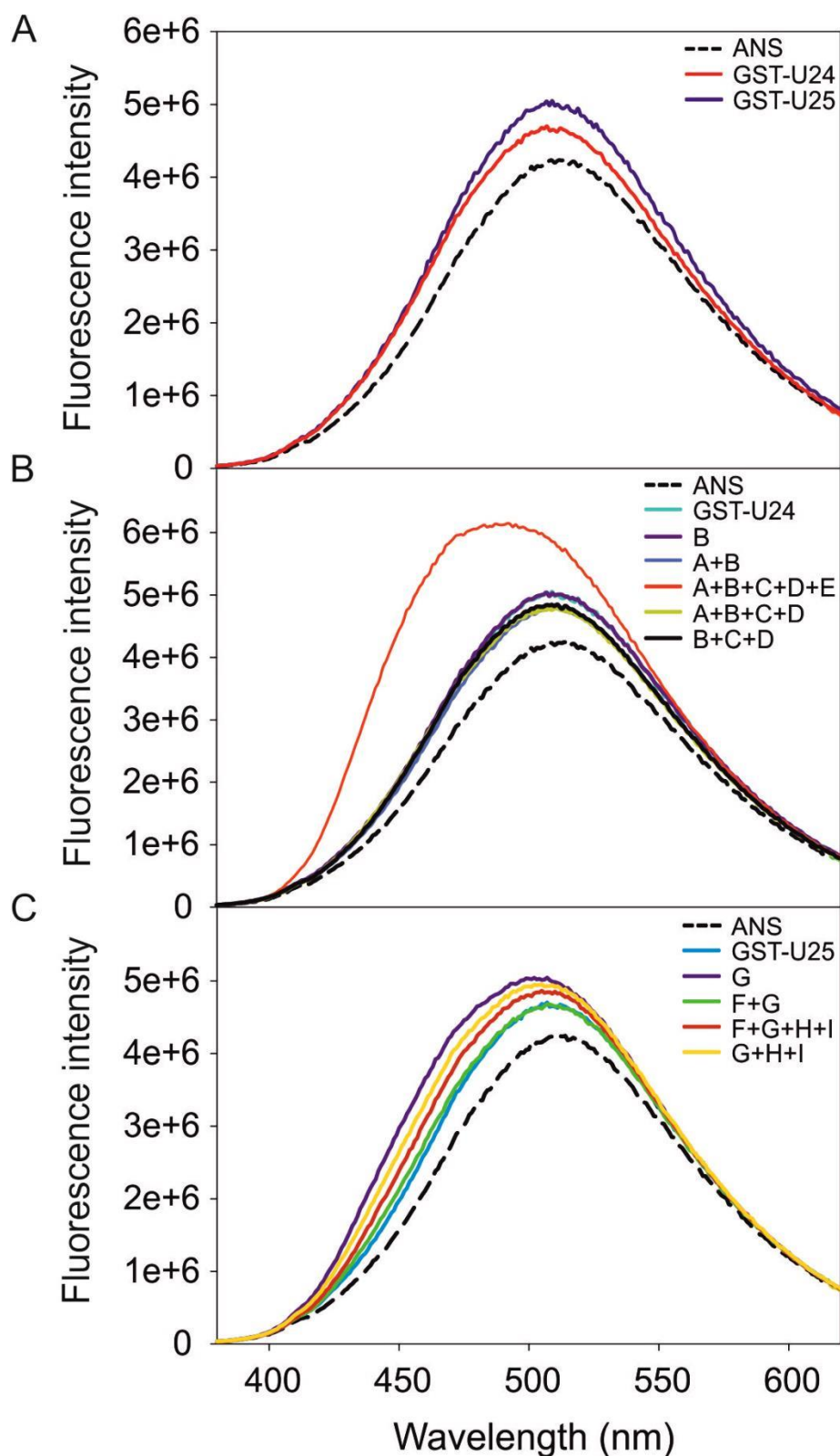


Figure 5.9: Fluorescence-emission spectra of ANS binding to the active site of the GSTs. (A) Spectra from GST-U24 and GST-U25. (B) Spectra from GST-U24 and its respective mutants. (C) Spectra from GST-U25 and its respective mutants. ANS, blank sample without enzyme; A-I, GST-U24 and GST-U25 mutants as presented in Table 5.3. Results are means of three technical replicates.

5.4 Discussion

The results of the site-directed mutagenesis confirm that the five targeted residues, forming part of the hydrophobic pocket, are indeed interacting with the substrate. Although TNT and CDNB are both substrates for GST-U24 and GST-U25, comparison of the effect of the mutations on the two activities showed that the effect of a mutation on the activity towards TNT does not necessarily have the same effect on the activity towards CDNB, although the two substrates share a similar structure. For example, mutant A+B increased the activity towards TNT by 66% comparing to wild-type GST-U24, but significantly decreased catalytic efficiency for CDNB. Furthermore, mutants F+G and G+H+I which decreased and increased the activity of wild-type GST-U25 towards TNT respectively, had little or no effect on the activity towards CDNB. These results imply that the two substrates bind differently within the hydrophobic pocket and are likely to interact with different, or additional, residues that were not targeted during this study. In addition, although it was not measured here, it should not be excluded the possibility that the mutations have a significant effect on the GPOX activity of GST-U24 and GST-U25.

5.4.1 Residues important to the activity towards TNT

The effects of the mutations on the activity towards TNT showed that the Tyr107 residue in GST-U25 is important for the catalytic efficiency and for determining the specificity of the conjugation reaction with GSH. The role of Tyr107 in the formation of conjugate 1 is demonstrated by the Asn107Tyr mutation in GST-U24. GST-U24 does not naturally produce conjugate 1, under the conditions tested; however, the Asn107Tyr mutation confers the ability to produce conjugate 1 in albeit small (6%) amounts.

The importance of Tyr107 to the catalytic activity towards TNT is not surprising since aromatic residues in the active site of GSTs have been hypothesised to stabilize substrates with aromatic groups [95, 164, 243]. Musdal et al. (2015) suggested that the aromatic residues Phe10 and Tyr107 in the active site of GST-U16 from poplar promote high activity towards

substrates bearing aromatic groups [164], while Tyr107 from the soybean Tau class GST *GmGSTU4-4* has been identified as an important structural moiety in the active site that modulates the catalytic efficiency towards aromatic substrates [95]. In *GmGSTU4-4*, Tyr107 points towards the aromatic ring of 4-nitrobenzyl and uses the hydroxyl group of its side chain to make a hydrogen bond between the hydroxyl group and the π -electron cloud of the aromatic ring, stabilizing the compound at the right orientation for conjugation [95]. Finally, the position and orientation of the aromatic residue Trp208 in UDP glucosyltransferases from Arabidopsis was responsible for the presence or absence of TNT-metabolising activity of these proteins [243].

It is possible that high activity towards TNT requires both Tyr107 and Pro12. This hypothesis is supported by the 60% increase in overall conjugating activity displayed by mutant A+B which bears both Tyr107 and Pro12. These two residues are adjacent in the active site and could act in a synergistic way or interact with each other. In *GmGSTU4-4*, an Arg residue adjacent to Tyr107 was found to be important to the catalytic activity by making a hydrogen bond with the hydroxyl group of Tyr107 and orientating it in the right way [95].

5.4.2 Leu211 involved in the production of conjugate 3

Leu211 appears to be implicated in the production of conjugate 3. Mutant A+B+C+D+E was able to produce all three conjugates, while all the remaining mutants of GST-U24 were not able to produce elevated amounts of conjugate 3. The Leu212 residue of *GmGSTU4-4* from soybean that shares high protein identity with GST-U24 and GST-U25 and whose structure was used for the homology modeling, was very close to the nitro group of 4-nitrobenzyl suggestive of a possible interaction [95]. It is possible that Leu at position 211 in GST-U24 and 212 in GST-U25 interacts with one of the nitro groups of TNT, altering its orientation in the active site and thus accounting for the production of conjugate 3.

5.4.3 Engineering the GST-U25 conjugate profile into GST-U24

The results of the site-directed mutagenesis studies showed that the conjugate production profile in both GST-U24 and GST-U25 can be manipulated. The five consecutive mutations present in A+B+C+D+E were predicted to engineer the near-complete active site of GST-U25 into GST-U24. The resulting conjugate profile and activity of A+B+C+D+E was similar to GST-U25 in that it produced all three conjugates and achieved similar levels of overall conjugating activity. Nonetheless, the fluorescence emission spectrum of A+B+C+D+E was significantly different from both GST-U24 and GST-U25, indicative of a conformational change of its hydrophobic site. Whether the increased activity and the altered conjugate profile is the result of the conformational change or is based solely on the interactions between TNT and the amino acid residues of the active site needs more investigation. Single mutations do not seem to contribute to catalysis by modulating specific conformational changes. Therefore their effect on catalytic efficiencies can be plausibly explained by their direct involvement on the reaction chemistry. However, multiple mutations at a catalytically important region could cause secondary effects and structural perturbations. In agreement with that, helices H4 and H5, which form part of the C-terminal domain, have been shown to be quite flexible and prone to movements [95, 242]. It is clear that determining the amino acid residues contributing to the catalytic efficiency is a significant task. To rationalize the variety of interactions and conformational changes, access to the detailed molecular structure of the respective enzymes is required. Crystallisation of GST-U24, GST-U25 and the A+B+C+D+E mutant, in complex with TNT, would be ideal for further investigation and would shed light on the how TNT interacts with the H-site of each enzyme.

Chapter 6: Final discussion

The fate and toxicity of TNT and its derivatives in plants remains largely unknown. Previous studies have shown that the TNT detoxification pathway starts with the rate-limiting step of nitroreduction followed by conjugation of the reduced derivatives by UDP-glucosyl transferases (UGTs) [26, 27]. In the past GSTs have been shown to be upregulated in response to TNT treatment and their involvement in TNT detoxification hypothesised [25, 26, 75, 76, 244]. The work described here shows that two GSTs, GST-U24 and GST-U25, upregulated in response to TNT treatment and mainly expressed in the roots (where TNT accumulates following uptake) also contribute to the TNT detoxification pathway in *Arabidopsis*. Over-expression of GST-U24 and GST-U25 conferred enhanced resistance to TNT toxicity, due to direct glutathionylation of TNT, along with an increased ability to remove and detoxify this environmental pollutant. The proposed detoxification pathway is given in Figure 6.1.

A previous study showed that an *Arabidopsis* line with a loss-of-function in GST-U24, caused by a T-DNA insert, was unaltered in its response to TNT treatment [191]. This is probably due to overlapping activities from other *Arabidopsis* GSTs. The high identity between GST-U24 and GST-U25, and other GSTs, coupled with the similar activity profiles, presented here for GST-U24 and GST-U25 agree with this conclusion. Furthermore, obtaining double knockout lines would be difficult due to their close proximity in the *Arabidopsis* genome (1.3 kb apart on chromosome I). However, with relatively new gene editing techniques now available, such as CRISPR/Cas [245, 246], generating *Arabidopsis* lines lacking both GST-U24 and GST-U25 activities would be possible. It is plausible, that additional redundancy from uncharacterised GSTs could still provide sufficient activity towards TNT to prevent a TNT-related phenotype appearing in lines lacking GST-U24 and GST-U25 activity. It is believed that redundancy within GST clades is a major factor in the lack of phenotypes in single knock-out lines; a feature that has hindered the characterisation of GSTs. Given the high identity between GSTs

in the Tau class, gene editing techniques could be extrapolated to remove sub-clades of GSTs with the aim of eliciting diagnostic phenotypes that will enable the characterisation of these intriguing families.

The CRISPR/Cas system has been successfully applied in a number of plant species including tobacco (*Nicotiana tabacum*), Arabidopsis and crops such as wheat (*Triticum aestivum*), maize (*Zea mays*) and rice (*Oryza sativa*), for gene editing [247], while detailed protocols regarding targeted mutagenesis in wheat and rice have recently been published [248, 249].

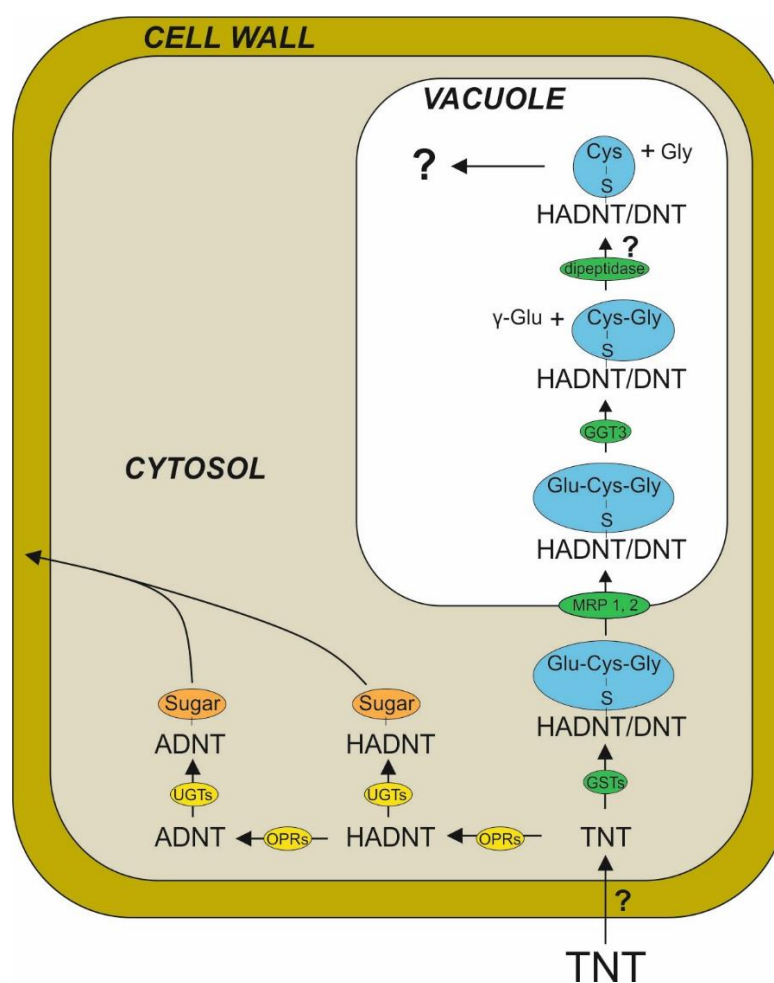


Figure 6.1: A schematic representation of the proposed TNT detoxification pathway in the roots of Arabidopsis. Steps bearing a question mark (?) represent steps where the mechanism or the respective enzyme catalysing the reaction is still unknown. OPRs, oxophytodienoate reductases; UGTs, UDP-glucosyl transferases; GSTs, glutathione transferases; MRP1, 2, multidrug resistance-associated protein, GGT, γ -glutamyl transpeptidase; HADNT, hydroxylamino dinitrotoluene; ADNT, amino dinitrotoluene; DNT, dinitrotoluene. Figure adapted from Rylott et al. [62].

A major role for plant GSTs is in the detoxification of herbicides, and related compounds. Given the importance of herbicides in agriculture it is perhaps unsurprising that much of what is known about plant GSTs is based on studies using these compounds. Alachlor, a member of chloroacetanilide family is used to control annual grasses and broadleaf weeds in crops. Fenclorim is used as a herbicide safener; its application prior to herbicide use can enhance herbicide resistance in crops by enhancing expression of herbicide detoxification enzymes, including GSTs, in the crop plant. Studies have shown that GSH-herbicide conjugates are rapidly sequestered in the vacuole by the ATP-binding cassette (ABC) transporters, Multidrug Resistance Protein 1 (MRP1) and MRP2 [85, 250], which are also upregulated in response to TNT [26]. Studies using monobromobimane (mBB) showed that although C-terminal degradation of the γ -Glu-Cys-Gly-mBB conjugate by phytochelatin synthase is possible in the Arabidopsis cytosol [139, 251], this is not the primary catabolic pathway in this species, as this mechanism is out-competed by vacuolar sequestration [140]. In the vacuole, γ -glutamyl transpeptidase (GGT3) has been shown to catalyse the N-terminal degradation of the γ -Glu-Cys-Gly-mBB to yield γ -Glu and Cys-Gly-mBB [143, 145]. Subsequently the Cys-Gly-conjugate is believed to be further catabolised to the Cys-conjugate by the activity of an uncharacterised vacuolar carboxypeptidase [145]. A barley (*Hordeum vulgare* L.) carboxypeptidase that cleaves alachlor GSH-conjugates C-terminally in the vacuole has been identified [141], however, such activity has not been reported for Arabidopsis. Whether the Cys-conjugate is the end product and whether it remains in the vacuole is also unknown. It is possible however that the Cys-conjugates are further metabolised. Fenclorim was found to be glutathionylated and rapidly processed to its corresponding Cys conjugate in Arabidopsis. Downstream metabolism derivatives included among other, S-(4-chloro-2-phenylpyrimidyl)-6-N-malonylcysteine and 4-chloro-6-(methylthio)-phenylpyrimidine [146]. It is not clear whether there is an advantage from salvaging the GSH-derived amino acids by subsequent catabolism of the GSH-conjugates, but both nitrogen and sulphur are elements that are likely to be found in limited amounts in TNT-contaminated training ranges. Further studies could, for

example, use soil-based studies to investigate whether limiting the amount of available nitrogen and sulphur affects the ability of wild-type and GST over-expressing lines to withstand and detoxify TNT.

Once TNT has been conjugated within the plant tissues, investigating its subsequent fate becomes technically more challenging. The use of ^{14}C radiolabelled TNT, combined with transmission electron microscopy (TEM), would enable the sub-cellular location of TNT in plants to be visualised. Using [^{14}C]-TNT in *in vitro* studies, such as whole plant extract-based experiments, would enable TNT-metabolites to be identified from LC-MS traces containing hundreds of plant metabolites. Radiolabels could also be used as substrates in assays containing purified GSTs to generate ^{14}C and/or ^{35}S -labelled glutathionylated-TNT conjugates. The fate of the radiolabelled conjugates could then be tracked. However, due to prohibitive costs, obtaining radiolabelled TNT was not possible for this study.

Other researchers have used [^{14}C]-TNT [64, 66-68] and found ^{14}C -activity to be mainly within cell-wall-derived fractions. Brentner et al., used phosphor imaging radiography to show that in poplar (*Populus deltoids X nigra* DN34) and switchgrass (*Panicum virgatum*) fed [^{14}C]-TNT for 5 days, most of the ^{14}C -activity associated with lignified tissues [68]. Studies in bean (*Phaseolus vulgaris*) and wheat (*Triticum aestivum*) fed with [^{14}C]-TNT for 14 days, showed that most of the TNT derivatives were evenly distributed between the cytoplasm and the cell wall, with most of the cell wall ^{14}C -activity associated mainly with the lignin and hemicellulose fraction and to a lesser extent with pectin [66, 67]. Schoenmuth et al report a similar distribution of TNT to that of Sens et al. for hybrid willow (*Salix spec.*, clone EW-20) and Norway spruce (*Picea abies*) fed [^{14}C]-TNT for 60 days, where TNT metabolites are evenly distributed between the cytoplasm and the cells wall and the lignins and hemicelluloses are the main targets for [^{14}C]-TNT deposition, followed by pectins [64]. Besides the root extracts of hybrid willow and Norway spruce where five unknown, very polar, TNT metabolites were detected [64], in the studies of Brentner et al. [68] and Sens et al. [66, 67] using radiolabelled TNT, the main extractable TNT metabolites were TNT, ADNTs and DANTs

suggesting that the conjugation of TNT and its subsequent incorporation into the plant biomass is a relatively fast process.

Following TNT uptake by the cell, conjugation by GSTs occurs in the cytosol. At pH values between 6.5 and 7.0, which are believed to be closer to the physiological pH [167-170], conjugate 3 production is favoured over the remaining two conjugates. A notion that is further supported by the fact that only conjugate 3 was recovered from the root extracts of GST-U25 OE plants grown on TNT-containing media [165]. The substitution of the nitro group at the two position in the TNT ring for sulphur could reduce the stability of conjugate 3, particularly if the sulphur could be subsequently cleaved in planta to release DNT.

Microbial biochemical pathways capable of mineralising the structurally-similar compounds 2,4- and 2,6-dinitrotoluene (DNT) have been well characterised in the past [228-230]. The DNT degradation pathway starts with the action of a dioxygenase, a three-component enzyme that hydroxylates the aromatic ring [230]. Although it is unlikely that dioxygenases will have activity towards the GSH-conjugate due to steric limitations, the Cys-conjugate, the hypothesised downstream derivative of the GSH-conjugate, could serve as a substrate and this is something that should be investigated. Production of the Cys-TNT conjugate from the GSH-TNT conjugate might be possible to be carried out enzymatically *in vitro*. In the past, affinity-purified PCS preparations were able to catalyse the removal of Gly from GSH conjugates to yield the Glu-Cys-conjugate [139]. In addition, Arabidopsis GGT3 that was initially thought to be tonoplast-associated was found through GFP fusion to be free in the vacuole, suggesting that recombinant expression and purification of this enzyme might be possible [143]. Should conjugate 3 or its downstream derivatives be more amenable to breakdown, this could be used to genetically engineer plants for increased conjugate 3 production, or screen GSTs from different species, with activity towards TNT, that produce higher amounts of conjugate 3. The site-directed mutagenesis studies conducted here highlighted Tyr107 and Pro12 as important in the catalytic activity towards TNT, and Leu211 as necessary for the production of conjugate 3. These residues give an idea of how TNT

resides in the active site of GST-U25 and help in the rational design and engineering of GSTs to manipulate the conjugate production profiles towards the formation of conjugate 3 [18]. The final aim would be the development of plant-based systems for the subsequent degradation and mineralisation of TNT, rather than the indefinite storage of TNT-transformation products in the environment.

Following from the work done with GST-U24 and GST-U25, the *DmGSTE6* was investigated for its TNT-detoxification abilities. *DmGSTE6* exhibited significantly higher activity towards TNT than GST-U24 and GST-U25, and produced almost exclusively conjugate 3. Expression of *DmGSTE6* in *Arabidopsis* conferred enhanced resistance to TNT toxicity, as shown by root length and biomass measurements, compared to that of the GST-U24/U25 OE lines. Nevertheless, *DmGSTE6* activity towards TNT was found to be limited by the availability of GSH, demonstrating that the enhanced tolerance of the *DmGSTE6* expressing plants is not the result of increased TNT uptake by the plant, but rather the result of a faster detoxification rate of TNT comparing to that of the GST-U24 and GST-U25 OE lines. There is enough evidence compiled in this study to support an important role of GSH in the detoxification of TNT and facilitate further research towards its abundance and localisation. The fact that GSH abundance is limiting the conjugation of TNT was unexpected as *Arabidopsis* cytosolic GSH concentration is believed to be in the low millimolar range [188-190] and should be theoretically more than enough to facilitate TNT conjugation by GST activities. A recent study showed that the intracellular distribution and redox state of GSH can be driven by stress conditions. Queval et al. showed that, in leaves, under conditions of oxidative stress, such as those induced by TNT, GSH oxidises to GSSG and accumulates in the vacuole and chloroplast [126]. The GSH measurements carried out here measured whole organ (root and shoots) GSH levels but not the GSH concentration in subcellular compartments. Methods currently available for measuring GSH in different organelles include monochloro- or monobromobimane staining, immunocytochemical analysis and redox-sensitive GFP [127, 128, 190], and this could be used to investigate how GSH

levels respond in the presence of TNT in wild-type and GST-overexpression lines.

The levels and biosynthesis of GSH can greatly affect plant stress defences. Glutathione serves a variety of important roles including detoxification of xenobiotics and ROS, storage and transport of reduced sulphur, and regulation of plastid and nuclear gene expression [117, 252]. Preliminary experiments where liquid media was supplemented with GSH resulted in increased TNT uptake by Arabidopsis plants, indicating that GSH abundance limited the TNT-glutathionylation reaction under these conditions. However, exogenously supplied GSH can also exhibit strong toxic effects, and is probably a rather crude method to investigate GST requirements. A more targeted strategy would perhaps be to genetically engineer the *DmGSTE6* expressing Arabidopsis to produce higher levels of GSH. Many factors can affect the synthesis of GSH but the most important are cysteine availability and γ -ECS activity [117, 119]. Consequently, increased GSH production can be driven by the over-expression of γ -ECS or by the over-expression of enzymes involved in cysteine synthesis [117, 119]. The γ -ECS enzyme catalyses the ATP-dependent condensation of glutamate and cysteine, the first and rate limiting step of GSH synthesis. Crossing, or re-transformation, of *DmGSTE6* expressing lines with γ -ECS over-expressing activity may help elucidate more about the mechanisms of GSH supply. Artificially depleting GSH levels in Arabidopsis showed that it does not have the same effect on plants as that observed when GSH synthesis is inhibited by the presence of the, exogenously supplied, GSH synthesis inhibitor buthionine sulfoximine (BSO) [130]. This suggests that through genetic engineering it might be possible to elevate GSH levels while at the same time omit the phytotoxic effects. In accordance with this, heterologous expression of a bacterial γ -ECS in the hybrid poplar (*Populus tremula* X *P. alba*) significantly increased the root and foliar levels of GSH [188, 253]. In addition, expression of an *E. coli*-derived γ -ECS in Arabidopsis alongside a microbial arsenate reductase increased the tolerance of the plant towards arsenic by elevating levels of GSH, which is required by arsenate reductase to detoxify arsenic [254]. Furthermore, over-expression of γ -ECS in Arabidopsis resulted in a two-fold

increase in GSH levels [255], while more recent studies with expression of a bifunctional γ -ECS/GSH synthetase (CSHS) enzyme from *Streptococcus thermophilus* in tobacco plants resulted in a dramatic increase of GSH concentration with no impact on plant growth [256]. Nevertheless, no toxic effects were reported for any of the above mentioned γ -ECS over-expressing plant lines; a possible result of internal regulation to prevent accumulation of GSH to levels that would be cytotoxic. The GSH and γ -EC levels could exert a regulatory feedback inhibition on γ -ECS [121-123], or the GSH:GSSG ratio could be balanced by stimulated GSH reductase activity as has been previously reported in transgenic poplar expressing a bacterial γ -ECS [253].

Arabidopsis is an excellent model organism for molecular genetics and laboratory studies but is in no case suitable for the remediation of TNT in the field. For such a purpose, the appropriate TNT-detoxifying traits need to be identified in field applicable species. Plant species suitable for the phytoremediation of TNT need to meet a number of requirements including: be low growing, have an extensive root system, ability to recover from mechanical disruption by military equipment operating at training ranges, and be fire-resistant [6, 56]. Several perennial grasses have been suggested as suitable candidates based on the above traits and ability to tolerate relatively high concentrations of TNT. Perennial grasses such as western (*Pascopyrum smithii*), slender (*Agropyron trachycaulum*) and Siberian (*Agropyron fragile*) wheatgrasses are native to the US training ranges [6]. Grasses are also characterised by fast growth and adaptability to a variety of soil types and climate [257] while the grasses bromegrass (*Bromus* spp.), wheat (*Thinopyrum intermedium*), oat (*Arrhenatherum elatius*) and switchgrass (*Panicum virgatum*) have demonstrated the ability to take up TNT [12]. Vetiver grass (*Vetiver zizaniodes*) has shown to have good characteristics for the phytoremediation of TNT. Vetiver grass was able to remove effectively TNT from soil, with Das et al. reporting TNT removal rates by Vetiver grass of 97% and 39%, from soil with initial concentrations of 40 mg kg⁻¹ and 80 mg kg⁻¹ respectively, within three days [258]. The plants were able to completely remove TNT from soil with a nominal concentration of 40 mg kg⁻¹ within 12 days, without displaying any phytotoxic symptoms. Poplar (*Populus* spp.) has

also been recommended as a plant species that could be used as a containment measure on the borders of a site or at non-active training ranges, due to its high biomass [6, 14]. With federal regulations limiting the use of genetically modified plant species in the field, future developments in phytoremediation are likely to include genetic use restriction technologies (GURTs) to control the dispersion of transgenes [259].

While TNT tolerance varies significantly among species, the higher concentrations ($>1000 \text{ mg kg}^{-1}$) of TNT found in the environment have been found to be toxic to all species tested so far [19]. A strategy to overcome this problem could be to utilise the knowledge obtained through this study for traditional breeding or genetic engineering techniques, to enhance tolerance and enable plants to detoxify TNT efficiently. In the past, Brentner et al. [76] have identified GST homologs in poplar following the results of a microarray study on TNT-treated *Arabidopsis* seedlings [75]. Among the GST homologues up-regulated in response to TNT was also the predicted poplar GST-U24 orthologue (GST173). GST173 (also referred to as GST-U16) was recently shown to have activity towards TNT, while protein sequence alignment showed that it bears Pro12, Tyr107, and Leu211, which is necessary for conjugate 3 production, in the respective positions [164]. These results suggest that engineering higher TNT tolerance could be possible for field applicable species as well.

To conclude, the present study demonstrates that GSTs contribute to the TNT detoxification pathway in *Arabidopsis* through the direct glutathionylation of TNT, and that their over-expression can lead to enhanced tolerance towards this toxic compound and increased removal from both soil and liquid media. In addition, a *Drosophila* Epsilon class GST (*DmGSTE6*) was characterised and recombinantly expressed in *Arabidopsis* showing that identifying GSTs from different species with higher activity towards TNT can further enhance the resistant phenotype. The identification of conjugate 3 brings us a step closer to TNT complete mineralisation. The removal of a nitro group that occurs during the formation of conjugate 3 is a beneficial reaction that restores, at least partially, the electrons of the aromatic ring and could potentially lead to

degradation by microbial oxygenases. The site-directed mutagenesis experiments identified Leu211 as necessary for conjugate 3 production. Following from that, looking into the use of C-S lyases to remove the glutathione moiety from conjugate 3 and release dinitrotoluene would be the ideal next step. Finally, it was shown that the TNT detoxification reaction catalysed by the GSTs can be limited by GSH abundance and in order to overcome this plants with increased GST activity will have to be engineered to also produce elevated levels of GSH. Ultimately, GSTs and the detoxification pathway described here can be employed to generate robust, potentially non-GM, plant phenotypes for environmental remediation. In such a case the technology will have to be transferred to field applicable species such as grasses which can tolerate relatively high levels of TNT concentration and are native to most military training ranges.

Abbreviations

½ MS	Murashige and Skoog medium half strength
2-ADNT	2-amino-dinitrotoluene
2-HADNT	2-hydroxylamino-4,6-dinitrotoluene
2,4-DNT	2,4-dinitrotoluene
2,6-DNT	2,6-dinitrotoluene
4-ADNT	4-amino-dinitrotoluene
4-HADNT	4-hydroxylamin-2,6-dinitrotoluene
5S-HpETE	Arachidonic acid 5-hydroperoxide (5S)-HpETE
γ-ECS	Gamma-glutamylcysteine synthase
ABC	ATP-binding cassette
ADNTs	Amino-dinitrotoluenes
AI	Autoinduction medium
ANS	1-anilino-8-naphthalene-sulfonate
BSO	Buthionine sulfoximine
CaMV 35S	Cauliflower mosaic virus 35S promoter
cDNA	Complementary DNA
CDNB	1-chloro-2,4-dinitrobenzene
Col0	Columbia 0 ecotype
dGST	<i>DmGSTE6</i> expressing Arabidopsis lines
DMSO	Dimethyl sulfoxide
DNA	Deoxyribonucleic acid
dNTP	Dinucleotide triphosphate
dsDNA	Double-stranded DNA
DTNB	5,5'-dithiobis(2-nitrobenzoic acid)
DTT	Dithiothreitol
EDTA	Ethylenediaminetetraacetic acid
EV	Empty vector

Abbreviations

fw	Fresh weight
g	Grams
GPOX	Glutathione peroxidase
GS⁻	Glutathione thiolate anion
GSH	Reduced glutathione
GSSG	Glutathione disulfide
GST	Glutathione S-transferase
GST-U24	AtGSTU24
GST-U25	AtGSTU25
GR	Glutathione reductase
HADNTs	Hydroxylamino-dinitrotoluenes
HPLC	High-performance liquid chromatography
kg	Kilogram
KO	Knockout
LB	Luria-Bertani medium
LC/MS	Liquid chromatography-mass spectrometry
M	Molar
μl	Microlitre
μM	Micromolar
mBB	Monobromobimane
ml	Millilitre
mM	Millimolar
NADPH	Nicotinamide adenine dinucleotide phosphate reduced
NADP⁺	Nicotinamide adenine dinucleotide phosphate
NED	N-(1-Naphthyl)ethylenediamine dihydrochloride
NMR	Nuclear magnetic resonance
OE	Over-expression.
OYE	Old yellow enzyme
O/N	Overnight

Abbreviations

PBS	Phosphate buffered saline
PCR	Polymerase chain reaction
PCS	Phytochelatin synthase
RNA	Ribonucleic acid
ROS	Reactive oxygen species
RT-PCR	Real time polymerase chain reaction
SDS-PAGE	sodium dodecyl sulfate polyacrylamide gel electrophoresis
SE	Standard error of the mean
TCA	Trichloroacetic acid
TNT	2,4,6-trinitrotoluene
U	Units
UGTs	uridine diphosphate (UDP)-glycosyltransferases
UV	Ultraviolet
VPD	2-vinylpyridine
v/v	Volume to volume ratio
w/v	Weight to volume ratio
WT	Wild Type (refers to <i>Arabidopsis thaliana</i> Columbia 0 ecotype unless stated otherwise)

References

1. Ponting, C., *Gunpowder An Explosive History - From the alchemists of China to the battlefields of Europe*. 2006.
2. Lewis, T.A., D.A. Newcombe, and R.L. Crawford, *Bioremediation of soils contaminated with explosives*. *J Environ Manage*, 2004. **70**(4): p. 291-307.
3. Boileau, J., et al., *Explosives*, in *Ullmann's Encyclopedia of Industrial Chemistry*. 2000, Wiley-VCH Verlag GmbH & Co. KGaA.
4. Snellinx, Z., et al., *Biological remediation of explosives and related nitroaromatic compounds*. *Environ Sci Pollut Res Int*, 2002. **9**(1): p. 48-61.
5. Rosser, S., C. French, and N. Bruce, *Engineering plants for the phytodetoxification of explosives*. *In Vitro Cellular & Developmental Biology - Plant*, 2001. **37**(3): p. 330-333.
6. Rylott, E.L. and N.C. Bruce, *Plants disarm soil: engineering plants for the phytoremediation of explosives*. *Trends Biotechnol*, 2009. **27**(2): p. 73-81.
7. Amaral, H.I., et al., *Assessing TNT and DNT groundwater contamination by compound-specific isotope analysis and 3H-3He groundwater dating: a case study in Portugal*. *Chemosphere*, 2009. **77**(6): p. 805-12.
8. Zheng, W., et al., *Fate and transport of TNT, RDX, and HMX in streambed sediments: Implications for riverbank filtration*. *Chemosphere*, 2009. **76**(9): p. 1167-77.
9. Talmage, S.S., et al., *Nitroaromatic munition compounds: environmental effects and screening values*. *Rev Environ Contam Toxicol*, 1999. **161**: p. 1-156.
10. Clark, B. and R. Boopathy, *Evaluation of bioremediation methods for the treatment of soil contaminated with explosives in Louisiana Army Ammunition Plant, Minden, Louisiana*. *J Hazard Mater*, 2007. **143**(3): p. 643-8.
11. Jenkins, T.F., et al., *Identity and distribution of residues of energetic compounds at army live-fire training ranges*. *Chemosphere*, 2006. **63**(8): p. 1280-90.
12. Rodgers, J.D. and N.J. Bunce, *Treatment methods for the remediation of nitroaromatic explosives*. *Water Res*, 2001. **35**(9): p. 2101-11.
13. General Accountability Office, U.S., *Department of Defense Operational Ranges: More Reliable Cleanup Cost Estimates and a Proactive Approach to Identifying Contamination Are Needed*. (GAO Publication GAO-04-601); www.gao.gov/products/GAO-04-601, 2004.
14. Schoenmuth, B.W. and W. Pestemer, *Dendroremediation of trinitrotoluene (TNT). Part 1: Literature overview and research concept*. *Environ Sci Pollut Res Int*, 2004. **11**(4): p. 273-8.
15. Hundal, L.S., et al., *Long-Term TNT Sorption and Bound Residue Formation in Soil*. *Journal of Environmental Quality*, 1997(26): p. 896-904.
16. Haigler, B.E., S.F. Nishino, and J.C. Spain, *Biodegradation of 4-methyl-5-nitrocatechol by Pseudomonas sp. strain DNT*. *J Bacteriol*, 1994. **176**(11): p. 3433-7.
17. Qasim, M., et al., *Structure and reactivity of TNT and related species: application of spectroscopic approaches and quantum-chemical approximations toward*

References

- understanding transformation mechanisms*. J Hazard Mater, 2009. **167**(1-3): p. 154-63.
18. Qasim, M.M., et al., *Structural Characteristics and Reactivity Relationships of Nitroaromatic and Nitramine Explosives – A Review of Our Computational Chemistry and Spectroscopic Research*. International Journal of Molecular Sciences, 2007. **8**(12): p. 1234-1264.
 19. Hannink, N.K., S.J. Rosser, and N.C. Bruce, *Phytoremediation of Explosives*. Critical Reviews in Plant Sciences, 2002. **21**(5): p. 511-538.
 20. Pavlostathis, S.G., et al., *Transformation of 2,4,6-trinitrotoluene by the aquatic plant *Myriophyllum spicatum**. Environmental Toxicology and Chemistry, 1998. **17**(11): p. 2266-2273.
 21. Mentewab, A., V. Cardoza, and C.N. Stewart Jr, *Genomic analysis of the response of *Arabidopsis thaliana* to trinitrotoluene as revealed by cDNA microarrays*. Plant Science, 2005. **168**(6): p. 1409-1424.
 22. Hannink, N., et al., *Phytodetoxification of TNT by transgenic plants expressing a bacterial nitroreductase*. Nat Biotechnol, 2001. **19**(12): p. 1168-72.
 23. Gong, P., B. Wilke, and S. Fleischmann, *Soil-based phytotoxicity of 2,4,6-trinitrotoluene (TNT) to terrestrial higher plants*. Arch Environ Contam Toxicol, 1999. **36**(2): p. 152-7.
 24. Vila, M., S. Lorber-Pascal, and F. Laurent, *Phytotoxicity to and uptake of TNT by rice*. Environ Geochem Health, 2008. **30**(2): p. 199-203.
 25. Mezzari, M.P., et al., *Gene Expression and Microscopic Analysis of Arabidopsis Exposed to Chloroacetanilide Herbicides and Explosive Compounds. A Phytoremediation Approach*. Plant Physiology, 2005. **138**(2): p. 858-869.
 26. Gandia-Herrero, F., et al., *Detoxification of the explosive 2,4,6-trinitrotoluene in Arabidopsis: discovery of bifunctional O- and C-glucosyltransferases*. Plant J, 2008. **56**(6): p. 963-74.
 27. Beynon, E.R., et al., *The Role of Oxophytodienoate Reductases in the Detoxification of the Explosive 2,4,6-Trinitrotoluene by Arabidopsis*. Plant Physiol, 2009. **151**(1): p. 253-61.
 28. Johnston, E.J., et al., *Monodehydroascorbate reductase mediates TNT toxicity in plants*. Science, 2015. **349**(6252): p. 1072-5.
 29. Lachance, B., et al., *Cytotoxic and genotoxic effects of energetic compounds on bacterial and mammalian cells in vitro*. Mutat Res, 1999. **444**(1): p. 25-39.
 30. Frische, T., *Screening for soil toxicity and mutagenicity using luminescent bacteria--a case study of the explosive 2,4,6-trinitrotoluene (TNT)*. Ecotoxicol Environ Saf, 2002. **51**(2): p. 133-44.
 31. Honeycutt, M.E., A.S. Jarvis, and V.A. McFarland, *Cytotoxicity and mutagenicity of 2,4,6-trinitrotoluene and its metabolites*. Ecotoxicol Environ Saf, 1996. **35**(3): p. 282-7.
 32. Neuwoehner, J., et al., *Toxicological characterization of 2,4,6-trinitrotoluene, its transformation products, and two nitramine explosives*. Environ Toxicol Chem, 2007. **26**(6): p. 1090-9.

References

33. Lima, D.R., et al., *Impact of ammunition and military explosives on human health and the environment*. Rev Environ Health, 2011. **26**(2): p. 101-10.
34. Rosenblatt, D.H., *Toxicology of explosives and propellants*. In *Encyclopedia of Explosives and Related Items* (Kaye, S.M. ed). 1980. **Vol. 9** p. 332-345.
35. Yinon, J., *Toxicity and Metabolism of Explosives*. Boca Raton, Florida, USA, CRC Press Inc., 1990.
36. George, I., et al., *Effect of 2,4,6-trinitrotoluene on soil bacterial communities*. J Ind Microbiol Biotechnol, 2008. **35**(4): p. 225-36.
37. Esteve-Núñez, A., A. Caballero, and J.L. Ramos, *Biological Degradation of 2,4,6-Trinitrotoluene*. Microbiology and Molecular Biology Reviews, 2001. **65**(3): p. 335-352.
38. Bryant, C. and M. Deluca, *Purification and characterization of an oxygen insensitive nadph nitroreductase from enterobacter cloacae*. Journal Of Biological Chemistry, 1991. **266**(7): p. 4119-4125.
39. Kitts, C.L., et al., *Type I nitroreductases in soil enterobacteria reduce TNT (2,4,6-trinitrotoluene) and RDX (hexahydro-1,3,5-trinitro-1,3,5-triazine)*. Can J Microbiol, 2000. **46**(3): p. 278-82.
40. Wittich, R.-M., et al., *OYE Flavoprotein Reductases Initiate the Condensation of TNT-Derived Intermediates to Secondary Diarylamines and Nitrite*. Environmental Science & Technology, 2008. **42**(3): p. 734-739.
41. Wittich, R.M., J.L. Ramos, and P. van Dillewijn, *Microorganisms and explosives: mechanisms of nitrogen release from TNT for use as an N-source for growth*. Environ Sci Technol, 2009. **43**(8): p. 2773-6.
42. van Dillewijn, P., et al., *Type II hydride transferases from different microorganisms yield nitrite and diarylamines from polynitroaromatic compounds*. Appl Environ Microbiol, 2008. **74**(21): p. 6820-3.
43. French, C.E., S. Nicklin, and N.C. Bruce, *Aerobic Degradation of 2,4,6-Trinitrotoluene by Enterobacter cloacae PB2 and by Pentaerythritol Tetranitrate Reductase*. Applied and Environmental Microbiology, 1998. **64**(8): p. 2864-2868.
44. Pak, J.W., et al., *Transformation of 2,4,6-trinitrotoluene by purified xenobiotic reductase B from Pseudomonas fluorescens I-C*. Appl Environ Microbiol, 2000. **66**(11): p. 4742-50.
45. Mercimek, H.A., et al., *Aerobic biodegradation of 2,4,6-trinitrotoluene (TNT) by Bacillus cereus isolated from contaminated soil*. Microb Ecol, 2013. **66**(3): p. 512-21.
46. Lee, B.U., et al., *Enhanced degradation of TNT by genome-shuffled Stenotrophomonas maltophilia OK-5*. Curr Microbiol, 2009. **59**(3): p. 346-51.
47. Ayoub, K., et al., *Application of advanced oxidation processes for TNT removal: A review*. J Hazard Mater, 2010. **178**(1-3): p. 10-28.
48. Ederer, M.M., T.A. Lewis, and R.L. Crawford, *2,4,6-Trinitrotoluene (TNT) transformation by clostridia isolated from a munition-fed bioreactor: comparison with non-adapted bacteria*. J Ind Microbiol Biotechnol, 1997. **18**(2-3): p. 82-8.
49. Khan, T.A., R. Bhadra, and J. Hughes, *Anaerobic transformation of 2,4,6-TNT and related nitroaromatic compounds by Clostridium acetobutylicum*. Journal of Industrial Microbiology and Biotechnology, 1997. **18**(2-3): p. 198-203.

References

50. Haïdour, A. and J.L. Ramos, *Identification of Products Resulting from the Biological Reduction of 2,4,6-Trinitrotoluene, 2,4-Dinitrotoluene, and 2,6-Dinitrotoluene by Pseudomonas sp.* Environmental Science & Technology, 1996. **30**(7): p. 2365-2370.
51. George, S.E., G. Huggins-Clark, and L.R. Brooks, *Use of a Salmonella microsuspension bioassay to detect the mutagenicity of munitions compounds at low concentrations.* Mutat Res, 2001. **490**(1): p. 45-56.
52. Fernando, T., J.A. Bumpus, and S.D. Aust, *Biodegradation of TNT (2,4,6-trinitrotoluene) by Phanerochaete chrysosporium.* Applied and Environmental Microbiology, 1990. **56**(6): p. 1666-1671.
53. Kim, H.Y. and H.G. Song, *Transformation and mineralization of 2,4,6-trinitrotoluene by the white rot fungus Irpex lacteus.* Appl Microbiol Biotechnol, 2003. **61**(2): p. 150-6.
54. Stahl, J.D., S.J. Rasmussen, and S.D. Aust, *Reduction of quinones and radicals by a plasma membrane redox system of Phanerochaete chrysosporium.* Arch Biochem Biophys, 1995. **322**(1): p. 221-7.
55. Spiker, J.K., D.L. Crawford, and R.L. Crawford, *Influence of 2,4,6-trinitrotoluene (TNT) concentration on the degradation of TNT in explosive-contaminated soils by the white rot fungus Phanerochaete chrysosporium.* Appl Environ Microbiol, 1992. **58**(9): p. 3199-202.
56. Rylott, E.L., A. Lorenz, and N.C. Bruce, *Biodegradation and biotransformation of explosives.* Curr Opin Biotechnol, 2011. **22**(3): p. 434-40.
57. Coleman, J., M. Blake-Kalff, and E. Davies, *Detoxification of xenobiotics by plants: chemical modification and vacuolar compartmentation.* Trends in Plant Science, 1997. **2**(4): p. 144-151.
58. Eapen, S., S. Singh, and S.F. D'Souza, *Advances in development of transgenic plants for remediation of xenobiotic pollutants.* Biotechnol Adv, 2007. **25**(5): p. 442-51.
59. Van Aken, B., *Transgenic plants for phytoremediation: helping nature to clean up environmental pollution.* Trends Biotechnol, 2008. **26**(5): p. 225-7.
60. Sandermann, H., Jr., *Higher plant metabolism of xenobiotics: the 'green liver' concept.* Pharmacogenetics, 1994. **4**(5): p. 225-41.
61. Kang, J., et al., *Plant ABC Transporters.* The Arabidopsis Book / American Society of Plant Biologists, 2011. **9**: p. e0153.
62. Rylott, E.L., et al., *Phytodetoxification of the environmental pollutant and explosive 2,4,6-trinitrotoluene.* Plant Signal Behav, 2015. **10**(1): p. e977714.
63. Pilon-Smits, E., *Phytoremediation.* Annu Rev Plant Biol, 2005. **56**: p. 15-39.
64. Schoenmuth, B.W. and W. Pestemer, *Dendroremediation of trinitrotoluene (TNT). Part 2: fate of radio-labelled TNT in trees.* Environ Sci Pollut Res Int, 2004. **11**(5): p. 331-9.
65. van Dillewijn, P., et al., *Bioremediation of 2,4,6-Trinitrotoluene by Bacterial Nitroreductase Expressing Transgenic Aspen.* Environmental Science & Technology, 2008. **42**(19): p. 7405-7410.
66. Sens, C., et al., *Distribution of 14C-TNT and derivatives in different biochemical compartments of Phaseolus vulgaris.* Environ Sci Pollut Res Int, 1998. **5**(4): p. 202-8.

References

67. Sens, C., P. Scheidemann, and D. Werner, *The distribution of ¹⁴C-TNT in different biochemical compartments of the monocotyledonous Triticum aestivum*. Environmental Pollution, 1999. **104**(1): p. 113-119.
68. Brentner, L.B., et al., *Localization of hexahydro-1,3,5-trinitro-1,3,5-triazine (RDX) and 2,4,6-trinitrotoluene (TNT) in poplar and switchgrass plants using phosphor imager autoradiography*. Environ Pollut, 2010. **158**(2): p. 470-5.
69. Hannink, N.K., et al., *Enhanced transformation of tnt by tobacco plants expressing a bacterial nitroreductase*. Int J Phytoremediation, 2007. **9**(5): p. 385-401.
70. Durringer, J.M., et al., *Uptake and transformation of soil [¹⁴C]-trinitrotoluene by cool-season grasses*. Environ Sci Technol, 2010. **44**(16): p. 6325-30.
71. Panz, K. and K. Miksch, *Phytoremediation of explosives (TNT, RDX, HMX) by wild-type and transgenic plants*. Journal of Environmental Management, 2012. **113**: p. 85-92.
72. Wang, C., et al., *Role of hydroxylamine intermediates in the phytotransformation of 2,4,6-trinitrotoluene by Myriophyllum aquaticum*. Environ Sci Technol, 2003. **37**(16): p. 3595-600.
73. Subramanian, M., D.J. Oliver, and J.V. Shanks, *TNT phytotransformation pathway characteristics in Arabidopsis: role of aromatic hydroxylamines*. Biotechnol Prog, 2006. **22**(1): p. 208-16.
74. Bhadra, R., et al., *Characterization of Oxidation Products of TNT Metabolism in Aquatic Phytoremediation Systems of Myriophyllum aquaticum*. Environmental Science & Technology, 1999. **33**(19): p. 3354-3361.
75. Ekman, D.R., et al., *SAGE analysis of transcriptome responses in Arabidopsis roots exposed to 2,4,6-trinitrotoluene*. Plant Physiol, 2003. **133**(3): p. 1397-406.
76. Brentner, L.B., et al., *Expression of glutathione S-transferases in poplar trees (Populus trichocarpa) exposed to 2,4,6-trinitrotoluene (TNT)*. Chemosphere, 2008. **73**(5): p. 657-62.
77. Lorenz, A., *Bioengineering transgenic plants to detoxify nitroaromatic explosive compounds*. University of York: PhD thesis, 2007.
78. Landa, P., et al., *Transferases and transporters mediate the detoxification and capacity to tolerate trinitrotoluene in Arabidopsis*. Funct Integr Genomics, 2010. **10**(4): p. 547-59.
79. Vila, M., et al., *Metabolism of [¹⁴C]-2,4,6-Trinitrotoluene in Tobacco Cell Suspension Cultures*. Environmental Science & Technology, 2005. **39**(2): p. 663-672.
80. Vila, M., S. Lorber-Pascal, and F. Laurent, *Fate of RDX and TNT in agronomic plants*. Environmental Pollution, 2007. **148**(1): p. 148-154.
81. Bhadra, R., et al., *Confirmation of Conjugation Processes during TNT Metabolism by Axenic Plant Roots*. Environmental Science & Technology, 1999. **33**: p. 446-452.
82. Frova, C., *The plant glutathione transferase gene family: genomic structure, functions, expression and evolution*. Physiologia Plantarum, 2003. **119**(4): p. 469-479.
83. Dixon, D.P., A. Laphorn, and R. Edwards, *Plant glutathione transferases*. Genome Biol, 2002. **3**(3): p. REVIEWS3004.
84. Dixon, D.P. and R. Edwards, *Glutathione Transferases*. The Arabidopsis Book / American Society of Plant Biologists, 2010. **8**: p. e0131.

References

85. Cummins, I., et al., *Multiple roles for plant glutathione transferases in xenobiotic detoxification*. Drug Metab Rev, 2011. **43**(2): p. 266-80.
86. Scalla, R. and A. Roulet, *Cloning and characterization of a glutathione S-transferase induced by a herbicide safener in barley (*Hordeum vulgare*)*. Physiologia Plantarum, 2002. **116**(3): p. 336-344.
87. Dixon, D.P., et al., *Enzyme activities and subcellular localization of members of the Arabidopsis glutathione transferase superfamily*. J Exp Bot, 2009. **60**(4): p. 1207-18.
88. Cummins, I., D.J. Cole, and R. Edwards, *Purification of Multiple Glutathione Transferases Involved in Herbicide Detoxification from Wheat (*Triticum aestivum*L.) Treated with the Safener Fenchlorazole-ethyl*. Pesticide Biochemistry and Physiology, 1997. **59**(1): p. 35-49.
89. Droog, F., *Plant Glutathione S-Transferases, a Tale of Theta and Tau*. Journal of Plant Growth Regulation, 1997. **16**(2): p. 95-107.
90. Jakobsson, P.J., et al., *Common structural features of MAPEG -- a widespread superfamily of membrane associated proteins with highly divergent functions in eicosanoid and glutathione metabolism*. Protein Science : A Publication of the Protein Society, 1999. **8**(3): p. 689-692.
91. Sheehan, D., et al., *Structure, function and evolution of glutathione transferases: implications for classification of non-mammalian members of an ancient enzyme superfamily*. Biochem J, 2001. **360**(Pt 1): p. 1-16.
92. Dixon, D.P., B.G. Davis, and R. Edwards, *Functional divergence in the glutathione transferase superfamily in plants. Identification of two classes with putative functions in redox homeostasis in Arabidopsis thaliana*. J Biol Chem, 2002. **277**(34): p. 30859-69.
93. Soranzo, N., et al., *Organisation and structural evolution of the rice glutathione S-transferase gene family*. Molecular Genetics and Genomics, 2004. **271**(5): p. 511-521.
94. Frova, C., *Glutathione transferases in the genomics era: New insights and perspectives*. Biomolecular Engineering, 2006. **23**(4): p. 149-169.
95. Axarli, I., et al., *Crystallographic and Functional Characterization of the Fluorodifen-inducible Glutathione Transferase from Glycine max Reveals an Active Site Topography Suited for Diphenylether Herbicides and a Novel L-site*. Journal of Molecular Biology, 2009. **385**(3): p. 984-1002.
96. Tajc, S.G., et al., *Direct Determination of Thiol pKa by Isothermal Titration Microcalorimetry*. Journal of the American Chemical Society, 2004. **126**(34): p. 10508-10509.
97. Zeng, Q.Y. and X.R. Wang, *Catalytic properties of glutathione-binding residues in a tau class glutathione transferase (PtGSTU1) from Pinus tabulaeformis*. FEBS Lett, 2005. **579**(12): p. 2657-62.
98. Bowman, A.L., et al., *Molecular determinants of xenobiotic metabolism: QM/MM simulation of the conversion of 1-chloro-2,4-dinitrobenzene catalyzed by M1-1 glutathione S-transferase*. Biochemistry, 2007. **46**(21): p. 6353-63.
99. Smith, A.P., et al., *Arabidopsis AtGSTF2 is regulated by ethylene and auxin, and encodes a glutathione S-transferase that interacts with flavonoids*. Plant J, 2003. **36**(4): p. 433-42.

References

100. Dixon, D.P., J.D. Sellars, and R. Edwards, *The Arabidopsis phi class glutathione transferase AtGSTF2: binding and regulation by biologically active heterocyclic ligands*. *Biochem J*, 2011. **438**(1): p. 63-70.
101. Dixon, D.P., D.J. Cole, and R. Edwards, *Characterisation of a zeta class glutathione transferase from Arabidopsis thaliana with a putative role in tyrosine catabolism*. *Arch Biochem Biophys*, 2000. **384**(2): p. 407-12.
102. Reumann, S., et al., *In-Depth Proteome Analysis of Arabidopsis Leaf Peroxisomes Combined with in Vivo Subcellular Targeting Verification Indicates Novel Metabolic and Regulatory Functions of Peroxisomes*. *Plant Physiology*, 2009. **150**(1): p. 125-143.
103. Chew, O., J. Whelan, and A.H. Millar, *Molecular definition of the ascorbate-glutathione cycle in Arabidopsis mitochondria reveals dual targeting of antioxidant defenses in plants*. *J Biol Chem*, 2003. **278**(47): p. 46869-77.
104. Prohaska, J.R., *The glutathione peroxidase activity of glutathione S-transferases*. *Biochim Biophys Acta*, 1980. **611**(1): p. 87-98.
105. Sappl, P.G., et al., *The Arabidopsis glutathione transferase gene family displays complex stress regulation and co-silencing multiple genes results in altered metabolic sensitivity to oxidative stress*. *Plant J*, 2009. **58**(1): p. 53-68.
106. Uquillas, C., et al., *NPR1-independent activation of immediate early salicylic acid-responsive genes in Arabidopsis*. *Mol Plant Microbe Interact*, 2004. **17**(1): p. 34-42.
107. Chen, W., G. Chao, and K.B. Singh, *The promoter of a H₂O₂-inducible, Arabidopsis glutathione S-transferase gene contains closely linked OBF- and OBP1-binding sites*. *Plant J*, 1996. **10**(6): p. 955-66.
108. Perl-Treves, R., et al., *Early induction of the Arabidopsis GSTF8 promoter by specific strains of the fungal pathogen Rhizoctonia solani*. *Mol Plant Microbe Interact*, 2004. **17**(1): p. 70-80.
109. Wangwattana, B., et al., *Characterization of *PAP1*-upregulated Glutathione *S*-transferase genes in *Arabidopsis thaliana**. *Plant Biotechnology*, 2008. **25**(2): p. 191-196.
110. Sun, Y., H. Li, and J.R. Huang, *Arabidopsis TT19 functions as a carrier to transport anthocyanin from the cytosol to tonoplasts*. *Mol Plant*, 2012. **5**(2): p. 387-400.
111. Dixon, D.P. and R. Edwards, *Selective binding of glutathione conjugates of fatty acid derivatives by plant glutathione transferases*. *J Biol Chem*, 2009. **284**(32): p. 21249-56.
112. DeRidder, B.P., et al., *Induction of glutathione S-transferases in Arabidopsis by herbicide safeners*. *Plant Physiol*, 2002. **130**(3): p. 1497-505.
113. Chen, I.-C., et al., *Glutathione S-Transferase Interacting with Far-Red Insensitive 219 Is Involved in Phytochrome A-Mediated Signaling in Arabidopsis*. *Plant Physiology*, 2007. **143**(3): p. 1189-1202.
114. Bresell, A., et al., *Bioinformatic and enzymatic characterization of the MAPEG superfamily*. *FEBS J*, 2005. **272**(7): p. 1688-703.
115. Klapheck, S., *Homoglutathione: isolation, quantification and occurrence in legumes*. *Physiologia Plantarum*, 1988. **74**(4): p. 727-732.
116. Klapheck, S., et al., *γ -Glutamylcysteinylserine — A New Homologue of Glutathione in Plants of the Family Poaceae**. *Botanica Acta*, 1992. **105**(3): p. 174-179.

References

117. Noctor, G., et al., *Glutathione in plants: an integrated overview*. Plant Cell Environ, 2012. **35**(2): p. 454-84.
118. Wachter, A., et al., *Differential targeting of GSH1 and GSH2 is achieved by multiple transcription initiation: implications for the compartmentation of glutathione biosynthesis in the Brassicaceae*. Plant J, 2005. **41**(1): p. 15-30.
119. Lu, S.C., *Regulation of glutathione synthesis*. Mol Aspects Med, 2009. **30**(1-2): p. 42-59.
120. Xiang, C. and D. Bertrand, *Glutathione synthesis in Arabidopsis: multilevel controls coordinate responses to stress*. In *Sulfure Nutrition and Sulphur Assimilation in Higher Plants*. Edited by Brunold C., Rennenberg H., De Kok L.J., Stulen I., Davidian J.C. Paul Haup, Bern Switzerland., 2000: p. 409-412.
121. Noctor, G., et al., *Interactions between biosynthesis, compartmentation and transport in the control of glutathione homeostasis and signalling*. J Exp Bot, 2002. **53**(372): p. 1283-304.
122. Pasternak, M., et al., *Restricting glutathione biosynthesis to the cytosol is sufficient for normal plant development*. Plant J, 2008. **53**(6): p. 999-1012.
123. Jez, J.M., R.E. Cahoon, and S. Chen, *Arabidopsis thaliana glutamate-cysteine ligase: functional properties, kinetic mechanism, and regulation of activity*. J Biol Chem, 2004. **279**(32): p. 33463-70.
124. Mhamdi, A., et al., *Arabidopsis GLUTATHIONE REDUCTASE1 plays a crucial role in leaf responses to intracellular hydrogen peroxide and in ensuring appropriate gene expression through both salicylic acid and jasmonic acid signaling pathways*. Plant Physiol, 2010. **153**(3): p. 1144-60.
125. Meyer, A.J., et al., *Redox-sensitive GFP in Arabidopsis thaliana is a quantitative biosensor for the redox potential of the cellular glutathione redox buffer*. Plant J, 2007. **52**(5): p. 973-86.
126. Queval, G., et al., *Increased intracellular H₂O₂ availability preferentially drives glutathione accumulation in vacuoles and chloroplasts*. Plant Cell Environ, 2011. **34**(1): p. 21-32.
127. Zechmann, B. and M. Muller, *Subcellular compartmentation of glutathione in dicotyledonous plants*. Protoplasma, 2010. **246**(1-4): p. 15-24.
128. Zechmann, B., et al., *Subcellular immunocytochemical analysis detects the highest concentrations of glutathione in mitochondria and not in plastids*. J Exp Bot, 2008. **59**(14): p. 4017-27.
129. Cairns, N.G., et al., *Maturation of arabidopsis seeds is dependent on glutathione biosynthesis within the embryo*. Plant Physiol, 2006. **141**(2): p. 446-55.
130. Marquez-Garcia, B., et al., *A new role for glutathione in the regulation of root architecture linked to strigolactones*. Plant Cell Environ, 2014. **37**(2): p. 488-98.
131. Schnaubelt, D., et al., *A phenomics approach to the analysis of the influence of glutathione on leaf area and abiotic stress tolerance in Arabidopsis thaliana*. Frontiers in Plant Science, 2013. **4**.
132. Koprivova, A., S.T. Mugford, and S. Kopriva, *Arabidopsis root growth dependence on glutathione is linked to auxin transport*. Plant Cell Rep, 2010. **29**(10): p. 1157-67.

References

133. Zechmann, B., B.E. Koffler, and S.D. Russell, *Glutathione synthesis is essential for pollen germination in vitro*. BMC Plant Biol, 2011. **11**: p. 54.
134. Ball, L., et al., *Evidence for a Direct Link between Glutathione Biosynthesis and Stress Defense Gene Expression in Arabidopsis*. Plant Cell, 2004. **16**(9): p. 2448-62.
135. Fratelli, M., et al., *Gene expression profiling reveals a signaling role of glutathione in redox regulation*. Proc Natl Acad Sci U S A, 2005. **102**(39): p. 13998-4003.
136. Han, Y., et al., *Functional analysis of Arabidopsis mutants points to novel roles for glutathione in coupling H₂O₂ to activation of salicylic acid accumulation and signaling*. Antioxid Redox Signal, 2013. **18**(16): p. 2106-21.
137. Sanchez-Fernandez, R., et al., *The Arabidopsis thaliana ABC protein superfamily, a complete inventory*. J Biol Chem, 2001. **276**(32): p. 30231-44.
138. Rea, P.A., et al., *FROM VACUOLAR GS-X PUMPS TO MULTISPECIFIC ABC TRANSPORTERS*. Annu Rev Plant Physiol Plant Mol Biol, 1998. **49**: p. 727-760.
139. Beck, A., et al., *Phytochelatase catalyzes key step in turnover of glutathione conjugates*. Phytochemistry, 2003. **62**(3): p. 423-31.
140. Grzam, A., et al., *Vacuolar sequestration of glutathione S-conjugates outcompetes a possible degradation of the glutathione moiety by phytochelatase synthase*. FEBS Letters, 2006. **580**(27): p. 6384-6390.
141. Wolf, A.E., K.J. Dietz, and P. Schroder, *Degradation of glutathione S-conjugates by a carboxypeptidase in the plant vacuole*. FEBS Lett, 1996. **384**(1): p. 31-4.
142. Storozhenko, S., et al., *Gamma-glutamyl transpeptidase in transgenic tobacco plants. Cellular localization, processing, and biochemical properties*. Plant Physiol, 2002. **128**(3): p. 1109-19.
143. Ohkama-Ohtsu, N., et al., *Glutathione conjugates in the vacuole are degraded by gamma-glutamyl transpeptidase GGT3 in Arabidopsis*. Plant J, 2007. **49**(5): p. 878-88.
144. Ohkama-Ohtsu, N., et al., *Characterization of the extracellular gamma-glutamyl transpeptidases, GGT1 and GGT2, in Arabidopsis*. Plant J, 2007. **49**(5): p. 865-77.
145. Grzam, A., et al., *gamma-Glutamyl transpeptidase GGT4 initiates vacuolar degradation of glutathione S-conjugates in Arabidopsis*. FEBS Lett, 2007. **581**(17): p. 3131-8.
146. Brazier-Hicks, M., et al., *Catabolism of glutathione conjugates in Arabidopsis thaliana. Role in metabolic reactivation of the herbicide safener fenclorim*. J Biol Chem, 2008. **283**(30): p. 21102-12.
147. Lieberman, M.W., et al., *Growth retardation and cysteine deficiency in gamma-glutamyl transpeptidase-deficient mice*. Proc Natl Acad Sci U S A, 1996. **93**(15): p. 7923-6.
148. Funk, S.B., et al., *Initial-phase optimization for bioremediation of munition compound-contaminated soils*. Applied and Environmental Microbiology, 1993. **59**(7): p. 2171-2177.
149. Brus-Nagel, D., et al., *Composting (humification) of nitroaromatic compounds*. In *Biodegradation of Nitroaromatic Compounds and Explosives*. Edited by Spain J., Hughes J.B., Knackmuss H.J. Boca Raton: Lewin Publishers, 2000: p. 357-393.
150. Lenke, H., C. Achtnich, and H.J. Knackmuss, *Perspectives of bioelimination of polynitroaromatic compounds*. In *Biodegradation of Nitroaromatic Compounds and*

References

- Explosives*. Edited by Spain J., Hughes J.B., Knackmuss H.J. Boca Raton: Lewin Publishers, 2000: p. 91-126.
151. Salt, D.E., R.D. Smith, and I. Raskin, *PHYTOREMEDIATION*. Annu Rev Plant Physiol Plant Mol Biol, 1998. **49**: p. 643-668.
 152. Rhodes, C.J., *Applications of bioremediation and phytoremediation*. Sci Prog, 2013. **96**(Pt 4): p. 417-27.
 153. Abhilash, P.C., S. Jamil, and N. Singh, *Transgenic plants for enhanced biodegradation and phytoremediation of organic xenobiotics*. Biotechnol Adv, 2009. **27**(4): p. 474-88.
 154. Sheoran, V., A.S. Sheoran, and P. Poonia, *Phytomining: A review*. Minerals Engineering, 2009. **22**(12): p. 1007-1019.
 155. Barac, T., et al., *Engineered endophytic bacteria improve phytoremediation of water-soluble, volatile, organic pollutants*. Nat Biotechnol, 2004. **22**(5): p. 583-8.
 156. Banuelos, G., et al., *Field trial of transgenic Indian mustard plants shows enhanced phytoremediation of selenium-contaminated sediment*. Environ Sci Technol, 2005. **39**(6): p. 1771-7.
 157. Meagher, R.B. and A.C. Heaton, *Strategies for the engineered phytoremediation of toxic element pollution: mercury and arsenic*. J Ind Microbiol Biotechnol, 2005. **32**(11-12): p. 502-13.
 158. Bizily, S.P., C.L. Rugh, and R.B. Meagher, *Phytodetoxification of hazardous organomercurials by genetically engineered plants*. Nat Biotech, 2000. **18**(2): p. 213-217.
 159. Rylott, E.L., et al., *Engineering plants for the phytoremediation of RDX in the presence of the co-contaminating explosive TNT*. New Phytol, 2011. **192**(2): p. 405-13.
 160. French, C.E., et al., *Biodegradation of explosives by transgenic plants expressing pentaerythritol tetranitrate reductase*. Nat Biotech, 1999. **17**(5): p. 491-494.
 161. Kurumata, M., et al., *Tolerance to, and uptake and degradation of 2,4,6-trinitrotoluene (TNT) are enhanced by the expression of a bacterial nitroreductase gene in Arabidopsis thaliana*. Z Naturforsch C, 2005. **60**(3-4): p. 272-8.
 162. Gleave, A.P., *A versatile binary vector system with a T-DNA organisational structure conducive to efficient integration of cloned DNA into the plant genome*. Plant Mol Biol, 1992. **20**(6): p. 1203-7.
 163. Ramos, J.L., et al., *Bioremediation of polynitrated aromatic compounds: plants and microbes put up a fight*. Curr Opin Biotechnol, 2005. **16**(3): p. 275-81.
 164. Musdal, Y. and B. Mannervik, *Substrate specificities of two tau class glutathione transferases inducible by 2,4,6-trinitrotoluene in poplar*. Biochimica et Biophysica Acta (BBA) - General Subjects, 2015. **1850**(9): p. 1877-1883.
 165. Gunning, V., *The role of glutathione transferases in TNT detoxification*, in *Department of Biology*. 2012, University of York: MSc Thesis.
 166. Sparrow, H., *The Role of Glutathione Transferases in the Detoxification of TNT*, in *Deptment of Biology*. 2010, University of York: PhD Thesis.
 167. Moseyko, N. and L.J. Feldman, *Expression of pH-sensitive green fluorescent protein in Arabidopsis thaliana*. Plant Cell Environ, 2001. **24**(5): p. 557-63.

References

168. Tournaire-Roux, C., et al., *Cytosolic pH regulates root water transport during anoxic stress through gating of aquaporins*. *Nature*, 2003. **425**(6956): p. 393-7.
169. Scott, A.C. and N. Allen, *Changes in Cytosolic pH within Arabidopsis Root Columella Cells Play a Key Role in the Early Signaling Pathway for Root Gravitropism*. *Plant Physiol*, 1999. **121**(4): p. 1291-8.
170. Fasano, J.M., et al., *Changes in root cap pH are required for the gravity response of the Arabidopsis root*. *Plant Cell*, 2001. **13**(4): p. 907-21.
171. Colville, L. and N. Smirnoff, *Antioxidant status, peroxidase activity, and PR protein transcript levels in ascorbate-deficient Arabidopsis thaliana vtc mutants*. *J Exp Bot*, 2008. **59**(14): p. 3857-68.
172. Habig, W.H., M.J. Pabst, and W.B. Jakoby, *Glutathione S-transferases. The first enzymatic step in mercapturic acid formation*. *J Biol Chem*, 1974. **249**(22): p. 7130-9.
173. Chow, T.M., et al., *Analysis of new generation explosives in the presence of u.s. EPA method 8330 energetic compounds by high-performance liquid chromatography*. *J Chromatogr Sci*, 2009. **47**(1): p. 40-3.
174. Sunahara, G.I., et al., *Ecotoxicological Characterization of Energetic Substances Using a Soil Extraction Procedure*. *Ecotoxicology and Environmental Safety*, 1999. **43**(2): p. 138-148.
175. Queval, G. and G. Noctor, *A plate reader method for the measurement of NAD, NADP, glutathione, and ascorbate in tissue extracts: Application to redox profiling during Arabidopsis rosette development*. *Anal Biochem*, 2007. **363**(1): p. 58-69.
176. Edwards, R. and D.P. Dixon, *Plant glutathione transferases*. *Methods Enzymol*, 2005. **401**: p. 169-86.
177. Cummins, I., et al., *Key role for a glutathione transferase in multiple-herbicide resistance in grass weeds*. *Proceedings of the National Academy of Sciences*, 2013. **110**(15): p. 5812-5817.
178. Dixon, D.P., M. Skipsey, and R. Edwards, *Roles for glutathione transferases in plant secondary metabolism*. *Phytochemistry*, 2010. **71**(4): p. 338-350.
179. Brazier-Hicks, M., et al., *Characterization and engineering of the bifunctional N- and O-glucosyltransferase involved in xenobiotic metabolism in plants*. *Proc Natl Acad Sci U S A*, 2007. **104**(51): p. 20238-43.
180. Singh, N., et al., *Degradation of trinitrotoluene in contaminated soils as affected by its initial concentrations and its binding to soil organic matter fractions*. *J Environ Sci Health A Tox Hazard Subst Environ Eng*, 2008. **43**(4): p. 348-56.
181. Park, C., et al., *Optimization for biodegradation of 2,4,6-trinitrotoluene (TNT) by Pseudomonas putida*. *J Biosci Bioeng*, 2003. **95**(6): p. 567-71.
182. Claus, H., et al., *Transformation of 2,4,6-trinitrotoluene (TNT) by Raoultella terrigena*. *Biodegradation*, 2007. **18**(1): p. 27-35.
183. Kubota, A., et al., *TNT biodegradation and production of dihydroxylamino-nitrotoluene by aerobic TNT degrader Pseudomonas sp. strain TM15 in an anoxic environment*. *Biodegradation*, 2008. **19**(6): p. 795-805.
184. Oh, B.T., et al., *TNT biotransformation and detoxification by a Pseudomonas aeruginosa strain*. *Biodegradation*, 2003. **14**(5): p. 309-19.

References

185. Conder, J.M., et al., *Recommendations for the assessment of TNT toxicity in sediment*. Environmental Toxicology and Chemistry, 2004. **23**(1): p. 141-149.
186. Singh, N., et al., *Effect of soil organic matter chemistry on sorption of trinitrotoluene and 2,4-dinitrotoluene*. J Hazard Mater, 2010. **173**(1-3): p. 343-8.
187. Singh, N., et al., *Sorption-desorption of trinitrotoluene in soils: effect of saturating metal cations*. Bull Environ Contam Toxicol, 2008. **80**(5): p. 443-6.
188. Arisi, A.C., et al., *Modification of thiol contents in poplars (Populus tremula x P. alba) overexpressing enzymes involved in glutathione synthesis*. Planta, 1997. **203**(3): p. 362-72.
189. Xiang, C. and D.J. Oliver, *Glutathione metabolic genes coordinately respond to heavy metals and jasmonic acid in Arabidopsis*. Plant Cell, 1998. **10**(9): p. 1539-50.
190. Meyer, A.J., M.J. May, and M. Fricker, *Quantitative in vivo measurement of glutathione in Arabidopsis cells*. Plant J, 2001. **27**(1): p. 67-78.
191. Yoon, J.M., D.J. Oliver, and J.V. Shanks, *Phytotoxicity and phytoremediation of 2,6-dinitrotoluene using a model plant, Arabidopsis thaliana*. Chemosphere, 2007. **68**(6): p. 1050-7.
192. Saisawang, C., J. Wongsantichon, and A.J. Ketterman, *A preliminary characterization of the cytosolic glutathione transferase proteome from Drosophila melanogaster*. Biochem J, 2012. **442**(1): p. 181-90.
193. Enayati, A.A., H. Ranson, and J. Hemingway, *Insect glutathione transferases and insecticide resistance*. Insect Mol Biol, 2005. **14**(1): p. 3-8.
194. Lee, K.W., et al., *Expression of glutathione S-transferase (GST) genes in the marine copepod Tigriopus japonicus exposed to trace metals*. Aquat Toxicol, 2008. **89**(3): p. 158-66.
195. Zhao, D., et al., *A delta-class glutathione transferase from the Chinese mitten crab Eriocheir sinensis: cDNA cloning, characterization and mRNA expression*. Fish Shellfish Immunol, 2010. **29**(4): p. 698-703.
196. Pettersson, E.U., et al., *Functional analysis and localisation of a delta-class glutathione S-transferase from Sarcoptes scabiei*. Int J Parasitol, 2005. **35**(1): p. 39-48.
197. Wang, Y., et al., *Structure of an insect epsilon class glutathione S-transferase from the malaria vector Anopheles gambiae provides an explanation for the high DDT-detoxifying activity*. J Struct Biol, 2008. **164**(2): p. 228-35.
198. Low, W.Y., et al., *Recognition and detoxification of the insecticide DDT by Drosophila melanogaster glutathione S-transferase D1*. J Mol Biol, 2010. **399**(3): p. 358-66.
199. Ketterman, A.J., C. Saisawang, and J. Wongsantichon, *Insect glutathione transferases*. Drug Metab Rev, 2011. **43**(2): p. 253-65.
200. Sawicki, R., et al., *Cloning, expression and biochemical characterization of one Epsilon-class (GST-3) and ten Delta-class (GST-1) glutathione S-transferases from Drosophila melanogaster, and identification of additional nine members of the Epsilon class*. Biochem J, 2003. **370**(Pt 2): p. 661-9.
201. Bonsor, D., et al., *Ligation independent cloning (LIC) as a rapid route to families of recombinant biocatalysts from sequenced prokaryotic genomes*. Org Biomol Chem, 2006. **4**(7): p. 1252-60.

References

202. USEPA, *Technical Fact Sheet - 2,4,6-Trinitrotoluene (TNT)*. 2014.
203. Griess, P., *Bemerkungen zu der Abhandlung der HH. Weselsky und Benedikt „Ueber einige Azoverbindungen“*. Berichte der deutschen chemischen Gesellschaft, 1879. **12**(1): p. 426-428.
204. Tsikas, D., *Analysis of nitrite and nitrate in biological fluids by assays based on the Griess reaction: appraisal of the Griess reaction in the L-arginine/nitric oxide area of research*. J Chromatogr B Analyt Technol Biomed Life Sci, 2007. **851**(1-2): p. 51-70.
205. Kumari, M., G.J. Taylor, and M.K. Deyholos, *Transcriptomic responses to aluminum stress in roots of Arabidopsis thaliana*. Mol Genet Genomics, 2008. **279**(4): p. 339-57.
206. Yilmaz, O., et al., *A Practical HPLC Method to Measure Reduced (GSH) and Oxidised (GSSG) Glutathione Concentrations in Animal Tissues*. Journal of Animal and Veterinary Advances, 2009. **8**(2): p. 343-347.
207. Melnyk, S., et al., *A new HPLC method for the simultaneous determination of oxidized and reduced plasma aminosulfhydryls using coulometric electrochemical detection*. J Nutr Biochem, 1999. **10**(8): p. 490-7.
208. Arnon, D.I., *COPPER ENZYMES IN ISOLATED CHLOROPLASTS. POLYPHENOLOXIDASE IN BETA VULGARIS*. Plant Physiol, 1949. **24**(1): p. 1-15.
209. Gunning, V., et al., *Arabidopsis Glutathione Transferases U24 and U25 Exhibit a Range of Detoxification Activities with the Environmental Pollutant and Explosive, 2,4,6-Trinitrotoluene*. Plant Physiol, 2014. **165**(2): p. 854-865.
210. Sheild, L.D., et al., *Mobility of 2-amino-4,6-dinitrobenzoic acid, a photodegradation product of TNT in a tropical soil under saturated abiotic conditions*. J Hazard Mater, 2013. **260**: p. 602-8.
211. Yang, X., X. Zhao, and H.M. Hwang, *Phototransformation of 2,4,6-trinitrotoluene: sensitized by riboflavin under different irradiation spectral range*. J Hazard Mater, 2007. **143**(1-2): p. 271-6.
212. Hwang, H.M., et al., *Photochemical and microbial degradation of 2,4,6-trinitrotoluene (TNT) in a freshwater environment*. Bull Environ Contam Toxicol, 2000. **65**(2): p. 228-35.
213. Lang, P.S., et al., *Oxidative Degradation of 2,4,6-Trinitrotoluene by Ozone in an Electrohydraulic Discharge Reactor*. Environmental Science & Technology, 1998. **32**(20): p. 3142-3148.
214. Schmelling, D.C. and K.A. Gray, *Photocatalytic transformation and mineralization of 2,4,6-trinitrotoluene (TNT) in TiO₂ slurries*. Water Research, 1995. **29**(12): p. 2651-2662.
215. Zeng, K., et al., *Assessing cytotoxicity of photosensitized transformation products of 2,4,6-trinitrotoluene (TNT) and atrazine with freshwater microbial assemblages*. Environ Toxicol, 2004. **19**(5): p. 490-6.
216. Schnaubelt, D., et al., *Low glutathione regulates gene expression and the redox potentials of the nucleus and cytosol in Arabidopsis thaliana*. Plant Cell Environ, 2015. **38**(2): p. 266-79.
217. Nakamura, C., et al., *Structural analysis of an epsilon-class glutathione transferase from housefly, Musca domestica*. Biochem Biophys Res Commun, 2013. **430**(4): p. 1206-11.

References

218. Daniel, R.M. and M.J. Danson, *Temperature and the catalytic activity of enzymes: A fresh understanding*. FEBS Letters, 2013. **587**(17): p. 2738-2743.
219. Honaker, M.T., et al., *Ensemble Perspective for Catalytic Promiscuity: CALORIMETRIC ANALYSIS OF THE ACTIVE SITE CONFORMATIONAL LANDSCAPE OF A DETOXIFICATION ENZYME*. Journal of Biological Chemistry, 2011. **286**(49): p. 42770-42776.
220. Irzyk, G.P. and E.P. Fuerst, *Purification and characterization of a glutathione S-transferase from benoxacor-treated maize (Zea mays)*. Plant Physiol, 1993. **102**(3): p. 803-10.
221. Guddewar, M.B. and W.C. Dauterman, *Purification and properties of a glutathione-S-transferase from corn which conjugates s-triazine herbicides*. Phytochemistry, 1979. **18**(5): p. 735-740.
222. Meyer, A.J. and M.D. Fricker, *Control of demand-driven biosynthesis of glutathione in green Arabidopsis suspension culture cells*. Plant Physiol, 2002. **130**(4): p. 1927-37.
223. Garcia-Gimenez, J.L., et al., *Nuclear glutathione*. Biochim Biophys Acta, 2013. **1830**(5): p. 3304-16.
224. Zhang, M.Y., et al., *A novel family of transporters mediating the transport of glutathione derivatives in plants*. Plant Physiol, 2004. **134**(1): p. 482-91.
225. Meyer, A.J. and R. Hell, *Glutathione homeostasis and redox-regulation by sulfhydryl groups*. Photosynth Res, 2005. **86**(3): p. 435-57.
226. Filomeni, G., G. Rotilio, and M.R. Ciriolo, *Cell signalling and the glutathione redox system*. Biochem Pharmacol, 2002. **64**(5-6): p. 1057-64.
227. Creissen, G., et al., *Elevated glutathione biosynthetic capacity in the chloroplasts of transgenic tobacco plants paradoxically causes increased oxidative stress*. Plant Cell, 1999. **11**(7): p. 1277-92.
228. Spanggard, R.J., et al., *Biodegradation of 2,4-dinitrotoluene by a Pseudomonas sp.* Appl Environ Microbiol, 1991. **57**(11): p. 3200-5.
229. Nishino, S.F., G.C. Paoli, and J.C. Spain, *Aerobic degradation of dinitrotoluenes and pathway for bacterial degradation of 2,6-dinitrotoluene*. Appl Environ Microbiol, 2000. **66**(5): p. 2139-47.
230. de Las Heras, A., M. Chavarria, and V. de Lorenzo, *Association of dnt genes of Burkholderia sp. DNT with the substrate-blind regulator DntR draws the evolutionary itinerary of 2,4-dinitrotoluene biodegradation*. Mol Microbiol, 2011. **82**(2): p. 287-99.
231. Crawford, R.L., *The microbiology and treatment of nitroaromatic compounds*. Current Opinion in Biotechnology, 1995. **6**(3): p. 329-336.
232. Ahmed, Z.U. and L.C. Vining, *Evidence for a chromosomal location of the genes coding for chloramphenicol production in Streptomyces venezuelae*. J Bacteriol, 1983. **154**(1): p. 239-44.
233. Kirner, S., et al., *Functions encoded by pyrrolnitrin biosynthetic genes from Pseudomonas fluorescens*. J Bacteriol, 1998. **180**(7): p. 1939-43.
234. Casalone, E., et al., *Site-directed mutagenesis of the Proteus mirabilis glutathione transferase B1-1 G-site*. FEBS Lett, 1998. **423**(2): p. 122-4.
235. Yamamoto, K., Y. Aso, and N. Yamada, *Catalytic function of an epsilon-class glutathione S-transferase of the silkworm*. Insect Mol Biol, 2013. **22**(5): p. 523-31.

References

236. Nishida, M., et al., *Molecular cloning and site-directed mutagenesis of glutathione S-transferase from Escherichia coli. The conserved tyrosyl residue near the N terminus is not essential for catalysis.* J Biol Chem, 1994. **269**(51): p. 32536-41.
237. Axarli, I., et al., *Crystal structure of Glycine max glutathione transferase in complex with glutathione: investigation of the mechanism operating by the Tau class glutathione transferases.* Vol. 422. 2009. 247-256.
238. Sali, A., et al., *Evaluation of comparative protein modeling by MODELLER.* Proteins, 1995. **23**(3): p. 318-26.
239. Yang, X., et al., *Biochemical and physiological characterization of a tau class glutathione transferase from rice (Oryza sativa).* Plant Physiol Biochem, 2009. **47**(11-12): p. 1061-8.
240. Schonbrunn, E., et al., *Structural basis for the interaction of the fluorescence probe 8-anilino-1-naphthalene sulfonate (ANS) with the antibiotic target MurA.* Proc Natl Acad Sci U S A, 2000. **97**(12): p. 6345-9.
241. Schonbrunn, E., et al., *Studies on the conformational changes in the bacterial cell wall biosynthetic enzyme UDP-N-acetylglucosamine enolpyruvyltransferase (MurA).* Eur J Biochem, 1998. **253**(2): p. 406-12.
242. Thom, R., et al., *Structure of a tau class glutathione S-transferase from wheat active in herbicide detoxification.* Biochemistry, 2002. **41**(22): p. 7008-20.
243. Bhattacharjee, A., et al., *Sequence and 3D structure based analysis of TNT degrading proteins in Arabidopsis thaliana.* J Mol Model, 2014. **20**(3): p. 2174.
244. Tanaka, S., et al., *Analysis of gene expression in poplar trees (Populus deltoides x nigra, DN34) exposed to the toxic explosive hexahydro-1,3,5-trinitro-1,3,5-triazine (RDX).* Int J Phytoremediation, 2007. **9**(1): p. 15-30.
245. Jinek, M., et al., *A programmable dual-RNA-guided DNA endonuclease in adaptive bacterial immunity.* Science, 2012. **337**(6096): p. 816-21.
246. Sander, J.D. and J.K. Joung, *CRISPR-Cas systems for editing, regulating and targeting genomes.* Nat Biotechnol, 2014. **32**(4): p. 347-55.
247. Belhaj, K., et al., *Editing plant genomes with CRISPR/Cas9.* Curr Opin Biotechnol, 2015. **32**: p. 76-84.
248. Shan, Q., et al., *Genome editing in rice and wheat using the CRISPR/Cas system.* Nat. Protocols, 2014. **9**(10): p. 2395-2410.
249. Ikeda, T., et al., *Generation of artificial drooping leaf mutants by CRISPR-Cas9 technology in rice.* Genes Genet Syst, 2015.
250. Klein, M., B. Burla, and E. Martinoia, *The multidrug resistance-associated protein (MRP/ABCC) subfamily of ATP-binding cassette transporters in plants.* FEBS Lett, 2006. **580**(4): p. 1112-22.
251. Blum, R., et al., *Function of phytochelatin synthase in catabolism of glutathione-conjugates.* Plant J, 2007. **49**(4): p. 740-9.
252. Meyer, A.J., *The integration of glutathione homeostasis and redox signaling.* J Plant Physiol, 2008. **165**(13): p. 1390-403.
253. He, J., et al., *Overexpression of bacterial gamma-glutamylcysteine synthetase mediates changes in cadmium influx, allocation and detoxification in poplar.* New Phytol, 2015. **205**(1): p. 240-54.

References

254. Dhankher, O.P., et al., *Engineering tolerance and hyperaccumulation of arsenic in plants by combining arsenate reductase and gamma-glutamylcysteine synthetase expression*. Nat Biotechnol, 2002. **20**(11): p. 1140-5.
255. Xiang, C., et al., *The biological functions of glutathione revisited in arabidopsis transgenic plants with altered glutathione levels*. Plant Physiol, 2001. **126**(2): p. 564-74.
256. Liedschulte, V., et al., *Exploiting plants for glutathione (GSH) production: Uncoupling GSH synthesis from cellular controls results in unprecedented GSH accumulation*. Plant Biotechnol J, 2010. **8**(7): p. 807-20.
257. Makris, K.C., et al., *High uptake of 2,4,6-trinitrotoluene by vetiver grass--potential for phytoremediation?* Environ Pollut, 2007. **146**(1): p. 1-4.
258. Das, P., et al., *Vetiver grass is capable of removing TNT from soil in the presence of urea*. Environ Pollut, 2010. **158**(5): p. 1980-3.
259. Hills, M.J., et al., *Genetic use restriction technologies (GURTs): strategies to impede transgene movement*. Trends in Plant Science, 2007. **12**(4): p. 177-183.